Mathematical analysis of the interaction of an inviscid fluid with immersed structures

Krisztian Benyo

Institut de Mathématiques de Bordeaux

université de BORDEAUX

Thèse de doctorat de
l'Université de Bordeaux

École doctorale de mathématiques et d'informatique
Spécialité : Mathématiques Appliquées

Présentée par

Krisztián Benyó

pour obtenir le grade de

docteur de l'Université de Bordeaux

Analyse mathématique de l'interaction d'un fluide non-visqueux avec des structures immergées

---

Date de soutenance : 25 septembre 2018

Directeurs de thèse :	M. David Lannes	DR CNRS (Université de Bordeaux)
	M. Franck Sueur	Professeur (Université de Bordeaux)
Rapporteurs :	M. Pascal Noble	Professeur (Université Paul Sabatier)
	M. Takéo Takahashi	CR Inria (Université de Lorraine)

Devant la commission d'examen composée de :

Emmanuel Audusse	MdC	Université Paris 13	Examinateur
Afaf Bouharguane	MdC	Université de Bordeaux	Examinatrice
Catherine Choquet	Professeur	Université de La Rochelle	Examinatrice
David Lannes	DR CNRS	Université de Bordeaux	Co-directeur
Pascal Noble	Professeur	Université Paul Sabatier	Rapporteur
Franck Sueur	Professeur	Université de Bordeaux	Directeur
Takéo Takahashi	CR Inria	Université de Lorraine	Rapporteur

– 2018 –

Institut de Mathématiques de Bordeaux

université de BORDEAUX

Doctoral dissertation
University of Bordeaux

Doctoral School of Mathematics and Computer Science
Discipline: Applied Mathematics

Presented by

Krisztián Benyó

for the degree of

Doctor of Philosophy

Mathematical analysis of the interaction of an inviscid fluid with immersed structures

---

PhD supervisors:	Prof. David Lannes	DR CNRS (Université de Bordeaux)
	Prof. Franck Sueur	Professeur (Université de Bordeaux)
Reviewers:	Prof. Pascal Noble	Professeur (Université Paul Sabatier)
	Prof. Takéo Takahashi	CR Inria (Université de Lorraine)
Examiners:	Prof. Emmanuel Audusse	MdC (Université Paris 13)
	Prof. Afaf Bouharguane	MdC (Université de Bordeaux)
	Prof. Catherine Choquet	Professeur (Université de La Rochelle)

– 2018 –

Résumé : Cette thèse porte sur l'analyse mathématique de l'interaction d'un fluide non-visqueux avec des structures immergées. Plus précisément, elle est structurée autour de deux axes principaux. L'un d'eux est l'analyse asymptotique du mouvement d'une particule infinitésimale en milieu liquide. L'autre concerne l'interaction entre des vagues et une structure immergée.

La première partie de la thèse repose sur l'analyse mathématique d'un système d'équations différentielles ordinaires non-linéaires d'ordre 2 modélisant le mouvement d'un solide infiniment petit dans un fluide incompressible en 2D. Les inconnues du modèle décrivent la position du solide, c'est-à-dire la position du centre de masse et son angle de rotation. Les équations proviennent de la deuxième loi de Newton avec un prototype de force de type Kutta-Joukowski.

Plus précisément, nous étudions la dynamique de ce système lorsque l'inertie du solide tend vers 0. Les principaux outils utilisés sont des développements asymptotiques multi-échelles en temps. Pour la dynamique de la position du centre de masse, l'étude met en évidence des analogies avec le mouvement d'une particule chargée dans un champ électromagnétique et la théorie du centre-guide. En l'occurrence, le mouvement du centre-guide est donné par une équation de point-vortex. La dynamique de l'angle est quant à elle donnée par une équation de pendule non-linéaire lentement modulée. Des régimes très différents se distinguent selon les données initiales. Pour de petites vitesses angulaires initiales la méthode de Poincaré-Lindstedt fait apparaitre une modulation des oscillations rapides, alors que pour de grandes vitesses angulaires initiales, un movement giratoire bien plus irrégulier est observé. C'est une conséquence particulière et assez spectaculaire de l'enchevêtrement des trajectoires homocliniques.

La deuxième partie de la thèse porte sur le problème des vagues dans le cas où le domaine occupé par le fluide est à surface libre et avec un fond plat sur lequel un objet solide se translate horizontalement sous l'effet des forces de pression du fluide. Nous avons étudié deux systèmes asymptotiques qui décrivent le cas d'un fluide parfait incompressible en faible profondeur. Ceux-ci correspondent respectivement aux équations de Saint-Venant et de Boussinesq. Grâce à leur caractère bien-posé en temps long, les modèles traités permettent de prendre en compte certains effets de la mécanique du solide, comme les forces de friction, ainsi que les effets non-hydrostatiques.

Notre analyse théorique a été complétée par des études numériques. Nous avons développé un schéma de différences finies d'ordre élevé et nous l'avons adapté à ce problème couplé afin de mettre en évidence les effets d'un solide (dont le mouvement est limité à des translations sur le fond) sur les vagues qui passent au dessus de lui. A la suite de ces travaux, nous avons souligné l'influence des forces de friction sur ce genre de systèmes couplés ainsi que sur le déferlement des vagues. Quant à l'amortissement dû aux effets hydrodynamiques, une vague ressemblance avec le phénomène de l'eau morte est mise en évidence.

Mots-clés : interaction fluide-structure, analyse asymptotique, dynamique des fluides, équations d'Euler, particules immergées, équation de Newton

Abstract: This PhD thesis concerns the mathematical analysis of the interaction of an inviscid fluid with immersed structures. More precisely it revolves around two main problems: one of them is the asymptotic analysis of an infinitesimal immersed particle, the other one being the interaction of water waves with a submerged solid object.

Concerning the first problem, we studied a system of second order non-linear ODEs, serving as a toy model for the motion of a rigid body immersed in a two-dimensional perfect fluid. The unknowns of the model describe the position of the object, that is the position of its center of mass and the angle of rotation; the equations arise from Newton's second law with the consideration of a Kutta-Joukowski type lift force. It concerns the detailed analysis of the dynamic of this system when the solid inertia tends to 0.

For the evolution of the position of the solid's center of mass, the study highlights similarities with the motion of a charged particle in an electromagnetic field and the well-known "guiding center approximation"; it turns out that the motion of the corresponding guiding center is given by a point-vortex equation. As for the angular equation, its evolution is given by a slowly-in-time modulated non-linear pendulum equation. Based on the initial values of the system one can distinguish qualitatively different regimes: for small angular velocities, by the Poincaré-Lindstedt method one observes a modulation in the fast time-scale oscillatory terms, for larger angular velocities however erratic rotational motion is observed, a consequence of Melnikov's observations on the presence of a homoclinic tangle.

About the other problem, the Cauchy problem for the water waves equations is considered in a fluid domain which has a free surface on the upper vertical limit and a flat bottom on which a solid object moves horizontally, its motion determined by the pressure forces exerted by the fluid. Two shallow water asymptotic regimes are detailed, well-posedness results are obtained for both the Saint-Venant and the Boussinesq system coupled with Newton's equation characterizing the solid motion. Using the particular structure of the coupling terms one is able to go beyond the standard scale for the existence time of solutions to the Boussinesq system with a moving bottom.

An extended numerical study has also been carried out for the latter system. A high order finite difference scheme is developed, extending the convergence ratio of previous, staggered grid based models. The discretized solid mechanics are adapted to represent important features of the original model, such as the dissipation due to the friction term. We observed qualitative differences for the transformation of a passing wave over a moving solid object as compared to an immobile one. The movement of the solid not only influences wave attenuation but it affects the shoaling process as well as the wave breaking. The importance of the coefficient of friction is also highlighted, influencing qualitative and quantitative properties of the coupled system. Furthermore, we showed the hydrodynamic damping effects of the waves on the solid motion, reminiscent of the so-called dead water phenomenon.

Keywords: fluid-structure interaction, asymptotic analysis, fluid dynamics, Euler equation, immersed particule, Newton equation

Laboratoire d'accueil : Institut de Mathématiques de Bordeaux,
Université de Bordeaux
Bât. A33, 351, cours de la Libération,
33405 Talence CEDEX, France

Remerciements

Mes premiers remerciements vont vers mes deux encadrants, David Lannes et Franck Sueur. C'est uniquement grâce à leur dévouement, leur disponibilité et leurs conseils professionnels ainsi que personnels que j'ai pu parvenir à conclure mes travaux de recherche au sein de l'Institut de Mathématiques de Bordeaux. Je sais très bien que j'étais loin de leur meilleur étudiant, néanmoins j'espère que malgré mes nombreux défauts j'ai été capable de récupérer tout mes occasions ratées.

J'aimerais également remercier Pascal Noble et Takéo Takahashi qui me font l'immense honneur d'être mes rapporteurs de thèse et, par conséquent, d'avoir consacré une partie considérable de leur temps pendant les vacances estivales. Je tiens à remercier également Afaf Bouharguane, Catherine Choquet et Emmanuel Audusse d'avoir accepter de faire partie de mon jury de thèse.

Je tiens à remercier les personnels de l'IMB et les collègues de l'équipe EDP et physique mathématique pour l'accueil chaleureux et pour les quotidiens vifs et dynamiques pendant ces trois années. En pensant au laboratoire, mes premières pensées vont vers Benjamin et Stevan qui m'ont guidé et accompagné pendant ma première année bordelaise. Malgré les difficultés et les inattendus, c'était grâce à eux que j'ai pu établir une excellente base à la fois sportive et scientifique.

Je voudrais ensuite remercier Benoit pour ses passages hilarantes, Stefano et Francesco pour un bon goût d'Italie pour les quotidiens, et Adrien pour sa présence très occasionnelle. Je dois également remercier Paul et Xiaoming pour m'avoir supporté, surtout ces derniers mois, en tant que collègue de bureau. Je remercie Edoardo pour les séjours et les conférences un peu partout en France. Je tiens à remercier également les autres membres de « l'équipe CNRS » : Debayan, Marco et Jared pour les repas inoubliables. Finalement un grand merci pour Olivier pour ses corrections et conseils de français.

Enfin je voulais remercier deux individus hongrois en particulier. Tout d'abord Kristóf pour m'avoir encourager (très) longuement de partir sur ce chemin. Ensuite János qui m'a servi comme un exemple pendant des années, qui m'a montré ce que cela signifie d'être un vrai mathématicien au XXIème siècle.

Mes derniers remerciements appartiennent à ma famille. Sans eux, rien ne serait possible.

Table of contents

Introduction (version française)

Sommaire

Les problèmes de l'interaction fluide-structure sont l'un des exemples les plus connus des problèmes multi-physiques. Ce sont des modèles qui impliquent plusieurs phénomènes physiques simultanément. Dans un problème d'interaction fluide-structure, on décrit l'interaction entre le mouvement ou la déformation d'une structure solide et un fluide s'écoulant à l'intérieur ou à l'extérieur de cette structure. Il s'agit de contextes physiques complexes dans lesquels le fluide et le solide interagissent à travers une surface de contact (par exemple le bord du solide). Plus précisément, le fluide exerce une pression sur la structure, ce qui engendre des changements dans l'état physique de celle-ci (sa position, sa forme etc.). En conséquence, l'objet modifie le domaine du fluide et son flot. Cet effet de couplage n'est pas stationnaire dans le sens où il se manifeste comme une action-réaction continument présente entre les deux milieux. Ainsi un échange d'énergie et de quantité de mouvement (a priori non-constant) se maintient dans le système complet.

Grâce à l'augmentation de la puissance du calcul ainsi qu'à son accès simple et facile, le domaine de l'interaction fluide-structure a connu un développement rapide ces dernières années. Des expériences et simulations numériques ont été mises en avant non seulement pour soutenir les résultats des recherches scientifiques menées sur ce sujet mais également pour venir en remplacement d'expérimentations chères et inefficaces, typiques de ce domaine. Il était également d'un grand intérêt de renforcer les connaissances théoriques. Cependant ce domaine n'a pas été aussi remarquablement influencé par le développement des moyens informatiques.

L'objectif principal de cette thèse est d'étudier deux problèmes en particulier, provenants de ce domaine de recherche très dynamique. Nous avons basé notre approche à des modèles asymptotiques qui conservent les caractéristiques essentielles des problèmes couplés complets et qui omettent des phénomènes physiques qui représentent des effets cumulatifs négligeables ou non pertinents. Ces problèmes s'inscrivent dans des directions de recherche récentes à cause de l'intérêt qu'ils représentent pour des applications dans l'ingénierie d'une part et pour leur pertinence par rapport à de nouvelles tentatives d'analyse asymptotique d'autre part.

1 Plan de la thèse

Dans cette partie introductive, nous présentons les deux problématiques de ce travail. D'abord nous introduisons les modèles principaux décrivant la dynamique du fluide ainsi que le mouvement du solide. Ensuite nous détaillons certains paradigmes et aspects essentiels liés au couplage de ces deux régimes. Enfin nous énonçons les principales techniques et méthodes de l'étude asymptotique des systèmes perturbés.

Le chapitre 1 présente l'analyse asymptotique d'un système d'équations différentielles ordinaires non-linéaires. Ce système intervient comme un modèle simplifié décrivant l'évolution d'un objet infinitésimal dans un milieu fluide parfait bi-dimensionnel. Une approche de développement à plusieurs échelles est adaptée à ce problème en régime asymptotique

lorsque l'inertie du solide tend vers 0.

Le chapitre 2 est largement inspiré de l'article [Ben17]. Nous détaillons le modèle couplé lié au problème de l'interaction entre des vagues et un objet se déplaçant au fond du fluide. Nous analysons deux systèmes asymptotiques en régime de faible profondeur. Notamment, nous établissons le caractère bien-posé du système couplé de Saint-Venant non-linéaire et de celui de Boussinesq faiblement non-linéaire.

Ensuite nous mettons en œuvre un schéma aux différences finies d'ordre élevé afin d'effectuer des simulations numériques sur les équations de Boussinesq couplées avec l'équation de Newton décrivant le mouvement du solide. Ce schéma numérique est une amélioration du schéma préexistant. De plus, il est adapté à l'intégration de l'EDO discrétisée qui caractérise le déplacement de l'objet. Enfin, la partie 3.3 présente les résultats de ces simulations et leur interprétation, tirée de [Ben18b].

Nous terminons en résumant les contributions principales de cette thèse et en détaillant quelques perspectives de recherche qui peuvent permettre de poursuivre les travaux présentés dans cette thèse. L'annexe complète les études présentées aux chapitre 2 et 3. Nous y faisons quelques remarques concernant les inégalités de Grönwall utilisées dans l'analyse des systèmes couplés.

2 La dynamique du fluide

La dynamique du fluide décrit le flot d'un fluide, que ce soit un liquide ou un gaz. En ce qui concerne le présent travail, nous nous intéressons en particulier à l'hydrodynamique afin de décrire le mouvement d'un milieu liquide. Une des principales hypothèses suppose que le liquide est décrit à l'échelle macroscopique, donc de manière continue. Le considérer comme un milieu continu permet de considérer les variables du flot et les propriétés du système (densité, pression, champ de vitesse etc.) comme des fonctions définies sur des éléments volumiques infinitésimaux. La structure moléculaire et une description discrète se manifeste néanmoins à travers certains coefficients, certaines équations d'état et les conditions aux limites.

Ainsi le mouvement du fluide peut être décrit par des équations différentielles qui caractérisent son évolution « continue ». Ces équations font suite à la description mathématique des lois de conservations générales, notamment la conservation de la masse et la conservation de la quantité de mouvement linéaire. Dans cette partie de l'introduction nous établissons ces équations en partant du principe que le fluide est parfait afin de mieux décrire la base dynamique de nos problèmes principaux.

2.1 Les équations d'Euler

Nous établissons ici de manière plutôt formelle des équations d'Euler incompressible. Ce sont les équations de base pour décrire le mouvement d'un fluide parfait et incompressible. Cette partie fait également office d'introduction à la partie modélisation du chapitre 2.

Nous commençons par supposer que le domaine du fluide est l'espace $\mathbb{R}^d$ tout entier, avec $d \in \mathbb{N}$, où $d = 2$ et 3 ce sont les dimensions physiquement pertinentes. Cela signifie que les effets de bord seront dans un premier temps négligés. Dans une description Eulerienne, nous associons à chaque point $x \in \mathbb{R}^d$ et à chaque instant $t \in \mathbb{R}_+$ des quantités telles que

- le champ de vitesse $\mathbf{U} = \mathbf{U}(t,x) \in \mathbb{R}^d$,
- la densité $\varrho = \varrho(t,x) \in \mathbb{R}_+$,
- la pression $P = P(t,x) \in \mathbb{R}$.

On peut aussi intégrer d'autres quantités, comme l'énergie interne ($e(t,x) \in \mathbb{R}$), l'entropie ($s(t,x) \in \mathbb{R}$) ou la température ($T = T(t,x) \in \mathbb{R}_+$). Nous avons énoncé ici ceux qui sont relatifs aux études présentées dans ce texte.

Les équations elles-mêmes proviennent des diverses lois de conservation de la mécanique classique et en général de la thermodynamique. L'interprétation de ces lois consiste à décrire la conservation de certaines quantités le long des trajectoires des particules, induites par le flot du champ de vitesse.

Définition 2.1. *Le flot ψ de $\mathbf{U} \in \mathrm{C}^0(\mathbb{R}_+, \mathrm{Lip}\,\mathbb{R}^d); \mathbb{R}^d)$ est l'unique solution de la classe $\mathcal{C}^1(\mathbb{R}_+, \mathcal{C}^0(\mathbb{R}^d); \mathbb{R}^d)$ de l'équation différentielle ordinaire suivante*

$$\frac{d}{dt}\psi(t,x) = \mathbf{U}(t,\psi(t,x)),\ t > 0, \quad \psi(0,x) = x,$$

où le point $x \in \mathbb{R}^d$ est un paramètre du système.

Pour un domaine $\omega \subset \mathbb{R}^d$, nous notons $\omega_t = \psi_t(\omega)$ avec $\psi_t(x) = \psi(t,x)$. Le lemme ci-dessous présente la réécriture adaptée à l'observation de la conservation des quantités le long des trajectoires.

Lemme 2.1. *Soient ω un sous-ensemble ouvert, borné, connexe et régulier de $\mathbb{R}^d$, ψ le flot de $\mathbf{U} \in \mathcal{C}^1(\mathbb{R}_+ \times \mathbb{R}^d; \mathbb{R}^d)$ avec $\omega_t = \psi_t(\omega)$ et $b \in \mathcal{C}^1(\mathbb{R}^+ \times \mathbb{R}^d; \mathbb{R}^d)$. Alors on a*

$$\begin{aligned}\frac{d}{dt}\int_{\omega_t} b(t,x)\,dx &= \int_{\omega_t} \Big(\partial_t b(t,x) + \nabla\cdot(b(t,x)\mathbf{U}(t,x))\Big)\,dx \\ &= \int_{\omega_t} \partial_t b(t,x)\,dx + \int_{\partial\omega_t} \Big(b(t,x)\mathbf{U}(t,x)\cdot\mathbf{n}\Big)\,d\Sigma.\end{aligned}$$

Ici, $\mathbf{n}$ désigne la normale unitaire sortante d'ω_t et Σ la mesure surfacique définie sur $\partial\omega_t$.

Dans ce qui suit, nous considérons un ω ouvert, borné et régulier pour représenter une partie arbitraire du domaine du fluide.

Conservation de la masse : nous travaillons sur un système de fluide fermé dans lequel il ne se passe aucune production ou perte de masse durant l'évolution en temps de la dynamique du fluide. La masse d'une quantité du fluide qui se retrouve dans ω à l'instant t s'écrit

$$M_\omega(t) = \int_\omega \varrho(t,x)\,dx.$$

Puisque la masse est conservée, nous en déduisons que

$$\frac{d}{dt}M_{\omega_t}(t) = \frac{d}{dt}\int_{\omega_t} \varrho(t,x) = 0.$$

De ce fait, par Lemme 2.1 nous obtenons l'équation du **bilan de masse** :

$$\partial_t \varrho + \nabla\cdot(\varrho\mathbf{U}) = 0. \tag{2.1}$$

Conservation de la quantité de mouvement : La deuxième loi de Newton dit que la force totale qui agit sur le fluide en ω est égale au changement instantané de la quantité de mouvement. Nous détaillerons cette loi plus précisément dans la Partie 3. La quantité de mouvement linéaire du fluide s'exprime sous la forme suivante

$$\mathbf{P}_\omega(t) = \int_\omega (\varrho\mathbf{u})(t,x)\,dx.$$

La force résultante exercée est constituée des forces à longue portée $\mathbf{F}_{ext}$ (la gravité, par exemple) et des forces surfaciques sur le bord du domaine (frottement ou pression externe, par exemple). Les forces à courte portée peuvent être représentées par un tenseur d'ordre 2 σ, dont la forme est précisée suivant des hypothèses physiques supplémentaires. Néanmoins, nous écrivons

$$\frac{d}{dt}\mathbf{P}_{\omega_t}(t) = \frac{d}{dt}\int_{\omega_t}(\varrho\mathbf{v})(t,x)\,dx = \int_{\omega_t}(\varrho\mathbf{F}_{ext})(t,x)\,dx + \int_{\partial\omega_t}(\sigma\cdot\mathbf{n})(t,x)\,d\Sigma.$$

L'équation du **bilan de la quantité de mouvement linéaire** est donc :

$$\partial_t(\varrho\mathbf{U}) + \nabla\cdot(\varrho\mathbf{U}\otimes\mathbf{U}) = \varrho\mathbf{F}_{ext} + \nabla\cdot\sigma. \tag{2.2}$$

De la même façon, on peut écrire le bilan d'énergie interne par la première loi de la thermodynamique, ou bien le bilan entropique fourni par la deuxième loi de la thermodynamique.

Afin d'obtenir les équations d'Euler, nous devons faire des hypothèses supplémentaires sur le fluide. Notamment, nous considérons un fluide parfait, ce qui signifie d'abord que celui-ci est isotrope, les quantités physiques principales ne dépendent que de (t,x). De

plus, nous supposons que le fluide n'admet pas de contrainte de cisaillement, qu'il n'est pas visqueux et que, finalement, aucun échange de chaleur ne se produit. Cela implique que le tenseur prend une forme assez simple : $\sigma = -P\,\mathrm{Id}$.

Par conséquent, les lois de conservation de la masse et de la quantité de mouvement s'écrivent

$$\begin{cases} \partial_t \varrho + \nabla \cdot (\varrho \mathbf{U}) = 0, \\ \partial_t (\varrho \mathbf{U}) + \nabla \cdot (\varrho \mathbf{U} \otimes \mathbf{U}) = -\nabla P + \varrho \mathbf{F}_{ext}. \end{cases} \tag{2.3}$$

EN faisant l'hypothèse supplémentaire que le fluide est homogène ($\varrho \equiv cst$), le système simplifie au point de parvenir à l'écriture classique des équations d'Euler incompressible :

$$\begin{cases} \nabla \cdot \mathbf{U} = 0, \\ \partial_t \mathbf{U} + (\mathbf{U} \cdot \nabla)\mathbf{U} = -\frac{1}{\varrho}\nabla P + \mathbf{F}_{ext}. \end{cases} \tag{2.4}$$

Le théorème suivant est un résultat classique concernant l'existence des solutions locales en temps de ce système sur l'espace tout entier :

Théorème 2.1. *Soit $\mathbf{U}_0 \in H^s(\mathbb{R}^d)$, avec $s > d/2 + 1$ et $\nabla \cdot \mathbf{U}_0 = 0$, il existe un temps T avec la borne supérieure*

$$0 < T \leqslant \frac{1}{c_s \|\mathbf{U}_0\|_{H^s}},$$

c_s constante dépendante uniquement de s et de d, il existe une unique solution classique $\mathbf{U}$ des équations (2.4) dans la classe $\mathcal{C}([0,T];\mathcal{C}^1(\mathbb{R}^d)) \cap \mathcal{C}^1([0,T];\mathcal{C}(\mathbb{R}))$.

Pour la démonstration, et pour des résultats plus généraux concernant la théorie générale, nous renvoyons au livre de [MB03].

Nous avons introduit précédemment les équations d'Euler sur l'espace tout entier. Maintenant nous voulons préciser le contexte de ce système dans le cas où le domaine du problème est borné. Prenons Ω ouvert, borné, connexe et simplement connexe. Le mouvement d'un fluide parfait incompressible dans le domaine Ω fixe (qui ne bouge pas en temps) est toujours décrit par les équations (2.4). Cependant, pour compléter le problème, nous devons imposer des conditions sur le bord $\partial\Omega$. Supposons que ce bord est fixe, non-déformable et imperméable. La condition de non-perméabilité, également connu sous le nom de condition de non-pénétration, s'exprime mathématiquement par la relation où le composant normal de la vitesse vaut 0 sur le bord.

Notons par $\mathbf{n}$ la normale sortante unitaire. Nous avons

$$\mathbf{U} \cdot \mathbf{n} = 0 \quad \text{sur } \partial\Omega \tag{2.5}$$

pour fermer le système d'équations.

Nous avons le résultat suivant concernant l'existence des solutions locales en temps ([KL84])

Theorem 2.1. *Soit $\Omega \subset \mathbb{R}^d$ ouvert et borné, avec un bord régulier $\partial\Omega$. Soit $s > d/2 + 1$, soit $\mathbf{U}_0 \in H^s(\Omega; \mathbb{R}^d)$ avec $\nabla \cdot \mathbf{U}_0 = 0$ et $\mathbf{F}_{ext} \in \mathcal{C}([0, T_0]; H^s(\Omega; \mathbb{R}^d))$ telle que $\nabla \cdot \mathbf{F}_{ext} = 0$ pout tout $t \in [0, T_0]$, $T_0 > 0$. Alors il existe un temps $T > 0$, $T \leqslant T_0$ tel qu'il existe une unique solution $\mathbf{U}$ dans la classe $\mathcal{C}([0, T]; H^s(\Omega; \mathbb{R}^d))$ du système (2.4) dans Ω.*

2.2 L'équation des vagues

Nous allons maintenant présenter les équations d'Euler à surface libre et leur réécriture dans le cadre du problème des vagues. Cela nécessite tout d'abord de préciser le domaine du fluide qui est désormais une bande infinie avec des bornes qui évoluent au cours du temps. Dans ce qui suit, nous désignons par $\zeta(t, x)$ l'élévation de la surface libre et par $b(t, x)$ les variations de la topographie du fond à un profondeur de base H_0. Avec cette notation, le domaine du fluide est donné par

$$\Omega_t = \left\{(x, z) \in \mathbb{R}^d \times \mathbb{R} \,:\, -H_0 + b(t, x) < z < \zeta(t, x)\right\},$$

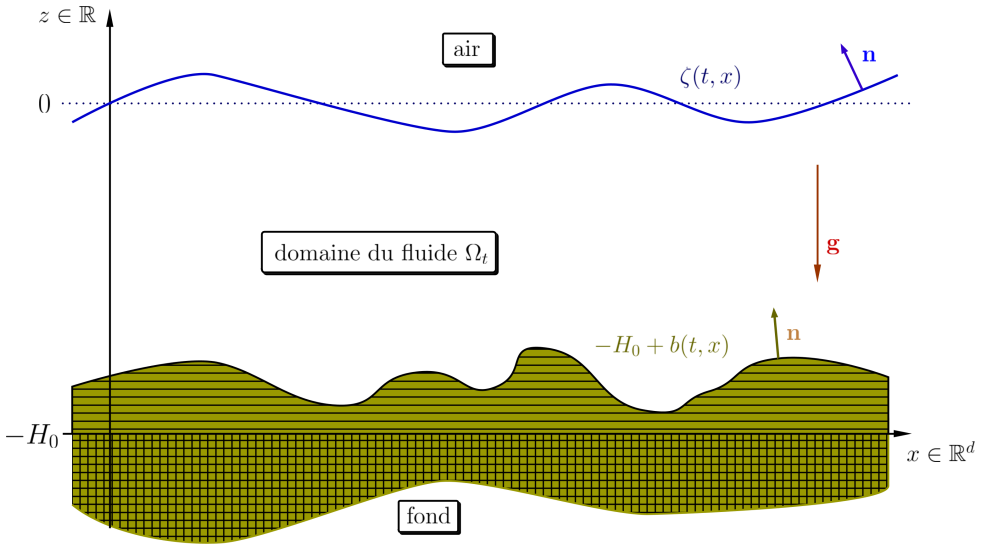

FIGURE 1 – Le problème des vagues avec un fond qui évolue au cours du temps

Pour éviter des cas physiques spécifiques liés aux irrégularités du domaine Ω_t (comme les îles, ou les plages), nous faisons l'hypothèse que la profondeur totale du fluide à chaque coordonnée horizontale est uniformément bornée inférieurement par une constante positive.

Dans le cadre du problème des vagues, nous considérons un fluide qui se déplace sous l'influence de la gravité dans le domaine Ω_t. Nous rappelons que la fonction $\mathbf{U}$ dénote le champ de vitesse et P la pression du fluide. Les équations d'Euler incompressible et

irrotationnel avec l'unique force extérieure due à la gravité s'écrivent

$$\begin{cases} \partial_t \mathbf{U} + \mathbf{U} \cdot \nabla \mathbf{U} = -\dfrac{\nabla P}{\varrho} + \mathbf{g}, \\ \nabla \cdot \mathbf{U} = 0, \\ \nabla \times \mathbf{U} = 0, \end{cases} \tag{2.6}$$

valable sur Ω_t. $\mathbf{g} = (0, -g)^\top$ désigne l'accélération gravitationnelle.

Les conditions aux limites peuvent être résumées ainsi :

- une condition cinématique (ou de non-pénétration) aux limites verticales (les particules du fluide ne peuvent pas pénétrer le bord) ;
- il n'y a pas de tension surfacique, la pression à la surface libre est donnée par la pression atmosphérique, qui est une constante du système.

Nous reformulons ces conditions physiques en langage mathématique :

- nous rappelons que $\mathbf{n}$ est la normale unitaire montante. Nous écrivons donc, pour le fond
$$\partial_t b - \sqrt{1 + |\nabla_x b|^2}\mathbf{U} \cdot \mathbf{n} = 0 \quad \text{sur } \{z = -H_0 + b(t,x)\}, \tag{2.7}$$
et pour la surface libre
$$\partial_t \zeta - \sqrt{1 + |\nabla_x \zeta|^2}\mathbf{U} \cdot \mathbf{n} = 0 \quad \text{sur } \{z = \zeta(t,x)\}; \tag{2.8}$$
- si nous désignons par P_{atm} la pression atmosphérique, nous avons la formule suivante
$$P = P_{atm} \quad \text{sur } \{z = \zeta(t,x)\}. \tag{2.9}$$

Le système (2.6), (2.7), (2.8) et (2.9) est appelé équations d'Euler à surface libre dans le domaine du fluide Ω_t.

Nous remarquons que le traitement analytique d'un système d'équations aux dérivées partielles sur un domaine Ω_t est complexe et nécessite beaucoup de subtilités. Toutefois nous constatons également que certaines reformulations de ce système peuvent être effectuées grâce à des hypothèses supplémentaires. En particulier, par la supposition d'incompressibilité et d'irrotationalité, nous pouvons représenter le champ de vitesse par le gradient d'un potentiel. Grâce à la décomposition de Helmholtz, il existe une fonction $\Phi(t,x)$, appelée potentiel de vitesse, telle que

$$\mathbf{U} = \nabla \Phi \quad \text{dans } \Omega_t.$$

Ce potentiel vérifie une équation de Laplace sur le domaine du fluide. Avec des conditions

au bord reformulées pour implémenter le potentiel, Φ vérifie l'équation

$$\begin{cases} \Delta\Phi = 0 \quad \text{dans } \Omega_t, \\ \Phi|_{z=\zeta} = \psi, \ \sqrt{1+|\nabla_x b|^2}\partial_{\mathbf{n}}\Phi|_{z=-H_0+b} = \partial_t b, \end{cases} \tag{2.10}$$

où $\psi = \Phi|_{z=\zeta}$ est une nouvelle inconnue du système. Par une méthode classique ([Mel15]) nous décomposons le potentiel Φ en un composant « au fond fixe » et un composant « au fond variable » de la façon suivante

$$\Phi = \Phi_{fb} + \Phi_{mb},$$

où

$$\begin{cases} \Delta\Phi_{fb} = 0 \quad \text{dans } \Omega_t, \\ \Phi_{fb}|_{z=\zeta} = \psi, \ \sqrt{1+|\nabla_x b|^2}\partial_{\mathbf{n}}\Phi_{fb}|_{z=-H_0+b} = 0, \end{cases}$$

et

$$\begin{cases} \Delta\Phi_{mb} = 0 \quad \text{dans } \Omega_t, \\ \Phi_{mb}|_{z=\zeta} = 0, \ \sqrt{1+|\nabla_x b|^2}\partial_{\mathbf{n}}\Phi_{mb}|_{z=-H_0+b} = \partial_t b. \end{cases}$$

De plus, nous avons la relation suivante ([Lan13])

$$\sqrt{1+|\nabla_x\zeta|^2}\partial_{\mathbf{n}}\Phi|_{z=\zeta} = G^{DN}[\zeta, b]\psi + G^{NN}[\zeta, b]\partial_t b,$$

où nous avons introduit l'opérateur de type Dirichlet–Neumann $G^{DN}[\zeta, b]$ associé au premier problème de Laplace :

$$G^{DN}[\zeta, b] : \psi \mapsto \sqrt{1+|\nabla_x\zeta|^2}\partial_{\mathbf{n}}\Phi_{fb}|_{z=\zeta}.$$

et l'opérateur de type Neumann–Neumann $G^{NN}[\zeta, b]$ associé au second problème de Laplace :

$$G^{NN}[\zeta, b] : \partial_t b \mapsto \sqrt{1+|\nabla_x\zeta|^2}\partial_{\mathbf{n}}\Phi_{mb}|_{z=\zeta}.$$

Au moyen de cette notation, nous énonçons enfin les équations des vagues avec un fond qui évolue au cours du temps :

$$\begin{cases} \partial_t\zeta - G[\zeta, b]\psi = G^{NN}[\zeta, b]\partial_t b, \\ \partial_t\psi + g\zeta + \frac{1}{2}|\nabla_x\psi|^2 - \dfrac{(G[\zeta, b]\psi + G^{NN}[\zeta, b]\partial_t b + \nabla_x\zeta\cdot\nabla_x\psi)^2}{2(1+|\nabla_x\zeta|^2)} = 0. \end{cases} \tag{2.11}$$

Nous remarquons que ces équations ont déjà été étudiées dans plusieurs contextes. Nous faisons référence à l'article d'Alazard, Burq et Zuily [ABZ11] pour le caractère bien-posée de ces équations pour des solutions locales en temps. Dans les travaux d'Iguchi [Igu11] et Melinand [Mel15] des régimes asymptotiques en faible profondeur ont été établis et justifiés.

3 La mécanique du solide

La mécanique du solide étudie le comportement des matériaux solides, plus précisément la description de leur mouvement et leurs déformations quand l'objet est soumis à des acteurs extérieurs ou intérieurs tels que l'action d'une force, le changement de la température, les réactions chimiques, etc. Tout comme dans le cas de l'hydrodynamique, nous faisons l'hypothèse de continuum que le solide est décrit de manière continue par des paramètres et variables. En revanche, nous allons vite nous apercevoir que son mouvement est beaucoup plus restreint que le flot d'un liquide.

Dans cette étude, nous considérons des solides qui sont rigides et non-déformables, ce qui nous permet de négliger des effets de tension de toute sorte dans le système physique. Sous ces hypothèses le mouvement du solide est essentiellement décrit par le vecteur de déplacement du centre de masse et sa rotation par rapport à un point de référence (l'origine du système) en 2 dimensions ou par rapport à des axes de rotations en plus grandes dimensions.

3.1 La deuxième loi de Newton

A la suite des hypothèses précédentes, nous décrivons le solide comme un objet physique macroscopique individuel, dont le mouvement est soumis aux lois de la mécanique classique. Il s'agit de trois (ou quatre, selon la littérature) principes physiques fondamentaux, établis par Newton en 1687.

1. Le *principe d'inertie* énonce que tout corps en repos ou en mouvement uniforme en ligne droit persévère dans cet état, à moins qu'une force externe ne s'exerce sur lui en le changeant d'état. La conséquence principale de ce principe est qu'à l'origine de tout type de changement de vitesse se trouve toujours une force qui agit vers l'extérieur.
2. Le *principe fondamental de la dynamique de translation* (la deuxième loi de Newton) a déjà été introduit dans le contexte de la dynamique des fluides. Il énonce que le taux de changement de la quantité de mouvement est proportionnel à la force résultante. Sous l'hypothèse que la masse du solide soit constante, cela implique que la force résultante peut être calculée comme le produit de la masse et de l'accélération de l'objet.
3. Le *principe d'action-réaction* établit que les actions de deux corps l'un sur l'autre sont toujours égales et de directions opposées. Ce principe est essentiellement derrière tout les effets liés au couplage dans nos systèmes de fluide-solide.
4. On fait souvent référence à une *quatrième loi de Newton*. Certains auteurs l'utilisent pour indiquer la loi universelle de la gravitation, même si celle-ci n'est pas censée être une véritable loi. Nous faisons plutôt référence au principe de superposition [Gre04], qui indique que le système des forces est un système linéaire, les forces

agissant comme des vecteurs d'un point de vue mathématique. Cette « loi » est plutôt une conséquence de la formulation moderne de la mécanique classique.

Grâce à ces principes fondamentaux, nous pouvons décrire le mouvement d'un solide par l'équation suivante

$$m\mathbf{a}_{solide}(t) = \mathbf{F}_{res} = \sum \mathbf{F}_i, \tag{3.1}$$

où m désigne la masse de l'objet (supposée constante), $\mathbf{a}_{solide}$ l'accélération et $\mathbf{F}_i$ les forces (internes ou externes) exercées sur l'objet. Notons que l'accélération n'est rien d'autre que la deuxième dérivée temporelle du déplacement du solide, qui implique que l'équation (3.1) est réellement une équation différentielle ordinaire du second ordre.

3.2 Des forces extérieures

Dans ces travaux, les effets internes dus à la structure moléculaire, aux réactions chimiques, au changement de la température sont supposés négligeables. Dans ce qui suit, nous détaillons des forces extérieures qui sont relatives aux études mathématiques de cette thèse. L'objectif est de préciser le mieux possible les termes à droite dans l'équation (3.1).

Les forces à longue portée, comme l'effet de la gravité $\mathbf{F}_{grav} = m\mathbf{g}$, ne nécessitent pas beaucoup de discussion. Représentant des actions constantes et uniformes sur l'ensemble du solide, elles peuvent être facilement représentées par des simples forces agissantes sur le centre de la masse. En revanche, les forces à courte portée intègrent des phénomènes physiques bien plus complexes. Nous en préciserons trois en particulier, qui réunissent les trois acteurs principaux de la mécanique du mouvement de l'objet.

3.2.1 Les effets hydrodynamiques

Quand on parle de l'interaction fluide-structure, les premières idées qui viennent à l'esprit sont les effets hydrodynamiques. Ces actions se manifestent quand un solide se retrouve immergé (au moins partiellement) dans un milieu fluide. Elles sont déterminées par la pression hydrodynamique exercée sur la surface mouillée du solide, qui est la partie du bord du solide en contact direct avec le fluide.

Comme elles représentent des effets moyennés, on les calcule au moyen d'une intégration le long de la surface mouillée de la pression $P(t, x)$. Notons $\mathcal{S}_t \subset \Omega$ l'espace occupé par le solide à l'instant t, et Σ_t la surface de contact. Alors, les forces (linéaires) hydrodynamiques s'expriment

$$\mathbf{F}_{hydro} = \int_{\Sigma_t} P\mathbf{n}_{solide}\, d\Sigma,$$

où $\mathbf{n}_{solide}$ est la normale unitaire sortante de $\partial\mathcal{S}_t$. Ce terme mathématique introduit le couplage dans les équations décrivant le mouvement de l'objet.

3.2.2 Des effets gyroscopiques

Dans la partie précédente nous avons détaillé les effets qui proviennent du changement de la quantité du mouvement linéaire. Ces effets concernaient essentiellement le mouvement linéaire du centre de masse. En regroupant les forces externes comme des acteurs agissant sur ce centre, nous avons réussi à caractériser le mouvement de manière simple. En revanche, certains effets physiques nécessitent la prise en compte des grandeurs physiques de l'objet, étant donné qu'il n'est pas ponctuel.

Le flot du fluide autour de l'objet immergé, ou du moins autour de la surface mouillée Σ_t, peut également engendrer des actions tangentielles. Le résultat de ces actions est le moment de la force hydrodynamique, mais il peut également s'agir de phénomènes plus complexes comme les traînées. Ce moment de force perturbe l'équilibre angulaire de l'objet, ce que nous pouvons également formuler grâce à la deuxième loi de Newton.

Le moment cinétique (ou moment angulaire) est l'équivalent du moment linéaire quand on considère les rotations. Si nous fixons l'origine comme point de référence, le moment cinétique d'une particule au point x est donné par le produit du moment d'inertie $\mathcal{I}$ (qui est analogue à la masse) et la vitesse angulaire ($\mathbf{v}_{ang}(x)$). A cause du fait qu'il dépende de la distance entre x et l'origine, le moment angulaire se réécrit de la manière suivante

$$\mathbf{r} \times \mathbf{v}_{solide},$$

où $\mathbf{r}$ est le vecteur de déplacement du point. Donc le moment d'une force $\mathbf{F}$ est de la forme

$$\mathbf{r} \times \mathbf{F}.$$

Pour toutes ces raisons, nous pouvons formuler le changement du moment cinétique dû aux effets hydrodynamiques le long de Σ_t :

$$\mathbf{F}_{giration} = \int_{\partial \mathcal{S}_t} (x - x_0(t)) \times P\mathbf{n}_{solide}\, d\Sigma,$$

où x_0 représente le centre de masse de l'objet.

La nature du moment cinétique dépend de la dimension physique : en 2 dimensions il est un scalaire ; en revanche, en 3 dimensions c'est un vecteur. Dans notre modèle océanographique basé sur l'équation des vagues, on a négligé les effets giratoires. Ils serviront pour la dérivation du model simplifié du chapitre 1, qui est faite dans la Partie 1.2.

3.2.3 La friction sèche

Le frottement sec se produit quand deux solides sont en contact direct l'un contre l'autre ; il correspond à l'opposition au mouvement relatif de ces objets. C'est une force non-conservatrice, qui représente un effet dissipatif dans le système parce que, physique-

ment, pendant le mouvement, il y a toujours une perte d'énergie sous forme de chaleur, qui n'est pas présente dans les équations. On explique cela par le fait que la friction n'est pas une force fondamentale, dans ce sens qu'elle n'est pas due à une interaction élémentaire, mais qu'elle résulte de l'adhérence le long des surfaces de contact, de la rugosité et de la déformation de ces surfaces. Cela implique que sa caractérisation est un problème physique de taille. Tout un domaine de la science (la tribologie) est dédié à l'étude de ce sujet.

Nous décrivons la friction sèche par les trois lois empiriques du contact entre solides ([Ber06]) :

1. Pour chaque point de contact x, l'action de contact exercé par un des solides sur l'autre est une force dont la ligne d'action passe par x. Notamment, la force de contact exercée par l'un des solides sur l'autre est décomposée en deux forces : une force de résultante normale ($\mathbf{F}_{normal}$) et une force de résultante tangentielle. Cette force tangentielle représente la résistance au glissement, elle est également appelée la force de frottement ($\mathbf{F}_{fric}$) et elle est entièrement contenue dans le plan tangent du contact.
2. La force de contact normale s'oppose à la pénétration d'un solide dans l'autre. Elle est de même direction que la normale entrante unitaire.
3. Généralement connue comme la loi de Coulomb dans la littérature, cette troisième loi établit qu'il existe un coefficient c_{fric} positif appelé coefficient de friction, dépendant des matériaux dont sont constitués les solides et de l'état des surfaces en contact, mais indépendant des mouvements ou de l'équilibre des solides, tel que à chaque instant
$$|\mathbf{F}_{fric}| \leqslant c_{fric}|\mathbf{F}_{normal}|.$$
Plus précisément, si l'un des solides glisse sur l'autre, donc si sa vitesse de glissement relative n'est pas nulle, alors d'une part c'est l'égalité qui est vérifiée, d'autre part $\mathbf{F}_{fric}$ est colinéaire avec la vitesse de glissement et de signe opposé. En revanche, si le solide ne glisse pas sur l'autre, donc si sa vitesse de glissement est nulle, alors c'est l'inégalité stricte qui est vérifiée.

Les lois de frottement ne sont applicables que dans le cas du frottement sec, donc nous ne pouvons pas prendre en compte les effets lubrifiants. Cela implique que dans les modèles considérés, le liquide ne passe pas entre les deux solides en contact.

De manière générale on tient compte de la dépendance du coefficient de frottement vis à vis de la vitesse. Un coefficient est désigné pour l'état de repos (friction statique) et un autre, généralement plus petit, pour l'état de glissement (friction dynamique). La considération mathématique de la friction statique fait intervenir une condition de saut dans le cas où la vitesse relative du solide s'annule. L'analyse précise de ce point reste un problème ouvert.

4 Interaction fluide-structure

Les problèmes d'interaction fluide-structure font partie des problèmes multi-physiques les plus étudiés et les plus complexes (au niveau des aspects de modélisation et de calcul). Le couplage de ces deux milieux physiquement assez différents engendre les adaptations nécessaires des systèmes présentés précédemment. Nous en détaillerons ici trois en particulier, qui sont des acteurs majeurs dans les systèmes étudiés dans cette thèse.

1. **Un domaine de fluide modifié :** La présence de l'objet $\mathcal{S}_t$ dans le domaine de fluide représente un obstacle pour le flot qui se manifeste dans le fait que le domaine du fluide est désormais donné par $\Omega_t = \Omega \backslash \mathcal{S}_t$. Dans le cadre du problème des vagues, nous avons déjà fait implicitement cette hypothèse dans le sens où l'Ω_t a été défini pour un fond $b(t, x)$ évoluant en temps, sans avoir explicitement précisé cette dépendance. Quand on laisse une partie du fond évoluer librement, la forme exacte de b va dépendre de ce mouvement, en faisant intervenir également un terme de couplage dans les équations.

   Même pour la formulation du problème dans le cas où nous considérons un domaine Ω fixe, introduire un solide $\mathcal{S}_t$ dans ce système implique une véritable dépendance en temps du domaine réel du fluide $\Omega_t = \Omega \backslash \mathcal{S}_t$. Cela implique notamment que nous devons ajouter des conditions à ces nouvelles limites (sur Σ_t). Encore une fois, une condition cinématique est intégrée dans le système, ce qui signifie que

   $$\mathbf{U} \cdot \mathbf{n}_{solide} = \mathbf{v}_{solide} \cdot \mathbf{n}_{solide} \quad \text{sur } \partial\mathcal{S}_t,$$

   que la direction normale du champ de vitesse est donnée par la direction normale de la vitesse du solide et que les particules du fluide ne peuvent pas pénétrer la surface du solide.
2. **Les effets sur le moment linéaire du solide :** Comme nous l'avons détaillé dans la partie précédente, le couplage dans les équations du mouvement du solide se manifeste à travers des forces hydrodynamiques. En particulier, la composante normale de la pression exerce une action sur la surface mouillée qui pousse le solide selon le flot du fluide.
3. **Les effets sur le moment angulaire du solide :** Les effets giratoires de la pression due au fluide à l'extérieur du solide ne doivent pas être négligés non plus. Nous pouvons les prendre en compte en établissant le bilan du changement du moment cinétique, par la deuxième loi de Newton également.

   En outre, dans le cas d'un solide complètement immergé, le flot du fluide peut circuler autour du solide, ce qui influence le moment linéaire et angulaire. Ce dernier effet peut être mesuré notamment par la contribution totale de la vitesse tangentielle du flot autour de l'objet :

   $$\gamma = \int_{\partial\mathcal{S}_t} \mathbf{U} \cdot \tau \, d\Sigma,$$

   avec $\tau^{\perp} = \mathbf{n}_{solide}$. Pour plus de détails, nous faisons référence à la Définition 1.2.3.

Au final, nous remarquons l'aspect numérique des problèmes de l'interaction fluide-structure. De nos jours, les logiciels dédiés à la mécanique des fluides numérique ou la mécanique des structures numérique sont aussi équipés par des solveurs spécialisés dans certains types d'interaction fluide-structure ([BS06]). L'approche générale pour traiter ce genre de problèmes d'un point de vue numérique est la suivante : on dédie des solveurs spécifiques pour calculer le flot du fluide et l'évolution de la structure, puis des schémas numériques du couplage sont appliqués pour mettre à jour les données communes de ces deux systèmes (pression du fluide, position de l'objet, etc.) (voir par exemple [Pes05],[LB10]). Mais cette façon de traiter les deux problèmes de manière semi-découplée pose des questions manifestes, en particulier par rapport à la conservation (numérique) de la masse, de la quantité du moment et de l'énergie totale.

Pour celle-ci et pour bien d'autres raisons, les problèmes numériques de l'interaction fluide-structure font partie d'une direction de recherches numériques majeure. La modélisation de manière efficace et optimale d'un tel couplage, ou l'uniformisation de certains schémas discrets pour prendre en compte à la fois le flot et la géométrie de la structure ([CM06], [CMM08], ou [Dor17] et ses références par exemple) restent encore des défis considérables.

5 Les modèles asymptotiques

Dans l'étude des problèmes venant de la physique ou d'autres domaines scientifiques, on rencontre souvent des problèmes de nature asymptotique, comme par exemple l'amortissement, la perturbation, la stabilisation, etc. Pour résoudre ce genre de problèmes, on est amené à utiliser certaines techniques de l'analyse asymptotique et de la théorie des perturbations. L'aspect théorique de ces domaines des mathématiques est désormais bien établi, contrairement à ce qu'on pouvait constater il y a quelques décennies.

En 1963, Kruskal [Kru64] a défini l'asymptotologie comme « l'art de traiter des systèmes de mathématiques appliquées dans les cas limites ». L'idée générale n'a toujours pas changé depuis lors, on souhaite toujours extraire des informations au moyen d'une approximation bien établie de la solution exacte du problème. Afin d'obtenir une telle approximation, on intègre des paramètres dans le système, dont certains apparaissent naturellement et dont d'autres sont introduits de manière artificielle. Grâce à la variation de ces paramètres on est capable de simplifier les équations, se sorte qu'on réduit la complexité du problème. L'outil mathématique principal est un développement limité autour d'un état prétendument stable, à travers certaines fonctions de ces paramètres de petitesse.

En général ([CK96]), on fait la différence entre deux types de problème qualitativement différents. Dans cette partie, nous détaillons ces deux types, puisqu'ils sont impliqués chacun dans les travaux de cette thèse.

5.1 Perturbations régulières

Dans les problèmes du type de la perturbation régulière, on peut faire un développement limité à l'ordre quelconque qui fournit une approximation de la forme d'une série par rapport au paramètre de petitesse. Les termes de cette série sont définis par des équations (différentielles) et des conditions aux bords déduites du système original au niveau de l'ordre de grandeur souhaité du paramètre. Ce système est résolu par récurrence, les solutions ont des bornes uniformes, valables sur le domaine du problème tout entier. L'exactitude de l'approximation s'améliore si l'on fait tendre le paramètre de petitesse vers 0.

Pour illustrer un problème typique qui appartient à cette catégorie, nous présentons les régimes asymptotiques en faible profondeur du problème des vagues. Cet exemple est loin d'être le plus simple, mais il est très pertinent par rapport aux études de la deuxième partie de cette thèse. A la base de ces modèles asymptotiques se trouve un développement limité de la vitesse horizontale verticalement moyennée autour du gradient du potentiel à la surface libre par rapport au paramètre de faible profondeur.

Afin d'introduire ces reformulations, nous allons tout d'abord définir les tailles caractéristiques associées au problème des vagues.

- H_0, la profondeur de base,
- L, la taille horizontale d'une vague typique,
- a_{surf}, l'amplitude d'une vague typique,
- a_{bott}, la taille verticale du solide au fond.

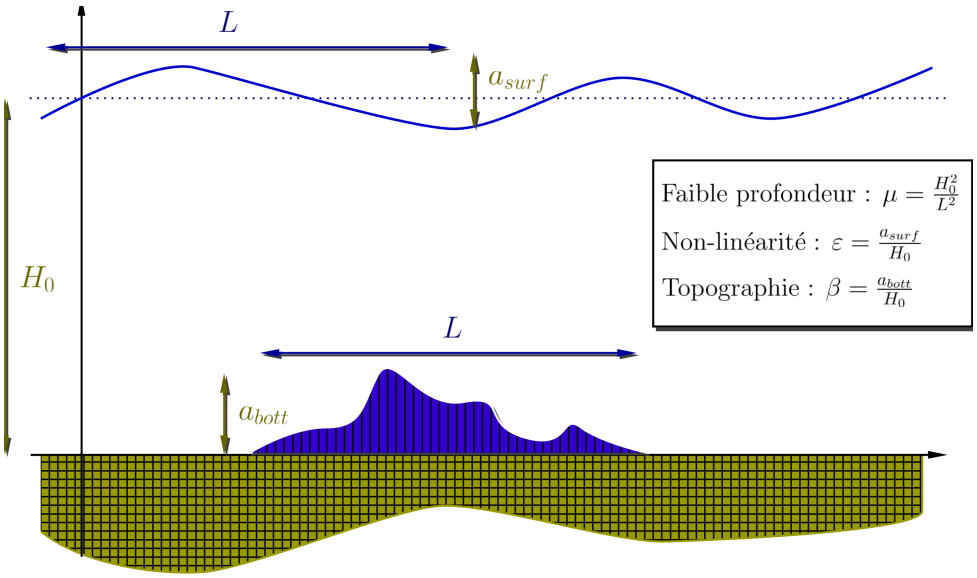

FIGURE 2 – Les ordres de grandeur typique pour le problème des vagues

Les paramètres de petitesse qui apparaissent dans l'adimensionnalisation sont les suivants :

- paramètre de faible profondeur $\mu = \frac{H_0^2}{L^2}$,
- paramètre de l'amplitude (de non-linéarité) $\varepsilon = \frac{a_{surf}}{H_0}$,
- paramètre de la topographie du fond $\beta = \frac{a_{bott}}{H_0}$.

Avec ces paramètres, nous pouvons adimensionner les équations (2.11). Tout d'abord, le problème de Laplace sur le domaine Ω_t, désormais sans dimensions s'écrit

$$\begin{cases} \Delta^\mu \Phi := \mu \Delta_x \Phi + \partial_z^2 \Phi = 0, & \text{dans } -1 + \beta b \leqslant z \leqslant \varepsilon\zeta, \\ \Phi|_{z=\varepsilon\zeta} = \psi, \quad \sqrt{1+\beta^2|\nabla_x b|^2}\partial_{\mathbf{n}}\Phi_{mb}|_{z=-H_0+b} = \partial_t b. \end{cases} \tag{5.1}$$

Comme dans la Partie 2.2, nous pouvons décomposer le potentiel de la vitesse $\Phi = \Phi_{fb} + \Phi_{mb}$ afin de définir les opérateurs de type Dirichlet–Neumann et Neumann–Neumann associés à leurs problèmes de Laplace respectifs :

$$\begin{aligned} G_\mu^{DN}[\varepsilon\zeta, \beta b]\psi &= \sqrt{1+\varepsilon^2|\nabla_x\zeta|^2}\partial_{\mathbf{n}}\Phi_{fb}|_{z=\varepsilon\zeta}, \\ G_\mu^{NN}[\varepsilon\zeta, \beta b]\partial_t b &= \sqrt{1+\varepsilon^2|\nabla_x\zeta|^2}\partial_{\mathbf{n}}\Phi_{mb}|_{z=\varepsilon\zeta}. \end{aligned}$$

Le problème des vagues sans dimension prend alors la forme suivante :

$$\begin{cases} \partial_t\zeta - \frac{1}{\mu}G_\mu^{DN}[\varepsilon\zeta, \beta b]\psi = \dfrac{\beta}{\varepsilon}G_\mu^{NN}[\varepsilon\zeta, \beta b]\partial_t b, \\ \partial_t\psi + \zeta + \dfrac{\varepsilon}{2}|\nabla_x\psi|^2 - \varepsilon\mu\dfrac{(\frac{1}{\mu}G_\mu^{DN}[\varepsilon\zeta, \beta b]\psi + \frac{\beta}{\varepsilon}G_\mu^{NN}[\varepsilon\zeta, \beta b]\partial_t b + \nabla_x(\varepsilon\zeta)\cdot\nabla_x\psi)^2}{2(1+\varepsilon^2\mu|\nabla_x\zeta|^2)} = 0. \end{cases}$$

Par l'équation (5.1), nous définissons la vitesse horizontale verticalement moyennée

$$\overline{V} = \overline{V}_\mu[\varepsilon\zeta, \beta b]\psi = \frac{1}{h}\int_{-1+\beta b}^{\varepsilon\zeta} \nabla_x\Phi(\cdot, z)\, dz, \tag{5.2}$$

où $h = 1 + \varepsilon\zeta - \beta b$. Avec cette notation, on peut établir d'abord que ([Lan13])

Proposition 5.1. *Soient $s > d/2 + 1$, $\zeta, b \in H^s(\mathbb{R}^d)$ telles que*

$$\exists h_{min} > 0,\ \forall X \in \mathbb{R}^d,\ 1 + \varepsilon\zeta(X) - \beta b(X) \geqslant h_{min}. \tag{5.3}$$

Soient $\psi \in \dot{H}^{3/2}(\mathbb{R}^d) = \{f \in L^2_{loc}(\mathbb{R}^d),\ \nabla f \in H^{1/2}(\mathbb{R}^d)^d\}$ et $\Phi \in \dot{H}^2(\mathbb{R}^d) = \{f \in L^2_{loc}(\mathbb{R}^d),\ \nabla f \in H^1(\mathbb{R}^d)^d\}$ la solution du problème de Laplace (5.1). Alors on a

$$\sqrt{1+\varepsilon^2|\nabla_x\zeta|^2}\partial_{\mathbf{n}}\Phi|_{z=\varepsilon\zeta} = \mu\frac{\beta}{\varepsilon}\partial_t b - \mu\nabla\cdot(h\overline{V}). \tag{5.4}$$

Cette proposition implique que nous pouvons réécrire les opérateurs de type Dirichlet–Neumann et Neumann–Neumann en utilisant $\overline{V}$.

La proposition qui établit le développement asymptotique de cette variable par rapport à μ est ([Lan13]) :

Proposition 5.2. *Soient $t_0 > \frac{d}{2}$, $s \geq 0$, $n \in \mathbb{N}$, et $\zeta, b \in H^{s+2+2n}(\mathbb{R}^d) \cap H^{t_0+2}(\mathbb{R}^d)$ telles qu'elles satisfont la condition de profondeur minimale précédente (5.3). Soit $\psi \in \dot{H}^{s+3+2n}(\mathbb{R}^d)$. Il existe une suite $(\overline{V}_j)_{0\leq j\leq n}$ telle que $\|\overline{V}_j\|_{H^s} \leq M(s+2j)\|\nabla_x\psi\|_{H^{s+2j}}$ $(0 \leq j \leq n)$ et*

$$\left\|\overline{V} - \sum_{j=0}^{n} \mu^j \overline{V}_j\right\|_{H^s} \leq \mu^{n+1} M(s+2+2n)\|\nabla_x\psi\|_{H^{s+2+2n}}, \tag{5.5}$$

avec une constante $M(\tilde{s})$ définie par

$$M(\tilde{s}) = C(M_0, \|\zeta\|_{H^{\tilde{s}}}, \|b\|_{H^{\tilde{s}}}), \text{ avec } M_0 = C\left(\frac{1}{h_{min}}, \mu_{max}, \|\zeta\|_{H^{t_0+1}}, \|b\|_{H^{t_0+1}}\right).$$

En particulier, on peut démontrer ([Lan13]) que

$$\overline{V} = \nabla_x\psi - \mu\mathcal{T}[h, \beta b]\nabla_x\psi - \mu\frac{\beta}{\varepsilon}\left(\frac{1}{2}h\nabla_x\partial_t b + \varepsilon\nabla_x\zeta\partial_t b\right) + \mathcal{O}(\mu^2),$$

où

$$\mathcal{T}[h, \beta b]V = -\frac{1}{3h}\nabla_x(h^3\nabla_x\cdot V) + \beta\frac{1}{2h}\left(\nabla_x(h^2\nabla_x b\cdot V) - h^2\nabla_x b\nabla_x\cdot V\right) + \beta^2\nabla_x b\nabla_x b\cdot V.$$

Sur la base de ce développement, on peut reformuler le problème des vagues pour introduire des modèles valables en faible profondeur. Pour plus de détails, de démonstrations ainsi qu'une justification robuste de ces modèles, nous renvoyons à [Lan13].

5.2 Perturbations singulières

Il y a de nombreux problèmes physiques qui ne nous ramènent pas à des problèmes de perturbation régulière. Par exemple, un développement asymptotique par rapport au paramètre de petitesse ne reste pas valable sur le domaine tout entier, ou les termes obtenus par le développement sont séculaires (ces termes deviennent non-bornés en temps long) à cause de la présence des couches limites (au bord) ou bien à l'intérieur. Dans ce cas, on dit que les problèmes sont de type perturbation singulière ou de type couche.

On peut facilement identifier les raisons générales de cette perte de la validité du développement. Un paramètre de petitesse devant le terme qui contient la dérivée à l'ordre le plus élevé engendre une perte dans l'ordre de l'équation dans la limite asymptotique. Notamment, une approximation du premier ordre fournit une équation caractéristique

d'un ordre plus bas que l'ordre du sytème originel, qui implique que certaines conditions initiales ne peuvent pas être garanties (le système est sur-déterminé). Quand le problème du domaine est non-borné, les effets cumulatifs de certains termes « asymptotiquement petits » peuvent devenir grands, lesquels font obstacle à des estimations uniformes.

Une méthode pour traiter ce genre de problèmes consiste à définir des échelles de temps supplémentaires pour le système et de faire un développement limité adapté à ces différentes échelles. Mise à part l'échelle de temps originel t, d'autres échelles de temps peuvent être associées à un problème en prenant compte de la dépendance par rapport à certains paramètres de petitesse. Cette méthode a des racines dans la méthode de Poincaré–Lindstedt ([Lin83], [Poi92]) développée originellement pour le problème des trois corps en mécanique céleste.

La première difficulté avec cette approche est de trouver les bonnes échelles de temps supplémentaires. Dans certains cas, la perte de la validité vient du fait que l'approximation ne reste pas uniformément bornée sur le domaine. Proche du bord, elle devient notamment non-bornée. La correction du développement asymptotique (externe) par un développement asymptotique supplémentaire (interne) autour du point qui représente la singularité asymptotique, afin d'en isoler la sécularité ([CK96]), peut fournir une approximation appropriée. L'échelle de temps supplémentaire requise par la méthode est donnée par ce développement supplémentaire.

Des méthodes d'homogénéisation ou une restriction à certaines classes de solutions souhaitées (par exemple des solutions périodiques) peuvent également donner une idée de la nature de l'échelle de temps supplémentaire. Ces techniques sont particulièrement utiles quand on n'est pas capable de découpler explicitement l'approximation en plusieurs séries selon les échelles de temps différentes, comme ce sera le cas au chapitre 1.

Notons que l'approche multi-échelle n'est pas la seule méthode pour traiter des problèmes de type perturbation singulière. Introduite originellement par Krylov et Bogoliubov en 1937 ([KB43]), la méthode de moyennage est devenue un outil largement utilisé pour des problèmes physiques de ce genre. Il s'agit d'une technique très générale et assez constructive, applicable à une large famille de systèmes ayant une structure Hamiltonienne (comme la plupart des problèmes physiques par exemple).

Au chapitre 1, nous sommes amenés à considérer le système simplifié suivant concernant la dynamique d'un solide infinitésimal dans un milieu liquide Ω :

$$I_\epsilon \ddot{q}(t) = F(q, \dot{q}), \tag{5.6}$$

où q est la position du solide, I_ϵ dénote l'inertie, qui est un paramètre de petitesse dans le système, et F représente les non-linéarités décrivant l'évolution dynamique du mouvement.

Ce système d'équations différentielles ordinaires du second ordre est un exemple typique d'un problème de perturbation singulière. En faisant tendre ϵ vers 0, I_ϵ disparaît, ce qui signifie qu'à la limite asymptotique le système devient d'ordre un uniquement. En outre, un détail reste moins visible, c'est la complexité du terme à droite, qui engendre

des difficultés additionnelles, la détermination d'une échelle de temps supplémentaire nécessitera donc des moyens analytiques autres que le développement externe-interne.

Introduction (English version)

Contents

Fluid-structure interaction problems are one of the most well-known examples of multi-physics problems. They involve the description of the interaction of some movable or deformable structure with an internal or surrounding fluid flow. They represent complex physical situations in which the flowing fluid exerts pressure on the object through a contact medium (for example the boundary of the solid), causing it to change its physical state (position, shape, etc.). In return the object alters the flow field by a change in the fluid domain. This coupling effect is non-stationary in the sense that there is a continuous action-reaction relation between the two physical media, maintaining an a priori non-constant exchange of momentum and energy.

The recent increase in massive computational power as well as its easy and cheap access has brought the domain of fluid-structure interactions to the fore as far as current research trends are concerned. Furthermore, new engineering trends concerning complex structures (such as off-shore structures and wave-energy converters in marine engineering) made it necessary to further our understanding of this domain. Numerical modeling, numerical simulations have become more and more involved in order to support or even replace experimental testing, especially in the case when engineering designs provide inefficient, costly or time consuming extensive experiments. The theoretical background of the domain has also enjoyed an increased interest, although it was far less affected by the skyrocketing hardware and software support.

The main objective of this thesis is to analyze two particular fluid-structure interaction problems. Our approach is based on asymptotic models that retain the most important characteristics of the full coupled problems, and neglect physical phenomena that have negligible or irrelevant cumulative effects. They have arisen as recent research interests due to new advancements in the corresponding theoretical analysis.

As far as the second half of this thesis is concerned, one can not avoid to discuss the real life applications of the models presented here. Submerged wave-energy converters have received relatively fewer attention as compared to their floating counterparts (such as off-shore wind turbines, wave converter arrays, etc.). This is not only true from a mathematical or modeling point of view but from an engineering point of view as well, despite the fact they have the advantage of being less exposed to the elements (for a more complete discussion of the advantages and drawbacks, we refer to [GIL+14]). Therefore, another objective of the current works is to highlight these features of submerged energy converters, mainly through the numerical analysis of our model in Chapter 3.

1 Outline of the thesis

This introduction presents the context of the fluid-structure interaction problems treated in this thesis. After detailing the mathematical models for the dynamics of the fluid flow as well as for the motion of the solid object we present some key aspects and particular paradigms arising from the coupling of these two systems. We will also high-

light the main methodology of asymptotic analysis implemented in the analysis to follow in later chapters.

The introduction is followed by an abbreviated introduction in French. The main part of the thesis consists of 3 independent chapters, presenting the two main problems of the manuscript. Each of these chapters starts with a French summary.

Chapter 1 presents a multiple-scale asymptotic analysis of a system of non-linear ordinary differential equations. It serves as an approximative model to describe the motion of an infinitesimal object in a bi-dimensional perfect fluid. The evolution equations of the motion are analyzed in the asymptotic regime when the solid inertia tends to 0. It is inspired by the article [Ben18a].

Chapter 2 is based on [Ben17]. It describes first of all a coupled model representing the interaction of water waves with a freely moving object on the bottom. Moreover it presents the analysis of this coupled water waves problem in two shallow water asymptotic regimes. We establish the well-posedness of the nonlinear Saint-Venant and the weakly nonlinear Boussinesq systems coupled with a Newton equation, describing the motion of the solid.

As a follow-up, Chapter 3 concerns the numerical analysis of the latter Boussinesq model. A high order accurate finite difference scheme is presented, improving on previous, staggered grid based numerical schemes, and adapted to incorporate a freely moving bottom topography. Section 3.3 of Chapter 3 shows an extended array of numerical simulations originating from [Ben18b].

After that, the main contributions of this thesis are presented as part of the Conclusion, followed by a detailed list of research perspectives. Finally, the Appendix contains some remarks on the applied methods and estimates throughout Chapters 2 and 3.

2 Fluid dynamics

Fluid dynamics in general describes the flow of fluids, that is liquids and gases as well. Concerning this thesis work, of particular interest is hydrodynamics, which concerns the study of liquids in motion. It is based on the description of the flow on a macroscopic scale, that is the so called “continuum assumption” is supposed. In reality liquids are composed of molecules that collide with each other (or the boundary of the domain for example), however by the continuum assumption we describe them as continuous media instead of discrete ones. Consequently, system properties and variables such as density, pressure, or flow velocity are well-defined at infinitesimal volume elements of the fluid domain, they are described by functions defined on the domain, corresponding to the infinitesimally averaged real physical quantities.

Hence, fluid movement can be described by differential equations capturing the “continuous evolution” of these variables. They arise as a mathematical implementation of

general conservation laws, in particular the conservation of mass and the conservation of (linear) momentum. In what follows we describe these equations under the hypothesis of a perfect fluid, and we present the fluid-dynamical setting of the two main problems.

2.1 The Euler equations

Now we provide a brief and formal derivation of the (incompressible) Euler equations, that serve as the basic equations describing the motion of the fluid flow throughout this work. It is to complement the modeling aspects of Chapter 2 as well.

For the sake of simplicity, for now the fluid domain is supposed to be the whole space $\mathbb{R}^d$ (with $d \in \mathbb{N}$ and $d = 2$, $d = 3$ being the relevant physical dimensions), thus boundary effects are neglected. In the Eulerian description, one can associate with every material point x in $\mathbb{R}^d$ at time $t \in \mathbb{R}_+$ the following physical quantities:

- the velocity field $\mathbf{U} = \mathbf{U}(t, x) \in \mathbb{R}^d$,
- the density $\varrho = \varrho(t, x) \in \mathbb{R}_+$,
- the pressure $P = P(t, x) \in \mathbb{R}$.

There are various other physical quantities as well, for example the internal energy ($e(t, x) \in \mathbb{R}$), the entropy ($s(t, x) \in \mathbb{R}$) or the temperature ($T(t, x) \in \mathbb{R}^+$), we only named the relevant ones for the derivation of the equations.

The equations governing the motion of the fluid arise from the fundamental conservation laws of mechanics (and in general from thermodynamics as well). Let us introduce the notion of the flow of the velocity field $\mathbf{U}$; the mathematical interpretation of the conservation laws is based on the fact that certain physical quantities are conserved along the particle trajectories.

Definition 2.1. *The flow ψ of $\mathbf{U} \in \mathcal{C}^0(\mathbb{R}_+; \mathrm{Lip}(\mathbb{R}^d))$ is the $\mathcal{C}^1(\mathbb{R}_+; \mathcal{C}^0(\mathbb{R}^d))$ solution of the following ordinary differential equation*

$$\frac{d}{dt}\psi(t, x) = \mathbf{U}(t, \psi(t, x)), \quad \psi(0, x) = x$$

(the point $x \in \mathbb{R}^d$ being treated as a parameter here).

For a domain $\omega \subset \mathbb{R}^d$ let us denote $\omega_t = \psi_t(\omega)$, where $\psi_t(x) = \psi(t, x)$. The lemma below serves to rewrite the conservation laws in a more appropriate fashion.

Lemma 2.1. *Let ω be an open, bounded, connected, smooth subdomain of $\mathbb{R}^d$, ψ be the flow of $\mathbf{U} \in \mathcal{C}^1(\mathbb{R}^+ \times \mathbb{R}^d)$ with $\omega_t = \psi_t(\omega)$. Let $b \in \mathcal{C}^1(\mathbb{R}^+ \times \mathbb{R}^d; \mathbb{R})$ be a scalar function.*

Then we have

$$\frac{d}{dt}\int_{\omega_t} b(t,x)\,dx = \int_{\omega_t}\Big(\partial_t b(t,x) + \nabla\cdot(b(t,x)\mathbf{U}(t,x))\Big)\,dx$$
$$= \int_{\omega_t}\partial_t b(t,x)\,dx + \int_{\partial\omega_t}\Big(b(t,x)\mathbf{U}(t,x)\cdot\mathbf{n}\Big)\,d\Sigma.$$

Here $\mathbf{n}$ *denotes the unit outer normal vector at the boundary of* Ω_t*, pointing outwards, and* Σ *is the surface measure defined on* $\partial\omega_t$*.*

We consider an arbitrary ω open subdomain of $\mathbb{R}^d$ for the description of the conservation laws.

Mass conservation: we are working with a closed fluid system, that is there is no production or loss of mass inside any part of the fluid during the time evolution of the motion. The mass of the fluid in ω at time t can be expressed by

$$M_\omega(t) = \int_\omega \varrho(t,x)\,dx.$$

Since the mass is conserved, we may deduce that

$$\frac{d}{dt}M_{\omega_t}(t) = \frac{d}{dt}\int_{\omega_t}\varrho(t,x) = 0.$$

That is, by Lemma 2.1 we obtain the equation for the **mass budget**:

$$\partial_t\varrho + \nabla\cdot(\varrho\mathbf{U}) = 0. \tag{2.1}$$

Momentum conservation: Newton's second law states that all the forces acting on the part of the fluid in ω are to be equal to the force arising from the change of momentum. We will discuss this law in detail later in Section 3. The momentum can be written in the following integral form

$$\mathbf{P}_\omega(t) = \int_\omega(\varrho\mathbf{u})(t,x)\,dx.$$

The change of the momentum equals the sum of all the forces acting on the body, that is the long range forces $\mathbf{F}_{ext}$ (gravity for example) and the surface forces at the boundary of the domain. This second force can be represented by the second order stress tensor σ, specified by further physical assumptions. So we obtain

$$\frac{d}{dt}\mathbf{P}_{\omega_t}(t) = \frac{d}{dt}\int_{\omega_t}(\varrho\mathbf{v})(t,x)\,dx = \int_{\omega_t}(\varrho\mathbf{F}_{ext})(t,x)\,dx + \int_{\partial\omega_t}(\sigma\cdot\mathbf{n})(t,x)\,d\Sigma,$$

and by the lemma we have the equation for the **momentum balance**:

$$\partial_t(\varrho\mathbf{U}) + \nabla\cdot(\varrho\mathbf{U}\otimes\mathbf{U}) = \varrho\mathbf{F}_{ext} + \nabla\cdot\sigma. \tag{2.2}$$

In a general setting, one writes in a similar fashion the conservation of internal energy (as a consequence of the first law of thermodynamics), as well as the entropy balance (dictated by the second law of thermodynamics).

In order to obtain the Euler equations, one makes the additional hypothesis of the fluid being a perfect fluid, which means first of all that it is isotropic, the physical quantities depend only on (t, x). Furthermore we make the additional hypotheses that the fluid has no shear stress, no viscosity, and no heat conduction. This in particular means that $\sigma = -P\,\mathrm{Id}$.

So the mass and momentum equations take the following form:

$$\begin{cases} \partial_t \varrho + \nabla \cdot (\varrho \mathbf{U}) = 0, \\ \partial_t (\varrho \mathbf{U}) + \nabla \cdot (\varrho \mathbf{U} \otimes \mathbf{U}) = -\nabla P + \varrho \mathbf{F}_{ext}. \end{cases} \tag{2.3}$$

By assuming that the fluid is homogeneous ($\varrho \equiv cst$), the system simplifies to the well-known incompressible Euler equations:

$$\begin{cases} \nabla \cdot \mathbf{U} = 0, \\ \partial_t \mathbf{U} + (\mathbf{U} \cdot \nabla)\mathbf{U} = -\frac{1}{\varrho}\nabla P + \mathbf{F}_{ext}. \end{cases} \tag{2.4}$$

A well-known result concerning the existence of a (local-in-time) solution to the Euler equation in the whole space is the following:

Theorem 2.1. *Given an initial condition $\mathbf{U}_0 \in H^s(\mathbb{R}^d)$, with $s > d/2+1$ and $\nabla \cdot \mathbf{U}_0 = 0$, and $\mathbf{F}_{ext} \in \mathcal{C}([0, T_0]; H^s(\mathbb{R}^d))$ such that $\nabla \cdot \mathbf{F}_{ext} = 0$ for every $t \in [0, T_0]$ with $T_0 > 0$. Then there exists a time $T > 0$ with an upper bound*

$$T \leqslant \max\left(\frac{1}{c_s \|\mathbf{U}_0\|_{H^s}}, T_0\right),$$

with c_s constant depending only on s and d, such that there exists a unique (classical) solution $\mathbf{U}$ of equations (2.4) in $\mathcal{C}([0, T]; \mathcal{C}^1(\mathbb{R}^d)) \cap \mathcal{C}^1([0, T]; \mathcal{C}(\mathbb{R})^d)$.

For the proof, and for more details on the general theory, one could refer for instance to [MB03].

2.1.1 Equations on a bounded domain

Previously we introduced the Euler equations for the whole space domain $\mathbb{R}^d$. Here, we will specify the context of the equations for a bounded domain. Let us suppose that Ω is an open, bounded, connected, and simply connected subset of $\mathbb{R}^d$.

The motion of a incompressible perfect fluid confined to the fixed domain Ω is still

described by the system (2.4). However, to close the problem, we have to impose conditions on the boundary $\partial\Omega$. We are considering a fixed, non-deformable fluid domain Ω whose stationary boundaries are supposed to be impermeable. This impermeability, or more commonly known as "no-penetration" condition, is expressed mathematically by the simple fact that the normal component of the fluid velocity (at the boundary) is 0.

So by denoting $\mathbf{n}$ the outward unit normal vector of the boundary, $\partial\Omega$, the boundary condition

$$\mathbf{U} \cdot \mathbf{n} = 0 \quad \text{on } \partial\Omega \tag{2.5}$$

completes the Euler equations on a bounded domain. For the corresponding well-posedness theory, we have for instance that ([KL84])

Theorem 2.2. *Let us consider $\Omega \subset \mathbb{R}^d$ an open bounded domain with smooth boundary $\partial\Omega$. Let $s > d/2 + 1$, an initial condition $\mathbf{U}_0 \in H^s(\Omega; \mathbb{R}^d)$, with $\nabla \cdot \mathbf{U}_0 = 0$, and $\mathbf{F}_{ext} \in \mathcal{C}([0, T_0]; H^s(\Omega; \mathbb{R}^d))$ such that $\nabla \cdot \mathbf{F}_{ext} = 0$ for every $t \in [0, T_0]$ with $T_0 > 0$. Then there exists a time $T > 0$, $T \leqslant T_0$, such that there exists a unique solution $\mathbf{U}$ in $\mathcal{C}([0, T]; H^s(\Omega; \mathbb{R}^d))$ of equations (2.4) in Ω.*

For now we have made no further assumptions on the vorticity of the fluid. In this work we will work with irrotational flows, verifying the additional hypothesis of

$$\nabla \times \mathbf{U} = 0 \quad \text{in } \Omega.$$

Nevertheless let us make a simple remark on the general rotational flow in a fixed domain Ω.

Remark 2.1. *By defining $\vec{\omega}(t, x) := \nabla \times \mathbf{U}(t, x)$ and by applying the* curl *operator on equation (2.4) we obtain the evolution of the vorticity, that is*

$$\partial_t \vec{\omega} + (\mathbf{U} \cdot \nabla)\, \vec{\omega} = (\vec{\omega} \cdot \nabla)\, \mathbf{U} + \nabla \times \mathbf{F}_{ext} \quad \text{in } \Omega. \tag{2.6}$$

According to Helmholtz's third theorem, in the absence of any rotational external force ($\nabla \times \mathbf{F}_{ext} \equiv 0$) the L^p norm of the vorticity is preserved by the flow (for $p > 1$). This implies that for an initially irrotational flow, it will stay irrotational, and that a control on the vorticity at time $t = 0$ assures an overall control of the vorticity at any given time.

2.1.2 Free surface Euler equations

In order to formulate the free surface equations, first of all we have to precise the domain of the fluid, given by an infinite horizontal layer. We denote by $\zeta(t, x)$ the free surface elevation function and $b(t, x)$ describes the bottom topography variation at a base depth of H_0. With this notation the fluid domain is given by

$$\Omega_t = \left\{(x, z) \in \mathbb{R}^d \times \mathbb{R} \,:\, -H_0 + b(t, x) < z < \zeta(t, x)\right\},$$

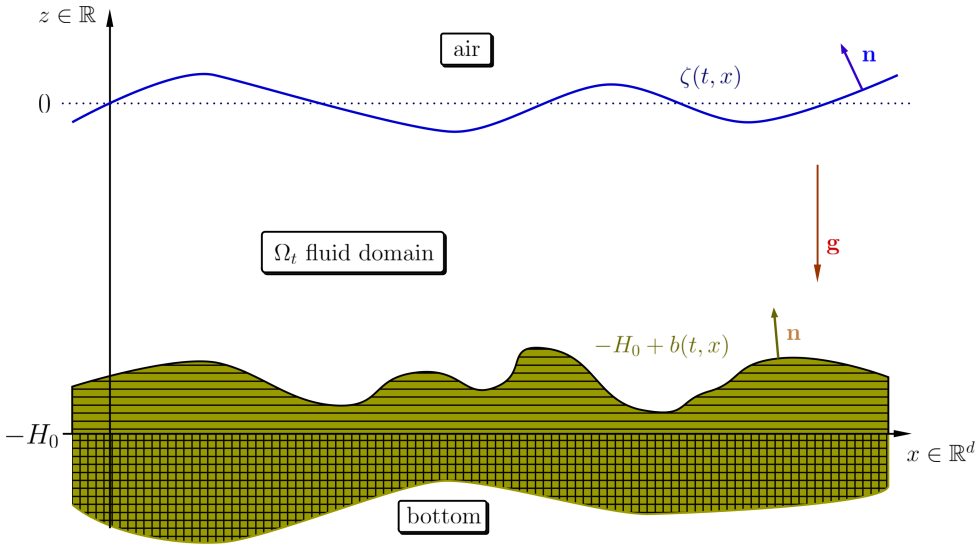

Figure 3 – The water waves setting for a moving bottom

In order to avoid special physical cases arising from the fluid domain Ω_t (such as islands or beaches, that are seen as vanishing shorelines), one usually makes use of the assumption that the water depth is uniformly bounded from below by a positive constant. Naturally, this is a considerable restriction, however a necessary one from an analytical point of view, see for example [dP16], [LM17] for an alleviation of this hypothesis.

In the water waves setting, we consider a fluid moving under the influence of gravity on the domain Ω_t. Denoting by $\mathbf{U}$ the velocity field and by P the fluid pressure, the homogeneous, incompressible, irrotational Euler equations take the following form:

$$\begin{cases} \partial_t \mathbf{U} + \mathbf{U} \cdot \nabla \mathbf{U} = -\dfrac{\nabla P}{\varrho} + \mathbf{g}, \\ \nabla \cdot \mathbf{U} = 0, \\ \nabla \times \mathbf{U} = 0, \end{cases} \tag{2.7}$$

valid in the entire fluid domain Ω_t. Here, $\mathbf{g} = (0, -g)^\top$ in the equations denotes the gravitational acceleration as a downwards pointing vector.

Remark 2.2. *The irrotationality condition allows us to reduce the problem to variables and equations given on the free surface only (the Zakharov / Craig–Sulem formulation, see below). It is not a necessary assumption for the mathematical analysis of the problem, however the water waves problem with vorticity requires more delicate approaches. For instance, a Lagrangian formulation ([Lin05]) does not require the irrotationality assumption. The approach to reduce the dimension has nevertheless been generalized in order to incorporate vorticity for the $d = 1$ case ([CL15], [Mé17]).*

The boundary conditions can be summarized as follows:

- the kinematic (or no-penetration) boundary conditions (that is, the fluid particles do not cross neither the bottom nor the free surface);
- there is no surface tension along the free surface, so the pressure at the surface is given by the atmospheric pressure, and assumed to be constant.

A mathematical restatement of the aforementioned conditions is the following:

- denoting by $\mathbf{n}$ the unit normal vector of the fluid domain pointing upward, we have the following reformulation for the no-penetration condition for the bottom

$$\partial_t b - \sqrt{1+|\nabla_x b|^2}\mathbf{U}\cdot\mathbf{n} = 0 \quad \text{on } \{z = -H_0 + b(t,x)\}, \tag{2.8}$$

  and for the free surface

$$\partial_t \zeta - \sqrt{1+|\nabla_x \zeta|^2}\mathbf{U}\cdot\mathbf{n} = 0 \quad \text{on } \{z = \zeta(t,x)\}; \tag{2.9}$$

- denoting by P_{atm} the atmospheric pressure, we have that

$$P = P_{atm} \quad \text{on } \{z = \zeta(t,x)\}. \tag{2.10}$$

The system of equations (2.7), (2.8), (2.9), and (2.10) together form the free surface Euler equations for the fluid domain Ω_t.

2.2 The water waves problem

As a follow-up of Section 2.1.2, one can first of all remark that the free boundary problem presented there requires the proper analytical treatment of a time dependent boundary Ω_t which is a complex task. However one can also remark that the incompressibility and irrotationality conditions assumed in the formulation of the free surface Euler equations allow for a rather useful reformulation of the problem.

Owing to the Helmholtz-decomposition of vector fields, the velocity field $\mathbf{U}$ can be represented by a velocity potential $\Phi(t,x)$. More precisely, we have that

$$\mathbf{U} = \nabla\Phi \quad \text{in } \Omega_t,$$

where Φ verifies a Laplace-problem on the same time-dependent domain:

$$\Delta\Phi = 0 \quad \text{in } \Omega_t. \tag{2.11}$$

With this potential one can reformulate the momentum equilibria as well as the boundary conditions to obtain the free surface Bernoulli equations. For more details we refer to

Section 2.1.1 of Chapter 2. The main advantage of this reformulation becomes apparent when one wishes to study the well-posedness of the water waves problem. It is possible (see e.g. [Lan13]) to straighten the fluid domain by a well-chosen diffeomorphism to reduce the complexity of the problem.

The previous Laplace equation requires boundary conditions as well. Therefore, we are left with the following:

$$\begin{cases} \Delta\Phi = 0 \quad \text{in } \Omega_t \\ \Phi|_{z=\zeta} = \psi, \quad \sqrt{1+|\nabla_x b|^2}\partial_{\mathbf{n}}\Phi|_{z=-H_0+b} = \partial_t b, \end{cases} \tag{2.12}$$

where $\psi = \Phi|_{z=\zeta}$, a priori an unknown of the system. This gives rise to the following natural decomposition of Φ into a "fixed bottom" and a "moving bottom" component

$$\Phi = \Phi_{fb} + \Phi_{mb},$$

where

$$\begin{cases} \Delta\Phi_{fb} = 0 \quad \text{in } \Omega_t \\ \Phi_{fb}|_{z=\zeta} = \psi, \quad \sqrt{1+|\nabla_x b|^2}\partial_{\mathbf{n}}\Phi_{fb}|_{z=-H_0+b} = 0, \end{cases}$$

and

$$\begin{cases} \Delta\Phi_{mb} = 0 \quad \text{in } \Omega_t \\ \Phi_{mb}|_{z=\zeta} = 0, \quad \sqrt{1+|\nabla_x b|^2}\partial_{\mathbf{n}}\Phi_{mb}|_{z=-H_0+b} = \partial_t b. \end{cases}$$

This leads to

$$\sqrt{1+|\nabla_x\zeta|^2}\partial_{\mathbf{n}}\Phi|_{z=\zeta} = G^{DN}[\zeta,b]\psi + G^{NN}[\zeta,b]\partial_t b,$$

where we introduced the Dirichlet-Neumann operator $G^{DN}[\zeta,b]$ associated with the first Laplace-problem:

$$G^{DN}[\zeta,b] : \psi \mapsto \sqrt{1+|\nabla_x\zeta|^2}\partial_{\mathbf{n}}\Phi_{fb}|_{z=\zeta}.$$

as well as the Neumann-Neumann operator $G^{NN}[\zeta,b]$ associated with the second Laplace-problem:

$$G^{NN}[\zeta,b] : \partial_t b \mapsto \sqrt{1+|\nabla_x\zeta|^2}\partial_{\mathbf{n}}\Phi_{mb}|_{z=\zeta}.$$

Based on these notations we can now establish the correct form of the water waves problem with moving bottom:

$$\begin{cases} \partial_t\zeta - G[\zeta,b]\psi = G^{NN}[\zeta,b]\partial_t b, \\ \partial_t\psi + g\zeta + \frac{1}{2}|\nabla_x\psi|^2 - \dfrac{(G[\zeta,b]\psi + G^{NN}[\zeta,b]\partial_t b + \nabla_x\zeta\cdot\nabla_x\psi)^2}{2(1+|\nabla_x\zeta|^2)} = 0. \end{cases} \tag{2.13}$$

We remark that this case has already been studied on multiple levels and is relatively well understood. For this particular formulation, the first results concerning the local-in-time existence date back to [Lan05]. We refer to the article of Alazard, Burq, and Zuily

[ABZ11] for the general local well-posedness theory. In the works of Iguchi [Igu11] and Melinand [Mel15] various shallow water regimes are examined (motivated by earthquake generated tsunami research).

This formulation is based on the initial remark of Zakharov in 1968 ([Zak68]) who noticed that the water waves problem can be represented as a set of evolution equations with the appropriate variables ζ, and ψ, in the case of infinite fluid depths. This observation was extended later on by Craig, Sulem, and Sulem ([CSS92],[CS93]).

3 Solid mechanics

Solid mechanics studies the behavior of solid materials, that is their motion and their deformation under external or internal effects (action of a force, temperature change, chemical reactions, etc.). Much like with the fluid model, the solid is also treated as a continuous material, although its evolution is much more restricted due to its different fundamental state.

Throughout this study we consider the solid to be rigid and non-deformable, eliminating any kind of stress actors from the physical models. Under these assumptions, the solid motion can be essentially described by the displacement and the angular evolution of the solid's center of mass.

3.1 Newton's second law

Since the solid is being described as a single macroscopic physical object, its motion is subjected to the laws of classical mechanics. This principally entails a set of three (four, depending on the literature) physical laws most commonly known as Newton's laws of motion:

1. The *first law* states that every object will remain at rest or in uniform motion in a straight line unless an external force exerts its action on it, thus changing its state. This is the basic principle of any inertia-based argument. A straightforward consequence is that the origin of any change in the velocity lies in some kind of (internal or external) force acting on the system.
2. The *second law* (also known as fundamental principle of dynamics) quantifies the net forces as the associated rate of change of momentum. More exactly, one has that the net forces acting on the body can be expressed as mass times acceleration of the object, provided the mass of the solid is constant in time (which will be assumed here).
3. Newton's *third law* incorporates the so called "action-reaction" principle that was already evoked in the beginning of the Introduction. It states that all forces acting between two objects exist in equal magnitude and of opposite direction. In complex

physical systems this law is the basis to describe the interaction of different media, or in our case the coupling terms between the fluid and the solid.

4. Often one describes a *fourth law* as well, which represents the "principle of superposition" [Gre04]. It states that forces acting on an object add up like vectors, which is more of a supplement than an actual law, it arises as a necessity in modern classical mechanics.

By these laws one can describe the motion of the solid through the following equation

$$m\,\mathbf{a}_{solid}(t) = \mathbf{F}_{net} = \sum \mathbf{F}_i, \tag{3.1}$$

where m denotes the mass of the object, $\mathbf{a}_{solid}$ is its acceleration and $\mathbf{F}_i$ represent the forces acting on the solid (internal or external). Observing that the acceleration can be expressed as the second derivative (with respect to time) of the solid displacement, equation (3.1) is in fact a general ordinary differential equation.

3.2 External forces

In what follows we precise some of the more important external forces acting on the solid object, that will appear throughout the analysis. The main objective is to clarify the terms on the right hand side of equation (3.1).

Long range forces, like the gravitational force $\mathbf{F}_{grav} = m\mathbf{g}$, require little to no discussion, since they represent a constant, uniform effect on the system as a whole. Short range forces, or surface forces however represent a more complex phenomenon, so they need to be addressed, especially since they are responsible for the interaction between the contacting media.

3.2.1 Hydrodynamic effects

The single most important external actors on the object in a fluid-structure interaction setting are the hydrodynamic forces. These arise when an object is at least partially submerged in a fluid domain, and are determined by the hydrodynamical pressure exerted on the wetted surface, the part of the boundary of the solid in direct contact with the fluid.

These can be calculated by a surface integral of the fluid pressure $P(t, x)$. For what follows let us denote by $\mathcal{S}_t \subset \Omega$ the area occupied by the solid in the fluid domain at time t. If we note by Σ_t the part of $\partial\mathcal{S}_t$ in direct contact with the fluid, we have that the linear hydrodynamical forces exerted by the fluid are

$$\mathbf{F}_{hydro} = \int_{\Sigma_t} P\mathbf{n}_{solid}\, d\Sigma,$$

where $\mathbf{n}_{solid}$ is the unit normal vector of $\partial\mathcal{S}_t$ pointing outwards. This is the principal coupling term in the solid equation, since it clearly incorporates the effects of the fluid flow on the object.

3.2.2 Gyroscopic effects

In the previous part we described effects arising from the variation of linear momentum. This concerned the linear motion of the center of mass, regrouping external forces acting on the solid as vector quantities originating from this center. However, as it was already evoked before, not all such effects can be described this easily. Since the object $\mathcal{S}_t$ has physical dimension, certain effects will involve these dimensions as well.

We have already elaborated the hydrodynamic effects arising as a normal force exerted by the pressure of the fluid. This took into account the impact of the normal component of the fluid velocity field. However, the fluid flow around the solid (or at least around the wetted surface) acts in the tangential direction as well, creating a torque of the hydrodynamical force. This creates a moment of force that introduces a rotational variation, acting on the angular component of the solid position as opposed to the linear component.

Angular momentum is the rotational analog of linear momentum, therefore, for a point particle at x, it is given by the product of angular inertia ($\mathcal{I}$) and angular velocity ($\mathbf{v}_{ang}(x)$) around a particular reference point or axis. However, the angular momentum depends on the distance of the point from the reference as well, since the angular velocity is given by the normalized vector cross product of the position vector of the particle ($\mathbf{r}$) and the velocity. So the angular moment is given by

$$\mathbf{r} \times \mathbf{v}_{solid},$$

implying that the torque, or rotational force by $\mathbf{F}$ is provided by

$$\mathbf{r} \times \mathbf{F}.$$

This implies that the net change of angular momentum for the solid $\mathcal{S}_t$ generated by the pressure is given by

$$\mathbf{F}_{giration} = \int_{\partial\mathcal{S}_t} (x - x_0(t)) \times P\mathbf{n}_{solid}\, d\Sigma,$$

where x_0 represents the center of mass of the object.

Angular momentum is described in a conceptually different way in 2 and 3 space dimensions, with the angular momentum being a scalar in the former case and a vector in the latter one. Since in our coupled water waves model, we neglected rotational effects on the solid (see Section 2.1.2), we shall only make use of angular effects in the 2 dimensional case, relevant to the toy model derived in Section 1.2 of Chapter 1.

3.2.3 Dry friction

Dry friction is a force that opposes the relative motion of two solid surfaces in contact. It represents a dissipative effect in the system, since it is accounted for as a non-conservative force. During the whole process, some energy is always lost in the form of heat. The reason for this is that friction itself is not a fundamental force, it arises as a combination of inter-surface adhesion, contact surface roughness, and deformation. This also implies that its determination is difficult, one is required to rely on empirical laws for an analysis.

The dry friction is most commonly described through the three empirical laws of friction ([Ber06]) that can be summarized as follows:

1. *The first law* (Amontons' second law) incorporates that the force arising from the contact of two solid media can be decomposed into two characteristically different components, acting on the solid as a whole. One of them is called the normal force ($\mathbf{F}_{normal}$), its direction is given by the normal vector of the contact surface. The other one is the friction force ($\mathbf{F}_{fric}$), or the resistance to sliding, whose direction is parallel to the contact plane.
2. *The second law* (Amontons' first law) states that the normal force $\mathbf{F}_{normal}$ opposes the penetration of the two solid into each other.
3. *The third law* (Coulomb's law of friction) indicates that there exists a positive coefficient c_{fric} (coefficient of friction), depending on the material properties of the two solids in contact, but independent of the motion of the objects, such that at all times
$$|\mathbf{F}_{fric}| \leqslant c_{fric}|\mathbf{F}_{normal}|.$$
More precisely, as long as there is a relative motion between the two objects with a non-zero sliding velocity, the equality holds in the above inequality (kinetic or dynamic friction), furthermore the direction of $\mathbf{F}_{fric}$ is the exact opposite of the sliding velocity's. However if this velocity is zero, the strict inequality holds (static friction).

These experimental laws are only applicable in the case of dry friction, that is when there is no lubrication between the two solids. This implies that in particular no amount of fluid is allowed between the two objects in contact.

It is important to remark that we have to distinguish between static and dynamic friction from a practical point of view as well. Not only is the direction of $\mathbf{F}_{fric}$ determined in a different way, but physical experiments show that the corresponding coefficients of friction differ as well, with the coefficient for static friction being generally larger than the coefficient for dynamic friction.

4 Fluid-structure interaction

Fluid-structure interaction problems are among the most important, and, with respect to both modeling and computational issues, most challenging of multi-physics problems. The coupling of these two systems can manifest in changes of the previously described equations on many levels. As far as the works in this thesis are concerned, we specify three effects in particular related to our coupled problems.

1. **Modified fluid domain:** The presence of the solid $\mathcal{S}_t$ in the fluid domain represents an obstruction in the fluid flow in the sense that the actual fluid domain is $\Omega_t = \Omega \backslash \mathcal{S}_t$. In the water waves problem this was already implicitly assumed in the sense that we defined the fluid domain Ω_t for a moving bottom $b(t, x)$ without specifying its actual evolution. When part of the bottom topography is allowed to move freely (not in a prescribed way), the actual expression for b depends on the solid motion, therefore introducing coupling in the system.

   The general implication is that even for the fixed bounded domain formulation of Ω, part of the boundary $\partial\Omega_t$ will depend on time for the coupled problem, therefore introducing the additional complexity of the moving domain. Naturally, this means that we have to prescribe boundary conditions on $\partial\mathcal{S}_t$ as well as for the fluid quantities. The kinematic boundary condition is still valid, indicating that fluid particles can't enter the solid domain, represented by

   $$\mathbf{U} \cdot \mathbf{n}_{solid} = \mathbf{v}_{solid} \cdot \mathbf{n}_{solid} \quad \text{on } \partial\mathcal{S}_t,$$

   which means that the normal velocity of the fluid is given by the normal component of the solid velocity $\mathbf{v}_{solid}$.
2. **Linear momentum effects:** As it was explained in the previous section, the main coupling term for the solid equations is the force arising from the pressure of the fluid flow. It incorporates a force acting on the normal direction of the wetted surface, exerted by the fluid flow, giving rise to the hydrodynamic force term in the equation for the solid motion (3.1).
3. **Angular momentum effects:** The fluid flow exerts a tangential force as well on the wetted surface of the solid. This gave rise to a gyroscopic force term in the Newton equation, acting on the angular variable.

   Another consequence of the fluid flowing around the submerged object is that it creates a circulation around the solid, influencing the angular momentum as well as the linear momentum. The latter effect can be quantified by measuring the total contribution of tangential fluid velocity around the solid:

   $$\gamma = \int_{\partial\mathcal{S}_t} \mathbf{U} \cdot \tau \, d\Sigma,$$

   with $\tau^{\perp} = \mathbf{n}_{solid}$. For more details, see also Definition 1.2.3.

Therefore the coupled fluid-solid system can be written in the following generic form

$$\begin{cases} \partial_t \mathbf{U} + \mathbf{U} \cdot \nabla \mathbf{U} = -\dfrac{\nabla P}{\varrho} + \mathbf{g}, & \text{in } \Omega_t \\ \nabla \cdot \mathbf{U} = 0, & \text{in } \Omega_t \\ m\, \ddot{\mathbf{X}}_{solid}(t) = \displaystyle\int_{\Sigma_t} P \mathbf{n}_{solid}\, d\Sigma + \sum_{\text{external forces}} \mathbf{F}_i. \end{cases} \tag{4.1}$$

Finally, let us mention some of the numerical aspects of fluid-structure interaction problems. Today's software packages specialized for computational fluid dynamics or computational structural mechanics often incorporate solvers to simulate more and more kinds of fluid-structure interactions ([BS06]). This illustrates well the general approach towards these kinds of problems, meaning that a separate, specialized solver is dedicated to computing the fluid flow and the motion (or deformation) of the structure, and a certain coupling scheme is applied to update the common data between the two systems (most notably the pressure field and the solid position/velocity) (see for example [Pes05],[LB10]). However this often raises the question of how well the (numerical) conservation of total mass, momentum, and energy are respected.

Although a lot of research has been done in this direction for the past few years, some questions still remain to be answered. In particular, modeling the coupling itself in an efficient, optimal way, or adapting the discretization scheme to incorporate the flow and the structure at the same time ([CM06], [CMM08], or [Dor17] and references therein) still prove to be relatively challenging.

5 Asymptotic models

When one is dealing with problems arising from physics, or other applied fields of science, one can frequently run into problems of asymptotic nature, such as certain damping, perturbation, stabilization, etc. problems. In order to solve these problems, one is led to apply techniques from asymptotic analysis, and perturbation theory. The theoretical aspects of this field are much more established nowadays than they were some decades ago.

In 1963, Kruskal [Kru64] defined asymptotology as "the art of dealing with applied mathematical systems in limiting cases". The general idea of the domain is still the same after all these years, one wishes to extract information through an approximation of the exact solution to a given problem. In order to derive such approximations, certain naturally appearing or artificially introduced small parameters are varied to obtain simplified equations, therefore reducing the complexity of the governing equations. The main mathematical tool is asymptotic expansion with respect to a suitable (asymptotic) sequence of functions of these smallness parameters.

One distinguishes in general ([CK96]) two types of qualitatively different problematics, in what follows we detail both, since the two main problems of this thesis each fall into a different category.

5.1 Regular perturbation problems

In a regular perturbation problem, one can carry out a straightforward Taylor expansion around a limiting case, leading to an approximation of the form of a series with respect to the smallness parameter. The terms of this series are defined by a system of (differential) equations and associated boundary conditions obtained for the corresponding order of magnitude of the parameter. This system is then solved recursively, with uniformly bounded terms on the whole domain of the problem, moreover the accuracy of the approximation improves as the parameter gets smaller and smaller.

5.1.1 The shallow water asymptotic regime

A typical, albeit not the simplest example of a regular perturbation problem is the derivation of shallow water asymptotic models for the water waves problem. It involves the asymptotic expansion of the vertically averaged horizontal velocity field with respect to the shallowness parameter associated with the domain Ω_t.

First of all we present the dimensionless parameters relevant to the system, bearing in mind that our aim is to derive (simpler) asymptotic models. For that we need to introduce the various characteristic scales of the problem

- H_0, the base water depth,
- L, characteristic horizontal scale of the wave motion (both for longitudinal and transversal directions),
- a_{surf} order of the free surface amplitude,
- a_{bott} vertical scale of the solid (order of the bottom topography variation in general).

Using these quantities, we can introduce several dimensionless parameters:

- shallowness parameter $\mu = \frac{H_0^2}{L^2}$,
- nonlinearity (or amplitude) parameter $\varepsilon = \frac{a_{surf}}{H_0}$,
- bottom topography parameter $\beta = \frac{a_{bott}}{H_0}$.

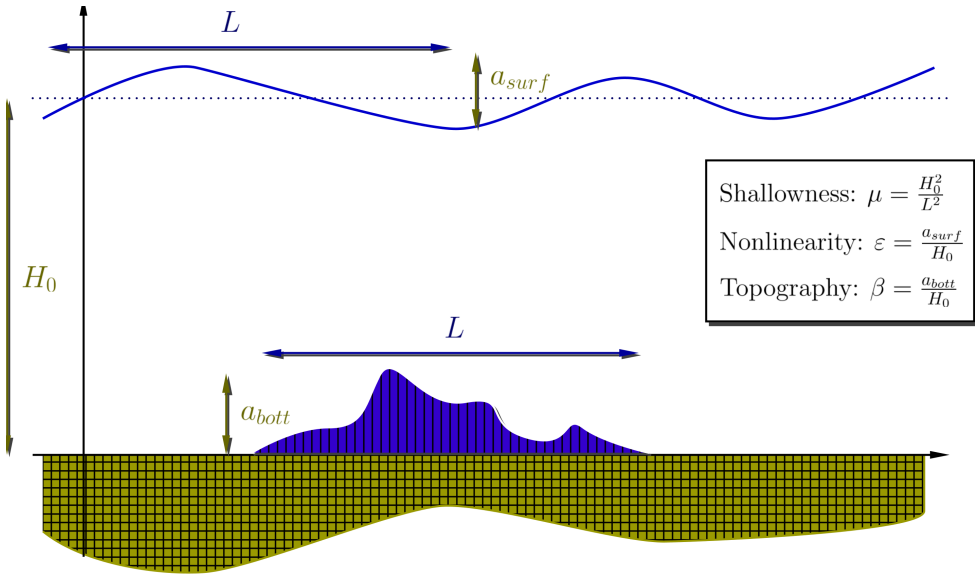

Figure 4 – The characteristic scales for the coupled water waves problem

With these parameters, one can nondimensionalize the water waves problem (2.13). First of all, the dimensionless Laplace-problem defining the velocity potential is

$$\begin{cases} \Delta^{\mu}\Phi := \mu\Delta_x\Phi + \partial_z^2\Phi = 0, \quad \text{on } -1+\beta b \leqslant z \leqslant \varepsilon\zeta, \\ \Phi|_{z=\varepsilon\zeta} = \psi, \quad \sqrt{1+\beta^2|\nabla_x b|^2}\partial_{\mathbf{n}}\Phi_{mb}|_{z=-H_0+b} = \partial_t b. \end{cases} \tag{5.1}$$

Decomposing the potential into two components $\Phi = \Phi_{fb} + \Phi_{mb}$ just as in Section 2.2, for the corresponding Laplace-problems one can once again define the Dirichlet–Neumann and Neumann–Neumann operators:

$$G_\mu^{DN}[\varepsilon\zeta, \beta b]\psi = \sqrt{1+\varepsilon^2|\nabla_x\zeta|^2}\partial_{\mathbf{n}}\Phi_{fb}|_{z=\varepsilon\zeta},$$
$$G_\mu^{NN}[\varepsilon\zeta, \beta b]\partial_t b = \sqrt{1+\varepsilon^2|\nabla_x\zeta|^2}\partial_{\mathbf{n}}\Phi_{mb}|_{z=\varepsilon\zeta}.$$

With this, the nondimensionalized form of the water waves equations arising from (2.13) is

$$\begin{cases} \partial_t\zeta - \frac{1}{\mu}G_\mu^{DN}[\varepsilon\zeta, \beta b]\psi = \frac{\beta}{\varepsilon}G_\mu^{NN}[\varepsilon\zeta, \beta b]\partial_t b, \\ \partial_t\psi + \zeta + \frac{\varepsilon}{2}|\nabla_x\psi|^2 - \varepsilon\mu\dfrac{(\frac{1}{\mu}G_\mu^{DN}[\varepsilon\zeta, \beta b]\psi + \frac{\beta}{\varepsilon}G_\mu^{NN}[\varepsilon\zeta, \beta b]\partial_t b + \nabla_x(\varepsilon\zeta)\cdot\nabla_x\psi)^2}{2(1+\varepsilon^2\mu|\nabla_x\zeta|^2)} = 0. \end{cases}$$

5.1.2 Shallow water approximative models

By (5.1), one can define the vertically averaged horizontal component of the velocity as

$$\overline{V} = \overline{V}_\mu[\varepsilon\zeta, \beta b]\psi = \frac{1}{h}\int_{-1+\beta b}^{\varepsilon\zeta} \nabla_x \Phi(\cdot, z)\, dz, \tag{5.2}$$

where $h = 1 + \varepsilon\zeta - \beta b$. The main interest of this new variable lies in the following proposition ([Lan13])

Proposition 5.1. *Let $s > d/2 + 1$ and $\zeta, b \in H^s(\mathbb{R}^d)$ such that*

$$\exists h_{min} > 0,\ \forall X \in \mathbb{R}^d,\ 1 + \varepsilon\zeta(X) - \beta b(X) \geqslant h_{min}. \tag{5.3}$$

Let $\psi \in \dot{H}^{3/2}(\mathbb{R}^d) = \{f \in L^2_{loc}(\mathbb{R}^d),\ \nabla f \in H^{1/2}(\mathbb{R}^d)^d\}$ and $\Phi \in \dot{H}^2(\mathbb{R}^d) = \{f \in L^2_{loc}(\mathbb{R}^d),\ \nabla f \in H^1(\mathbb{R}^d)^d\}$ be the solution of the Laplace equation (5.1). Then the following relation holds

$$\sqrt{1 + \varepsilon^2|\nabla_x\zeta|^2}\partial_{\mathbf{n}}\Phi|_{z=\varepsilon\zeta} = \mu\frac{\beta}{\varepsilon}\partial_t b - \mu\nabla\cdot(h\overline{V}). \tag{5.4}$$

This implies that one can rewrite the Dirichlet-Neumann and Neumann-Neumann operators by using this expression of $\overline{V}$.

The main motivation for this is that an asymptotic expansion can be obtained for this variable, more precisely

Proposition 5.2. *Let $t_0 > \frac{d}{2}$, $s \geq 0$, $n \in \mathbb{N}$, and $\zeta, b \in H^{s+2+2n}(\mathbb{R}^d) \cap H^{t_0+2}(\mathbb{R}^d)$ such that they satisfy the previous minimal water depth condition (5.3). Let $\psi \in \dot{H}^{s+3+2n}(\mathbb{R}^d)$. One can construct a sequence $(\overline{V}_j)_{0\leq j\leq n}$ of class $H^s(\mathbb{R}^d)$, independent of μ, such that $\|\overline{V}_j\|_{H^s} \leq M(s+2j)\|\nabla_x\psi\|_{H^{s+2j}}$ $(0 \leq j \leq n)$ and*

$$\left\|\overline{V} - \sum_{j=0}^{n}\mu^j\overline{V}_j\right\|_{H^s} \leq \mu^{n+1}M(s+2+2n)\|\nabla_x\psi\|_{H^{s+2+2n}}, \tag{5.5}$$

with a constant $M(\tilde{s})$ defined by

$$M(\tilde{s}) = C(M_0, \|\zeta\|_{H^s}, \|b\|_{H^s}),\ \text{with } M_0 = C\left(\frac{1}{h_{min}}, \mu_{max}, \|\zeta\|_{H^{t_0+1}}, \|b\|_{H^{t_0+1}}\right).$$

In particular, one has the following:

$$\overline{V} = \nabla_x\psi - \mu\mathcal{T}[h, \beta b]\nabla_x\psi - \mu\frac{\beta}{\varepsilon}\left(\frac{1}{2}h\nabla_x\partial_t b + \varepsilon\nabla_x\zeta\partial_t b\right) + \mathcal{O}(\mu^2),$$

where

$$\mathcal{T}[h,\beta b]V = -\frac{1}{3h}\nabla_x(h^3\nabla_x\cdot V) + \beta\frac{1}{2h}\left(\nabla_x(h^2\nabla_x b\cdot V) - h^2\nabla_x b\nabla_x\cdot V\right) + \beta^2\nabla_x b\nabla_x b\cdot V.$$

From this one can derive the shallow water equations analyzed in the current work. For more details as well as the demonstrations of the aforementioned propositions, we refer to [Lan13].

5.2 Singular perturbation problems

Many problems of physical interest however do not fall into the category of regular perturbation problems. This manifests in the fact that a straightforward expansion fails over the whole domain of the problem, the terms obtained from the development are secular (they become unbounded), due to the presence of one (or more) thin layer(s) at the boundary, or in the interior of the domain. In this case one is talking about singular perturbation problems, or layer-type problems.

This failure is in general attributed to one of the two following main causes. The presence of the smallness parameter as a multiplier of the highest order derivative term in the equations leads to the fact that in the asymptotic limit, the leading order approximation is defined by a lower-order equation, which in turn can not satisfy all the initial and boundary conditions of the original system. Often, problems are defined on an infinite domain, in which small terms can have cumulatively significant effects, therefore uniform estimates are not assured for the whole domain of the problem.

5.2.1 A multiple scale approach

A well-established method to overcome the difficulties arising from a singular perturbation problem is the introduction of new timescales beyond the standard timescale t of the problem itself. These new timescales are in general well-defined functions of the time t and the smallness parameters of the problem. The foundations of this method date back to 1883 when Lindstedt ([Lin83]) introduced the idea to analyze the three body problem of celestial mechanics. It was justified later on by Poincaré ([Poi92]), therefore it became known as the Poincaré–Lindstedt method.

The main issue with this approach is to find the appropriate timescales for the problem. In some cases the failure of a regular asymptotic expansion comes from the fact that this expansion ceases to be uniformly valid over the whole domain, in particular around part of the boundary. Therefore, complementing the standard (external) asymptotic expansion with a secondary (internal) asymptotic development around the problematic point or area, and superposing the two expansions provides an adequate approximation for the whole domain ([CK96]). These two expansions often involve different functions of the smallness parameter, which in turn provides the two natural timescales of the original problem.

In other cases, homogenization methods, or restricting the search for specific types of solutions (for example periodic solutions) can give an idea of the nature of the additional timescales. These techniques are useful in the case when the terms involving these different times can't be explicitly decoupled, as it is going to be the case in Chapter 1.

We remark that, apart from the multiple-scale approach, there exist other methods to handle these problems. The method of averaging for instance is another well-established approach. It was originally introduced by Krylov and Bogoliubov [KB43] in 1937 and has been extensively applied to a variety of physical problems. Its main feature is that it makes use of the Hamiltonian structure of the equations, providing a relatively general and constructive method that applies to problems originating from a physical context.

5.2.2 The dynamics of an infinitesimal object

Following the derivation in Section 1.2, we have that the simplified first order system describing the motion of an infinitesimal object in Ω is of the form

$$I_\epsilon \ddot{q}(t) = F(q, \dot{q}), \tag{5.6}$$

where q stands for the position vector of the solid, I_ϵ represents the inertia, with ϵ a smallness parameter of the system, and F on the right hand side incorporates the dynamics and the nonlinearity of the system.

It is clear that this system of second order ordinary differential equations falls into the case when a straightforward asymptotic development would fail, since by $\epsilon \to 0$, the left hand side would disappear, meaning that the limiting equation would be only a first order system. Moreover, due to the complexity of the nonlinearity, the internal-external asymptotic expansion approach is not applicable, therefore we are required to ascertain in a different way the natural timescales associated with this system.

Chapter 1

Multiple-scale analysis of the dynamics of a point particle in a two dimensional perfect incompressible and irrotational flow

Contents

Version française abrégée

Nous étudions un modèle simplifié qui décrit le mouvement d'un solide dans un milieu fluide parfait sur un domaine $\Omega \subset \mathbb{R}^2$, qui est supposé borné, connexe et simplement connexe. Les équations sont données par

$$\begin{cases} \mu h'' = (h' - u(h))^\perp, & \text{(1.0.1a)} \\ \varepsilon \vartheta'' = R_\vartheta \xi \cdot (h' - u(h)), & \text{(1.0.1b)} \end{cases}$$

où les variables principales sont le vecteur de déplacement du centre de masse du solide $h(t) \in \Omega$ et sa position angulaire $\vartheta(t) \in [-\pi, \pi]$. R_ϑ est la matrice de rotation par ϑ, et en particulier $x^\perp = R_{\pi/2} x$ pour $x \in \mathbb{R}^2$. La non-linéarité du système est décrite par $u \in \mathcal{C}^\infty(\Omega)$ qui correspond essentiellement la vitesse de Kirchhoff–Routh. Les conditions initiales sont $h(0) = \bar{h}_0 \in \Omega$, $h'(0) = \bar{h}_1 \in \mathbb{R}^2$, $\vartheta(0) = \vartheta_0 \in (-\pi, \pi]$ et $\vartheta'(0) = \vartheta_1 \in \mathbb{R}$.

Dans cette étude, nous présentons trois résultats principaux, qui concernent à la fois la dynamique de ces équations et leur développement asymptotique par rapport à des paramètres de petitesse μ et ε. Notons que μ représente la masse de l'objet, ε sa taille.

Un premier résultat consiste à établir un développement d'ordre quelconque du vecteur de déplacement h, caractérisé par l'équation (1.0.1a), qui est a priori découplée de l'autre équation du système. Par une estimation d'énergie, nous avons que pour chaque $\mu >$, la solution existe pour un temps T_μ. En nous rassurant que cette solution n'approche pas trop le bord, nous définissons pour $\delta > 0$

$$T_{\mu,\delta} = \sup\{t \in (0, T_\mu) \Big| \operatorname{dist}(h(t), \partial\Omega) \geqslant \delta\},$$

nous obtenons le développement suivant :

Théorème 1.0.1. *Soit $d \in \mathbb{N}$, $d > 1$ et soient $\mu_0 > 0$, $\delta > 0$ suffisamment petits. Pour tout $0 < \mu < \mu_0$, et pour tout indices (j, k), $1 \leqslant j \leqslant d$, $0 \leqslant k \leqslant d - j$, il existe $h_k(t) \in \mathcal{C}^\infty([0, \infty))$, $h_{j,k}(t, \tau) \in \mathcal{C}^\infty([0, \infty), 2j\pi\mathbb{T})$, qui sont périodiques en leur deuxième variable, et $(h_R)_{\mu \in (0,\mu_0)}$ une famille de fonctions uniformément bornées sur $[0, T_{\mu,\delta}]$ dans le sens que pour tout $\delta > 0$ suffisamment petit, on a*

$$\sup_{\mu \in (0,1)} \sup_{t \in [0, T_{\mu,\delta}]} (\|h_R\|(t) + \|h_R'\|(t)) < +\infty,$$

tels que pour tout $t \in [0, T_{\mu,\delta}]$ l'unique solution de (1.0.1a) avec données initiales $h(0) = \bar{h}_0 \in \Omega$, $h'(0) = \bar{h}_1 \in \mathbb{R}^2$ s'écrit

$$h(t) = h_0(t) + \sum_{k=1}^{d-1} \mu^k h_k(t) + \sum_{j=1}^{d} \sum_{k=0}^{d-j} \mu^{j+k} h_{j,k}\left(t, \frac{t}{\mu}\right) + \mu^{d-1} h_R. \tag{1.0.2}$$

Ce théorème a des conséquences diverses. Tout d'abord, en étudiant les conditions

initiales et leurs implications sur le développement (1.0.2), nous déduisons une condition de compatibilité entre l'équation (1.0.1a) et l'équation de limite vérifiée par h_0 (qui n'est rien d'autre qu'une équation de point-vortex). Cette condition consiste à établir la relation entre $h_0'(0)$ et $\bar{h}_1$. En particulier, nous avons les résultats suivantes :

- si $\bar{h}_1 = u(\bar{h}_0)$, alors $h \to h_0$ dans $W^{1,\infty}$;
- si $\bar{h}_1 \neq u(\bar{h}_0)$, alors $h't) \neq u(h(t))$ pour tout t tel que la solution $h(t)$ existe ;
- de plus, si $\bar{h}_1 \neq u(\bar{h}_0)$, alors $g(t) := h't) - u(h(t))$ se comporte de manière quasi-périodique dans le sens qu'ils existent λ, ν réels positifs et deux suites croissantes $\{a_n\}_{n\in\mathbb{N}}$, $\{b_n\}_{n\in\mathbb{N}}$ tels que $\frac{d}{dt}|g(t)| \geqslant \lambda$ sur $[a_n - \nu, a_n + \nu]$ et $\frac{d}{dt}|g(t)| \leqslant \lambda$ sur $[b_n - \nu, b_n + \nu]$.

Par rapport à la variable angulaire, nous établissons que, pour des données initiales petites, nous avons l'approximation asymptotique suivante :

Théorème 1.0.2. *Ils existent $\phi \in \mathcal{C}^\infty(\mathbb{R}^+)$ et $\theta \in \mathcal{C}^\infty(\mathbb{R}^+)$ uniquement définies,*

$$\psi = \frac{\theta(t)}{\sqrt{\varepsilon}} + \phi(t),$$

$t = \sqrt{\varepsilon}$ et ils existent $\Theta^0 \in \mathcal{C}^\infty((-\pi,\pi],\mathbb{R}^+)$, $\Theta^1 \in \mathcal{C}^\infty((-\pi,\pi],\mathbb{R}^+)$ telles que l'approximation

$$\Theta_A(\tau) = \Theta_A(\psi(\tau), t(\tau)) = \Theta^0(\psi, t) + \sqrt{\varepsilon}\Theta^1(\psi, t) \tag{1.0.3}$$

est périodique par rapport à sa première variable et qu'elle vérifie pour un temps $\tau \in [0, T/\sqrt{\varepsilon}]$

$$\begin{cases} \frac{d^2}{d\tau^2}\Theta(\tau)_{App} = R_{\Theta(\tau)_{App}}\xi \cdot g(t) + \mathcal{O}_{L^\infty}(\varepsilon), \\ \Theta_{App}(0) = \vartheta_0 + \mathcal{O}_{L^\infty}(\varepsilon), \quad \frac{d}{d\tau}\Theta_{App}(0) = \mathcal{O}_{L^\infty}(\varepsilon). \end{cases} \tag{1.0.4}$$

Ici, T est défini par Remarque 1.4.1.

En revanche, nous obtenons des résultats différents tant que nous supposons que les données initiales sont assez éloignées de l'origine. Dans ce cas il s'agit d'une étude dynamique du système non-autonome (1.0.1b) pour mettre en évidence un caractère dynamique assez complexe.

Cet étude dynamique repose sur l'analyse d'un système de trois équations du premier ordre, obtenu de l'équation (1.0.1b) :

$$\begin{aligned} \Theta' &= v, \\ v' &= |\xi||g(t)|\sin(\Theta + \alpha(t)), \\ t' &= \sqrt{\varepsilon}, \end{aligned} \tag{1.0.5}$$

ou de manière plus compacte :

$$\mathbf{x}' = f_\varepsilon(\mathbf{x}),$$

avec $\mathbf{x} = (\Theta, v, t)^\top$ et $f_\varepsilon = (f_1, f_2, f_3)(\Theta, v, t) = (v, |\xi||g(t)|\sin(\Theta + \alpha(t)), \sqrt{\varepsilon})$. Ici $\alpha(t)$ est l'angle orienté entre les vecteurs $\xi^\perp$ et $g(t)$.

Ce système, désormais autonôme, ne peut pas être traité par des techniques classiques à cause de la dégénérescence dans la troisième variable (t), par conséquent nous sommes ammenés à introduire des outiles généralisés, suite à des travaux récents dans le domaine de comportement chaotique des systèmes dynamiques ([CW15]).

Définition 1.0.1. *Nous notons par Σ l'ensemble de Cantor des suites indexées par $\mathbb{Z}$ de deux symboles (0 et 1). Soit $\sigma : \Sigma \to \Sigma$ l'opérateur de décalage défini pour $s = (s_i)_{i\in\mathbb{Z}}$ par $\sigma(s)_i = s_{i+1}$.*

Théorème 1.0.3. *Pour ε suffisamment petit, il existe une ligne non-horizontale $\mathcal{N}_\varepsilon$ dans $\mathbb{R}^3$, invariante sous l'action de f_ε, autour de laquelle il existe un ensemble invariant Λ_ε tel que Λ_ε est topologiquement conjugué à $\Sigma \times \mathcal{N}_\varepsilon$, Λ_ε est un ensemble de Cantor des lignes non-horizontales, et un itéré de l'application de Poincaré associée à la restriction $f_\varepsilon|_{\Lambda_\varepsilon}$ est topologiquement conjugué au décalage de Bernoulli σ.*

1.1 Introduction

Studies on the motion of rigid bodies immersed in a fluid domain have existed for the past few decades, especially in the viscous fluid case, when the fluid motion is governed by the Navier–Stokes equations (see for example [CSMT00],[TC08], [GM00], [GVH14], [Bra18]). In the case of a perfect fluid, with the governing fluid equations being the Euler equations instead of the Navier–Stokes equations, the literature is sparser; we refer to [ORT07] concerning one of the first main results, or to a series of recent articles ([GLS14],[GMS18],[GS15],[GLS16]) covering the physically relevant cases in this setting.

Here we study a simplified model for this system with an emphasis on the angular variable and its evolution, a quantity that a priori vanishes when the size of the solid tends to 0 (see Theorem 1.2.4). As remarked in [Sue17], strong oscillations are present in the system, hindering convergence of the solution in regular spaces. We establish the exact nature of these oscillations, moreover a compatibility condition is obtained with which these oscillatory terms can be cancelled out. Another focus concerns the sensitivity to the body's shape present in the correction terms when passing to the limit.

1.1.1 The model system

Let us fix Ω, a bounded, open, regular, connected, and simply connected domain of $\mathbb{R}^2$; the domain of the perfect fluid. Let us also fix $\mathcal{S}_0 \subset \Omega$ a non-empty, closed, connected, and simply connected subset; the initial position of the solid, submitted to a rigid motion inside the fluid domain. For a time $t > 0$, let us denote by $h(t) \in \Omega$ the position of the

center of mass of the solid, and by $\vartheta(t) \in (-\pi, \pi]$ the angle of its rotation. The simplified system describing the motion of the object is given by

$$\begin{cases} \mu h'' = (h' - u(h))^{\perp}, & \text{(1.1.1a)} \\ \varepsilon \vartheta'' = R_{\vartheta}\xi \cdot (h' - u(h)). & \text{(1.1.1b)} \end{cases}$$

Here R_{ϑ} is the rotation matrix by ϑ, that is

$$R_{\vartheta(t)} = \begin{pmatrix} \cos\vartheta(t) & -\sin\vartheta(t) \\ \sin\vartheta(t) & \cos\vartheta(t) \end{pmatrix},$$

and, in particular, for a vector $x \in \mathbb{R}^2$, $x^{\perp} = R_{\pi/2}x$.

The vector ξ is the conformal center of the object, thus incorporating the essentials on the geometry of the solid (see also Definition 1.2.5). The function $u \in \mathcal{C}^{\infty}(\Omega)$ is the nonlinearity of the system, a Kirchhoff–Routh velocity defined by

Definition 1.1.1. *Let*

$$u = \nabla^{\perp}\psi_{\Omega}, \tag{1.1.2}$$

where the Kirchhoff–Routh stream function ψ_{Ω} is given by the trace

$$\psi_{\Omega}(x) = \frac{1}{2}\psi^0(x, x),$$

where the function $\psi^0(h, \cdot)$ is the solution of the following Dirichlet-problem

$$\begin{cases} \Delta\psi^0(h, \cdot) = 0 & \text{in } \Omega, \\ \psi^0(h, \cdot) = -\frac{1}{2\pi}\ln|\cdot - h| & \text{on } \partial\Omega. \end{cases} \tag{1.1.3}$$

Remark 1.1.1. *As long as $h \in \Omega$, the Dirichlet boundary condition is a smooth function for the system (1.1.3), thus the solution of this Laplace problem is regular. In particular, by the chain rule, the function $u(h(t))$ is as regular as the function $h(t)$.*

We remark that the right hand side of equation (1.1.1a) corresponds to a Kutta–Joukowski type lift force arising from the effects of the fluid pressure. The initial conditions of the system are $h(0) = \bar{h}_0 \in \Omega$, $h'(0) = \bar{h}_1 \in \mathbb{R}^2$, $\vartheta(0) = \vartheta_0 \in (-\pi, \pi]$, and $\vartheta'(0) = \vartheta_1 \in \mathbb{R}$.

The two parameters of the system are μ, representing the mass of the object, and ε, the size (diameter) of the solid. The asymptotic analysis involves at least one of these quantities tending to 0, this will be clarified at the beginning of each section.

For further details, as well as the derivation of this system, we refer to Section 1.2.

1.1.2 Outline of the study

The outline of this study is as follows. First of all, we present the origins of system 1.1.1. We detail the physical system describing the flow of a bidimensional fluid (on an unbounded or a bounded domain) with the addition of a solid body within. We state the reduction of this system to an ODE, and finally we detail the asymptotic limit of a vanishing body (when the size of the solid tends to 0).

Section 1.3 is devoted to the analysis of the evolution of the position of the solid's center of mass, as well as the limiting point-vortex system which characterizes the zeroth order expansion of the displacement vector of the solid. More precisely we show that, given a massive point-vortex system (equation (1.1.1a)), by letting the mass μ tend to zero, one obtains indeed a classical point-vortex equation, following the ideas of Kruskal ([Kru58]) and Berkowitz and Gardner in [BG59]. A necessary compatibility condition is established to connect these two point-vortex systems, based on which one can deduce convergence in $W^{1,\infty}$. This has some important consequences not only on the behavior of the displacement but on the equation describing the angle as well.

In Section 1.4 we address the asymptotic development of the angular equation (1.1.1b) and we present the essential tools to handle the arising singular perturbation problem. We analyze the equation for small initial data, when periodic trajectories can be observed, and establish a power series expansion for two timescales simultaneously. Following the ideas of Bourland and Haberman ([BH88]) we describe the naturally appearing shift as well as the modulation induced by the equations.

Section 1.5 presents a particular result on the angular equation, concerning the case when the initial data is sufficiently large, leading to amplified instabilities from a dynamical point of view. Applying a Wiggins type theorem ([Wig88b]) on the angular equation we highlight the complexity of the underlying dynamics for this system. In particular, a theorem involving the sensitivity to initial data is presented, followed by some existence results on homoclinic and almost periodic orbits.

1.2 On the motion of a rigid body in a bidimensional perfect fluid

Now we state some classical and some more recent results concerning the study of the motion of a rigid body in a two-dimensional fluid flow. In general for a detailed discussion and for more references on the origin of the system we refer to [Sue17], as well as to [GLS14], [GLS16], [GMS18].

1.2.1 The case of an unbounded irrotational flow

We considered the motion of a rigid body immersed in a 2 dimensional incompressible, irrotational perfect fluid. The domain of the full fluid-solid system is taken to be the whole space $\mathbb{R}^2$. Initially the solid occupies a non-empty, closed, connected, and simply connected subset $\mathcal{S}_0 \subset \mathbb{R}^2$. We suppose that the body moves rigidly so that at time t it occupies the domain $\mathcal{S}(t)$ which is isometric to $\mathcal{S}_0$. Let us assume that the origin is the center of mass for $\mathcal{S}_0$. Initially the fluid occupies the domain $\mathcal{F}_0 = \mathbb{R}^2 \backslash \mathcal{S}_0$, and at time t the domain $\mathcal{F}(t) = \Omega \backslash \mathcal{S}(t)$.

1.2.1.1 The equations of the system

Based on our physical assumptions on the fluid (it being incompressible, irrotational, and inviscid), its dynamics are governed by the two dimensional incompressible irrotational Euler equations

$$\begin{cases} \partial_t U + (U \cdot \nabla)U + \nabla P = 0 & \text{for } t \in (0,\infty), x \in \mathcal{F}(t), \quad (1.2.1a) \\ \nabla \cdot U = 0 & \text{for } t \in [0,\infty), x \in \mathcal{F}(t), \quad (1.2.1b) \\ \nabla \times U = 0 & \text{for } t \in [0,\infty), x \in \mathcal{F}(t), \quad (1.2.1c) \end{cases}$$

where $U = (U_1, U_2)^\top$ is the fluid velocity field and P denotes the fluid pressure. The fluid is supposed to be homogeneous with a density of 1 for the sake of simplicity.

The motion of the solid is governed by the forces exerted by the fluid (by Newton's second law), thus the balance of the linear and the angular momentum writes as follows

$$\begin{cases} \mu h''(t) = \displaystyle\int_{\partial\mathcal{S}(t)} P\mathbf{n}\, d\Sigma & \text{for } t \in (0,\infty), \quad (1.2.2a) \\ \mathcal{I}\vartheta''(t) = \displaystyle\int_{\partial\mathcal{S}(t)} (x - h(t))^\perp \cdot P\mathbf{n}\, d\Sigma & \text{for } t \in (0,\infty), \quad (1.2.2b) \end{cases}$$

where h is the position of the center of mass of the solid with respect to a fixed point of reference (the origin of the system), ϑ denotes the angle of its rotation with respect to its initial position. In the equations, $\mathbf{n} = (n_1, n_2)^\top$ stands for the unit normal vector of the surface of the solid ($\partial\mathcal{S}(t)$) pointing outwards, $\mu > 0$ is the mass of the solid, $\mathcal{I} > 0$ the momentum of inertia of the object.

We remark that, due to the isometric property of the solid displacement, we may introduce the rotation matrix $R_{\vartheta(t)}$ in order to describe the exact position of the solid, that is

$$\mathcal{S}(t) = \{h(t) + R_{\vartheta(t)}x,\ x \in \mathcal{S}_0\}. \quad (1.2.3)$$

Finally, for the boundary conditions of the system, we impose that the boundary of the solid is impermeable (a kinematic boundary condition on $\partial\mathcal{S}(t)$), as well as the hypothesis

that the fluid is at rest at infinity. Thus we have that

$$U \cdot \mathbf{n} = \left(h'(t) + \vartheta'(t)(x - h(t))^{\perp}\right) \cdot \mathbf{n} \quad \text{for } t \in [0, \infty), x \in \partial\mathcal{S}(t), \tag{1.2.4}$$

and

$$\lim_{|x| \to \infty} |U(t, x)| = 0 \quad \text{for } t \in [0, \infty). \tag{1.2.5}$$

The system (1.2.1)-(1.2.5) forms the coupled problem of the incompressible Euler equations with a rigid body. The initial conditions can be stated as follows

$$\begin{aligned} &U|_{t=0} = U_0 \qquad \text{for } x \in \mathcal{F}_0; \\ &h(0) = 0, \quad h'(0) = \bar{h}_1, \quad \vartheta(0) = 0, \quad \vartheta'(0) = \vartheta_1. \end{aligned} \tag{1.2.6}$$

The position h and orientation ϑ of the solid is the basis of its movement (see the characteristic equations of its motion in (1.2.2)), thus we shall make use of the position vector $q = (h, \vartheta)^{\top}$. Let us denote its time derivative by the vector p. Since the solid position is entirely described by the vector q (due to (1.2.3)), we may also denote the domains $\mathcal{S}(t)$ and $\mathcal{F}(t)$ by $\mathcal{S}(q)$ and $\mathcal{F}(q)$ respectively.

1.2.1.2 The geometry of the unbounded flow

In this part, we state the essential parts of the analysis of the case of an unbounded irrotational flow ([Sue17]). Some of these expressions originate from complex analysis due to the computations involved in the associated theorems. We introduce quantities defined for the whole plane, that describe the fundamental geometry of the object and its impact on the dynamics of the system.

In the potential case, the fluid velocity can be globally taken as a gradient. This motivates the following particular extension.

Definition 1.2.1. *The global Kirchhoff-potentials $\Phi_{gl} = (\Phi_{gl,i})_{i=1,2,3}$ are defined as the solutions of the following Laplace problems*

$$\begin{cases} \Delta\Phi_{gl,i} = 0 & \text{in } \mathbb{R}^2 \backslash \mathcal{S}_0, \\ \Phi_{gl,i} \to 0 & \text{when } |x| \to \infty, \\ \dfrac{\partial \Phi_{gl,i}}{\partial n} = K_{gl,i} & \text{on } \partial\mathcal{S}_0; \end{cases} \tag{1.2.7}$$

where we have that

$$(K_{gl,1}, K_{gl,2}, K_{gl,3}) = (n_1, n_2, x^{\perp} \cdot \mathbf{n}).$$

These potentials contain information on the solid geometry which may be expressed by introducing the added inertia matrix.

Definition 1.2.2. *For $i, j \in \{1, 2, 3\}$ let us define*

$$m_{gl;i,j} = \int_{\mathbb{R}^2 \setminus \mathcal{S}_0} \nabla \Phi_{gl,i} \cdot \nabla \Phi_{gl,j} \, dx, \tag{1.2.8}$$

Then the matrix $\mathcal{M}_{gl,a}$, which has $m_{gl;i,j}$ as its entries, is called the global added inertia matrix, that is

$$\mathcal{M}_{gl,a} = [m_{gl;i,j}]_{i,j \in \{1,2,3\}}.$$

This matrix actually encodes the so called added mass phenomenon and it shall serve as an additional inertia in the soon-to-be-formulated solid equations, as opposed to the genuine inertia matrix

$$\mathcal{M}_g = \begin{pmatrix} \mu & 0 & 0 \\ 0 & \mu & 0 \\ 0 & 0 & \mathcal{I} \end{pmatrix}.$$

We also define the extended rotational matrix $\mathcal{R}(\vartheta)$ as

$$\mathcal{R}_\vartheta = \begin{pmatrix} R_\vartheta & 0 \\ 0 & 1 \end{pmatrix} \in SO(3).$$

An important parameter regarding the solid is the circulation of the fluid velocity around the object $\mathcal{S}_0$, defined by

Definition 1.2.3. *The circulation of velocity around the solid is*

$$\gamma = \int_{\partial \mathcal{S}_0} U \cdot \tau \, d\Sigma, \tag{1.2.9}$$

where τ is the unit tangent vector of the solid surface verifying $\tau^\perp = \mathbf{n}$.

Due to Kelvin's theorem, the circulation is constant in time.

Much like the potential case giving rise to the global Kirchhoff-potentials, the circulation motivates the introduction of a particular harmonic field as well.

Definition 1.2.4. *Let us define by H the unique solution vanishing at infinity of the following harmonic problem*

$$\begin{cases} \nabla \cdot H = 0 & \text{in } \mathbb{R}^2 \setminus \mathcal{S}_0, \\ \nabla \times H = 0 & \text{in } \mathbb{R}^2 \setminus \mathcal{S}_0, \\ H \cdot \mathbf{n} = 0 & \text{on } \partial \mathcal{S}_0, \\ \displaystyle\int_{\partial \mathcal{S}_0} H \cdot \tau \, d\Sigma = 1. \end{cases} \tag{1.2.10}$$

The field H allows for the definition of the conformal center of the solid, yet another important geometric parameter.

Definition 1.2.5. *The conformal center* $\xi = (\xi_1, \xi_2)^\top$ *of the solid* $\mathcal{S}_0$ *is defined by*

$$\xi_1 + i\xi_2 = \oint_{\partial\mathcal{S}_0} zH^* \, dz, \tag{1.2.11}$$

where the integral is a complex line integral along the curve $\partial\mathcal{S}_0$.

With these definitions at our disposal, we have the following for an unbounded, bidimensional, irrotational flow (Theorem 2.2. of [Sue17])

Theorem 1.2.1. *The motion of a rigid body immersed in a two dimensional incompressible and irrotational perfect fluid can be described by the following equation*

$$(\mathcal{M}_g + \mathcal{M}_{gl,a})q'' + \langle \Gamma_{gl,a}, q', q' \rangle = \gamma q' \times B_{gl}. \tag{1.2.12}$$

Here

- *the Christoffel-symbol* $\Gamma_{gl,a}$ *is defined for* $p = (l, r)^\top$ *by*

$$\langle \Gamma_{gl,a}, p, p \rangle = -\begin{pmatrix} \mathcal{P}_a \\ 0 \end{pmatrix} \times p - r\mathcal{R}_\vartheta \mathcal{M}_{gl,a} \mathcal{R}_\vartheta^t \begin{pmatrix} 0 \\ l^\perp \end{pmatrix},$$

  where $\mathcal{P}_a$ *are the two first coordinates of* $\mathcal{R}_\vartheta \mathcal{M}_{gl,a} \mathcal{R}_\vartheta^t p$;

- *and* $B_{gl} = \mathcal{R}_\vartheta \begin{pmatrix} \xi^\perp \\ -1 \end{pmatrix}$.

  The fluid velocity is then determined as the unique solution of the associated div-curl system, namely

$$U(t,x) = R_\vartheta \left(\nabla(\Phi_{gl} \cdot q)(t, R_\vartheta^T(x-h)) + \gamma \nabla^\perp \psi_{\mathbb{R}^2}(t, , R_\vartheta^T(x-h)) \right) \tag{1.2.13}$$

For a proof, we refer to [Sue17].

1.2.1.3 The vanishing body problem for an unbounded fluid domain

We are interested in an asymptotic study in the sense that the body present in the system has a vanishingly small size. So, the rigid body initially occupies the domain $\mathcal{S}_0^\varepsilon = \varepsilon\mathcal{S}_0$ for $\varepsilon \in (0,1)$. This means that the solid at time t is given by

$$\mathcal{S}^\varepsilon(t) = R_{\vartheta(t)}\mathcal{S}_0^\varepsilon + h(t).$$

Then for a fixed ε, we may establish the same systems of equations as the ones presented in the previous part: (1.2.1)-(1.2.5) as well as (1.2.12).

The main interest is the asymptotic behavior of our variables as $\varepsilon \to 0$. For a fixed ε, we have U^ε solution of the Euler equations (1.2.1), and $(h^\varepsilon, \vartheta^\varepsilon)$ solutions to the Newton equations (1.2.2) with the appropriate boundary conditions. Notice that this general problem depends on how we define the relation of the data with ε.

The most notable interest is the definition of the inertia. We may distinguish two different cases depending on whether the body shrinks to a massive or a massless limit:

1. *The case of a point-mass particle:* the mass and the moment of inertia of the solid is assumed to have the form

$$\mu(\varepsilon) = \mu \quad \text{and} \quad \mathcal{I}(\varepsilon) = \varepsilon^2 \mathcal{I},$$

with $m > 0$ and $\mathcal{I} > 0$ fixed.

2. *The case of a massless point particle:* the mass and the moment of inertia of the solid is assumed to have the form

$$\mu(\varepsilon) = \varepsilon^\alpha \mu \quad \text{and} \quad \mathcal{I}(\varepsilon) = \varepsilon^{2+\alpha} \mathcal{I},$$

with $\mu > 0$, $\mathcal{I} > 0$, and $\alpha > 0$ fixed. In particular the case $\alpha = 2$ corresponds to the fixed solid density case, furthermore the limit case of $\alpha = 0$ would yield the point-mass particle.

The initial solid velocity $(\bar{h}_1^\varepsilon, \vartheta_1^\varepsilon) = (\bar{h}_1, \vartheta_1)$ is taken independently of ε. The circulation of the solid, γ is assumed to be a constant independent of ε as well.

We have the following for the massive (and for the massless) limit cases (Theorem 2.16. of [GMS18])

Theorem 1.2.2. *Let $\mathcal{S}_0 \subset \mathbb{R}^2$, $(\alpha > 0)$ $\gamma \in \mathbb{R}$ (respectively $\gamma \in \mathbb{R}^*$), $(\mu, \mathcal{I}) \in (0,\infty) \times (0,\infty)$, and $(\bar{h}_1, \vartheta_1) \in \mathbb{R}^2 \times \mathbb{R}$. Let, for each $\varepsilon > 0$, the solution $h^\varepsilon \in \mathcal{C}^\infty([0,\infty); \mathbb{R}^2)$ of equation (1.2.12) associated with an initial solid domain $\mathcal{S}_0^\varepsilon$, with $\mu(\varepsilon) = \mu$, $\mathcal{I}(\varepsilon) = \varepsilon^2 \mathcal{I}$ (respectively $\mu(\varepsilon) = \varepsilon^\alpha \mu$, $\mathcal{I}(\varepsilon) = \varepsilon^{2+\alpha} \mathcal{I}$, and initial data $q(0) = 0$, $p(0) = (\bar{h}_1, \vartheta_1)$. Then, for all $T > 0$, we have that as $\varepsilon \to 0$ in the case of a massive particle (respectively massless particle):*

- *h^ε converges to h weakly-* in $W^{2,\infty}([0,T]; \mathbb{R}^2)$ (respectively in $W^{1,\infty}([0,T]; \mathbb{R}^2)$);*
- *$\varepsilon \vartheta^\varepsilon$ converges to 0 weakly-* in $W^{2,\infty}([0,T]; \mathbb{R})$ (respectively in $W^{1,\infty}([0,T]; \mathbb{R}^2)$).*

Moreover, the limit time-dependent vector h satisfies the equation $\mu h'' = \gamma (h')^\perp$ (respectively $h' = 0$).

1.2.2 The case of a bounded fluid domain

From now on we take Ω a bounded, open, regular, connected, and simply connected domain of $\mathbb{R}^2$. This Ω will represent the domain of our fluid-solid system in the bounded

case. Initially the solid occupies a non-empty, closed, connected, and simply connected subset $\mathcal{S}_0 \subset \Omega$; without loss of generality, we can assume that $0 \in \Omega$ and the origin is the center of mass of the solid at the initial phase. Just as before, the solid at time t occupies the domain $\mathcal{S}(t)$ and the corresponding fluid domain is given by $\mathcal{F}(t) = \Omega \backslash \mathcal{S}(t)$.

For the new fluid domain, the incompressible, irrotational Euler equations (1.2.1) are still valid. The same holds for the equations describing the solid motion (1.2.2). The kinematic boundary condition on the solid boundary (1.2.4) still has to be verified, however the "rest at infinity" condition must be replaced by a second kinematic boundary condition, this time on the boundary $\partial\Omega$:

$$u \cdot \mathbf{n} = 0 \qquad \text{on } \partial\Omega. \tag{1.2.14}$$

It is essential to avoid collision with the boundary of the domain ($\partial\Omega$), thus we set

$$\mathcal{Q} = \{q \in \mathbb{R}^3 \ : \ \operatorname{dist}(\mathcal{S}(q), \partial\Omega) > 0\}.$$

By our assumptions, $0 = q(0) \in \mathcal{Q}$.

1.2.2.1 Reformulation as an ODE

One can reduce the fluid-system to an ODE in the bounded case in a similar fashion as it was presented previously in Theorem 1.2.1, although with more complicated terms (Theorem 2.2. of [GMS18]).

Theorem 1.2.3. *Let us take Ω open, regular, connected, and simply connected, a $\mathcal{S}_0 \subset \Omega$ closed initial solid domain. Let us suppose that $\gamma \in \mathbb{R}$, $(\bar{h}_1, \vartheta_1) \in \mathbb{R}^2 \times \mathbb{R}$, and that U_0 is a compatible initial fluid velocity, meaning that it is the unique vector field satisfying the following div-curl type system:*

$$\begin{cases} \nabla \cdot U_0 = 0, \quad \nabla \times U_0 = 0 & \text{in } \mathcal{F}_0 \\ U_0 \cdot \mathbf{n} = \left(\bar{h}_1 + \vartheta_1 x^{\perp}\right) \cdot \mathbf{n} & \text{for } x \in \partial\mathcal{S}_0, \\ \int_{\partial\mathcal{S}_0} U_0 \cdot \tau \, d\Sigma = \gamma, \\ U_0 \cdot \mathbf{n} = 0 \quad \text{for } x \in \partial\Omega. \end{cases} \tag{1.2.15}$$

There exists a $\mathcal{C}^\infty$ mapping $q \in \mathcal{Q} \mapsto \mathcal{M}_a(q) \in S_3^+(\mathbb{R})$, depending only on $\mathcal{S}_0$ and Ω, and $F \in \mathcal{C}^\infty(\mathcal{Q} \times \mathbb{R}^3; \mathbb{R}^3)$ depending only on $\mathcal{S}_0$, γ, and Ω, such that, up to the first collision, the motion of a rigid body immersed in a two dimensional incompressible and irrotational perfect fluid can be described by the following second order ordinary differential equation

$$(\mathcal{M}_g + \mathcal{M}_a(q))q'' + \langle \Gamma_a(q), q', q' \rangle = F(q, q'), \tag{1.2.16}$$

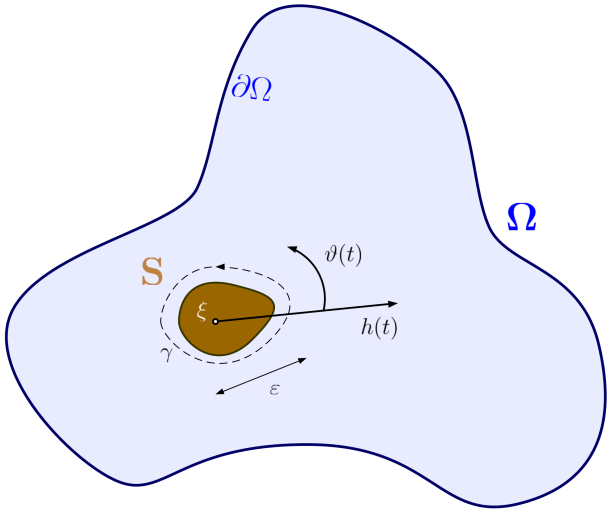

Figure 1.1 – The infinitesimally small object in a fluid domain

with Cauchy data

$$q(0) = 0 \in \mathcal{Q},\ p(0) = (\bar{h}_1, \vartheta_1)^\top \in \mathbb{R}^2 \times \mathbb{R}.$$

Here the assciated a-connection Γ_a *is given by*

$$\langle \Gamma_a(q), p, p\rangle = \left(\sum_{1\le i,j\le 3} (\Gamma_a(q))^k_{i,j} p_i p_j \right)_{1\le k\le 3} \in \mathbb{R}^3,$$

where for every $i, j, k \in \{1, 2, 3\}$ *we have*

$$(\Gamma_a(q))^k_{i,j} = \frac{1}{2}\left(\frac{\partial(\mathcal{M}_a)_{k,j}}{\partial q_i} + \frac{\partial(\mathcal{M}_a)_{k,i}}{\partial q_j} - \frac{\partial(\mathcal{M}_a)_{i,j}}{\partial q_k} \right)(q).$$

1.2.2.2 Derivation of the equations at first order

Now we address the derivation of the coupled problem (1.1.1) by means of the first order approximative system of equations (1.2.16) describing the solid movement. For detailed arguments, we refer to [GLS14].

We start from the differential geometric reformulation of the system (Theorem 1.2.3), recast for a shrunken solid of size ε, that is

$$\begin{cases} (q^\varepsilon)' = p^\varepsilon, & \text{(1.2.17a)} \\ \mathcal{M}^\varepsilon(q^\epsilon)(p^\epsilon)' = -\langle \Gamma^\epsilon(q^\varepsilon), p^\varepsilon, p^\varepsilon\rangle + F^\epsilon(q^\varepsilon, p^\varepsilon), & \text{(1.2.17b)} \end{cases}$$

for the position (q^ε) and velocity (p^ε) of the solid $\mathcal{S}^\varepsilon(t)$. The main idea is to perform an asymptotic expansion of the various terms in the equation with respect to ε. The

motivation for this is that the leading order terms in these asymptotic developments are in fact the corresponding global quantities presented in Section 1.2.1.2.

In order to establish proper boundedness, especially for properly estimating the error terms of the approximation, it is imperative to assure a safe distance from the boundary $\partial\Omega$. So we introduce the following:

Definition 1.2.6. *For $\delta > 0$, $\varepsilon_0 > 0$ let us define the set $\mathcal{D}_{\delta,\varepsilon_0}$ as follows*

$$\mathcal{D}_{\delta,\varepsilon_0} = \{(\varepsilon, q) \in (0, \varepsilon_0) \times \mathbb{R}^3 \Big| \operatorname{dist}(S^\varepsilon(q), \partial\Omega) > \delta\}.$$

By Proposition 3 of [GMS18], for $\delta > 0$ there exists a ε_0 and $H_r \in L^\infty(\mathcal{D}_{\delta,\varepsilon_0} \times \mathbb{R}^3; \mathbb{R}^3)$ (depending on $\mathcal{S}_0$, γ, and Ω, and weakly nonlinear) such that (1.2.17) has the following form

$$\begin{cases} (q^\varepsilon)' = p^\varepsilon, & \text{(1.2.18a)} \\ \mathcal{M}_g(\hat{p}^\epsilon)' = \gamma\tilde{p}^\varepsilon \times B_{gl} + \varepsilon H_r(\varepsilon, q^\varepsilon, \hat{p}^\varepsilon), & \text{(1.2.18b)} \end{cases}$$

with $\hat{p}^\varepsilon = \begin{pmatrix} l^\varepsilon \\ \varepsilon r^\varepsilon \end{pmatrix}$, and $\tilde{p} = \begin{pmatrix} \tilde{l}^\varepsilon \\ \varepsilon r^\varepsilon \end{pmatrix}$, where $\tilde{l}^\varepsilon = l^\varepsilon - \gamma u(h^\varepsilon)$.

By computing the vectorial product (see definition of B_{gl} in Theorem 1.2.1.) and by neglecting the higher order terms in (1.2.18), we are left with the analysis of the following system

$$\begin{cases} \mu(h^\varepsilon)'' = \gamma((h^\varepsilon)' - \gamma u(h^\varepsilon))^\perp & \text{(1.2.19a)} \\ \varepsilon\mathcal{I}(\vartheta^\varepsilon)'' = R_{\vartheta^\varepsilon}\xi \cdot ((h^\varepsilon)' - u(h^\varepsilon)), & \text{(1.2.19b)} \end{cases}$$

where we recall that R_ϑ is the rotation matrix by ϑ, ξ is the conformal center of the solid, and the function u is a given function depending on Ω. For $\gamma = \mathcal{I} = 1$ this gives rise to exactly (1.1.1).

1.2.2.3 The vanishing body problem for a bounded fluid domain

Finally, we state some recent results concerning the analysis of the vanishing body problem for a bounded domain ([GLS14],[GLS16]).

The massive limit: In order to be able to state an asymptotic result for the bounded regime, to define the limit equation for the solid displacement, recall the Kirchhoff–Routh velocity, u, defined by Definition 1.1.1, which is a generalization of the drift velocity known from the classical point-vortex system on $\mathbb{R}^2$.

We have that for a bounded domain Ω (Theorem 2.11. of [GMS18]):

Theorem 1.2.4. *Let $\mathcal{S}_0 \subset \Omega$, $\gamma \in \mathbb{R}$, $(\mu, \mathcal{I}) \in (0, \infty) \times (0, \infty)$, and $(\bar{h}_1, \vartheta_1) \in \mathbb{R}^2 \times \mathbb{R}$.*

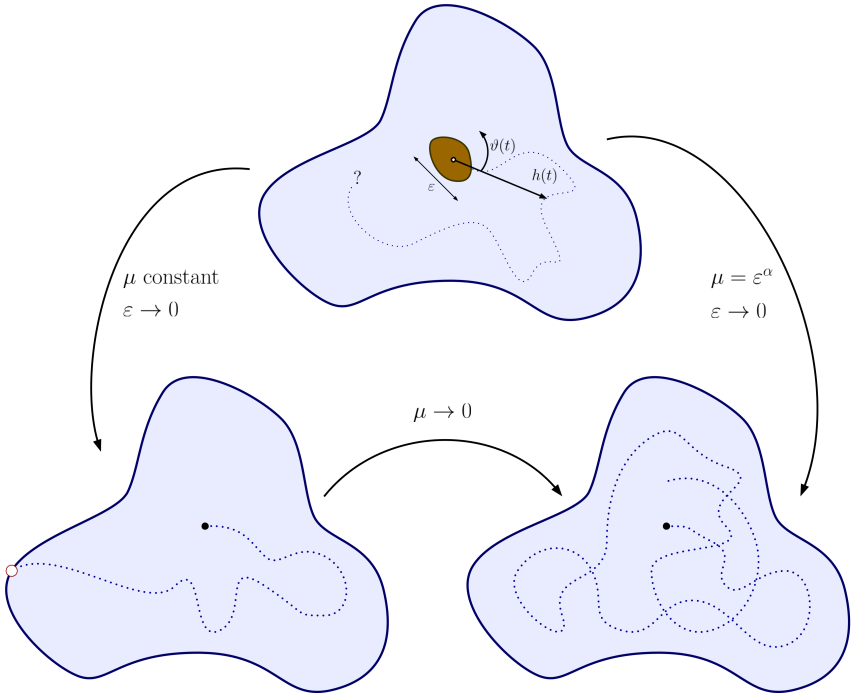

Figure 1.2 – The connection between the systems

Moreover, let (h, T) *be the maximal solution to*

$$\mu h''(t) = \gamma\Big(h'(t) - \gamma u(h(t))\Big)^\perp \tag{1.2.20}$$

with $h(0) = 0$ *and* $h'(0) = \bar{h}_1$.

Then, for every $\varepsilon \in (0, 1]$ *sufficiently small so that* $\mathcal{S}_0^\varepsilon \subset \Omega$, *we denote by* T^ε *the maximal lifetime of the solution given by Theorem 1.2.3. Thus we have that as* $\varepsilon \to 0$ $\liminf T^\varepsilon \geq T$, h^ε *converges to* h *weakly-* in* $W^{2,\infty}([0, T]; \mathbb{R}^2)$, *and* $\varepsilon\vartheta^\varepsilon$ *converges to* 0 *weakly-* in* $W^{2,\infty}([0, T]; \mathbb{R})$.

The massless limit: When Ω is a bounded domain, again supposing the fluid is irrotational, we have the following for any $\alpha > 0$ (Theorem 2.12. of [GMS18]):

Theorem 1.2.5. *Let* $\mathcal{S}_0 \subset \Omega$, $\gamma \in \mathbb{R}^*$, $(\mu, \mathcal{I}) \in (0, \infty) \times (0, \infty)$, *and* $(\bar{h}_1, \vartheta_1) \in \mathbb{R}^2 \times \mathbb{R}$. *Moreover, let* h *be the global solution to*

$$h'(t) = \gamma u(h(t)) \tag{1.2.21}$$

with $h(0) = 0$.

Then, for every $\varepsilon \in (0,1]$ sufficiently small so that $\mathcal{S}_0^\varepsilon \subset \Omega$, we denote by T^ε the maximal lifetime of the solution given by Theorem 1.2.3. Thus we have that as $\varepsilon \to 0$ $\liminf T^\varepsilon \to \infty$, and h^ε converges to h weakly- in $W^{1,\infty}([0,T];\mathbb{R}^2)$ for all $T > 0$.*

Remark 1.2.1. *Equation (1.2.21) has a global solution due to the Hamiltonian structure of the equation. Since*

$$\frac{d}{dt}\Big(\psi_\Omega(h(t))\Big) = h'(t)\cdot\nabla\psi_\Omega(h(t)) = \gamma\nabla^\perp\psi_\Omega(h(t))\cdot\nabla\psi_\Omega(h(t)) = 0,$$

the solutions are moving along the level sets of the Kirchhoff-Routh stream function, the particle cannot touch the border of the domain, and as such, there is no finite time explosion.

For further details and the proof of these theorems, we refer to [GMS18].

1.3 The zero-mass limit of the massive point-vortex system

The basis of the analysis is the point-vortex system; notice the right hand sides of equations (1.1.1a) and (1.1.1b), both are governed by the same quantity of the displacement vector. Therefore, a deeper qualitative understanding of this quantity is necessary; of particular interest will be whether it can become 0 or not. In this section we analyze the equation characterizing the solid displacement (equation (1.1.1a)) when the mass μ tends to 0.

1.3.1 The results of this section

Let us recall the classical (massless) **point-vortex system**:

$$\begin{cases} h_0'(t) = u(h_0(t)), \\ h_0(0) = \overline{h}_0, \end{cases} \tag{1.3.1}$$

with u the nonlinearity (given by Definition 1.1.1.) incorporating the evolution of the vortex motion within the fluid domain Ω. This is the well-known single vortex system and has been extensively studied. In particular, we have the following existence and uniqueness result, attributed to Turkington ([Tur87]).

Theorem 1.3.1. *For $\overline{h}_0 \in \Omega$, with $u \in \mathcal{C}^\infty(\Omega)$ the Kirchhoff–Routh velocity defined in Definition 1.1.1 there exists a unique solution $h_0 \in \mathcal{C}^\infty(0,+\infty;\Omega)$ of the system (1.3.1).*

We also introduce the following **massive point-vortex system**:

$$\begin{cases} \mu h''(t) = (h'(t) - u(h(t)))^{\perp}, \\ h(0) = \overline{h}_0, \quad h'(0) = \overline{h}_1, \end{cases} \tag{1.3.2}$$

with $\mu > 0$ corresponding to the mass of the object. We impose $\overline{h}_0 \in \Omega$ and $\overline{h}_1 \in \mathbb{R}^2$.

Notice that this system is of order 2 with two initial conditions, as compared to the classical point-vortex system (1.3.1) that is of order 1.

Similar to Theorem 1.3.1, we can establish existence and uniqueness for (1.3.2) as well:

Lemma 1.3.1. *For any $\overline{h}_0 \in \Omega$, $\overline{h}_1 \in \mathbb{R}^2$, and for any $\mu \in (0,1)$, there exists a unique (h, T_μ) maximal solution of (1.3.2) on the interval $(0, T_\mu)$, with $h \in \mathcal{C}^\infty([0, T_\mu); \Omega)$. Here T_μ denotes the first collision time between the particle and the boundary of the domain Ω.*

Proof: Let us fix $\mu \in (0,1)$. The right hand side of (1.3.2), as a functional of (t, h, v_μ), is continuous in time (since it is time-variable independent) and (locally) Lipschitz continuous in its other variables, due to the assured regularity (the object is initially inside Ω) for $h \in \Omega$. So by the Cauchy–Lipschitz theorem, there exists a unique local solution for some time $t \in (0, T_\mu)$. By defining the energy associated with this system as

$$E(x, y) = \frac{1}{2}\mu y^2 + \psi_\Omega(x),$$

with $\nabla\psi_\Omega = u^\perp$, it can be easily verified that this quantity is conserved, since

$$\frac{d}{dt}[E(h(t), h'(t))] = h''(t) \cdot \mu h'(t) + \nabla\psi_\Omega(h(t)) \cdot h'(t) = 0$$

by the equation. This implies that the velocity of the system can not become unbounded, thus the only possibility for the solution to explode in finite time is if h hits the boundary of Ω, thus making u (or equivalently ψ_Ω) become unbounded. So the maximal solution exists until the first collision with $\partial\Omega$. □

Observe that by letting the mass μ tend to 0, one formally expects to obtain (1.3.1) from equation (1.3.2). However obtaining a first order differential equation as the limit of a second order differential equation requires some attention. The question of the second initial data that disappears in the limit, in particular, will imply that for higher order convergence results, a compatibility condition has to arise. Furthermore, the existence time T_μ of the system (1.3.2) clearly depends on μ, and by the energy argument one could assume that in fact it tends to $+\infty$ as μ tends to 0. This will be addressed later on as well.

As implied by Lemma 1.3.1, for a precise analysis it is important to secure a safe distance from the boundary $\partial\Omega$. For this, let us introduce the followings:

Definition 1.3.1. *For $\delta > 0$ let us define the compact set*

$$\overline{D}_\delta = \{x \in \mathbb{R}^2 \Big| \operatorname{dist}(x, \partial\Omega) \geqslant \delta\},$$

as well as the existence time

$$T_{\mu,\delta} = \sup\{t \in (0, T_\mu) \Big| h(t) \in \overline{D}_\delta\}.$$

The main theorem of this section is the following:

Theorem 1.3.2. *Let $d \in \mathbb{N}$, $d > 1$ and let $\mu_0 > 0$, $\delta > 0$ sufficiently small. For $0 < \mu < \mu_0$, $1 \leqslant j \leqslant d$, $0 \leqslant k \leqslant d - j$, there exist $h_k(t) \in \mathcal{C}^\infty([0, \infty))$ and $h_{j,k}(t, \tau) \in \mathcal{C}^\infty([0, \infty), 2j\pi\mathbb{T})$, periodic in the second variable, and independent of μ; furthermore there exists $(h_R)_{\mu\in(0,\mu_0)}$ uniformly bounded in Lipschitz-norm in $[0, T_{\mu,\delta}]$ in the sense that for any $\delta > 0$ sufficiently small, we have that*

$$\sup_{\mu\in(0,\mu_0)} \sup_{t\in[0,T_{\mu,\delta}]} (\|h_R\|(t) + \|h_R'\|(t)) < +\infty,$$

such that for every $0 < \mu < \mu_0$, $t \in [0, T_{\mu,\delta}]$ we have

$$h(t) = h_0(t) + \sum_{k=1}^{d-1} \mu^k h_k(t) + \sum_{j=1}^{d} \sum_{k=0}^{d-j} \mu^{j+k} h_{j,k}\left(t, \frac{t}{\mu}\right) + \mu^{d-1} h_R. \tag{1.3.3}$$

The hearth of the proof of this theorem is based on the work of Berkowitz and Gardner ([BG59]) and it will take place in Section 1.3.2. The demonstration entails a thorough asymptotic expansion, formerly elaborated by Kruskal in [Kru58]. For now we state some straightforward consequences. First of all, let us turn our attention to the time of existence for the solutions h. We know that h_0 is a global solution to (1.3.1). We also have that up until the first collision that occurs at time T_μ, the exact solution h exists as well.

Corollary 1.3.1. *We have that $\liminf_{\mu\to 0} T_\mu = +\infty$.*

Proof: Let us choose an arbitrary μ. By (1.3.3), we have that for sufficiently small $\delta > 0$, $h(t) = h_0(t) + \mathcal{O}_{L^\infty}(\mu)$ for any $t \in [0, T_{\mu,\delta}]$. As such, there exists a K, independent of μ, such that $|h(t) - h_0(t)| \leqslant K\mu$.

Now let us fix $T > 0$ and denote by d_T the minimal distance between the solution $h_0(t)$ and the boundary of Ω (which is strictly positive), that is $d_T = \inf_{t\in(0,T)} \operatorname{dist}\Big(h_0(t), \partial\Omega\Big)$.

For $\mu \leqslant d_T/(2K)$ and for $t \leqslant \inf(T_{\mu,\delta}, T)$ we have that $\operatorname{dist}\Big(h(t), \partial\Omega\Big) > d_T/2$. Since $\lim_{\delta\to 0} T_{\mu,\delta} = T_\mu$, by the continuity in time, we have that $T_\mu > T$ or else we could extend the solution for a time $T_\mu + \epsilon$, with a small positive ϵ. This means that for every $\mu \leqslant d_T/(2K)$, $T_\mu > T$, and therefore $\overline{T} = \liminf_{\mu\to 0} T_\mu \geqslant T > 0$. However $T > 0$ was chosen arbitrarily, implying that in fact $\overline{T} = +\infty$. □

Now we turn our attention towards the exact nature of the convergence of h when $\mu \to 0$. To this end, let us first of all examine the initial data. We have that

$$h'(0) = \overline{h}_1 = h_0'(0) + \partial_\tau h_{1,0}(0,0) + \mathcal{O}_{L^\infty}(\mu),$$

implying that the initial data for the fast time scale variation of the first order oscillatory term is given by

$$\partial_\tau h_{1,0}(0,0) = \overline{h}_1 - h_0'(0) = \overline{h}_1 - u(\overline{h}_0). \tag{1.3.4}$$

This quantity can also be interpreted as a natural measure of compatibility of the two point-vortex systems (equations (1.3.1) and (1.3.2)) on the level of the initial conditions.

If we assume that this quantity is 0, in addition to the hypotheses of Theorem 1.3.2, then we can conclude in a straightforward way that

Corollary 1.3.2. *For every $T > 0$, if the compatibility condition $\overline{h}_1 = u(\overline{h}_0)$ is verified, we have that $h \xrightarrow{W^{1,\infty}} h_0$ over $(0,T)$.*

The details of this corollary as well as its proof will be elaborated in Section 1.3.3.

On the other hand, if the aforementioned compatibility condition is not verified, one can deduce first of all that

Corollary 1.3.3. *If $\overline{h}_1 \neq u(\overline{h}_0)$, then there exists $\mu_0 \in (0,1)$ such that for every $\delta > 0$, $\mu \in (0,\mu_0)$, and for any $t \in [0, T_{\mu,\delta}]$ $g(t) := h'(t) - u(h(t)) \neq 0$.*

This corollary has multiple implications. It will be an essential tool for the asymptotic analysis of Section 1.4. Furthermore it allows for a non-degenerate reformulation of the angular system, detailed in Section 1.4.1.

Also, for every $T > 0$ we remark that we can not have a convergence in $W^{1,\infty}$ for

$$h \xrightarrow{\mu \to 0} h_0 \quad \text{in } (0,T).$$

Indeed, the non-compatibility condition assumed in the corollary ($\overline{h}_1 \neq u(\overline{h}_0)$) implies that $\partial_\tau h_{1,0}$ has a non-zero norm, and as such it hinders the proper convergence of the derivative.

In fact, we can say even more concerning the right hand side of equation (1.3.2), provided that the difference $|\overline{h}_1 - u(\overline{h}_0)|$ is different from zero. We have the following proposition, that will be used in Section 1.5 to derive the results concerning the dynamics of the angular equation.

Proposition 1.3.1. *Let $|\overline{h}_1 - u(\overline{h}_0)| \neq 0$. Then the quantity $|g(t)| = |h'(t) - u(h(t))|$ changes monotonicity almost periodically, meaning that there exist λ and η positive real numbers, as well as two sequences of intervals, $I_n = [a_n - \eta, a_n + \eta]$ and $J_n = [b_n - \eta, b_n + \eta]$, with a_n and b_n increasing, such that $\frac{d}{dt}|g(t)| \geqslant \lambda$ on each I_n and $\frac{d}{dt}|g(t)| \leqslant -\lambda$ on each J_n.*

For the proof of this proposition, we refer to Section 1.3.4.

1.3.2 Proof of Theorem 1.3.2.

The main goal is to establish the asymptotic representation of the exact solution of the equation (1.3.2) up to an arbitrary order with uniformly bounded terms. The idea is to make use of the structural similarities with a system describing the motion of a charged particle in an electromagnetic field, and in particular apply the principles of the guiding center theory. In 1958 Kruskal ([Kru58]) formally derived an asymptotic development to arbitrary order for the corresponding system. By applying similar ideas regarding the construction of the asymptotic development as well as the arguments of Berkowitz and Gärdner ([BG59]) one can provide an adequate justification.

We will construct an approximation to the unique solution h for (1.3.2), bearing in mind the fact that we wish to recover h_0, solution to the classical point-vortex system (1.3.1) when $\mu \to 0$. One of the main issues is addressing the second boundary condition in (1.3.2), since $h_0'(0)$ is in general not equal to $\overline{h}_1$. This gave rise to the compatibility condition elaborated in Section 1.3.1 and the multiple different consequences of Theorem 1.3.2.

1.3.2.1 The guiding center approximation

The general idea is to introduce terms in the fast time variable to ensure that the compensation for h_0' can be done by terms that disappear in the asymptotic limit. The fast time variable $\tau = t/\mu$ arises naturally due to the smallness parameter in the second derivative term of equation (1.3.2), implying oscillations in this time scale.

One can be more precise, remarking the structural similarities of equation (1.3.2) with the equation characterizing the non-relativistic motion of a charged particle in an electromagnetic field ([Kru58]). The main idea is the so called "guiding-center approximation" according to which the motion of the particle can be approximated as a gyration (uniform circular motion) orthogonal to the magnetic field, of small radius but large frequency. For more details one can consult for example [Sul05].

Hence, a straightforward first approach would be to search an approximation of the form

$$h \simeq h_0 + \mu H\left(\frac{\cdot}{\mu}\right),$$

where h_0 verifies the classical point-vortex equation (1.3.1), providing for the finite velocity motion of the so called guiding center, and H is a periodic function (solution of a rotational equation), incorporating the uniform circular motion, dictated by solely the dynamics of the equation. The μ factor signifies that the motion is of small scale (small radius) and the τ fast time variable implies a high frequency motion.

The main issue is that this simple approach does not capture sufficiently the effect of higher order oscillatory terms on lower order terms, meaning that with this approach the error term is no longer bounded in Lipschitz norm. Furthermore, a straightforward generalization of the construction ceases to work starting from a second order approximation due to the fact that the nonlinear term (through the Taylor expansion of u) can no longer ensure the periodicity in the fast time variable on the $\mathcal{O}(\mu)$ scale.

Therefore, as part of the formulation by Kruskal, the periodicity in the fast time scale has to be prescribed. It is important for two reasons: first, it corresponds to the small radius circular motion expected by the aforementioned physical background of the equivalent system. Secondly the periodicity ensures boundedness over $[0, \infty)$ independently of the time scale, therefore one can avoid a situation where the function may explode at infinity in the fast time variable, which would imply that the existence time tends to 0 as μ tends to 0.

To guarantee the periodicity in τ, we will prescribe the fast time scale dependence as a linear combination of sine and cosine functions of τ. However, since the Taylor expansion involves many multiplications, it is more convenient to present this combination with the aid of complex analysis.

1.3.2.2 A higher order approximation

Let us fix $d \in \mathbb{N}$, $d > 1$. Following Kruskal, one writes:

$$h \simeq h_{App} := h_0 + \sum_{k=1}^{d-1} \mu^k H_{0,k}(t) + \sum_{j=1}^{d} \sum_{k=0}^{d-j} \mu^{j+k} \left(H_{j,k}(t) e^{ij\frac{t}{\mu}} + H_{-j,k}(t) e^{-ij\frac{t}{\mu}} \right), \qquad (1.3.5)$$

here $H_{0,k} \in \mathbb{R}^2$, $H_{j,k} \in \mathbb{C}^2$ for $|j| \geqslant 1$, making use of the inclusion $\mathbb{R}^2 \hookrightarrow \mathbb{C}^2$, and in particular $H_{-j,k} = H_{j,k}^*$ to ensure that the sum is real valued, the approximation is indeed in $\mathbb{R}^2$. The first index (j) corresponds to the period in the fast time scale (with $j = 0$ signifying that there is no dependence on τ) and the second index (k) measures how far one goes in the asymptotic development for each term.

Here, and in what follows, we will have to work with higher order derivatives of the function u. For $k \in \mathbb{N}$, $k \geqslant 1$ we denote by $\mathcal{D}^k u$ the total derivative of order k, as a k-linear function from $(\mathbb{R}^2)^k$ to $\mathbb{R}^2$. Owing to the matrix representation of linear maps, this definition can be extended in a straightforward way to the complex plane (associated of the linear map), therefore $\mathcal{D}^k u$ can also be interpreted as a k-linear map from $(\mathbb{C}^2)^k$ to $\mathbb{C}^2$, and it shall be denoted the same way, in order to avoid overcomplicating the notations.

We have to define the functions $H_{j,k}$ adequately in order to obtain the approximation of h. By substituting this approximation in equation (1.3.2) and by regrouping the terms according to the power of the factor μ as well as separating the terms based on the periodicity in the fast time variable (the power of the complex exponential) one obtains the characterizing equations. The definition is by induction based on $n = |j| + k$.

Remarks on the underlying linear operator: In order to establish the equations determining the terms associated to the fast time variation ($H_{j,k}$ for $|j| \geqslant 1$) in general, we have to use the following linear operator:

$$\mathrm{Op}\, w = \mathrm{Op}\begin{pmatrix} w_1 \\ w_2 \end{pmatrix} := -iw^{\perp} = \begin{pmatrix} iw_2 \\ -iw_1 \end{pmatrix} \qquad \text{for } w \in \mathbb{C}^2 \tag{1.3.6}$$

which is a bijective operator from $\mathbb{C}^2$ to $\mathbb{C}^2$ with eigenvalues ± 1 and eigenvectors

$$e_- = \begin{pmatrix} 1 \\ i \end{pmatrix}, \quad e_+ = \begin{pmatrix} 1 \\ -i \end{pmatrix}, \tag{1.3.7}$$

hence the corresponding projector operators on the respective 1 complex dimensional eigenspaces are

$$P_- = \frac{1}{2}(\mathrm{Id} - \mathrm{Op}), \quad P_+ w = \frac{1}{2}(\mathrm{Id} + \mathrm{Op}). \tag{1.3.8}$$

1.3.2.3 The initial steps

The first step ($n = 0$): For $n = 0$ one finds exactly the point vortex system (1.3.1), that is

$$(h_0')^{\perp} - u(h_0) = 0. \tag{1.3.9}$$

The initial condition is simply $h_0(0) = \overline{h}_0$ due to the zeroth order term in $h_{App}(0)$.

The second step ($n = 1$): Let us start with $H_{1,0}$. Since $H_{-1,0}$ is its complex conjugate, defining $H_{1,0}$ defines it as well. We have that $H_{1,0}$ verifies the following linear equation:

$$H_{1,0} + iH_{1,0}^{\perp} = 0, \tag{1.3.10}$$

from which one infers that

$$H_{1,0}(t) = c_{1,0}(t)\begin{pmatrix} 1 \\ -i \end{pmatrix}. \tag{1.3.11}$$

It is in fact the eigenvector e_+ of the associated linear operator (for more details, see below)Op. Here $c_{1,0}(t) \in \mathcal{C}^1(\mathbb{R}^+; \mathbb{C})$ is a complex valued function verifying the following complex scalar system of linear ordinary differential equations

$$2e_+ c_{1,0}'(t) + \mathcal{D}^1 u(h_0(t)) e_+ c_{1,0}(t) = 0. \tag{1.3.12}$$

The corresponding initial condition is determined by the initial data of $(h_{App})'$, since

$$(h_{App})'(0) = \bar{h}_1 = h_0'(0) + i(H_{1,0}(0) - H_{-1,0}(0)) + \mathcal{O}(\mu),$$

from which one can establish that

$$i(H_{1,0}(0) - H_{-1,0}(0)) = -2\mathfrak{Im}\, H_{1,0}(0) = \bar{h}_1 - h_0'(0).$$

Owing to the particular structure of $H_{1,0}$ we have

$$\begin{pmatrix} \mathfrak{Im}\, c_{1,0}(0) \\ -\mathfrak{Re}\, c_{1,0}(0) \end{pmatrix} = -\frac{1}{2}\left(\bar{h}_1 - h_0'(0)\right). \tag{1.3.13}$$

As for the $H_{0,1}$ term, following a straightforward computation, it verifies the following real valued linear ordinary differential equation:

$$H_{0,1}'(t) - \mathcal{D}^1(h_0(t))(H_{0,1}(t)) = -(h_0'')^{\perp}(t). \tag{1.3.14}$$

Let us look at the initial conditions. We have that

$$h_{App}(0) = \overline{h}_0 = h_0(0) + \mu(H_{0,1}(0) + H_{1,0}(0) + H_{-1,0}(0)) + \mathcal{O}(\mu^2).$$

Therefore, from the $\mathcal{O}(\mu)$ terms of $h_{App}(0)$ one obtains $H_{0,1}(0)$ as

$$H_{0,1}(0) = -H_{1,0}(0) - H_{-1,0}(0) = -2\mathfrak{Re}\, H_{1,0}(0) = \left(\bar{h}_1 - h_0'(0)\right)^{\perp}. \tag{1.3.15}$$

1.3.2.4 The induction step

Let us assume that we are at the n^{th} step ($n \geqslant 2$), that is, all $H_{j',k'}$ terms are already known for $|j'|+k' < n$. We have to distinguish three characteristically different cases: terms not involving τ_μ ($j = 0$), terms with the smallest period ($|j| = 1$), and the rest ($|j| > 1$). We have that the $|j| > 1$ terms arise as a solution of a linear algebraic equation, determined by terms of summed indices less than n. The $|j| \leqslant 1$ terms however are determined through first order linear ordinary differential equations, whose initial conditions are dictated by the initial conditions obtained from h_{App}, hence the order of determination (see also Figure 1.3).

For what follows, it is going to be necessary to determine the index set of the terms involved in the higher order terms of the Taylor expansion of u. Therefore let us define

$$\mathcal{N}_{j,l}^n := \left\{ \underline{i} \in (\mathbb{Z}\times\mathbb{N})^l; \sum_{m=1}^{2l} |i_m| = n,\ \sum_{m=1}^{l} i_{2m-1} = j,\ \forall m \in [l], |i_{2m-1}| + |i_{2m}| \geqslant 1 \right\}.$$

Here we made use of the notation $[l] := \{k \in \mathbb{N} : k \leqslant l\}$

Determining the $|j| > 1$ terms: As mentioned before, we obtain the characterizing equations for $H_{j,n-j}$ by collecting all the terms with a factor μ^{n-1} and $\exp(ij/\mu)$. They involve time derivative terms stemming from the two derivatives of h_{App} as well as many terms coming from the Taylor expansion of the nonlinearity u. Note that it is the $\mathcal{O}(\mu^{n-1})$ level equation that determines the terms of cumulative index n for the terms with a fast time dependence.

More exactly, one has the followings. For $j = n$ the only terms arising from the equation (1.3.22) are the time derivatives of the exponential factors of $H_{n,0}$, yielding

$$0 = -iH_{n,0}^{\perp}(t) - nH_{n,0}(t) = (\mathrm{Op} - n\,\mathrm{Id})H_{n,0}(t). \tag{1.3.16}$$

Since n is not an eigenvalue of Op for $n \geqslant 2$, we have an invertible operator, resulting in

$$H_{n,0} \equiv 0. \tag{1.3.17}$$

For $1 < j < n$ ($n \geqslant 3$) the equation incorporates the aforementioned operator but with a source term, namely we have that for $\mathcal{O}(\mu^n)$ for the $\exp(ij/\mu)$ terms

$$j(\mathrm{Op} - j\,\mathrm{Id})H_{j,n-j}(t) = R_{j,n-j}, \tag{1.3.18}$$

where

$$\begin{aligned} R_{n-1,1} =& (H'_{n-1,0})^{\perp}(t) - 2(n-1)iH'_{n-1,0}(t) - \mathcal{D}^1(h_0(t))(H_{n-1,0}(t))^{\perp}, \\ R_{j,n-j} =& (H'_{j,n-j-1})^{\perp}(t) - 2jiH'_{j,n-j-1}(t) - H''_{j,n-j-2}(t) - \mathcal{D}^1(h_0(t))(H_{j,n-j-1}(t))^{\perp} \\ & - \sum_{l=2}^{n-1} \sum_{\underline{i} \in \mathcal{N}_{j,l}^{n-1}} \mathcal{D}^l u(h_0(t)) \left(H_{i_1,i_2}(t), H_{i_3,i_4}(t), \ldots, H_{i_{2l-1},i_{2l}}(t)\right)^{\perp} \end{aligned}$$

which is a linear algebraic equation, the right hand side is already determined, since it only depends on terms of index less than n. Therefore the functions $H_{j,n-j}$ are given by $j^{-1}(\mathrm{Op} - j\,\mathrm{Id})^{-1}R_{j,n-j}$.

Determining the $j = 1$ term: Let us suppose that we are at an induction step n (with $n > 1$). The idea is the same as before, we determine $H_{1,n-1}$ by regrouping the terms with factors μ^{n-1} and $\exp(i/\mu)$.

Once again we will find ourselves with the operator $(\mathrm{Op} - \mathrm{Id})$ but contrary to the previous part, 1 is an eigenvalue, so we have to change our reasoning, we can no longer invert the operator.

We have that the corresponding characterizing equation is

$$(\mathrm{Op} - \mathrm{Id})H_{1,n-1}(t) = R_{1,n-1}, \tag{1.3.19}$$

where $R_{1,n-1}$ is defined by

$$\begin{aligned} R_{1,1} =&(H'_{1,0})^{\perp}(t) - 2iH'_{1,0}(t) - \mathcal{D}^1(h_0(t))(H_{1,0}(t))^{\perp}, \\ R_{1,n-1} =&(H'_{1,n-2})^{\perp}(t) - 2iH'_{1,n-2}(t) - H''_{1,n-3}(t) - \mathcal{D}^1(h_0(t))(H_{1,n-2}(t))^{\perp} \\ &- \sum_{l=2}^{n-1} \sum_{\underline{i}\in\mathcal{N}_{1,l}^{n-1}} \mathcal{D}^l u(h_0(t)) \left(H_{i_1,i_2}(t), H_{i_3,i_4}(t), \dots, H_{i_{2l-1},i_{2l}}(t)\right)^{\perp}, \end{aligned}$$

separating the cases $n = 2$, and $n > 2$. From this one can only determine part of $H_{1,n-1}$. Decomposing $\mathbb{C}^2$ into the eigenspaces associated with e_- and e_+ one writes

$$H_{1,n-1}(t) = c_{1,n-1}(t)e_+ + \tilde{c}_{1,n-1}(t)e_-. \tag{1.3.20}$$

Equation (1.3.19) defines the coefficient $\tilde{c}_{1,n-1}(t)$ associated with the other eigenvector of Op (e_-). In order to determine $c_{1,n-1}(t)$ one has to remark that (1.3.19) is not necessarily solvable. Indeed, a Fredholm-type criterion has to be satisfied in order to guarantee the existence of a solution of the linear equation. This criterion is nothing else than $R_{1,n-1} = P_+R_{1,n-1}$, that is the source term is in the eigenspace of the eigenvector e_+. Hence we are left with a recursive condition concerning the solvability, which in turn provides for the necessary differential equation to define $c_{1,n-1}(t)$.

By induction, $c_{1,n-2}(t)$ was defined such that $P_-R_{1,n-1} = 0$ is verified, which guarantees that we can solve (1.3.19) to obtain $\tilde{c}_{1,n-1}(t)$. Then, $c_{1,n-1}(t)$ is defined by the consecutive solvability condition, $P_-R_{1,n} = 0$, which is a complex scalar system of linear ordinary differential equations, having the form of

$$\begin{aligned} c'_{1,n-1}(t)e_+ + c_{1,n-1}(t)\mathcal{D}^1(h_0(t))(e_+) =& c''_{1,n-2}(t)e_+^{\perp} \\ &- \sum_{l=2}^{n} \sum_{\underline{i}\in\mathcal{N}_{1,l}^{n}} \mathcal{D}^l u(h_0(t)) \left(H_{i_1,i_2}(t), H_{i_3,i_4}(t), \dots, H_{i_{2l-1},i_{2l}}(t)\right)^{\perp}, \end{aligned}$$

where the additional terms on the right hand side have already been determined.

The initial condition, just as before, is provided by the initial value of $(h_{App})'$ for the $\mathcal{O}(\mu^{n-1})$ terms, that is

$$\begin{aligned} \mathfrak{Im}\, H_{1,n-1}(0) =& \frac{1}{2}H'_{0,n-1}(0) + \mathfrak{Re}\, H'_{1,n-2}(0) - \mathfrak{Im}\, H_{n,0}(0) \\ &+ \sum_{l=2}^{n-1} \left(\mathfrak{Re}\, H'_{l,n-l-1}(0) - \mathfrak{Im}\, H_{l,n-l}(0)\right) \end{aligned}$$

which defines $c_{1,n-1}(0)$ due to the special structure of $H_{1,n-1}$.

The ODE for the $j = 0$ term: Once again let us suppose that we are at the induction step n (with $n > 1$). In order to determine $H_{0,n}$ we collect the terms with a factor μ^n and

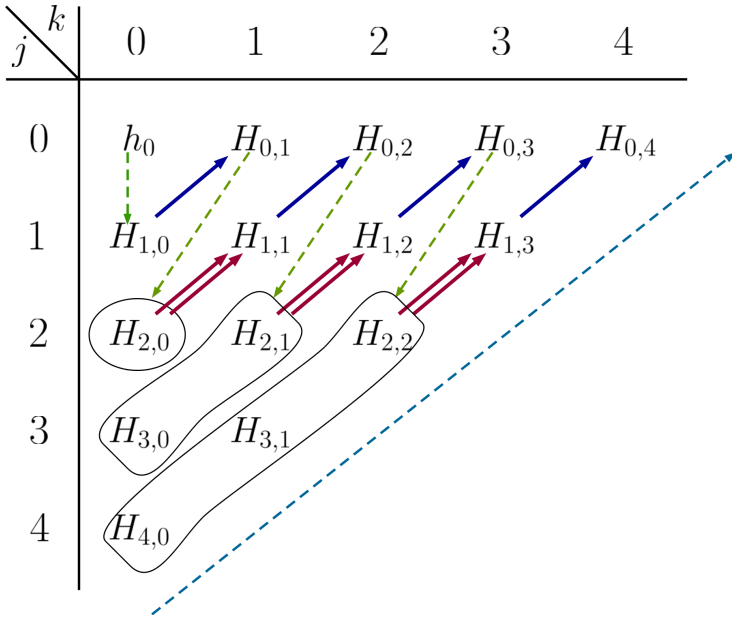

Figure 1.3 – The order of determination for the functions

without any exponential terms, resulting in

$$H'_{0,n}(t) - \mathcal{D}^1 u(h_0) H_{0,n}(t) = -(H''_{0,n-1})^\perp(t) - \sum_{l=2}^{n} \sum_{\underline{i} \in \mathcal{N}^n_{0,l}} \mathcal{D}^l u(h_0(t)) \left(H_{i_1,i_2}(t), H_{i_3,i_4}(t), \dots, H_{i_{2l-1},i_{2l}}(t) \right).$$

Notice that the right hand side only involves terms that have already been determined. Therefore this linear ordinary differential equation defines completely the term $H_{0,n}$. As for the initial condition, evaluating h_{App} at 0 on the $\mathcal{O}(\mu^n)$ level gives

$$H_{0,n}(0) = -2 \sum_{l=1}^{n} \mathfrak{Re}\, H_{l,n-l}(0). \tag{1.3.21}$$

With this all the terms have been defined for the induction step.

1.3.2.5 A summary on the approximation

The aim was to satisfy the massive point-vortex equation (1.3.2) up to order d in μ of the form

$$\begin{cases} \mu (h_{App})''(t) = ((h_{App})'(t) - u(h_{App}(t)))^\perp + \mathcal{O}_{L^\infty}(\mu^d), \\ h_{App}(0) = \overline{h}_0, \quad (h_{App})'(0) = \overline{h}_1. \end{cases} \tag{1.3.22}$$

Proposition 1.3.2. *For any $T > 0$ the approximative solution $h_{App} \in \mathcal{C}^\infty(0, +\infty)$ is bounded in Lipschitz-norm over $[0, T]$, moreover for $\delta > 0$ and $\mu \leqslant \mu_0$ sufficiently small,*

we have that $h_{App}(t) \in \overline{D}_\delta$ *for any* $t \in (0, T_{\delta,\mu})$.

Proof: The $\mathcal{C}^\infty$ regularity follows from the definition, since each term was defined by a linear or an algebraic equation. For any $T > 0$, by the defining equations, each term in h_{App} has bounded derivatives on $[0, T]$, since the derivatives of $u(h_0)$ are bounded on the respective interval. Thus the boundedness of the Lipschitz-norm is assured on any compact interval.

As for the distance to the boundary, let us choose δ such that

$$\delta < \frac{1}{2} \min_{t\in(0,\infty)} \operatorname{dist}(h_0(t), \partial\Omega).$$

Then, since $H_{j,k}$ are bounded on any $(0, T)$ with $T > 0$, we can choose $\mu \leqslant \mu_0$ sufficiently small such that for the remainder term

$$\mu \sup_{t\in(0,T_{\mu_0})} \left| \sum_{k=1}^{d-1} \mu^{k-1} H_{0,k}(t) + \sum_{j=1}^{d} \sum_{k=0}^{d-j} \mu^{j+k-1} \left(H_{j,k}(t) e^{ij\frac{t}{\mu}} + H_{-j,k}(t) e^{-ij\frac{t}{\mu}} \right) \right| < \frac{1}{2}\delta.$$

□

1.3.2.6 Error estimate

The approximation constructed in the previous part satisfies the massive point-vortex system (1.3.2) up to an error term of order d. Now, with an error term h_R, we write

$$h(t) = h_{App}(t) + \mu^{d-1} h_R(t). \tag{1.3.23}$$

Notice that albeit the approximation was up to order d, we allow for errors in the μ^{d-1} scale.

By working on $[0, T_{\mu,\delta}]$ we are assured that the solution stays away from the boundary of Ω, as such no regularity issues arise from the nonlinearity u. Therefore, the $u(h)$ term is developed according to a first order Taylor expansion with an exact error term around h_{App}, as a real vector. In order to avoid regularity issues with u, it is necessary to work on the compact subset $\overline{D}_\delta \subset \Omega$ for a δ chosen to be sufficiently small. Thus for $h \in \overline{D}_\delta$

$$u(h) = u(h_{App}) + \mu^{d-1} r_u(h, h_R), \tag{1.3.24}$$

where r_u is the first order remainder term, a $(2, 0)$ tensor over $\mathbb{R}^2$ with coordinate functions

$$r_u(h, h_R)_i = \sum_{\substack{\beta\in\mathbb{N}^2,\\ |\beta|=1}} r_{i,\beta}(h) h_R^\beta,$$

$$r_{i,\beta}(h) = \int_0^1 (1-s) D^\beta \partial_i u(h_{App} + s h_R)\, ds,$$

for $i \in \{1,2\}$, where $\beta \in \mathbb{N}^2$ is a multi-index and D^β is the corresponding partial derivative operator.

Remark 1.3.1. *For the Taylor expansion, we used an exact integral remainder term. It is worth mentioning that we have the following uniform estimate:*

$$|r_{i,\beta}(x)| \leqslant \max_{|\alpha|=|\beta|} \max_{y\in\overline{D}_\delta} |D^\alpha \partial_i u(y)| \text{ for } x \in \overline{D}_\delta$$

By substituting into the massive point-vortex system (1.3.2) and regrouping the terms, we obtain the equation characterizing the error term:

$$\begin{cases} \mu(h_R)'' = ((h_R)')^\perp + r_u(h, h_R) + \mu r_{App}(t), \\ h_R(0) = (h_R)'(0) = 0. \end{cases} \tag{1.3.25}$$

Here we introduced the error of the approximation as $\mu^d r_{App}(t)$, quantifying the $\mathcal{O}_{L^\infty}(\mu^d)$ term of (1.3.22), namely

$$\mu^d r_{App}(t) = \sum_{k=d}^{d^2} \mu^k \sum_{j=-d^2}^{d^2} \sum_{l=2}^{d} \sum_{\underline{i}\in\mathcal{N}_{j,l}^k} e^{ij\frac{t}{\mu}} \mathcal{D}^l u(h_0(t)) \left(H_{i_1,i_2}(t), H_{i_3,i_4}(t), \dots, H_{i_{2l-1},i_{2l}}(t)\right)^\perp.$$

Notice that the time derivative of r_{App} is of order μ^{d-1} due to the fast timescale dependence, this is the reason why we had to approximate up to an order of μ^d.

Now we turn our attention towards analyzing this system. One may observe that the system (1.3.25) has the same structure as the original massive point-vortex system, only with some additional terms. It is at this point that we will make use of the results of Berkowitz and Gardner ([BG59]).

First, we can rewrite equation (1.3.25) as follows:

$$\begin{cases} \mu(h_R)''(t) = E(t, h_R; \mu) + ((h_R)')^\perp(t), \\ r(0) = 0, \quad r'(0) = 0, \end{cases} \tag{1.3.26}$$

with

$$E(t, h_R; \mu) = r_u(h, h_R) + \mu r_{App},$$

where, according to the definition of r_u, it is an affine function of h_R. Furthermore, we can also deduce that E is continuous in time and is well defined on $[0, T_{\mu,\delta}]$.

To ascertain correctly the solvability of the system, let us first show the uniform boundedness of the variable of the system (1.3.25).

Proposition 1.3.3. *Let h_R be a solution of the equation (1.3.25). Then we have that for $\delta > 0$*

$$\forall t \in [0, T_{\mu,\delta}]; \quad h_R(t) = \mathcal{O}_{L^\infty}(1), \quad (h_R)'(t) = \mathcal{O}_{L^\infty}(1), \tag{1.3.27}$$

meaning the solution and its derivative are uniformly bounded in μ. Here $T_{\mu,\delta}$ denotes the maximal time of existence for the solution inside the compact subset of Ω which of distance at least δ away from its boundary $\partial\Omega$.

Proof: Making use of the formulation introduced in (1.3.26), we can write it as a system

$$\begin{cases} (h_R)' = v_R, \\ (v_R)' = \dfrac{1}{\mu}E(t, h_R; \mu) + \dfrac{1}{\mu}(v_R)^{\perp}. \end{cases} \tag{1.3.28}$$

By introducing the so called drift velocity

$$V = V(t, h_R) = (E(t, h_R; \mu))^{\perp}, \tag{1.3.29}$$

with a shift in the velocity variable: $w := v_R - V$ we can rewrite system (1.3.28):

$$\begin{cases} (h_R)' = w + V, \\ w' = \dfrac{1}{\mu}w^{\perp} - V'. \end{cases} \tag{1.3.30}$$

Remark 1.3.2. *The notation E and the term called drift velocity are not a coincidence. They indicate the connection between system (1.3.26) and the equation describing the movement of a particle in an electromagnetic field, treated in [BG59]. In fact, if we looked at our system as a 3-dimensional system having 0s as the third coordinates, the $^{\perp}$ operator could be interpreted as a vectorial product with the vector $B = (0, 0, 1)^{\top}$. In this sense, the drift velocity introduced before is just*

$$V = \frac{E \times B}{|B|^2}.$$

We remark that in our system, we have $E \cdot B = 0$ which simplifies the case of Berkowitz and Gardner.

Making use of some simple computations, one may see that

$$\frac{d}{dt}(V(t, h_R(t))) = \partial_t V + ((V + w) \cdot \nabla_{h_R})V.$$

Thus, multiplying the second equation of (1.3.30) by w, we get

$$\frac{1}{2}\frac{d}{dt}(|w|^2) = -w \cdot \partial_t V - w \cdot ((V + w) \cdot \nabla_{h_R})V. \tag{1.3.31}$$

Furthermore, by multiplying the first equation of (1.3.30) by h_R, and adding it to the

previous one, we obtain

$$\frac{1}{2}\frac{d}{dt}(|h_R|^2)+\frac{1}{2}\frac{d}{dt}(|w|^2)=w\cdot h_R+V\cdot h_R-w\cdot\partial_t V-w\cdot((V+w)\cdot\nabla_{h_R})V. \quad (1.3.32)$$

The right hand side is a quadratic polynomial in (h_R,w) with coefficients polynomial in μ, bounded in time over $t\in[0,T_{\mu,\delta}]$ and in spatial variables. This means that for some constant a_0,a_1,a_2 independent of h_R, t, and μ one may write

$$\frac{d}{dt}(|h_R|^2)+\frac{d}{dt}(|w|^2)\leqslant a_1|h_R|^2+a_2|w|^2+a_0, \quad (1.3.33)$$

so by Grönwall's inequality

$$|h_R|^2+|w|^2(t)\leqslant e^{\max(a_1,a_2)t}(|h_R|^2(0)+|w|^2(0))+\frac{a_0}{\max(a_1,a_2)}(e^{\max(a_1,a_2)t}-1), \quad (1.3.34)$$

implying a uniform bound on w and on h_R for any $t\in[0,T_{\mu,\delta}]$.

So, by definition, v_R is also uniformly bounded over $[0,T_{\mu,\delta}]$ (since V is bounded independently of μ). □

With this at our disposal, we are assured that system (1.3.25) admits a unique solution over $[0,T_{\mu,\delta}]$, since a local solution is given, once again, by the Cauchy–Lipschitz theorem, and the boundedness of h_R and $(h_R)'$ implies that this local solution extends to the whole interval at hand.

1.3.3 The proof of the convergence results

Now we proceed with the proof of Corollary 1.3.2. Let us assume the compatibility condition

$$\overline{h}_1=u(\overline{h}_0).$$

Let us examine the term $H_{1,0}$ of the approximation (1.3.5) involved in the fast timescale development. We have that $H_{1,0}(t)=c_{1,0}(t)e_+$, moreover the coefficient $c_{1,0}$ is defined by a linear ordinary differential equation (1.3.12) without a source term, whose initial condition is given by (1.3.13). By our assumption, this quantity is zero, therefore $c_{1,0}\equiv 0$.

This means that $H_{1,0}\equiv 0$, the fast time scale compensation disappears at first order, guaranteeing a convergence in $W^{1,\infty}$.

We cannot say more about convergence due to the influence of the slow time quantities on the fast time scale for the higher order terms. This can be easily seen from the defining equation of $H_{0,1}$ (1.3.14). It is also a linear ordinary differential equation, but with a source term $-(h_0'')^\perp$ which is not constant zero. Even though the initial condition given by (1.3.15) is also 0 due to the assumption on the compatibility condition, the solution of the system, $H_{0,1}$ is not constantly zero.

Moreover, for the $n = 2$ terms, we have that $H_{2,0} \equiv 0$, and that $H_{0,2}$ is not zero for the same reason as $H_{0,1}$. Finally, $H_{1,1}$ is not guaranteed to be zero either. This is deduced from the corresponding initial condition

$$\mathfrak{Im}\, H_{1,1}(0) = \frac{1}{2} H'_{0,1}(0) + \mathfrak{Re}\, H'_{1,0}(0)$$

that is not 0 due to the first term.

These imply that from $n \geqslant 2$ the source terms $R_{j,n-j}$ contain nonzero terms as well, which prevent us from establishing convergence results incorporating higher order derivatives.

1.3.4 The proof of the quasi-periodicity

In order to prove Proposition 1.3.1. and Corollary 1.3.3. we turn our attention towards the right hand side of the equation (1.3.2). The quantity we would like to examine is

$$g(t) := h'(t) - u(h(t)).$$

Let us prove first of all Corollary 1.3.3. Owing to Theorem 1.3.2, and in particular to the approximation defined in (1.3.5), one has that

$$(h_{App})'(t) = h'_0(t) + i(H_{1,0}(t)e^{i\frac{t}{\mu}} - H_{-1,0}(t)e^{-i\frac{t}{\mu}}) + \mathcal{O}_{L^\infty}(\mu),$$

as well as

$$u(h_{App}(t)) = u(h_0(t)) + \mathcal{O}_{L^\infty}(\mu).$$

This means that we have

$$g(t) = i(H_{1,0}(t)e^{i\frac{t}{\mu}} - H_{-1,0}(t)e^{-i\frac{t}{\mu}}) + \mu H_R, \tag{1.3.35}$$

with H_R bounded over $[0, T]$ for every $T > 0$. Here we made use of the point-vortex equation (1.3.9). It is clear that the first term is dominant, since by choosing μ sufficiently small the remainder term can be chosen arbitrarily small.

Following a straightforward computation, one has that

$$i(H_{1,0}(t)e^{i\frac{t}{\mu}} - H_{-1,0}(t)e^{-i\frac{t}{\mu}}) = -2\mathfrak{Im}\left(H_{1,0}(t)e^{i\frac{t}{\mu}}\right) = -2R_{\frac{\pi}{2}-\frac{t}{\mu}} \begin{pmatrix} \mathfrak{Re}\, c_{1,0}(t) \\ \mathfrak{Im}\, c_{1,0}(t) \end{pmatrix}, \tag{1.3.36}$$

with $R_{\frac{\pi}{2}-\frac{t}{\mu}}$ being the rotational matrix by the angle $(\pi/2 - t/\mu)$.

From the assumption of the non-compatibility condition $\overline{h}_1 \neq u(\overline{h}_0)$, one can deduce by (1.3.13) that the initial condition $c_{1,0}(0)$ is not 0, implying that $c_{1,0}(t)$, a solution of a homogeneous linear ODE, is never 0. Therefore the aforementioned quantity (1.3.36),

being a rotation of this vector, will never be zero either. This concludes the proof of this corollary. □

By the approximative solution (1.3.5), we have that for $\delta > 0$ sufficiently small, for $t \in [0, T_{\mu,\delta}]$

$$\begin{aligned}|g(t)| = \Big| & i(H_{1,0}(t)e^{i\frac{t}{\mu}} - H_{-1,0}(t)e^{-i\frac{t}{\mu}}) + \mu H'_{0,1}(t) \\ & + \mu(H'_{1,0}(t)e^{i\frac{t}{\mu}} + H'_{-1,0}(t)e^{-i\frac{t}{\mu}}) + \mu i(H_{1,1}(t)e^{i\frac{t}{\mu}} - H_{-1,1}(t)e^{-i\frac{t}{\mu}}) \\ & - \mathcal{D}^1 u((h_0)(t)) \left(H_{0,1}(t) + H_{1,0}(t)e^{i\frac{t}{\mu}} + H_{-1,0}(t)e^{-i\frac{t}{\mu}}\right) + \mu\mathcal{R}(t)\Big|\end{aligned}$$

where $\mathcal{R}$ is regular and uniformly bounded in Lipschitz norm on $[0, T_{\mu,\delta}]$. We made use of equation (1.3.9) to eliminate the other $\mathcal{O}(1)$ terms with respect to μ.

Remark 1.3.3. *Owing to the uniform boundedness of $\mathcal{R}$ on $[0, T_{\mu,\delta}]$ as well as the global regularity of h_0, $H_{0,1}$, and $H_{\pm 1,0}$, we have that for sufficiently small μ the value $|N(t)|$ is almost constant, equaling approximatively to*

$$\left|H_{1,0}(t)e^{i\frac{t}{\mu}} - H_{-1,0}(t)e^{-i\frac{t}{\mu}}\right|,$$

as it was established in Corollary 1.3.3.

We aim to prove a statement concerning the monotonicity of $|g(t)|$. For that, let us calculate the derivative. We have that

$$\begin{aligned}\frac{d}{dt}|g(t)| &= \frac{1}{|g(t)|} g(t) \cdot g'(t) \\ &= \frac{1}{|g(t)|}\left(-\frac{i}{\mu}\left(H_{1,0}(t)e^{i\frac{t}{\mu}} - H_{-1,0}(t)e^{-i\frac{t}{\mu}}\right) \cdot \left(H_{1,0}(t)e^{i\frac{t}{\mu}} + H_{-1,0}(t)e^{-i\frac{t}{\mu}}\right) + \overline{\mathcal{R}}(t)\right)\end{aligned}$$

where $\bar{\mathcal{R}}$ is bounded on $[0, T_{\mu,\delta}]$. Hence

$$\frac{d}{dt}|g(t)| = \frac{|H_{1,0}(t)|^2}{|g(t)|}\frac{2}{\mu}\sin\frac{2t}{\mu} + \mathcal{O}_{L^\infty}(1).$$

The first term is dominant for small values of μ, moreover, since its first factor is always positive, the sign is determined entirely by the sine function, which is $\mu\pi$ periodic. Hence, by choosing λ sufficiently small and I_n and J_n subintervals of each period of length $\mu\pi$, we can conclude. □

1.4 Multiple-scale analysis of the angular equation

Now we turn our attention towards the second part of the asymptotic analysis, that is the study of the equation characterizing the angle (equation (1.1.1b)). Here our analysis concerns the parameter ε tending to 0.

1.4.1 An adapted scaling for the angular equation

One of the first issues is to determine a good scaling for the variables with respect to ε. Just as before, remark the presence of the smallness parameter in the term involving the second derivative, that is, we have $\varepsilon(\vartheta)''$.

Let us suppose that $h(t)$ is already given (determined by equation (1.1.1a)) and let us look at the equation of the angle (1.1.1b). We get that

$$\varepsilon(\vartheta)''(t) = R_{\vartheta(t)}\xi \cdot (h'(t) - u(h(t))),$$

where $((h)'(t) - u(h(t)))$ is now a given function of time and $R_{\vartheta(t)}\xi$ is a periodic function of ϑ since it is a linear combination of sine and cosine functions. If we set $\Theta(t) = \vartheta(\varepsilon^{1/2}t)$, we get

$$\frac{d^2}{d\tau^2}\Theta(\tau) = R_{\Theta(\tau)}\xi \cdot (h'(\sqrt{\varepsilon}\tau) - u(h(\sqrt{\varepsilon}\tau))) \tag{1.4.1}$$

by defining the fast time variable as $\tau = \varepsilon^{-1/2}t$. The presence of two different timescales, the fast time τ and the slow time t, in the equations foreshadows nontrivial (asymptotic) dynamical properties.

Nevertheless, this means that a reasonable scale for the angle, motivated by equation (1.1.1b) is $\sqrt{\varepsilon}$.

Let us elaborate the influence of the point-vortex system on the angular system. Recalling that $g(t) = h'(t) - u(h(t))$, we reformulate equation (1.1.1b). We have that

$$\begin{aligned} R_{\Theta(\tau)}\xi \cdot g(t) &= \begin{pmatrix} \cos\Theta(\tau)\xi_1 - \sin\Theta(\tau)\xi_2 \\ \sin\Theta(\tau)\xi_1 + \cos\Theta(\tau)\xi_2 \end{pmatrix} \cdot \begin{pmatrix} g_1(t) \\ g_2(t) \end{pmatrix} \\ &= (\xi_1 g_1(t) + \xi_2 g_2(t))\cos\Theta(\tau) + (\xi_1 g_2(t) - \xi_2 g_1(t))\sin\Theta(\tau) \\ &= \xi^{\perp} \cdot g(t)\sin\Theta(\tau) + \xi \cdot g(t)\cos\Theta(\tau) \\ &= |\xi||g(t)|\sin(\Theta(\tau) + \alpha(t)), \end{aligned}$$

where $\alpha(t)$ is the oriented angle of the constant $\xi^{\perp}$ vector and $g(t)$, a continuous function from $\mathbb{R}^+$ to $\mathbb{R}$ with $\alpha(0) \in (-\pi, \pi]$.

The right hand side of (1.1.1b) becomes constant 0 if either $\xi = 0$ or $g(t) \equiv 0$. The first case can be excluded since ξ is a geometric constant of the solid, we suppose that it is not 0 (in order to observe nontrivial geometric effects). The second case is excluded by

Corollary 1.3.3. based on our hypothesis concerning the non-compatibility condition.

Remark 1.4.1. *The function $g(t)$ is well-defined for $t \in [0, T_{\mu,\delta}]$. Owing to Corollary 1.3.1. the time $T_{\mu,\delta}$ can be chosen arbitrarily large by setting μ and δ sufficiently small. Let us take an arbitrary $T > 0$ such that $T < T_{\mu,\delta}$ for sufficiently small μ and δ.*

1.4.2 The modulated phase shift

An important observation concerning the angular equation (1.1.1b) is that physically speaking it falls into the type of equations which may experience modulated oscillations, which means that the right hand side gives a (nearly) periodic structure over a time interval comparable to a few cycles (in τ), however after sufficiently long time, the local parameters with respect to the amplitude, frequency and even the shape can experience significant changes ([Neu15]). This is even more apparent if one looks at equation (1.4.1) where both the slow time variable t and the fast time variable τ are present in the equations.

Systems with these type of strongly nonlinear slowly varying oscillators have already been analyzed ([Kuz59], [Luk66]), we adapt one of the more recent techniques, detailed in [BH88] and aptly called the modulated phase shift.

The aim is to introduce a phase shift alongside with the scaling $\sqrt{\varepsilon}$ in order to avoid secular terms in the development. The equation concerning the angle (1.4.1), writes as

$$\frac{d^2}{d\tau^2}\Theta(\tau) - R_{\Theta(\tau)}\xi \cdot g(t) = 0, \tag{1.4.2}$$

or equivalently

$$\frac{d^2}{d\tau^2}\Theta(\tau) - |\xi||g(t)|\sin(\Theta(\tau) + \alpha(t)) = 0. \tag{1.4.3}$$

Here τ is the fast time variable and $t = \sqrt{\varepsilon}\tau$ is the slow time variable. This is a second order nonlinear ODE, whose second term can be interpreted as a nonlinear term coming from the potential $V(\Theta, t)$, where

$$V(\Theta, t) = R_{\frac{\pi}{2}+\Theta}\xi \cdot g(t) = |\xi||g(t)|\cos(\Theta + \alpha(t)),$$

since with this choice, we have that

$$\partial_\Theta V(\Theta, t) = -R_\Theta \xi \cdot g(t).$$

Notice that for a fixed t equation (1.4.1) admits a periodic solution for Θ. The reasoning for this is as follows: presented in the form of (1.4.3) it is a pendulum type system (for more details, see also Section 1.5). More precisely, Theorem 1 of [KO85] applies due to the fact that $g(t)$ is bounded (by Corollary 1.3.3), $V(\Theta, t)$ is bounded and periodic in Θ. More precisely, we have that ([BPVM+06]):

Lemma 1.4.1. *For any $t \in \mathbb{R}^+$, $\vartheta_0 \in (-\pi, \pi)$ there exists a family $(\tilde{\Theta}(\tau, t)_{f\in\mathbb{R}}$ of periodic solutions to the problem*

$$\begin{cases} f^2\partial^2_{\tau\tau}\tilde{\Theta} + \partial_\Theta V(\tilde{\Theta}, t) = 0, \\ \tilde{\Theta}(0,t) = \vartheta_0, \quad \partial_\tau\tilde{\Theta}(0,t) = 0. \end{cases} \tag{1.4.4}$$

Moreover the unique solution $\tilde{\Theta}$ depends on f in a continuously differentiable manner.

The energy associated with (1.4.4) for any $t \in \mathbb{R}^+$ is

$$\tilde{E}(t) = \frac{1}{2}f^2(\partial_\tau\tilde{\Theta})^2 + V(\tilde{\Theta}, t). \tag{1.4.5}$$

It is obtained by multiplying (1.4.4) with $\partial_\tau\tilde{\Theta}$ and integrating with respect to τ. From this one can deduce the extrema of $\tilde{\Theta}(\tau; t)$, that are independent of the value of f. For an extremum $\bar{\Theta}$, we have that

$$\tilde{E}(t) = V(\bar{\vartheta}, t) = |\xi||g(t)|\cos(\bar{\Theta} + \alpha(t)),$$

that admits two solutions on the interval $(-\pi, \pi]$ which correspond to the minimum (Θ_{min}) and the maximum values (Θ_{max}), defined by

$$\Theta_{min,max} = \pm\arccos\left(\frac{\tilde{E}(t)}{|\xi||g(t)|}\right) - \alpha(t). \tag{1.4.6}$$

It is clear to see that $\Theta_{min,max} = \Theta_{min,max}(\tilde{E}(t), t)$ depends on t and $\tilde{E}(t)$ continuously.

Also, in order to make sense of formula (1.4.6), one needs to consider the domain of definition of arccos being $[-1, 1]$, which imposes an upper and lower bound for the energy functional in the case when a periodic solution exists:

$$|\tilde{E}(t)| < |\xi||g(t)|. \tag{1.4.7}$$

By the formal construction of [BH88], the main result of this section is the following theorem:

Theorem 1.4.1. *There exist $\phi \in \mathcal{C}^\infty(\mathbb{R}^+)$, $\theta \in \mathcal{C}^\infty(\mathbb{R}^+)$, as well as $\Theta^0 \in \mathcal{C}^\infty((-\pi, \pi] \times \mathbb{R}^+)$, $\Theta^1 \in \mathcal{C}^\infty((-\pi, \pi] \times \mathbb{R}^+)$ periodic with respect to their first variable, such that for $\tau \in [0, T]$*

$$\Theta_A(\tau) := \Theta^0\left(\frac{\theta(\sqrt{\varepsilon}\tau)}{\sqrt{\varepsilon}} + \phi(\sqrt{\varepsilon}\tau), \sqrt{\varepsilon}\tau\right) + \sqrt{\varepsilon}\Theta^1\left(\frac{\theta(\sqrt{\varepsilon}\tau)}{\sqrt{\varepsilon}} + \phi(\sqrt{\varepsilon}\tau), \sqrt{\varepsilon}\tau\right) \tag{1.4.8}$$

that satisfies

$$\begin{cases} \partial^2_{\tau\tau}\Theta_A(\tau) = R_{\Theta_A(\tau)}\xi \cdot g(t) + \mathcal{O}_{L^\infty}(\varepsilon), \\ \Theta_A(0) = \vartheta_0 + \mathcal{O}_{L^\infty}(\varepsilon), \quad \partial_\tau\Theta_A(0) = \mathcal{O}_{L^\infty}(\varepsilon). \end{cases} \tag{1.4.9}$$

1.4.3 Proof of the asymptotic development

As mentioned before, we follow the ideas presented in [BH88], but in a more structured manner. Also, some of the computations were adapted to fit our system. The structure of the proof is as follows:

1. *Definition of the energy:* We define the energy associated with the nonlinear oscillator equation (1.4.4) and establish the bounds of a corresponding periodic solution.
2. *Definition of the functions:* We define θ and ϕ that provide the shifted fast time scale, as well as Θ^0 and Θ^1 the two terms of the development.
3. *Reformulation of the system:* With the help of the approximation Θ_A defined in (1.4.8) we reformulate equation (1.4.2) and separate the terms with different orders of magnitude in $\sqrt{\varepsilon}$;
4. *The zeroth order expansion:* We verify the characterizing equation for Θ^0, and by analyzing this system we deduce the formulas for the frequency and the fast variable ψ;
5. *The action of the system:* In order to treat the higher order equations, we deduce a Fredholm-alternative type argument to provide us with non-secularity conditions. By defining the action of the system, we deduce the defining formula for the energy;
6. *The higher order terms:* By examining the equations that are verified by the higher order terms, we deduce the formula for Θ^1;
7. *Initial conditions:* We remark how certain initial conditions are computed in order to close all the systems.

Definition of the energy: By setting $E(0) = V(\vartheta_0, 0) = |\xi||g(0)|\cos(\vartheta_0 + \alpha(0))$, the following formula implicitly defines an energy function $E(t)$ associated with the general problem:

$$\int_{\Theta_{min}(E(t),t)}^{\Theta_{max}(E(t),t)} (E(t) - V(\vartheta, t))^{1/2}\, d\vartheta - \int_{\Theta_{min}(E(0),0)}^{\Theta_{max}(E(0),0)} (E(0) - V(\vartheta, 0))^{1/2}\, d\vartheta = 0. \tag{1.4.10}$$

Since the potential V is essentially a cosine function, these integrals are elliptic integrals of the second kind (up to a change of variables). Therefore, from (1.4.10) we have that

$$\mathcal{F}(E(t), t, \vartheta_0) = 0,$$

for a well-defined functional $\mathcal{F}$ with continuous partial derivatives, $E(t)$ can be recovered (locally in time t) by the implicit function theorem. This is due to the fact that the

derivative of $\mathcal{F}$ with respect to E is, by the chain rule:

$$\frac{d}{dE}\mathcal{F} = \frac{1}{2}\int_{\Theta_{min}(E(t),t)}^{\Theta_{max}(E(t),t)} (E(t) - V(\vartheta,t))^{-1/2}\, d\vartheta,$$

a complete elliptic integral of the first kind with modulus based on $E(t)/(|\xi||g(t)|)$, which is strictly positive. Notice that the energy must verify at all times t the inequality

$$|E(t)| \leqslant |\xi||g(t)| \tag{1.4.11}$$

in order for the elliptic integrals to stay real, which imposes the locality condition, since for the initial $t = 0$ it is verified.

Definition of the functions: Given the well-defined energy function $E(t)$, we define first of all θ as

$$\theta(t) = \int_0^t \left(\frac{1}{\pi}\int_{\Theta_{min}(E(t'),t')}^{\Theta_{max}(E(t'),t')} \frac{d\vartheta}{(2[E(t') - V(\vartheta,t')])^{1/2}}\right)^{-1} dt'. \tag{1.4.12}$$

This involves an elliptic integral of the first kind (up to a change of variables), hence the formula (and consequently θ) depends on E in a continuously differentiable manner. This implies that in particular, the quantity $\partial_E\theta$ is well-defined.

Then $\Theta^0(\cdot,t)$ is defined as the unique solution to the system (1.4.4) with $f = f(E,t) = \theta'(t)$ which is given by Lemma 1.4.1. From now on let us fix this $f(E,t)$ frequency. Continuing the previous argument, one has that Θ^0 also depends on E in a continuously differentiable manner.

We define $\phi(0) = 0$, then ϕ is defined as

$$\phi(t) = \int_0^t \frac{(f\partial_E f)(E(t'),t')}{f^2(E(0),0)} \cdot \phi(0) \int_0^1 \partial_t V(\Theta^0(\psi,0),0)\, d\psi. \tag{1.4.13}$$

Finally, Θ^1 is given by

$$\Theta^1 = C_1(t)\partial_\psi\Theta^0 + \frac{(\phi)'}{\partial_E f}\partial_E\Theta^0 + \Theta^1_{p_{odd}}, \tag{1.4.14}$$

with

$$\begin{aligned}\Theta^1_{p_{odd}} = &-\frac{1}{f}(f\partial_E\Theta^0 + \partial_E f\psi\partial_\psi\Theta^0)\int_0^\psi ((\theta)''\partial_\psi\Theta^0 + 2(\theta)'\partial_{\psi t}\Theta^0)\partial_\psi\Theta^0\, d\tilde{\psi}\\ &+\frac{1}{f}\partial_\psi\Theta^0\int_0^\psi ((\theta)''\partial_\psi\Theta^0 + 2(\theta)'\partial_{\psi t}\Theta^0)(f\partial_E\Theta^0 + \partial_E f\psi\partial_\psi\Theta^0)\, d\tilde{\psi},\end{aligned}$$

and $C_1(t)$ defined later.

Reformulation of the system: In order to analyze our strongly nonlinear, slowly varying oscillator equation (1.4.1), we make use of the method of multiple scales by using the fast time scale ψ and the slow time scale t such that

$$\psi = \frac{\theta(t)}{\sqrt{\varepsilon}} + \phi(t), \qquad t = \sqrt{\varepsilon}\tau. \tag{1.4.15}$$

Here the scaling θ and the shift ϕ are defined by (1.4.12) and (1.4.13) . With these scales, we have that

$$\partial_\tau \Theta_A(\tau) = \left(\theta'(t) + \sqrt{\varepsilon}\phi'(t)\right)\partial_\psi \Theta_A + \sqrt{\varepsilon}\partial_t \Theta_A,$$

thus substituting Θ_A into equation (1.4.2) that we aim to satisfy up to order $\mathcal{O}_{L^\infty}(\varepsilon)$, we get

$$\begin{aligned}(\theta' + \sqrt{\varepsilon}\phi')^2\partial_{\psi\psi}\Theta_A + \sqrt{\varepsilon}\left[(\theta'' + \sqrt{\varepsilon}\phi'')\partial_\psi\Theta_A + 2(\theta' + \sqrt{\varepsilon}\phi')\partial_{\psi t}\Theta_A\right] \\ + \varepsilon\partial_{tt}\Theta_A + \partial_\Theta V(\Theta_A, t) = 0.\end{aligned} \tag{1.4.16}$$

Remark 1.4.2. *Multiplying equation (1.4.16) by $\partial_\psi\Theta_A$ and integrating with respect to ψ, for solutions Θ_A^ε 2π-periodic in ψ, we may deduce the following, action related identity*

$$\frac{d}{dt}\left[(\theta' + \sqrt{\varepsilon}\phi')\int_0^{2\pi}(\partial_\psi\Theta_A)^2\,d\psi\right] + \sqrt{\varepsilon}\int_0^{2\pi}\partial_{tt}\Theta_A\partial_\psi\Theta_A\,d\psi = 0. \tag{1.4.17}$$

Defining the perturbation expansion (1.4.8) as

$$\Theta_A(\psi, t) = \Theta^0(\psi, t) + \sqrt{\varepsilon}\Theta^1(\psi, t) + \mathcal{O}_{L^\infty}(\varepsilon),$$

and plugging it into equation (1.4.16) leads to the nonlinear oscillator equation for the $\mathcal{O}(1)$ part

$$(\theta'(t))^2\partial_{\psi\psi}\Theta^0 + \partial_\Theta V(\Theta^0, t) = 0, \tag{1.4.18}$$

and its higher order perturbations for $\mathcal{O}\left(\varepsilon^{1/2}\right)$

$$L(\Theta^1) = R_1, \tag{1.4.19}$$

where $L = (\theta')^2\partial_{\psi\psi} + \partial_{\Theta\Theta}V(\Theta^0, t)$ is the linearization of the nonlinear operator in (1.4.18), and R_1 is the remainder term such that

$$R_1 = -2\theta'\phi'\partial_{\psi\psi}\Theta^0 - \theta''\partial_\psi\Theta^0 - 2\theta'\partial_{\psi t}\Theta^0,$$

Here we made use of the asymptotic development

$$\partial_\Theta V(\Theta_A, t) = \partial_\Theta V(\Theta^0, t) + \sqrt{\varepsilon}\Theta^1\partial_{\Theta\Theta}V(\Theta^0, t) + \mathcal{O}_{L^\infty}(\varepsilon).$$

In what follows, we will essentially search for the necessary and sufficient conditions for the existence of solutions periodic in ψ for the oscillation equation and its higher order perturbation, since periodic solutions are admitted by the nonlinear potential V. Furthermore, the periodicity condition guarantees their boundedness as well.

The zeroth order expansion: We start our analysis of the $\mathcal{O}(1)$ equation by multiplying (1.4.18) by $\partial_\psi \Theta^0$. By integrating with respect to ψ (for any t) we obtain the following energy equation

$$\frac{1}{2}(\theta'(t))^2(\partial_\psi \Theta^0)^2 + V(\Theta^0, t) = E(t), \tag{1.4.20}$$

with the energy $E(t)$ slowly varying over time, given by (1.4.10). Since the potential V is periodic in its first variable, this equation defines closed curves on the phase plane $(\Theta^0, \partial_\psi \Theta^0)$ for a fixed t. This means that Θ^0 is periodic in ψ and oscillates between some well-defined Θ_{min} and Θ_{max} values, satisfying $V(\Theta_{min}, t) = V(\Theta_{max}, t) = E(t)$, as they were defined for (1.4.10).

We have that Θ^0 is an even function of ψ, thus $\psi = 0$ corresponds to $\Theta^0(0, t) = \Theta_{min}(E(t), t)$ and $\partial_\psi \Theta^0(0, t) = 0$.

By quadrature method on (1.4.20), we obtain that

$$\psi = \theta'(t) \int_{\Theta_{min}(E(t),t)}^{\Theta^0(\psi,t)} \frac{d\vartheta}{(2[E(t) - V(\vartheta, t)])^{1/2}}, \tag{1.4.21}$$

so that the period of the fast variable is

$$P(E, t) = 2\theta'(t) \int_{\vartheta_{min}(E(t),t)}^{\vartheta_{max}(E(t,t)} \frac{d\vartheta}{(2[E(t) - V(\vartheta, t)])^{1/2}}. \tag{1.4.22}$$

By deriving the periodicity condition $\Theta^0(\psi, t) = \Theta^0(\psi + P, t)$ with respect to time or energy, it can be shown that the period is actually independent of the time (or else Θ^0 would blow up) and that $\partial_E P$ is non zero for almost all t in our case.

Furthermore we can normalize the period to any constant of time2π, which leads us to the frequency formula

$$f(E, t) = \theta'(t) = \left\{ \frac{1}{\pi} \int_{\Theta_{min}(E(t),t)}^{\Theta_{max}(E(t),t)} \frac{d\vartheta}{(2[E(t) - V(\vartheta, t)])^{1/2}} \right\}^{-1}, \tag{1.4.23}$$

that justifies our definition of θ. The initial condition is $\theta(0) = 0$.

The action of the system: Let us examine the linearized operator L.

Lemma 1.4.2. *The differential operator $L = (\theta')^2 \partial_{\psi\psi} + \partial_{\Theta\Theta} V(\Theta^0, t)$ admits the homoge-*

neous solutions

$$\partial_\psi \Theta^0, \quad \text{and} \quad \Theta_h = f\partial_E \Theta^0 + \partial_E f \psi \partial_\psi \Theta^0.$$

Proof: Take the derivative with respect to ψ in (1.4.18). It yield exactly $L(\partial_\psi \Theta^0) = 0$, thus $\partial_\psi \Theta^0$ is an odd, periodic, homogeneous solution.

Take the derivative with respect to E in (1.4.18) we get that $L(\partial_E \Theta^0) = -2f\partial_E f \partial_{\psi\psi}\Theta^0$. However by direct substitution we get that $L(\psi\partial_\psi \Theta^0) = 2f^2 \partial_{\psi\psi}\Theta^0$. This provides us with $\Theta_h = f\partial_E \Theta^0 + \partial_E f \psi \partial_\psi \Theta^0$, an even, non-periodic homogeneous solution. Its aperiodicity is due to the fact that $\partial_E P \neq 0$. □

A consequence of this lemma is that $\partial_\psi \Theta^0$ is the only periodic homogeneous solution, thus by the Fredholm alternative theorem, the remainder terms must be orthogonal to this solution in the fast time space to assure the existence of periodic-in-ψ solutions for the non-homogeneous problem. This provides us with the condition

$$\int_0^1 \partial_\psi \Theta^0 R_1 \, d\psi = 0, \tag{1.4.24}$$

an equivalent to the fact that we eliminate secular terms to assure the boundedness of the approximation.

In particular, we get that

$$\frac{d}{dt}\left(f(E,t) \int_0^1 (\partial_\psi \Theta^0)^2 \, d\psi \right) = 0,$$

by using parity argument. This is nothing else than the time derivative of the action of the system, thus the action is conserved. By a simple change of variables this gives us exactly the formula for the energy function

$$2\int_{\Theta_{min}}^{\Theta_{max}} (2[E(t) - V(\Theta,t)])^{1/2} \, d\Theta = c_E. \tag{1.4.25}$$

Thus, up to an integration constant c_E, and with the knowledge of the initial energy, the energy constant $E(t)$ was fully defined from this formula. We remark that this equation is nothing else than the leading order expansion of (1.4.17).

The higher order terms: Due to Lemma 1.4.2. we already know the homogeneous solutions of the operator L, so it is enough to find a particular solution for the perturbation equation. Separating the terms in R_1 with respect to parity in ψ hints that

$$\Theta_p^1 = -\frac{(\phi)'}{f}\psi\partial_\psi \Theta^0 + \Theta^1_{p_{odd}}$$

is a good candidate. Here the periodic odd part of the particular solution may be obtained by variation of parameters.

The general periodic solution Θ^1 is a linear combination of the two homogeneous solutions and the particular solution. Due to the presence of the coefficient ψ in the homogeneous solution Θ_h, we have a restriction in terms of the coefficients of the linear combination (to assure the boundedness). Thus, we obtain a simplified expression

$$\Theta^1 = C_1(t)\partial_\psi \Theta^0 + \frac{(\phi)'}{\partial_E f}\partial_E \Theta^0 + \Theta^1_{p_{odd}}, \tag{1.4.26}$$

where $C_1(t)$ can be determined from the action equation (1.4.17) in $\mathcal{O}_{L^\infty}(\sqrt{\varepsilon})$.

Closing arguments: The differential equation determining the phase shift ϕ arises from the $\mathcal{O}(\sqrt{\varepsilon})$ analysis of the general action equation (1.4.17). So we deduce

$$\phi'(t) = \frac{(f\partial_E f)(E,t)}{(f\partial_E f)(E(0),0)}\phi'(0), \tag{1.4.27}$$

we only need to determine the initial conditions.

To close up the system, we only need to determine the initial conditions $E(0)$ and $\phi(0)$. This can be done using the initial conditions on Θ^0, since

$$\begin{aligned} \Theta^0(\phi(0),0) &= \theta_0 \\ \theta'(0)\partial_\psi \Theta^0(\phi(0),0) &= 0 \end{aligned} \tag{1.4.28}$$

forms a closed system for the only remaining parameters, $E(0)$ and $\phi(0)$.

The missing initial condition for ϕ is then given by

$$\phi'(0) = \partial_E f(E(0),0)\cdot\phi(0)\int_{\phi(0)}^{1}\frac{\partial_t V(\Theta^0(\psi,0),t)}{f(E(0),0)}\,d\psi. \tag{1.4.29}$$

□

1.5 Erratic behavior for a particular set of initial data

In this section we examine the dynamical properties of the angular equation (1.1.1b) for small ε parameter. More exactly, we study the equation

$$\Theta''(\tau) = G(t)\sin\left(\Theta(\tau) + \alpha(t)\right), \tag{1.5.1}$$

that, for $t = \sqrt{\varepsilon}\tau$, is a slowly shifted, parametrically excited pendulum equation. Here, G is continuously differentiable function on $(0,\infty)$, bounded away from 0 for all time, and almost periodic in the sense of Proposition 1.3.1, and α is a continuously differentiable function. From here on throughout this section, prime will denote the derivative with

respect to the fast time scale variable τ as opposed to before. The initial conditions are taken as $\Theta(0) = \vartheta_0 \in (-\pi, \pi]$, $\Theta'(0) = \vartheta_1 \in \mathbb{R}$.

Remark 1.5.1. *By setting $G(t) = |\xi||g(t)|$ and $\alpha(t)$ the signed angle between $\xi^\perp$ and $g(t)$, one finds exactly (1.4.1). By assuming $\overline{h}_1 \neq u(\overline{h}_0)$, Corollary 1.3.3. and Proposition 1.3.1, we obtain that we verify the aforementioned boundedness and periodicity condition for $G(t)$. The existence of $g(t)$ is assured for a time $t \in [0, T_{\mu,\delta}]$. However, by choosing μ and δ sufficiently small, Corollary 1.3.1. guarantees that $T_{\mu,\delta}$ is as large as we want, indicating that for sufficiently small parameters we indeed obtain dynamical information on the original (1.1.1b) system as well.*

1.5.1 Sensitivity to the initial data

Equation (1.5.1) is not an autonomous system in this form due to the two different timescales present in the equations. However, rewriting it as a three dimensional system, one can consider it as an autonomous one:

$$\begin{aligned} \Theta' &= v, \\ v' &= G(t)\sin(\Theta + \alpha(t)), \\ t' &= \sqrt{\varepsilon}. \end{aligned} \tag{1.5.2}$$

With this one finds the classical structure of a 3 dimensional autonomous system

$$\mathbf{x}' = f_\varepsilon(\mathbf{x}), \tag{1.5.3}$$

with $\mathbf{x} = (\Theta, v, t)^\top$ and $f_\varepsilon = (f_1, f_2, f_3)(\Theta, v, t) = (v, G(t)\sin(\Theta + \alpha(t)), \sqrt{\varepsilon})$.

For a dynamical study, one is led to examine invariant structures:

Definition 1.5.1. *Consider the differential equation $x' = f(x)$ $x \in \mathbb{R}^n$, with an associated flow $x(t) = \phi_t(x_0)$ being the solution of the differential equation for $x(0) = x_0$. A set $S \subset \mathbb{R}^n$ is called an invariant set for the differential equation if, for each $x_0 \in S$ the solution $t \mapsto \phi_t(x_0)$, defined for its maximal time of existence, has its image in S (the orbit passing through each $x_0 \in S$ lies in S). In addition, S is called an invariant manifold if it is an invariant set and a manifold.*

It is for the dynamical system (1.5.3) that we can state sensitivity to the initial data. For this, let us first of all define the source of the erratic behavior.

Definition 1.5.2. *Let Σ denote the Cantor set of all bi-infinite sequences of two symbols:*

$$\Sigma := \{(s_i)_{i\in\mathbb{Z}};\ s_i \in \{0, 1\} \forall i \in \mathbb{Z}\},$$

with the natural product topology. It is a compact metric space with no isolated points. Let $\sigma : \Sigma \to \Sigma$ be the shift map defined for $s = (s_i)_{i\in\mathbb{Z}}$ as $\sigma(s)_i = s_{i+1}$. This map is invertible and uniformly continuous in the given topology.

Definition 1.5.3. *The generalised Poincaré map P_ε, associated with the flow of f_ε is the application mapping $\mathbb{R}^2$ to $\mathbb{R}^2$, with*

$$P : (\Theta, v)(0) \mapsto (\Theta, v)\left(\frac{\mu}{\sqrt{\varepsilon}}\pi\right).$$

Remark 1.5.2. *Since the function G is almost $\mu\pi$ periodic in the sense of Proposition 1.3.1, this indeed defines a generalized Poincaré map between the $t = 0$ and $t = \mu\pi$ level sets.*

Then, the main results of this section can be summarized in what follows:

Conjecture 1.5.1. *There exists ε_0 sufficiently small such that for every $\varepsilon \in (0, \varepsilon_0)$, there exists a non-horizontal line $\mathcal{N}_\varepsilon$ in $\mathbb{R}^3$, invariant under the action of f_ε, around which there exists an invariant set Λ_ε such that Λ_ε is topologically conjugate to $\Sigma \times \mathcal{N}_\varepsilon$, Λ_ε is a Cantor set of non-horizontal lines.*

Moreover, there exist $n_\varepsilon \in \mathbb{N}$ such that the iterate of the generalised Poincaré map restricted to Λ_ε, $P_\varepsilon(f_\varepsilon|_{\Lambda_\varepsilon})^{n_\varepsilon}$ is topologically conjugate to the Bernoulli shift σ over two symbols.

The reason why this is only a conjecture will be elaborated at the end of the series of proofs given in the next sections. The missing step in its demonstration is at the very end, in order to conclude the behaviour of the trajectories from what we can establish on the local stable and unstable manifolds.

This implies a sensitivity to initial conditions around the invariant line $\mathcal{N}_\varepsilon$, which is a necessary condition of deterministic chaos (albeit not a sufficient one). A particular consequence of the theorem is that there are uncountably many erratic solutions of this system, due to the symbolic dynamical property around the invariant set. These solutions have initial conditions ϑ_0 close to $\pi - \alpha(0)$ and ϑ_1 close to 0, which means that they are initially around the invariant line $\mathcal{N}_\varepsilon$. Most notably one observes infinitely many unstable periodic solutions of arbitrary high period, uncountably many unstable non-periodic solutions as well as solutions whose trajectory is dense in Λ_ε meaning that it approaches any element of Λ_ε arbitrarily closely ([Wig88b]).

This however does not necessarily imply that the system is chaotic in a dynamical sense ([HM93]), since we have no information on whether the map f_ε is topologically mixing or whether there exists any dense periodic orbits.

Definition 1.5.4. *For a topological space X, the continuous map $f : X \to X$ is said to be topologically mixing (or topologically transitive) if, for every pair of non-empty open sets $A, B \subset X$, there exists an $n \in \mathbb{N}$ such that $f^n(A) \cap B \neq \emptyset$.*

We remark that G being only almost periodic requires a dynamical toolset that has only recently been developed ([CW15],[CW05]). For a periodic perturbation function $G(t)$,

to some extent the original results of Melnikov ([Mel63]) apply as well (see also [Wig88b]). Other, more exact methods have also been developed (see for example the shooting technique of Hastings and McLeod [HM93] and references therein), they are based on direct computations with the associated energy functional of the system. However the presence of a time-dependent shift α in our system complicates these types of reasoning.

The rest of this section is dedicated to the demonstration of the main steps of the previous conjecture. The structure of the proof is as follows:

1. **Analysis of the unperturbed system:** In the next section we establish the basics of the dynamics of this system and we reason why these equations require non-classical tools to handle. Then we analyze the system corresponding to $\varepsilon = 0$ (the unperturbed system).
2. **Persistence for small parameters:** We proceed with establishing some fundamental results on the dynamical structure of system (1.5.2). Most notably we show the existence of a line invariant under the action of f_ε, and an associated stable and unstable manifold.
3. **The generalized Smale–Birkhoff theorem:** We state a classical result and its more recent generalizations in Section 1.5.4. By regrouping the previously obtained results we are then led to verify a single condition concerning the intersection of the stable and unstable manifolds.
4. **Intersection of the stable and unstable manifold:** In Section 1.5.5 we show that these manifolds intersect transversally, which is the condition with which one would apply a generalized Smale–Birkhoff theorem. For this we present the essentials of the theory introduced by Melnikov ([Mel63] in order to analyze tangential intersections of homoclinic trajectories and to show what it implies for the overall dynamics.

1.5.2 The perturbed and unperturbed system

A huge drawback of the formulation as a 3-dimensional first order system (1.5.4) is that the associated map f_ε is not hyperbolic. This degeneracy is due to the fact that the Jacobian matrix of f_ε,

$$\mathrm{Jac}(f_\varepsilon) = \begin{pmatrix} 0 & 1 & 0 \\ G(t)\cos(\Theta + \alpha(t)) & 0 & G'(t)\sin(\Theta + \alpha(t)) + G(t)\cos(\Theta + \alpha(t))\alpha'(t) \\ 0 & 0 & 0 \end{pmatrix}$$

always has at least one 0 eigenvalue (associated with the artificial direction of t). This in turn prevents one to perform a classical dynamical analysis, since essential notions like hyperbolicity are by definition not verified.

In order to overcome this obstacle, one is led to consider the unperturbed system. This means that we consider the case $\varepsilon = 0$, or equivalently, the original system (1.5.1) for a

fixed t. This yields the following

$$\begin{aligned} \Theta' &= v, \\ v' &= G(t)\sin(\Theta + \alpha(t)), \\ t' &= 0, \end{aligned} \tag{1.5.4}$$

now t is a constant, a parameter of the two dimensional system defined by the first two equations.

In particular, normally hyperbolic invariant manifolds will play an essential part of the analysis (see for example [HPS77]).

Definition 1.5.5. *Let M be a smooth manifold, X a $\mathcal{C}^r$ ($r \geqslant 1$) vector field on M, f_t the associated flow and Df_t the differential of f_t. An f_t-invariant sub-manifold V of M is said to be a normally hyperbolic invariant manifold if the restriction to V of the tangent bundle of M ($T_V M$) splits into three continuous Df_t-invariant sub-bundles*

$$T_V M = TV \oplus E^s \oplus E^u,$$

with TV being the tangent bundle of V, E^s and E^u the stable and unstable linear bundles, respectively, meaning that the restriction of Df_t to E^s is a contraction, and the restriction of Df_t to E^u is an expansion.

Remark 1.5.3. *This one-parameter family of planar systems has a Hamiltonian structure, as it was remarked in the previous section, with the Hamiltonian (energy functional)*

$$E(\Theta, v; t) = \frac{v^2}{2} + G(t)\cos(\Theta + \alpha(t)). \tag{1.5.5}$$

The main idea is the following: analyzing the unperturbed system is rather simple since it permits to work with explicit quantities. We establish a normally hyperbolic invariant structure for this system. Then, with a persistence theory one can show that this structure, and the desired properties are preserved for the perturbed system.

1.5.2.1 Hyperbolic saddle points

Let us make some remarks on the unperturbed system (1.5.4). For each parameter value of t, the planar system is nothing else than a shifted pendulum equation, whose dynamics are well known, the solutions and trajectories can be explicitly calculated.

Figure 1.4a depicts the phase portrait of the planar equation for a single period of 2π in the horizontal (Θ) direction, restricted to not too large angular velocities (v). We remark that the natural phase space for the planar equation is the cylinder $(-\pi, \pi] \times \mathbb{R}$.

In the cylindrical phase portrait, there are two fixed points of the system, of which one is always a center, the other one being a hyperbolic saddle point. The fixed points

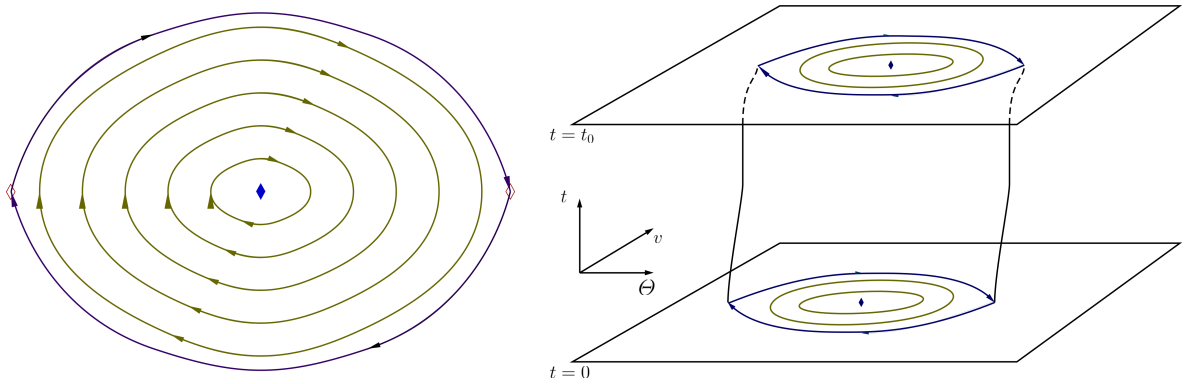

(a) A section of the periodic phase por-(b) The structure of the phase portrait of the unper-
trait of the classical pendulum equationturbed system

Figure 1.4 – The periodic phase portrait of the unperturbed system (1.5.4)

are given by

$$(\vartheta_-(t), v_-(t)) = (-\alpha(t), 0) \tag{1.5.6}$$

associated with saddle points, with eigenvalues of the corresponding planar Jacobian $(\mathrm{Jac}((f_1, f_2)^\top))$

$$\pm\sqrt{G(t)},$$

that, by our hypothesis on $G(t)$, stay away from zero uniformly for every parameter value of t. The fixed points $(\vartheta_+(t), v_+(t)) = (-\alpha(t) + \pi, 0)$ are centers.

1.5.2.2 Normally hyperbolic invariant lines

For each value of t, the points $(\vartheta_\pm(t), v_\pm(t))$ form an invariant set of the corresponding planar problem of the unperturbed system. By grouping together these points from each level of t we obtain a natural parametrization of the invariant set of the complete (3 dimensional) unperturbed problem (1.5.4). More precisely, for the set of saddle points

$$\mathcal{N}_0 := \{(\vartheta_{-,fix}(t), 0, t);\ t \in \mathbb{R}^+\}, \tag{1.5.7}$$

we have that

Lemma 1.5.1. *The set of hyperbolic saddle points $\mathcal{N}_0$ forms a normally hyperbolic one-dimensional invariant manifold.*

Proof: By definition, it is invariant under the action of f_0. The normally hyperbolicity is a straightforward consequence of the definition and the fact that at each level t they correspond to hyperbolic saddle points, with eigenvalues uniformly bounded away from zero ([Wig88b]). See also [HPS77].

The consequences of being a normally hyperbolic invariant manifold are summarized for instance in Theorem 4.1. of [HPS77]. From this we would like to cite only what is relevant to our current analysis:

Proposition 1.5.1. *For the unperturbed system (1.5.4), there exists a locally f_0-invariant 2 dimensional sub-manifold $W^s_{loc}(\mathcal{N}_0)$ (called the stable manifold of $\mathcal{N}_0$) that consists of all the points whose forward f_0-orbits stay ϵ-close to $\mathcal{N}_0$. Respectively, there exists a locally f_0-invariant 2 dimensional sub-manifold $W^u_{loc}(\mathcal{N}_0)$ (called the unstable manifold of $\mathcal{N}_0$) that consists of all the points whose backward f_0-orbits stay ϵ-close to $\mathcal{N}_0$.*

1.5.3 Persistence of normally hyperbolic invariant manifolds

The remarkable property of normally hyperbolic structures is that they are relatively stable with respect to regular perturbations. We have that

Proposition 1.5.2. *There exists ε_0 sufficiently small, such that for $\varepsilon < \varepsilon_0$ the perturbed system (1.5.2) possesses a normally hyperbolic invariant manifold, which is topologically a line*

$$\mathcal{N}_\varepsilon := \{(z;\varepsilon) = \vartheta_{-,fix}(0;z) + \mathcal{O}_{L^\infty}(\varepsilon), z \in \mathbb{R}^+\}. \tag{1.5.8}$$

Moreover, $\mathcal{N}_\varepsilon$ has local stable and unstable manifolds $W^s_{loc}(\mathcal{N}_\varepsilon)$ and $W^u_{loc}(\mathcal{N}_\varepsilon)$ that are ϵ-close to the local stable and unstable manifolds of $\mathcal{N}$, $W^s_{loc}(\mathcal{N}_0)$ and $W^u_{loc}(\mathcal{N}_0)$.

Proof: This is an immediate consequence of the persistence theory for normally hyperbolic invariant manifolds. See Theorem 3 of [Fen71] for the classical persistence theory, Theorem 4.1. of [HPS77] for the general result on compact manifolds, and Proposition 3.3 [Rob83] for the relaxation to unbounded invariant sets.

1.5.4 The Smale horseshoe map

Transverse homoclinic orbits, or in a more general sense transverse homoclinic invariant manifolds indicate a complexity in the dynamics of the system. A well-known result of Smale ([Sma65]) states the following

Theorem 1.5.1. *Let $P : \mathbb{R}^n \to \mathbb{R}^n$ be a $\mathcal{C}^r$ $(r \geqslant 1)$ diffeomorphism having a hyperbolic fixed point p whose stable and unstable manifolds intersect transversely in $q \neq p$. Then, in a neighborhood of q, there exist an invariant Cantor set of points, Λ, on which f is topologically conjugate to the Bernoulli shift on a countable set of symbols.*

With the notion of normally hyperbolic invariant manifolds ([HPS77]), this theorem has been generalized for invariant tori (Theorem 4.2. of [Wig88b]), as well as for simpler but unbounded structures (Theorem 2.3. of [Rob83], Theorem 5 of [MS86]).

The transverse intersection of the stable and unstable manifolds around $\mathcal{N}_\varepsilon$ are guaranteed by our a priori analysis on the Melnikov-function, therefore the second part of the

conjecture would be consequence of the generalized Smale–Birkhoff homoclinic theorem (By the main results of [CW05], Theorem 2 of [CW15])

Conjecture 1.5.2. *Let $P : \mathbb{R}^3 \to \mathbb{R}^3$ be a $\mathcal{C}^r$ ($r \geqslant 1$) diffeomorphism having a 1-dimensional normally hyperbolic invariant manifold, $\mathcal{N}$, possessing 2-dimensional (locally invariant) stable and unstable manifolds $W^s_{loc}(\mathcal{N})$ and $W^u_{loc}(\mathcal{N})$. If $W^s_{loc}(\mathcal{N})$ and $W^u_{loc}(\mathcal{N})$ intersect transversely, then there exists $n\mathbb{N}$ such that f^n contains an invariant Cantor set of 1-dimensional manifolds on which it acts like a Bernoulli shift.*

We remark that this invariant set Λ is often referred to as the Smale horseshoe map ([GH83]). By the persistence result of Proposition 1.5.2. we have already showed that for f_ε there exists a normally hyperbolic invariant line $\mathcal{N}_\varepsilon$ whose stable and unstable manifolds are well defined. In the final section we show that these manifolds intersect transversely.

1.5.5 A Melnikov/Wiggins type theorem

In his article, Melnikov ([Mel63]) introduced a quantity to measure the relative orientation of the local stable and unstable manifolds around a (normally) hyperbolic invariant structure. He gave the general definition of this signed distance and provided an asymptotic development with respect to the smallness parameter ε in order to obtain computable formulae. This gave rise to the so-called Melnikov-functional, a first order approximation of the aforementioned quantity, that has been since re-adapted to many other scenarios ([Rob83], [MS86], [Wig88b] for example).

This allowed him to establish the dynamical properties of a large class of slowly varying non-autonomous ODE systems. This theory was later extended to many other types of systems, see for example Chapter 4 of [Wig88a].

The critical observation concerning our system is that homoclinic trajectories are often the precursors of complex dynamics ([Poi90]). In particular, we remarked the presence of the homoclinic trajectories in the unperturbed system (on a cylinder ($(-\pi, \pi] \times \mathbb{R}$)). These are in fact a "fragile" particular state, one that breaks down into a special type of bifurcation under perturbation, the so called homoclinic tangle ([GH83]), see also Figure 1.5.

1.5.5.1 The homoclinic trajectories

Let us remark that the unperturbed system (1.5.4) admits a pair of homoclinic orbits. These solutions are explicit for each parameter value t, they are given by

$$\begin{aligned} \Theta_\pm(\tau) &= \pm 2 \sin^{-1}(\tanh(G(t)\tau)) + \pi - \alpha(t), \\ V_\pm(\tau) &= \pm 2 G(t) \operatorname{sech}(G(t)\tau), \end{aligned} \tag{1.5.9}$$

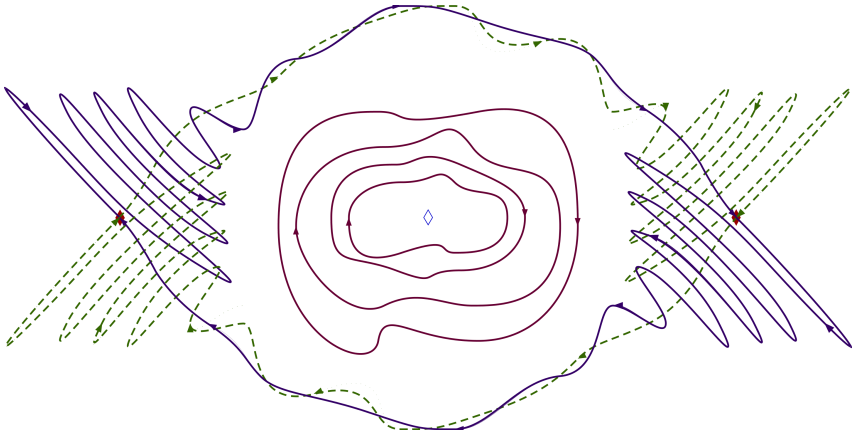

Figure 1.5 – A section of the perturbed phase portrait

and connect the saddle point of the system at $-\alpha(t)$ by itself.

The corresponding unique pair of homoclinic trajectories on the plane $\mathbb{R}^2$ will be denoted by $\mathbf{x}_{\pm,0}(\tau)$.

1.5.5.2 Geometry of the Melnikov function

First of all, the signed distance of the locally invariant manifolds $W^s_{loc}(\mathcal{N}_\varepsilon)$ and $W^u_{loc}(\mathcal{N}_\varepsilon)$ is given by

Definition 1.5.6. *For $0 < \varepsilon \ll 1$, the separation of the manifolds $W^s_{loc}(\mathcal{N}_\varepsilon)$ and $W^u_{loc}(\mathcal{N}_\varepsilon)$ at level t is given by*

$$d(t;\varepsilon) = \frac{1}{|\mathbf{f}(\mathbf{x}_{+,0}(0))|}\mathbf{f}^\perp(\mathbf{x}_{+,0}(0)) \cdot (\mathbf{x}^u_\varepsilon(t) - \mathbf{x}^s_\varepsilon(t)), \tag{1.5.10}$$

where $\mathbf{f} = (f_1, f_2)$, $\mathbf{x}^s_\varepsilon(t)$ (respectively $\mathbf{x}^u_\varepsilon(t)$) is the first intersection point of $W^s_{loc}(\mathcal{N}_\varepsilon)$ (respectively $W^u_{loc}(\mathcal{N}_\varepsilon)$) with the line defined by $\mathbf{f}^\perp(\mathbf{x}_{+,0}(0))$.

We remark that the choice of the homoclinic trajectory does not influence this distance, and that the intersection points $\mathbf{x}^s_\varepsilon(t)$ and $\mathbf{x}^u_\varepsilon(t)$ are well-defined (Theorems 4 and 5 of [Mel63]).

By a Taylor expansion (Lemma 4.5.2 of [GH83]), one has that

$$d(t;\varepsilon) = \frac{\sqrt{\varepsilon}}{|\mathbf{f}(\mathbf{x}_{+,0}(0))|}\mathbf{f}^\perp(\mathbf{x}_{+,0}(0)) \cdot \left(\frac{\partial}{\partial\varepsilon}\mathbf{x}^u_\varepsilon(t)|_{\varepsilon=0} - \frac{\partial}{\partial\varepsilon}\mathbf{x}^s_\varepsilon(t)|_{\varepsilon=0}\right) + \mathcal{O}_{L^\infty}(\varepsilon),$$

where the first term of the asymptotic development defines the Melnikov-function $M^+(t)$:

$$M^+(t) = \mathbf{f}^\perp(\mathbf{x}_{+,0}(0)) \cdot \left(\frac{\partial}{\partial\varepsilon}\mathbf{x}^u_\varepsilon(t)|_{\varepsilon=0} - \frac{\partial}{\partial\varepsilon}\mathbf{x}^s_\varepsilon(t)|_{\varepsilon=0}\right). \tag{1.5.11}$$

This quantity, given the particular structure of our system (1.5.2), can be reformulated into (Proposition 3.4 of [Rob83], Appendix A of [Wig88b])

$$M^+(t) = \int_{-\infty}^{\infty} \tau \left(f_1(\mathbf{x}_{+,0}(\tau))\partial_t f_2(\mathbf{x}_{+,0}(\tau)) - f_2(\mathbf{x}_{+,0}(\tau))\partial_t f_1(\mathbf{x}_{+,0}(\tau)) \right) d\tau$$

Therefore, using (1.5.9), the Melnikov-function (Section 5 of [Wig88b]) associated with the perturbed system (1.5.2) is given by

$$\begin{aligned} M^+(t) = &- \int_{-\infty}^{\infty} 2\tau G(t)G'(t)\,\mathrm{sech}(G(t)\tau)\cdot \sin(2\sin^{-1}(\tanh(G(t)\tau)))\,d\tau \\ &- \int_{-\infty}^{\infty} 2\tau G(t)\alpha'(t)\,\mathrm{sech}(G(t)\tau)\cdot \cos(2\sin^{-1}(\tanh(G(t)\tau)))\,d\tau, \end{aligned} \tag{1.5.12}$$

or, by calculating the integral, with a more explicit expression

$$M^+(t) = 4\frac{G'(t)}{G(t)} \tag{1.5.13}$$

This changes sign almost periodically in the sense of Proposition 1.3.1, since we have the corresponding estimate on the nominator and the denominator stays bounded away from 0.

By the main theorem of Melnikov (see also Theorem 4.5.3. of [GH83])

Theorem 1.5.2. *If $M^+(t)$ is almost periodic in the sense of Proposition 1.3.1, then for sufficiently small ε, $W^s_{loc}(\mathcal{N}_\varepsilon)$ and $W^u_{loc}(\mathcal{N}_\varepsilon)$ intersect transversely.*

This concludes the demonstration of the main results of this section.

Acknowledgement: The author, as well as the current work was partially supported by the Conseil Régional Nouvelle Aquitaine, the ANR-15-CE40-0010 IFSMACS and the Fondation Del Duca.

Chapter 2

Wave-structure interaction for long wave models in the presence of a freely moving object on the bottom

Contents

Version française abrégée

Le problème des vagues consiste à décrire le mouvement des vagues d'un milieu fluide non-visqueux, incompressible, irrotationel et à densité constante, soumises à la gravité. Nous nous intéressons à l'étude d'une formulation particulière de ce problème dans laquelle le fond du domaine de fluide évolue en temps de façon non-forcée. Son évolution est alors déterminée par les forces hydrodynamiques engendrées par les vagues. La théorie mathématique d'une telle configuration n'a pas encore étée étudiée, par conséquent, pour une première approche, le but de cet article est de dériver et analyser des modèles asymptotiques de faibles profondeurs provenant de ce problème à double frontière libre.

En particulier, nous considérons un fond plat sur lequel un corps rigide peut se déplacer horizontalement, dont le mouvement est complètement déterminé par le mouvement des vagues. Le principal intérêt de ce modèle simplifié concerne d'une part l'énergie maritime côtière et les nouvelles tentatives pour construire des convertisseurs de l'énergie des vagues submergés ([AELS14], [GIL+14]) et d'autre part les études océanographiques menées sur les glissements de terrain sous-marins. En raison de cet intérêt au niveau des applications, des expériences physiques ([ACDNn17]) ainsi que des simulations numériques approfondies ([CM06], [GN07], [Mit09], [DNZ15]) ont été effectuées.

Mise en équation du problème : Pour introduire le système décrivant la dynamique du fluide, notons par $\zeta(t,x)$ l'élévation de la surface libre et par $b(t,x)$ la fonction caractérisant la topographie du fond à une profondeur de base H_0. Le domaine de fluide s'écrit comme

$$\Omega_t = \left\{(x,z) \in \mathbb{R}^d \times \mathbb{R} \,:\, -H_0 + b(t,x) < z < \zeta(t,x)\right\},$$

La fonction décrivant la profondeur totale du fluide $h(t,x) = H_0 + \zeta(t,x) - b(t,x)$ va jouer un rôle important dans l'analyse. Nous supposerons en effet qu'elle a une borne inférieure uniforme $h_{min} > 0$ pour éviter certaines situations physiques particulières (comme les îles ou les plages).

En raison des hypothèses physiques sur le fluide (notamment l'incompressibilité et l'irrotationalité), nous exprimons le mouvement du fluide à travers le potentiel de vitesse Φ. Ce potentiel vérifie une équation de Laplace :

$$\begin{cases} \Delta\Phi = 0 \quad \text{dans } \Omega_t, \\ \Phi|_{z=\zeta} = \psi, \;\; \sqrt{1+|\nabla_x b|^2}\partial_{\mathbf{n}}\Phi|_{z=-H_0+b} = \partial_t b, \end{cases} \tag{2.0.1}$$

où ψ est le potentiel de vitesse à la surface libre. En écrivant la loi de conservation du moment ainsi que la condition au bord cinématique (à la surface libre), nous retrouvons le problème de Bernoulli à surface libre, dans le domaine Ω_t. Issue du problème précédent,

la vitesse horizontale verticalement moyennée est une quantité importante :

$$\overline{V} = \frac{1}{h}\int_{-H_0+b}^{\zeta} \nabla_x \Phi(\cdot, z)\, dz, \tag{2.0.2}$$

cette variable est plus adaptée aux études asymptotiques dans le régime à faible profondeur. Avec cette notation, le problème des vagues avec un fond qui évolue en temps s'écrit sous la forme suivante

$$\begin{cases} \partial_t \zeta + \nabla \cdot (h\overline{V}) = \partial_t b, \\ \partial_t \psi + g\zeta + \dfrac{1}{2}|\nabla_x \psi|^2 - \dfrac{(-\nabla \cdot (h\overline{V}) + \partial_t b + \nabla_x \zeta \cdot \nabla_x \psi)^2}{2(1+|\nabla_x \zeta|^2)} = 0. \end{cases} \tag{2.0.3}$$

Concernant le solide qui se déplace librement au fond, nous supposons qu'il est rigide, homogène (de masse M), et que sa surface mouillée est décrite par une fonction de classe $\mathcal{C}^\infty$ à support $(I(t))$ compact. Le solide est contraint à un mouvement horizontal selon le vecteur de déplacement $X_S(t)$, avec une vitesse $v_S(t)$, les effets rotationnels sont exclus. Grâce à cette notation, nous pouvons exprimer la topographie du fond par une translation ; on a $b(t,x) = \mathfrak{b}\,(x - X_S(t))$ où $\mathfrak{b}$ correspond à l'état initial (voir également Figure 2.1). D'après la deuxième loi de Newton sur la force totale agissant sur le solide, on obtient

$$\begin{aligned} M\ddot{X}_S(t) = &- c_{\text{fric}} \left(Mg + \int_{I(t)} P|_{z=-H_0+b(t,x)}\, dx \right) \frac{\dot{X}_S(t)}{\left|\dot{X}_S(t)\right| + \sqrt{gH_0\delta}} \\ &+ \int_{I(t)} P|_{z=-H_0+b(t,x)} \nabla_x b\, dx. \end{aligned}$$

Ici, nous avons implémenté une loi de friction purement dynamique, dont la direction de la force de frottement est opposée à la direction de vitesse v_S (avec une $\delta \ll 1$ constante mathématique régularisant cette fonction), et dont c_{fric}, appelé coefficient de friction, représente les propriétés physiques du système couplé. En outre, $P|_{z=-H_0+b(t,x)}$ signifie la pression du fluide évaluée au fond.

Pour une analyse asymptotique, nous sommes amenés à réécrire les équations dans une formulation sans dimensions (physiques), en utilisant des paramètres sans dimensions. Notamment, on pose que $\mu = H_0^2/L^2$, qui est le rapport de la profondeur de base (H_0) et la taille horizontale caractéristique des vagues (L) au carré, qui représente le paramètre de faible profondeur. On a également $\varepsilon = a_{surf}/H_0$, le paramètre de non-linéarité, qui n'est rien d'autre que le rapport entre l'amplitude caractéristique des vagues (a_{surf}) et H_0. Avec l'hypothèse supplémentaire que les tailles caractéristiques du solide sont du même ordre de grandeur que celles des vagues, on peut introduire les équations sans dimensions de notre problème couplé (voir les équations (2.1.22), (2.1.24) et (2.1.26)).

Etude des régimes asymptotiques : Nous nous intéressons à l'étude de deux régimes asymptotiques, selon les hypothèses sur les paramètres de petitesse μ et ε. Pour le cas

des équations de Saint-Venant, nous réalisons une approximation à l'ordre $\mathcal{O}(\mu)$ de la formulation sans dimensions des équations des vagues (2.0.3) en supposant que ε vaut 1. Par conséquent, les équations à surface libre avec un solide qui se déplace au fond dans le cadre de Saint-Venant non-linéaire ont la forme suivante :

$$\begin{cases} \partial_t \zeta + \nabla_x \cdot (h\overline{V}) = \nabla_x \mathfrak{b}(x - X_S) \cdot \dot{X}_S, & \text{(2.0.4a)} \\ \partial_t \overline{V} + \nabla_x \zeta + (\overline{V} \cdot \nabla_x)\overline{V} = 0, & \\ \ddot{X}_S = -\dfrac{c_{\text{fric}}}{\sqrt{\mu}} \left(c_{solid} + \dfrac{1}{\tilde{M}} \displaystyle\int_{I(t)} \zeta \, dx \right) \dfrac{\dot{X}_S}{\left|\dot{X}_S\right| + \bar{\delta}} + \dfrac{1}{\tilde{M}} \displaystyle\int_{\mathbb{R}^d} \zeta \nabla_x \mathfrak{b}(x - X_S) \, dx. & \text{(2.0.4b)} \end{cases}$$

Le premier résultat consiste à établir le caractère bien-posé de ces équations. Plus précisément

Théorème 2.0.1. *On suppose que $\varepsilon = 1$. Si les données initiales ζ_{in} et $\overline{V}_{in}$ sont dans l'espace $H^s(\mathbb{R}^d)$ avec $s \in \mathbb{R}$, $s > d/2 + 1$, et que $X_S(0) = 0$, $\dot{X}_S(0) = v_{S_0} \in \mathbb{R}^d$ est arbitraire, alors il existe une solution*

$$\begin{aligned} &(\zeta, \overline{V}) \in \mathcal{C}([0,T]; H^s(\mathbb{R}^d)) \cap \mathcal{C}^1([0,T]; H^{s-1}(\mathbb{R}^d)), \\ &X_S \in \mathcal{C}^2([0,T]), \end{aligned}$$

du système (2.0.4) pour un temps $T > 0$ suffisamment petit, indépendant de $\mu \in (0,1)$.

La démonstration s'appuie sur le théorème de point fixe appliqué à un schéma itératif construit du système (2.0.4). Ce schéma permet de découpler la partie EDO et la partie EDP de ce système. Grâce à la structure hyperbolique quasi-linéaire des équations de Saint-Venant, nous établissons de manière directe des estimations d'énergie pour l'EDP. Les points critiques concernent les estimations des termes de source venant du couplage et l'estimation de la vitesse du solide.

Pour l'approximation de Boussinesq, on fait l'approximation des équations du fluide (2.0.3) d'ordre $\mathcal{O}(\mu^2)$ pour obtenir un système qui est consistant d'ordre 2 avec les équations originelles. En faisant l'hypothèse supplémentaire de $\varepsilon = \mathcal{O}(\mu)$, nous regardons le problème couplé dans le cadre de Boussinesq faiblement non-linéaire suivant :

$$\begin{cases} \partial_t \zeta + \nabla_x \cdot (h\overline{V}) = \partial_t b, & \\ \left(1 - \dfrac{\mu}{3}\Delta_x\right) \partial_t \overline{V} + \nabla_x \zeta + \varepsilon(\overline{V} \cdot \nabla_x)\overline{V} = -\dfrac{\mu}{2} \nabla_x \partial_t^2 b, & \text{(2.0.5a)} \\ \ddot{X}_S = -\dfrac{c_{\text{fric}}}{\sqrt{\mu}} \left(\dfrac{1}{\varepsilon}\tilde{c}_{solid} + \dfrac{1}{\tilde{M}} \displaystyle\int_{I(t)} \zeta \, dx \right) \dfrac{\dot{X}_S}{\left|\dot{X}_S\right| + \bar{\delta}} + \dfrac{\varepsilon}{\tilde{M}} \displaystyle\int_{\mathbb{R}^d} \zeta \nabla_x \mathfrak{b}(x - X_S) \, dx. & \text{(2.0.5b)} \end{cases}$$

Le résultat principal de cet article établit l'existence d'une solution unique à longue portée.

Théorème 2.0.2. *On suppose que $\varepsilon = \mathcal{O}(\mu)$. On suppose également que pour les valeurs*

initiales ζ_{in} *et* $\mathfrak{b}$ *il existe* $h_{min} > 0$ *tel que* $1 + \zeta_{in} - \mathfrak{b} \geqslant h_{min}$. *Si les données initiales* ζ_{in} *et* $\overline{V}_{in}$ *sont dans l'espace* $H^s(\mathbb{R}^d)$ *avec* $s \in \mathbb{R}$, $s > d/2 + 1$, *et que* $V_{S_0} \in \mathbb{R}^d$, *alors il existe un temps maximal* $T_0 > 0$, *indépendant de* ε *tel qu'il existe une unique solution*

$$(\zeta, \overline{V}) \in C\left(\left[0, \frac{T_0}{\sqrt{\varepsilon}}\right]; \mathcal{X}^s(\mathbb{R}^d)\right) \cap C^1\left(\left[0, \frac{T_0}{\sqrt{\varepsilon}}\right]; \mathcal{X}^{s-1}(\mathbb{R}^d)\right),$$
$$X_S \in C^2\left(\left[0, \frac{T_0}{\sqrt{\varepsilon}}\right]\right)$$

du système (2.0.5) avec des données initiales $(\zeta_{in}, \overline{V}_{in})$ *et* $(0, \sqrt{\varepsilon} V_{S_0})$. *Les espaces* $\mathcal{X}^s(\mathbb{R}^d)$ *sont définis par la définition 2.3.1.*

La preuve, contrairement au régime précédent, est basée sur une régularisation due à Friedrichs. La raison de ce changement de méthode est motivée par le fait que certaines annulations ne peuvent pas être adaptées à un schéma itératif basé sur les équations de Boussinesq, principalement à cause de leur terme dispersif. Cependant, l'établissement d'une estimation d'énergie pour le modèle couplé garantit l'existence d'une solution en temps long. Cette estimation est obtenue pour la fonctionnelle d'énergie suivante

$$E_B(t) = \frac{1}{2}\int_{\mathbb{R}^d} \zeta^2\, dx + \frac{1}{2}\int_{\mathbb{R}^d} h(\overline{V}\cdot\overline{V})\, dx + \frac{1}{2}\sum_{j=1}^{d}\int_{\mathbb{R}^d} \frac{\mu}{3} h(\partial_j \overline{V}\cdot\partial_j\overline{V})\, dx + \frac{1}{2\varepsilon}\left|\dot{X}_S\right|^2,$$

qui n'est pas un Hamiltonien du système, puisqu'elle n'est pas conservée en temps, mais est contrôlée en temps long.

Introduction

The water waves problem, which consists in describing the motion of waves at the surface of an inviscid, incompressible, and irrotational fluid of constant density under the action of gravity, has attracted a lot of attention in the last decades. The local well-posedness theory is now well-understood following the works of Wu [Wu97, Wu99] establishing the relevance of the Taylor sign condition. In the case of finite depth, which is of interest here, we refer for instance to [Lan05, Igu09, ABZ14]; the case where the bottom is also allowed to depend on time has also been treated in [ABZ11, Igu11, Mel15]. In this paper, we are interested in a particular configuration where the bottom depends on time, but instead of being in forced motion as in the above references, it evolves under the action of the hydrodynamic forces created by the surface waves. Finding its evolution is therefore a free boundary problem, which is coupled to the standard water waves problem, itself being a free boundary problem. The mathematical theory for such a configuration has not been considered yet; we refer however to [Lan17] for a related problem where the moving object is floating instead of lying on the bottom, as it is in the present paper.

Here, our goal is not to address the local well-posedness theory for this double free

boundary problem, but to give some qualitative insight on its behavior by deriving and analyzing simpler asymptotic models. The focus is on a regime which is particularly interesting for applications, namely, the shallow water regime, where the typical horizontal scale of the flow is much larger than the depth at rest. For a fixed bottom, several models arise in this setting such as the Korteweg–de Vries (KdV) equation (justified in [Cra85, KN86, SW00]), the nonlinear shallow water equations (justified in [Ovs74, KN86, ASL08a, Igu09]), the Boussinesq systems (justified in [Cra85, KN86, BCS02, BCL05]) – see also [Per67, PR83, GKSW95, Cha07, CLS12] for particular focus on topography effects – the Green–Naghdi equations [Li06, ASL08b, HI15], etc. We refer to [Lan13] for more exhaustive references.

For a bottom with prescribed motion in general, the problem has already been considered, local well-posedness results ([ABZ11]) and long time existence results ([Mel15]) have been proven recently. Numerical experiments and attempts to adapt existing and known shallow water models for a moving bottom regime have been present for a while in literature, however lacking rigorous justifications. After observing successively generated solitary waves due to a disturbance in the bottom topography advancing at critical speed ([Wu87]) they formally derived a set of generalized channel type Boussinesq systems ([TW92]), their work was extended later on in a formal study on more general long wave regimes ([Che03]). Tsunami research has also proved to be an important motivating factor with the consideration of water waves type problems with a moving bottom (see for example [GN07] or [Mit09] for an extensive numerical study). The mathematical justification of these models as approximations of the full problem was carried out not too long ago ([Igu11] for Saint-Venant type systems, or [HI15] for the precise Green–Naghdi system).

Here, we present a new class of problems where the bottom is still moving, but its movement is not prescribed, instead it is generated by the wave motion. A good approach to this is to place a freely moving object on the bottom of the fluid domain. The main physical motivation of this study lies in the recent development of submerged wave energy converters (submerged pressure differential devices, [AELS14] and references therein) and oscillating wave surge converters (WaveRollers and Submerged plate devices, [GIL+14]), as well as reef-evolution and submarine landslide modeling problems. Bibliography in the more theoretical approach is rather lacking, existing studies are heavily oriented to physical experiments (most notably in [ACDNn17] where the authors investigate a submerged spring-block system and its numerical simulation through an adapted level set method, for further details, see for example [CM06]), as well as numerical applications ([DNZ15] for instance).

The structure of the article is as follows. In the first section the free surface fluid dynamics system and its possible reformulations in the water waves setting are presented. The equations governing the motion of an object lying on the bottom are established, they derive from Newton's second law and take into account the hydrodynamic force exerted by the fluid and a dynamic friction force. The characteristic scales of the variables of the system are also introduced in order to derive the nondimensionalized equivalents of the

different equations and formulae, preparing for the study of the asymptotic models.

In Section 2, we detail the first order asymptotic regime with respect to the shallowness parameter μ; the resulting approximation is the well-known (nonlinear) Saint-Venant equations, in the presence of a solid moving on the bottom of the fluid domain. A key step is to derive an asymptotic approximation of the hydrodynamic force exerted on the solid. Then we establish a local in time well-posedness result for the coupled system.

In the third section, we elaborate our study on a second order asymptotic regime with respect to the shallowness parameter μ. This study concerns the so called long wave regime where the vertical size of the waves and of the solid are assumed to be small compared to the mean fluid height. The resulting approximation is the so called (weakly nonlinear) Boussinesq system. A local in time well-posedness is shown for this coupled system as well. The standard existence time for a Boussinesq system with a moving bottom is $\mathcal{O}(1)$ with respect to the nonlinearity parameter ε, due to the presence of a source term involving time derivatives of the topography, which can potentially become large (as remarked in [Mel15]). By a precise analysis of the wave-structure coupling one is able to extend the existence time to the $\mathcal{O}(\varepsilon^{-1/2})$ time scale. This time scale is therefore intermediate between the aforementioned $\mathcal{O}(1)$ scale, and the $\mathcal{O}(\varepsilon^{-1})$ scale that can be achieved for fixed bottoms ([ASL08a, Bur16]).

2.1 The fluid-solid coupled model

In this section we present our model in general, that is, the equations characterizing the fluid dynamics as well as the equation describing the solid motion. The dimensionless equations are formulated at the end of the section to prepare the upcoming analysis for the shallow water asymptotic models.

2.1.1 The dynamics of a fluid over a moving bottom

As a basis for our model and our computations, we consider a fluid moving under the influence of gravity. The fluid domain Ω_t (depending on the time t) is delimited from below by a moving bottom and from above by a free surface. In our case the fluid is homogeneous with a constant density ϱ, moreover it is inviscid, incompressible, and irrotational.

To clarify the upcoming notations, the spatial coordinates take the form $(x, z) \in \mathbb{R}^d \times \mathbb{R}$ with x denoting the horizontal component and z the vertical one. Regarding differential operators, x or z as a subscript refers to the operator with respect to that particular variable, the absence of subscript for an operator depending on spatial variables means that it is to be taken for the whole space $(x, z) \in \mathbb{R}^{d+1}$. From a theoretical point of view arbitrary horizontal dimensions $d \in \mathbb{N}^+$ can be considered even though the physically relevant cases are $d = 1$ and 2 only.

In what follows, we denote by $\zeta(t,x)$ the free surface elevation function and $b(t,x)$ describes the bottom topography variation at a base depth of H_0. With this notation at our disposal the fluid domain is

$$\Omega_t = \left\{(x,z) \in \mathbb{R}^d \times \mathbb{R} \,:\, -H_0 + b(t,x) < z < \zeta(t,x)\right\},$$

Let us also introduce the height function $h(t,x) = H_0 + \zeta(t,x) - b(t,x)$ that describes the total depth of the fluid at a given horizontal coordinate x and at a given time t.

In order to avoid special physical cases arising from the fluid domain Ω_t (such as islands or beaches), throughout our analysis we suppose the following (or similar) minimal water height condition

$$\exists h_{min} > 0,\ \forall (t,x) \in [0,T) \times \mathbb{R}^d,\ h(t,x) \geqslant h_{min}, \tag{2.1.1}$$

we refer to [dP16] for an analysis of the water waves equation allowing vanishing depth, and to [LM17] where the evolution of the shoreline is considered for the one dimensional nonlinear Saint-Venant and Serre–Green–Naghdi equations.

2.1.1.1 The free surface Bernoulli equations

To describe the fluid motion under the aforementioned physical assumptions, the free surface Euler equations could be considered, however for what follows the formulation involving a potential (the Bernoulli equations) is more adapted. Due to the fluid being incompressible and irrotational, one can describe its dynamics by utilizing the velocity potential Φ, and with the knowledge of this potential one may recover the actual velocity field as the gradient.

The velocity potential is obtained as a solution of the following Laplace equation

$$\begin{cases} \Delta\Phi = 0 \quad \text{in } \Omega_t, \\ \Phi|_{z=\zeta} = \psi, \ \ \sqrt{1+|\nabla_x b|^2}\partial_{\mathbf{n}}\Phi|_{z=-H_0+b} = \partial_t b, \end{cases} \tag{2.1.2}$$

where ψ is the velocity potential on the free surface (an unknown of the problem). Here we made use of the notation $\partial_{\mathbf{n}}$ signifying the upwards normal derivative (with $\mathbf{n}$ being the unit normal vector of the fluid domain pointing upward). Notice that the Neumann boundary condition on the bottom of the fluid domain corresponds to a kinematic (or no-penetration) boundary condition (that is, the fluid particles do not cross the bottom). Naturally the same condition applies to the free surface, meaning that

$$\partial_t \zeta - \sqrt{1+|\nabla_x \zeta|^2}\partial_{\mathbf{n}}\Phi = 0 \quad \text{on } \{z = \zeta(t,x)\}. \tag{2.1.3}$$

Additionally we also require that there is no surface tension along the free surface, so

the pressure P at the surface is given by the atmospheric pressure P_{atm}, hence

$$P = P_{atm} \quad \text{on } \{z = \zeta(t,x)\}. \tag{2.1.4}$$

By the momentum conservation of the fluid system we get that

$$\partial_t \Phi + \frac{1}{2}|\nabla\Phi|^2 + gz = -\frac{1}{\varrho}(P - P_{atm}) \tag{2.1.5}$$

in the domain Ω_t. Here g in the equation denotes the gravitational acceleration, furthermore ϱ denotes the density of the fluid (constant due to the homogeneity assumption).

So the free surface Bernoulli equations are the system of equations (2.1.2)-(2.1.5).

Based on equation (2.1.5), we can recover the pressure in terms of the velocity potential:

$$P = -\varrho\left(\partial_t\Phi + \frac{1}{2}|\nabla\Phi|^2 + gz\right) + P_{atm}. \tag{2.1.6}$$

This relation allows to compute the hydrodynamical force exerted on the solid by the fluid (derived from Newton's second law in Section 2.1.2).

2.1.1.2 The Zakharov / Craig–Sulem framework

We present another formulation of the equations (also referred to as the water waves problem). This formulation is attributed to Zakharov in his studies regarding gravity waves [Zak68] and is based on the fact that the variables ζ and $\psi = \Phi|_{z=\zeta}$ fully determine the flow. More precisely, the water waves problem reduces to a set of two evolution equations in ζ and ψ,

$$\begin{cases} \partial_t\zeta - \sqrt{1+|\nabla_x\zeta|^2}\partial_{\mathbf{n}}\Phi|_{z=\zeta} = 0, \\ \partial_t\psi + g\zeta + \frac{1}{2}|\nabla_x\psi|^2 - \dfrac{(\sqrt{1+|\nabla_x\zeta|^2}\partial_{\mathbf{n}}\Phi|_{z=\zeta} + \nabla_x\zeta\cdot\nabla_x\psi)^2}{2(1+|\nabla_x\zeta|^2)} = 0, \end{cases} \tag{2.1.7}$$

where Φ solves the boundary value problem (2.1.2).

In more general terms, one can introduce a natural decomposition of Φ into a "fixed bottom" and a "moving bottom" component which could be used to define the so-called Dirichlet-Neumann and Neumann-Neumann operators associated to the Laplace problem (2.1.2) (assuming sufficient regularity for the limiting functions), but we will not pursue further this path, for more details we refer to the works of Craig and Sulem [CSS92, CS93]. For a more specific analysis of the moving bottom case we refer to the article of Alazard, Burq, and Zuily [ABZ11] for the local well-posedness theory or to [Igu11] for specific studies motivated by earthquake generated tsunami research. For a comprehensive and detailed analysis as well as the well-posedness of the water waves problem in the general

setting, we refer to [Lan13] and references therein.

Since our study focuses on shallow water regimes, it is convenient to bypass the aforementioned technicalities by introducing the following variable:

Definition 2.1.1. *The vertically averaged horizontal component of the velocity is given by*

$$\overline{V} = \frac{1}{h}\int_{-H_0+b}^{\zeta} \nabla_x \Phi(\cdot, z)\, dz, \tag{2.1.8}$$

where Φ solves (2.1.2).

The interest of this new variable $\overline{V}$ is that a closed formulation of the water waves problem in terms of ζ and $\overline{V}$ (instead of ζ and ψ) can be obtained, see for example [Lan17]. For our case, it is sufficient to observe that ([Lan13])

Proposition 2.1.1. *If Φ solves (2.1.2) and $\overline{V}$ is defined as in (2.1.8), then*

$$\sqrt{1+|\nabla_x\zeta|^2}\partial_{\mathbf{n}}\Phi|_{z=\zeta} = \partial_t b - \nabla\cdot(h\overline{V}), \tag{2.1.9}$$

assuming sufficient regularity on the data concerning ζ, ψ, and b as well as the minimal water depth condition (2.1.1).

Remark 2.1.1. *Let $\zeta, b \in W^{1,\infty}(\mathbb{R}^d)$ such that they satisfy the minimal water depth condition (2.1.1). Moreover, let $\psi \in \dot{H}^{3/2}(\mathbb{R}^d) = \{f \in L^2_{loc} : \nabla_x f \in H^{1/2}(\mathbb{R}^d)\}$. Then the Laplace equation (2.1.2) can be solved with $\Phi \in \dot{H}^2(\Omega) = \{f \in L^2_{loc} : \nabla_x f \in H^1(\Omega)\}$ and relation (2.1.9) holds true, where*

$$\Omega = \{(X,z) \in \mathbb{R}^d \times \mathbb{R},\ -1 + b(X) < z < \zeta(X)\} \tag{2.1.10}$$

is a known fluid domain. For more details, we refer to Chapter 2 of [Lan13].

With this, the water waves problem with a moving bottom takes the following form

$$\begin{cases} \partial_t\zeta + \nabla\cdot(h\overline{V}) = \partial_t b, \\ \partial_t\psi + g\zeta + \dfrac{1}{2}|\nabla_x\psi|^2 - \dfrac{(-\nabla\cdot(h\overline{V}) + \partial_t b + \nabla_x\zeta\cdot\nabla_x\psi)^2}{2(1+|\nabla_x\zeta|^2)} = 0. \end{cases} \tag{2.1.11}$$

This system seemingly depends on three variables, namely ζ, $\overline{V}$ and ψ, but in fact the Laplace equation provides a connection between the latter two. Exploiting this connection to express (asymptotically) one variable with the other gives rise to various well-known asymptotic equations under the shallow water assumption. In Section 2.1.3 detailing the nondimensionalization of the system we shall provide the necessary tools as well as some references concerning this asymptotic expansion.

2.1.2 A freely moving object on a flat bottom

The aim of this paper is to understand a particular case in which the bottom of the domain contains a freely moving object, the movement of which is determined by the gravity driven fluid motion. We will work with a flat bottom in the presence of a freely moving solid object on it (see Figure 2.1).

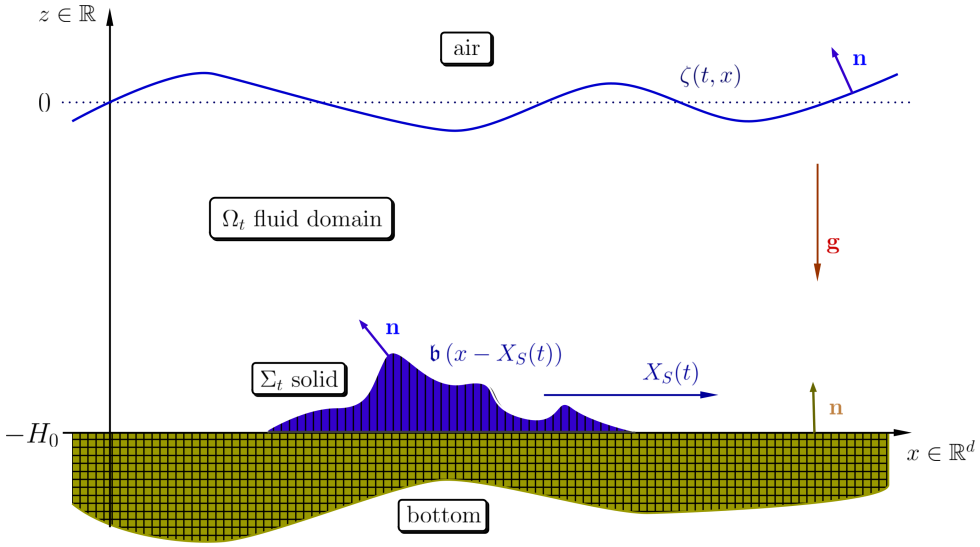

Figure 2.1 – The setting of the water waves problem in the presence of a solid on the bottom

For the solid we suppose it to be rigid and homogeneous with a given mass M. The surface of the object can be characterized by two components: the part of the surface in direct contact with the fluid, denoted by Σ_t and the rest, that is the part in direct contact with the flat bottom, denoted by $I(t)$. For convenience reasons we shall suppose that Σ_t is a graph of a $\mathcal{C}^\infty$ function with compact support $I(t)$ for any instance of t.

The solid moves horizontally in its entirety, we denote by $X_S(t)$ the displacement vector, and $v_S(t)$ the velocity (with $\dot{X}_S = v_S$). We make the additional hypothesis that the object is neither overturning, nor rotating so its movement is completely described by its displacement vector, which will be restrained to horizontal movement only. In particular, this means that the object is not allowed to start floating, the domain $I(t)$ has a constant (nonzero) area.

Under these assumptions a simplified characterization of the function describing the bottom variation is possible:

$$b(t,x) = \mathfrak{b}\,(x - X_S(t))\,, \tag{2.1.12}$$

where $\mathfrak{b}$ corresponds to the initial state of the solid at $t = 0$ (so that we have $X_S(0) = 0$).

Taking into account all the external forces acting on the object, Newton's second law provides us with the correct equation for the movement of the solid. The total force acting on the solid is

$$\begin{aligned}\mathbf{F}_{\text{total}} &= \mathbf{F}_{\text{gravity}} + \mathbf{F}_{\text{solid-bottom interaction}} + \mathbf{F}_{\text{solid-fluid interaction}} \\ &= M\mathbf{g} + [\mathbf{F}_{\text{normal}} + \mathbf{F}_{\text{friction}}] + \mathbf{F}_{\text{pressure}}.\end{aligned}$$

Here we made use of the fact that the force emerging from the contact of the solid with the bottom may be decomposed in two components: the normal force, perpendicular to the surface of the bottom, expressing the fact that the bottom is supporting the solid, and the (kinetic or dynamic) friction force, the tangential component, hindering the sliding of the solid. By making use of the three empirical laws of friction [Ber06], most notably the third law often attributed to Coulomb regarding the existence of a coefficient $c_{\text{fric}} > 0$ of kinetic friction (describing the material properties of the contact medium), we may reformulate the tangential contact force as follows

$$\mathbf{F}_{\text{friction}} = \mathbf{F}_{\text{sliding friction}} = -c_{\text{fric}}|\mathbf{F}_{\text{normal}}|\frac{v_S(t)}{|v_S(t)| + \sqrt{gH_0\bar{\delta}}}, \tag{2.1.13}$$

where $\bar{\delta} \ll 1$ is a purely mathematical dimensionless parameter serving as a regularizing term in order to avoid a singularity in the equation when the solid stops, that is when $v_S(t)$ is equal to 0. Normally, when the solid comes to a halt, the kinetic friction detailed just before turns into static friction, a tangential force component preventing the solid from restarting its movement. The static friction has its own coefficient, which is usually greater than c_{fric}, and its direction is determined by the horizontal force component rather than the velocity.

Remark 2.1.2. *The coefficient of friction c_{fric} is a dimensionless scalar constant, it describes a ratio proportional to the hindering effect generated by the parallel motion of two surfaces. It is in fact a property of the system, in reality it not only depends on the material of the two surfaces but their geometry (surface microstructure), temperature, atmospheric conditions, velocity of the motion, etc. and as such it is impossible to accurately determine it. To give the reader an idea, an almost frictionless sliding (for example objects on ice, lubricated materials) corresponds to a coefficient of $10^{-2} \sim 10^{-3}$, while a frictional sliding (for example rubber on paper) has a coefficient of order 1.*

In order to prevent the complications that would arise by implementing the physically more relevant threshold for $v_S(t) = 0$ and the associated jump in friction force, we simplify the system by regularizing the friction force, thus neglecting static effects. A more specific modeling and analysis of the transition between static and dynamic friction will be addressed in future works.

Treating the horizontal and vertical component of $\mathbf{F}_{\text{total}} = (\mathbf{F}^h_{\text{total}}, \mathbf{F}^v_{\text{total}})^\top$ separately and using the fact that the solid is constrained to horizontal motion, we have that the

vertical components are in equilibrium, thus

$$0 = -M\mathbf{g} + \mathbf{F}_{\text{normal}} + \mathbf{F}^{v}_{\text{pressure}}, \tag{2.1.14}$$

and we obtain that the horizontal movement of the solid is given by

$$M\ddot{X}_S(t) = \mathbf{F}_{\text{sliding friction}} + \mathbf{F}^{h}_{\text{pressure}}. \tag{2.1.15}$$

Finally, by making use of the fact that

$$\mathbf{F}_{\text{pressure}} = \int_{\Sigma_t} P\mathbf{n}_{\text{solid}}\, d\Sigma = \int_{I(t)} P|_{z=-H_0+b(t,x)} \begin{pmatrix} \nabla_x b \\ -1 \end{pmatrix} dx,$$

due to the fact that the inwards normal vector for the surface of the solid $\mathbf{n}_{\text{solid}} = -\mathbf{n}$ can be easily expressed by the bottom variation $b(t,x)$, since

$$\mathbf{n}_{\text{solid}} = \frac{1}{\sqrt{1+|\nabla_x b|^2}} \begin{pmatrix} \nabla_x b \\ -1 \end{pmatrix}.$$

Therefore we obtain from (2.1.14) that

$$F_{\text{normal}} = Mg + \int_{I(t)} P|_{z=-H_0+b(t,x)}\, dx, \tag{2.1.16}$$

now as a scalar quantity since the vertical direction is one dimensional. Let us remark that $F_{\text{normal}} \geqslant 0$, since the right hand side is nonnegative, due to the pressure being positive. Therefore, by (2.1.13), (2.1.15) writes as

$$M\ddot{X}_S(t) = -c_{\text{fric}} F_{\text{normal}} \frac{\dot{X}_S(t)}{\left|\dot{X}_S(t)\right| + \sqrt{gH_0\delta}} + \int_{I(t)} P|_{z=-H_0+b(t,x)} \nabla_x b\, dx. \tag{2.1.17}$$

So we have that Newton's equation characterizing the motion of the solid takes the following form

$$\begin{aligned} M\ddot{X}_S(t) = &- c_{\text{fric}} \left(Mg + \int_{I(t)} P|_{z=-H_0+b(t,x)}\, dx \right) \frac{\dot{X}_S(t)}{\left|\dot{X}_S(t)\right| + \sqrt{gH_0\delta}} \\ &+ \int_{I(t)} P|_{z=-H_0+b(t,x)} \nabla_x b\, dx. \end{aligned} \tag{2.1.18}$$

A key step in our study is to handle the force term exerted by the fluid, which requires the computation of the integral of the pressure on the bottom over the solid domain. For this we will establish an appropriate formula for the pressure to be used in the integral.

In both the case of the freely moving bottom (due to the moving object) and the free surface, the kinematic no-penetration condition still applies, most notably we still have that

$$\partial_t b - \sqrt{1+|\nabla_x b|^2}\mathbf{U}\cdot\mathbf{n} = 0 \quad \text{for } \{z = -H_0 + b(t,x)\},$$

or equivalently, on the part of the surface of the solid in contact with the fluid (Σ_t), the normal component of the fluid velocity field coincides with the normal component of the velocity of the solid, that is

$$\mathbf{U}\cdot\mathbf{n}_{\text{solid}} = v_S\cdot\mathbf{n}^h_{\text{solid}} \quad \text{for } \{z = -H_0 + b(t,x)\}. \tag{2.1.19}$$

To sum up, the water waves problem in the presence of a solid on the bottom is given by equations (2.1.11) and (2.1.2), where in the Neumann boundary condition, the bottom function b and its time derivative are given by (3.1.1), with X_S arising from (2.1.18) and the pressure P derived from (2.1.6).

2.1.3 Dimensionless form of the equations

The main part of the analysis consists of establishing and analyzing the wave-structure interaction system for shallow water regimes, for that we need first of all the correct parameters involving the characteristic orders of magnitude of our variables as well as the dimensionless equations obtained with the help of these quantities.

2.1.3.1 The different scales of the problem

First of all we present the proper dimensionless parameters relevant to the system. For that we need to introduce the various characteristic scales of the problem: as already mentioned before, the base water depth is H_0. The characteristic horizontal scale of the wave motion (both for longitudinal and transversal directions) is L, the order of the free surface amplitude is a_{surf}, and the characteristic height of the solid (order of the bottom topography variation in general) is a_{bott}.

Using these quantities, we can introduce several dimensionless parameters:

$$\mu = \frac{H_0^2}{L^2}, \quad \varepsilon = \frac{a_{\text{surf}}}{H_0}, \quad \text{and } \beta = \frac{a_{\text{bott}}}{H_0},$$

where μ is called the shallowness parameter, ε stands for the nonlinearity (or amplitude) parameter, and β is the bottom topography parameter.

Our goal in this paper is to examine asymptotic models when μ is small (shallow water regime), and under various assumptions on the characteristic size of ε and β.

With these parameters in our hand, we may remark that the natural scaling for the

horizontal spatial variable x is L, and for its vertical counterpart z it is H_0. Moreover the natural order of magnitude for the function characterizing the free surface ζ is a_{surf}, and for the bottom b it is a_{bott}. Thus the nondimensionalized form for the water depth is

$$h = 1 + \varepsilon\zeta - \beta b.$$

Furthermore, one can establish the correct scale of the velocity potential through linear wave analysis, which gives rise to

$$\Phi_0 = \frac{a_{\text{surf}}}{H_0} L\sqrt{gH_0}.$$

As for the pressure, we choose the typical order of the hydrostatic pressure, that is $P_0 = \varrho g H_0$. For the time parameter, from linear wave theory one can deduce the scaling as

$$t_0 = \frac{L}{\sqrt{gH_0}}.$$

Finally, for the parameters concerning the solid, we impose that the characteristic horizontal dimension of the solid is comparable to L (which was already implicitly assumed). It would be relevant to consider solids with a smaller size, but this raises important difficulties. Even in the case of a fixed bottom there is no fully justified model yet in general (see for example [CLS12]).

Following this, by taking into account the volume integral of the density, the mass can be rescaled by the nondimensionalisation parameter $\tilde{M}$:

$$M = M_0\tilde{M} = \varrho L^d a_{\text{bott}}\tilde{M}.$$

Thus the proper nondimensionalized parameters are obtained by

$$x' = \frac{x}{L}, \quad z' = \frac{z}{H_0}, \quad \zeta' = \frac{\zeta}{a_{\text{surf}}}, \quad \Phi' = \frac{\Phi}{\Phi_0}, \quad t' = \frac{t}{t_0}, \quad \text{etc.}$$

For the sake of clarity we shall omit the primes on the variables from here on.

Our main interest will be to express the equations principally with the different orders of magnitude of μ (the shallowness parameter) to pass on to the different asymptotic regimes. Given the particular structure of the asymptotic regimes we are going to examine we shall make an a priori hypothesis concerning certain parameters.

Remark 2.1.3. *Since all the regimes handled in this article involve the hypothesis that ε and β are of the same order of magnitude we assume, without loss of generality, that $\beta = \varepsilon$.*

An additional precision shall be made concerning the quantities involving the bottom.

The explicit form of the nondimensionalized form for the water depth is

$$h(t,x) = 1 + \varepsilon(\zeta(t,x) - b(t,x)) \tag{2.1.20}$$

with

$$b(t,x) = \mathfrak{b}\left(x - X_S(t)\right). \tag{2.1.21}$$

2.1.3.2 Nondimensionalized equations

Using the previous section and in particular taking $\varepsilon = \beta$ as in Remark 2.1.3, one easily derives the dimensionless version of (2.1.11), namely

$$\begin{cases} \partial_t \zeta + \nabla \cdot (h\overline{V}) = \partial_t b, \\ \partial_t \psi + \zeta + \dfrac{\varepsilon}{2}|\nabla_x \psi|^2 - \varepsilon\mu \dfrac{(-\nabla \cdot (h\overline{V}) + \partial_t b + \nabla_x(\varepsilon\zeta)\cdot\nabla_x\psi)^2}{2(1+\varepsilon^2\mu|\nabla_x\zeta|^2)} = 0, \end{cases} \tag{2.1.22}$$

where $\overline{V}$ is now defined as

$$\overline{V} = \frac{1}{h}\int_{-1+\varepsilon b}^{\varepsilon\zeta} \nabla_x \Phi(\cdot, z)\, dz, \tag{2.1.23}$$

with $h = 1 + \varepsilon\zeta - \varepsilon b$, furthermore Φ solves

$$\begin{cases} \Delta^\mu \Phi = \mu\Delta_x\Phi + \partial_z^2\Phi = 0, \quad \text{on } -1+\varepsilon b \leqslant z \leqslant \varepsilon\zeta, \\ \Phi|_{z=\varepsilon\zeta} = \psi, \quad (\partial_z\Phi - \mu\nabla_x(\varepsilon b)\cdot\nabla_x\Phi)\,|_{z=-1+\varepsilon b} = \mu\partial_t b, \end{cases} \tag{2.1.24}$$

the nondimensionalized equivalent of the Laplace problem (2.1.2).

It is also necessary to nondimensionalize the formula describing the pressure (2.1.6), thus

$$P = \frac{P_{atm}}{\varrho g H_0} - z - \varepsilon\partial_t\Phi - \frac{\varepsilon^2}{2}|\nabla_x\Phi|^2 - \frac{\varepsilon^2}{2\mu}|\partial_z\Phi|^2. \tag{2.1.25}$$

Here we had to separate the horizontal and the vertical part of the gradient due to the different scaling parameters for the different directions.

We remark that the normal derivative is given by

$$\mathbf{n}_{solid} = \frac{1}{\sqrt{1+\varepsilon^2\mu|\nabla_x b|^2}}\begin{pmatrix}\sqrt{\mu}\varepsilon\nabla_x b \\ -1\end{pmatrix}.$$

Thus we may reformulate Newton's equation (2.1.18) in the following way

$$\begin{aligned}\ddot{X}_S(t) = &- \frac{c_{\text{fric}}}{\sqrt{\mu}} \left(1 + \frac{1}{\varepsilon \tilde{M}} \int_{I(t)} P|_{z=-1+\varepsilon b}\, dx\right) \frac{\dot{X}_S(t)}{\left|\dot{X}_S(t)\right| + \bar{\delta}} \\ &+ \frac{1}{\tilde{M}} \int_{\mathbb{R}^d} P_{z=-1+\varepsilon b} \nabla_x b\, dx,\end{aligned} \tag{2.1.26}$$

taking into consideration the characteristic scales of the variables.

2.2 The $\mathcal{O}(\mu)$ asymptotic regime: The nonlinear Saint-Venant equations

We shall now start our analysis for shallow water regimes, that is an asymptotic analysis with respect to the shallowness parameter μ for the nondimensionalized water waves problem (2.1.22) coupled with Newton's equation (2.1.26) for the solid. With our notations, this means that we would like to consider systems that are valid for $\mu \ll 1$.

In this section we treat the general first order approximate system, more specifically a model with $\mathcal{O}(\mu)$ approximation that allows large wave amplitudes and large bottom variations ($\varepsilon = \mathcal{O}(1)$). So, the asymptotic regime writes as follows

$$0 < \mu \leqslant 1, \quad \varepsilon = 1. \tag{SV}$$

2.2.1 The fluid equations in the asymptotic regime

As mentioned before, the important step in deducing asymptotic models relies on how we establish the connection between the variables $\overline{V}$ and ψ. More precisely, it is possible to construct an asymptotic expansion of $\overline{V}$ with respect to μ (depending on ζ, b and ψ). For details, we refer to Chapter 3 of [Lan13]. One can equally obtain an asymptotic expansion of Φ with respect to μ, depending on the aforementioned variables. Quite obviously the equation $\Delta^\mu \Phi = 0$ in (2.1.24) reduces to $\partial_z^2 \Phi = 0$ at leading order in z; since the Neumann boundary condition in (2.1.24) is $\mathcal{O}(\mu)$, it follows that Φ does not depend on z at leading order, and therefore

$$\overline{V} = \nabla_x \psi + \mathcal{O}(\mu),$$

see Proposition 3.37. in [Lan13] for a rigorous proof.

So the system (2.1.22) for the $(\zeta, \overline{V})$ variables simplifies as follows

$$\begin{cases} \partial_t \zeta + \nabla_x \cdot (h\overline{V}) = \partial_t b, \\ \partial_t \overline{V} + \nabla_x \zeta + (\overline{V} \cdot \nabla_x)\overline{V} = 0, \end{cases} \tag{2.2.1}$$

where we considered the gradient of the second equation in (2.1.22), and then neglected terms of order $\mathcal{O}(\mu)$. This system is known as the (nonlinear) Saint-Venant or nonlinear shallow water equations.

2.2.2 Formal derivation of a first order asymptotic equation for the solid motion

Our strategy is as follows: we establish an asymptotic formula of order $\mathcal{O}(\mu)$ for the pressure P based on (2.1.25). With this at our disposal, we rewrite Newton's equation (2.1.26) at order approximately μ describing the displacement of the solid.

For an $\mathcal{O}(\mu)$ approximation, we shall start with the corresponding development for the velocity potential, that is

$$\Phi = \psi + \mathcal{O}(\mu), \tag{2.2.2}$$

where $\psi = \Phi|_{z=\varepsilon\zeta}$ as before, the restriction of the velocity potential on the free surface. Knowing this we recover the following for the time derivative of ψ (based on the second equation of the water waves problem (2.1.22))

$$\partial_t \psi = -\zeta - \frac{1}{2}|\nabla_x \psi|^2 + \mathcal{O}(\mu).$$

So by substituting the first order asymptotic expansion of the velocity potential described in (2.2.2) into the general nondimensionalized formula of the pressure (2.1.25) the corresponding $\mathcal{O}(\mu)$ approximation for the pressure takes the form

$$P = \frac{P_{atm}}{\varrho g H_0} + (\zeta - z) + \mathcal{O}(\mu),$$

using the fact that ψ does not depend on the variable z.

So in particular, at the bottom, we find that the pressure is given by the hydrostatic formula

$$P|_{z=-1+b} = \frac{P_{atm}}{\varrho g H_0} + h + \mathcal{O}(\mu). \tag{2.2.3}$$

Thus for Newton's equation (2.1.26),

$$\begin{aligned}\ddot{X}_S = &-\frac{c_{\text{fric}}}{\sqrt{\mu}}\left(1 + \frac{1}{\tilde{M}}\int_{I(t)}\left(\frac{P_{atm}}{\varrho g H_0} + h\right)\,dx\right)\frac{\dot{X}_S}{\left|\dot{X}_S\right| + \overline{\delta}} \\ &+ \frac{P_{atm}}{\varrho g H_0 \tilde{M}}\int_{\mathbb{R}^d}\nabla_x b\,dx + \frac{1}{\tilde{M}}\int_{\mathbb{R}^d} h\nabla_x b\,dx + \mathcal{O}\left(\frac{c_{\text{fric}}}{\tilde{M}}\sqrt{\mu}\right).\end{aligned}$$

Using the fact that b is of compact support, the integral of its (and b^2's) gradient on

the whole horizontal space is 0, and the equation simplifies to

$$\ddot{X}_S = -\frac{c_{\text{fric}}}{\sqrt{\mu}}\left(1 + \frac{|\operatorname{supp}(\mathfrak{b})|}{\tilde{M}}\left(\frac{P_{atm}}{\varrho g H_0} + 1\right) - \frac{|\operatorname{Volume}_{Solid}|}{\tilde{M}} + \frac{1}{\tilde{M}}\int_{I(t)} \zeta\, dx\right)\frac{\dot{X}_S}{\left|\dot{X}_S\right| + \overline{\delta}} + \frac{1}{\tilde{M}}\int_{\mathbb{R}^d} \zeta \nabla_x b\, dx + \mathcal{O}\left(\frac{c_{\text{fric}}}{\tilde{M}}\sqrt{\mu}\right).$$

Notice the presence of the friction term (the first term on the right hand side). Even though it is of order $\mu^{-1/2}$, it will not pose a problem when controlling the solid velocity, as we are going to see in Lemma 2.2.5. later on (since it acts as a damping force).

Recalling that b is given by (2.1.21) the corresponding approximative equation characterizing the motion of the body is

$$\ddot{X}_S = -\frac{c_{\text{fric}}}{\sqrt{\mu}}\left(c_{solid} + \frac{1}{\tilde{M}}\int_{\operatorname{supp}(\mathfrak{b})+X_S} \zeta\, dx\right)\frac{\dot{X}_S}{\left|\dot{X}_S\right| + \overline{\delta}} + \frac{1}{\tilde{M}}\int_{\mathbb{R}^d} \zeta \nabla_x \mathfrak{b}(x - X_S)\, dx, \quad (2.2.4)$$

where we made use of the following abbreviation:

$$c_{solid} = 1 + \frac{|\operatorname{supp}(\mathfrak{b})|}{\tilde{M}}\left(\frac{P_{atm}}{\varrho g H_0} + 1\right) - \frac{|\operatorname{Volume}_{Solid}|}{\tilde{M}}. \quad (2.2.5)$$

We remark that the quantity corresponding to F_{normal},

$$c_{solid} + \frac{1}{\tilde{M}}\int_{\operatorname{supp}(\mathfrak{b})+X_S} \zeta\, dx > 0$$

positive, since it contains positive constants as well as the integral of the approximate hydrostatic pressure $P|_{z=-1+b}$ (given by (2.2.3), which is positive, by the minimal water height assumption (2.1.1.

Therefore, we have the following concerning the consistency of the solid equation:

Proposition 2.2.1. *Let $s_0 \geqslant 0$, and let us assume that $\zeta \in \mathcal{C}([0,T]; H^{s_0+4}(\mathbb{R}^d))$ and that $\mathfrak{b} \in H^{s_0+4}(\mathbb{R}^d)$ compactly supported. Let us suppose that $\nabla_x \psi \in \mathcal{C}([0,T]; H^{s_0+4}(\mathbb{R}^d))$. The solid equation (2.1.26) is consistent at order $\mathcal{O}(\sqrt{\mu})$ with the model (3.1.3) on $[0,T]$ with $T > 0$.*

Proof: By the regularity assumptions (Lemma 3.42. of [Lan13]), we can write that $\Phi = \psi + \mu R_1$ with

$$\begin{aligned} |||R_1|||_{T,H^{s_0}} &\leqslant C(|||\zeta|||_{T,H^{s_0+2}}, \|\mathfrak{b}\|_{H^{s_0+2}})|||\nabla_x \psi|||_{T,H^{s_0+2}} \\ |||\partial_t R_1|||_{T,H^{s_0}} &\leqslant C(|||\zeta|||_{T,H^{s_0+4}}, \|\mathfrak{b}\|_{H^{s_0+4}}, |||\nabla_x \psi|||_{T,H^{s_0+4}}), \end{aligned}$$

here the second estimate is due to Lemma 5.4. of [Lan13]. This means that, following the

same computations as before, we have that

$$P|_{z=-1+b} = \frac{P_{atm}}{\varrho g H_0} + h + \mu R_{P,1}$$
$$|||R_{P,1}|||_{T,H^{s_0}} \leqslant C(|||\zeta|||_{T,H^{s_0+4}}, \|\mathfrak{b}\|_{H^{s_0+4}}, |||\nabla_x \psi|||_{T,H^{s_0+4}}).$$

Here the $|||\,|||_{T,\mathcal{X}}$ notation was adopted based on Definition 2.2.1.

Hence, in the equation for the solid motion (2.1.26), we recover the approximate equation (3.1.3) with the additional error terms

$$-\sqrt{\mu}\frac{c_{\text{fric}}}{\tilde{M}}\frac{\dot{X}_S}{|\dot{X}_S| + \overline{\delta}}\int_{I(t)} R_{P,1}\,dx + \mu\frac{1}{\tilde{M}}\int_{I(t)} R_{P,1}\nabla_x\mathfrak{b}(x - X_S)\,dx,$$

that can be estimated as an $\mathcal{O}(\sqrt{\mu})$ total error term, that is, it is less than

$$\sqrt{\mu}C(\tilde{M}^{-1}, |||\zeta|||_{T,H^{s_0+4}}, \|\mathfrak{b}\|_{H^{s_0+4}}, |||\nabla_x\psi|||_{T,H^{s_0+4}}).$$

□

2.2.3 The wave-structure interaction problem at first order

With (3.1.3) in our hand, we have all three equations for our coupled system. Indeed, notice that for the first equation in the nonlinear Saint-Venant system (2.2.1), the right hand side depends on X_S, since $b(t,x)$ depends on it. Hence, by the chain rule the right hand side is

$$\partial_t b(t,x) = -\nabla_x\mathfrak{b}(x - X_S(t)) \cdot \dot{X}_S(t).$$

Our remark concerning the friction term present in the acceleration equation (3.1.3) becomes even more pertinent now, since we can observe a direct influence of the solid velocity in the first equation of the fluid system (2.2.1). This implies that a careful attention has to be paid on the velocity estimate for the solid.

To sum it up, the free surface equations with a solid moving at the bottom in the case of the nonlinear Saint-Venant approximation take the following form

$$\begin{cases} \partial_t\zeta + \nabla_x\cdot(h\overline{V}) = \nabla_x\mathfrak{b}(x - X_S)\cdot\dot{X}_S, \quad x\in\mathbb{R}^d \\ \partial_t\overline{V} + \nabla_x\zeta + (\overline{V}\cdot\nabla_x)\overline{V} = 0, \quad x\in\mathbb{R}^d \end{cases} \tag{2.2.6a}$$

$$\ddot{X}_S = -\frac{c_{\text{fric}}}{\sqrt{\mu}}\left(c_{solid} + \frac{1}{\tilde{M}}\int_{I(t)}\zeta\,dx\right)\frac{\dot{X}_S}{|\dot{X}_S| + \overline{\delta}} + \frac{1}{\tilde{M}}\int_{\mathbb{R}^d}\zeta\nabla_x\mathfrak{b}(x - X_S)\,dx. \tag{2.2.6b}$$

In what follows, we proceed to the mathematical analysis of this system. We shall establish a local in time existence result for the coupled equations.

2.2.4 Local in time existence of the solution

The main result on the local well-posedness of the wave-structure interaction problem (2.2.6) is the following:

Theorem 2.2.1. *Suppose that $\varepsilon = 1$, and that μ is sufficiently small so that we are in the shallow water regime (SV). Let us suppose that for the initial value ζ_{in} and $\mathfrak{b}$ the lower bound condition (2.1.1) is satisfied. If the initial values ζ_{in} and $\overline{V}_{in}$ are in $H^s(\mathbb{R}^d)$ with $s \in \mathbb{R}$, $s > d/2 + 1$, and $X_S(0) = 0$, $\dot{X}_S(0) = v_{S_0} \in \mathbb{R}^d$ is an arbitrary initial condition for the solid motion, then there exists a solution*

$$(\zeta, \overline{V}) \in \mathcal{C}([0, T_0]; H^s(\mathbb{R}^d)) \cap \mathcal{C}^1([0, T_0]; H^{s-1}(\mathbb{R}^d)),$$
$$X_S \in \mathcal{C}^2([0, T_0]),$$

to (2.2.6) for a sufficiently small time $T_0 > 0$ independent of μ.

Proof: The demonstration is based on the fixed point theorem applied to an iterative scheme presented in the following subsections. The brief outline of our proof is as follows:

1. Reformulation of the system,
2. Construction of the iterative scheme,
3. Existence and a priori estimates for the iterative scheme,
4. Convergence of the iterative scheme solutions.

2.2.4.1 Reformulation of the coupled fluid-solid system

Let us remark the following: the nonlinear Saint-Venant equations (2.2.1) admit a quasilinear hyperbolic structure. More precisely, we have the following classical reformulation using the new variable $\mathcal{U} = (\zeta, \overline{V})^\top \in \mathbb{R}^{d+1}$:

$$\partial_t \mathcal{U} + \sum_{j=1}^{d} A_j(\mathcal{U}, X_S)\partial_j \mathcal{U} + B(\mathcal{U}, X_S) = 0. \tag{2.2.7}$$

Let us take the following real valued $(d+1) \times (d+1)$ matrices

$$A_j(\mathcal{U}, X_S) = \left(\begin{array}{c|c} \overline{V}_j & hI_j \\ \hline I_j^\top & \overline{V}_j \, \mathrm{Id}_{d\times d} \end{array}\right) \text{ for } 1 \leqslant j \leqslant d, \tag{2.2.8}$$

where for every $1 \leqslant j \leqslant d$ we have $I_j = e_j \in \mathbb{R}^d$ the j^{th} coordinate vector with respect to the standard Euclidean basis of $\mathbb{R}^d$.

We recall that $h = 1 + \zeta - b$ thus implying that the matrices $A_j(\mathcal{U}, X_S)$ indeed depend on X_S, however only through the bottom variation (2.1.21).

Following the notation in (2.2.7), the additional term $B(\mathcal{U}, X_S)$ is the vector

$$B(\mathcal{U}, X_S) = \left(-\overline{V} \cdot \nabla_x \mathfrak{b}(x - X_S) + \nabla_x \mathfrak{b}(x - X_S) \cdot \dot{X}_S, 0, \dots, 0\right)^\top.$$

From here on, we shall also use the following uniform notation for the coordinate functions of $\mathcal{U}$:

$$\mathcal{U}_0 = \zeta, \quad \mathcal{U}_j = \overline{V}_j \text{ for } 1 \leqslant j \leqslant d.$$

As for the initial values, we have $\mathcal{U}(0, \cdot) = \mathcal{U}_{in} = (\zeta_{in}, \overline{V}_{in})$ and $X_S(0) = 0$, $\dot{X}_S(0) = v_{S_0}$. There is no restriction necessary on the initial values concerning the solid motion.

There exists a symmetrizer matrix $S(\mathcal{U}, X_S)$ defined by

$$S(\mathcal{U}, X_S) = \left(\begin{array}{c|c} 1 & 0 \\ \hline 0 & h\,\mathrm{Id}_{d\times d} \end{array}\right), \tag{2.2.9}$$

such that the matrices $S(\mathcal{U}, X_S)A_j(\mathcal{U}, X_S)$ are symmetric. Moreover, based on our imposed lower boundary condition on h_{in}, one can establish that

$$S(\mathcal{U}_{in}, 0) \geqslant \min(1, h_{min})\,\mathrm{Id}_{(d+1)\times(d+1)},$$

which guarantees that the matrix is positive definite.

Owing to the existence of such a symmetrizer S, the local well-posedness for a bottom with a prescribed motion follows from classical results [Tay97]. In our case and additional step is needed due to the presence of the coupling with the equation describing the solid motion.

Let us make one further remark, concerning the second order (nonlinear) ordinary differential equation characterizing the displacement of the solid X_S in (2.2.6b). Let us define the functional $\mathcal{F}[\mathcal{U}](t, Y, Z)$ as

$$\mathcal{F}[\mathcal{U}](t, Y, Z) = -\frac{c_{\text{fric}}}{\sqrt{\mu}} \left(c_{solid} + \frac{1}{\tilde{M}} \int\limits_{\text{supp}(\mathfrak{b})+Y} \mathcal{U}_0\, dx \right) \frac{Z}{|Z| + \bar{\delta}} + \frac{1}{\tilde{M}} \int_{\mathbb{R}^d} \mathcal{U}_0 \nabla_x \mathfrak{b}(x - Y)\, dx.$$

The coupled system (2.2.6) has the following equivalent form

$$\begin{cases} \partial_t \mathcal{U} + \displaystyle\sum_{j=1}^{d} A_j(\mathcal{U}, X_S)\partial_j \mathcal{U} + B(\mathcal{U}, X_S) = 0, & \text{(2.2.10a)} \\ \ddot{X}_S = \mathcal{F}[\mathcal{U}]\left(t, X_S, \dot{X}_S\right). & \text{(2.2.10b)} \end{cases}$$

2.2.4.2 The iterative scheme

To solve the coupled system (2.2.10) we construct a sequence $\left(\{\mathcal{U}^k(t,x)\},\{X^k(t)\}\right)_{k\in\mathbb{N}}$ of approximate solutions through the scheme

$$\begin{cases} S(\mathcal{U}^k,X^k)\partial_t\mathcal{U}^{k+1}+\sum_{j=1}^{d}S(\mathcal{U}^k,X^k)A_j(\mathcal{U}^k,X^k)\partial_j\mathcal{U}^{k+1}= \\ \qquad\qquad =-S(\mathcal{U}^k,X^k)B(\mathcal{U}^k,X^k), \end{cases} \tag{2.2.11a}$$

$$\begin{cases} \ddot{X}^{k+1}=\mathcal{F}[\mathcal{U}^{k+1}]\left(t,X^{k+1},\dot{X}^{k+1}\right); \\ \mathcal{U}^{k+1}(0,\cdot)=\mathcal{U}_{in},\quad X^{k+1}(0)=0,\ \dot{X}^{k+1}(0)=v_{S_0}. \end{cases} \tag{2.2.11b}$$

Here the matrices A_j and S are the matrices defined in (2.2.8) and (2.2.9). In what follows we will make use of the following abbreviations

$$S^k=S(\mathcal{U}^k,X^k),\quad A_j^k=A_j(\mathcal{U}^k,X^k),\ \text{ and }\ B^k=B(\mathcal{U}^k,X^k).$$

The main goal is to prove the existence and convergence of this sequence. We will follow the footsteps of a classical method, presented by Alinhac and Gérard in [AG07] for instance, detailing only the parts where additional estimates are necessary due to the coupling terms.

The iterative scheme works as follows: we choose the initial $k=0$ elements to be $(\mathcal{U}^0,X^0)=(\mathcal{U}_{in},0)$. From then on, at each step k ($k\in\mathbb{N}$) we have to solve a linear symmetric hyperbolic PDE system (2.2.11a) to recover $\mathcal{U}^{k+1}$, and then a second order nonlinear ODE (2.2.11b) to obtain X^{k+1}.

2.2.4.3 Existence and a priori estimates

Now, the aim is to establish the existence of solutions $(\mathcal{U}^{k+1},X^{k+1})$ ($k\geqslant 0$) for the iterative scheme to justify their definition in (2.2.11). Furthermore we shall also obtain a control of the velocity fields for our coupled system. In particular an upper bound on $\mathcal{U}^{k+1}$ in a "large norm", partially in order to guarantee the boundedness conditions required for the existence result presented, as well as to introduce certain inequalities which will be useful for the convergence of the series.

In what follows, we will make use of the following notation

Definition 2.2.1. *For an $f(t,x)\in L^\infty([0,T];\mathcal{X}(\mathbb{R}^d))$ function let us define*

$$|||f|||_{T,\mathcal{X}}=\sup_{t\in[0,T]}\|f(t,\cdot)\|_{\mathcal{X}}. \tag{2.2.12}$$

With this definition at our disposal, we can state the induction hypothesis (H_k) for

the boundedness of solutions $(\mathcal{U}^l, X^l)_{l\leqslant k}$ of (2.2.11):

$$\text{for } 0 \leqslant l \leqslant k, \quad \left|\!\left|\!\left|\mathcal{U}^l\right|\!\right|\!\right|_{T,H^s} \leqslant C_f, \ \left|\!\left|\!\left|\mathcal{U}^l - \mathcal{U}_{in}\right|\!\right|\!\right|_{T,L^\infty} \leqslant \delta_0, \ \sup_{t\in[0,T]} \left|\dot{X}^l - v_{S_0}\right| \leqslant C_v T, \quad (H_k)$$

for a sufficiently large constant $C_f = C(\tilde{M}^{-1}, S_0^{-1}, \|\mathcal{U}_{in}\|_{H^s}, \|\mathfrak{b}\|_{H^s})$, with $\delta_0 > 0$ a small constant to be defined, independent of k, and $C_v = C(\tilde{M}^{-1}, \|\mathfrak{b}\|_{H^s}; C_f)$,

Proposition 2.2.2. *For $k \geq 0$, assuming the induction hypothesis (H_k), there exists a solution $\mathcal{U}^{k+1} \in \mathcal{C}([0,T]; H^s(\mathbb{R}^d))$, $X^{k+1} \in \mathcal{C}^2([0,T])$ of (2.2.11), moreover, by an adequate choice of C_f, δ_0, and T (independent of k and of μ)*

$$(H_k) \Rightarrow (H_{k+1}).$$

Proof: The proof goes by induction. For $k = 0$, (H_0) is clearly verified. For the induction step, we shall treat separately the case of the PDE (part A) and the case of the ODE (part B), for the sake of clarity.

Part A: existence and energy estimate for $\mathcal{U}^{k+1}$: The initial values $\mathcal{U}^{k+1}(0,\cdot)$ are bounded since they are equal to the original initial values $\mathcal{U}_{in}$. Since we are operating by induction with respect to k, for the respective $\mathcal{U}^k$ term we already have existence, moreover we also have the large norm estimates (H_k) at hand, which in particular guarantees the uniform bounds for $\mathcal{U}^k$ (independently of the index k) for small time T and δ_0. Also, given the simple structure of S^k and $S^k A_j^k$, they are bounded as well in Lipschitz norm.

Lemma 2.2.1. *For $k \geq 0$, with the initial condition $\mathcal{U}^{k+1}(0,\cdot) = \mathcal{U}_{in}$ and the hypothesis (H_k) there exists a $\mathcal{C}([0,T]; H^s(\mathbb{R}^d))$ solution $\mathcal{U}^{k+1}$ for the linear symmetric hyperbolic PDE system defined in (2.2.11a).*

Proof: Notice that (2.2.11a) has a particular symmetric structure which may be exploited based on the following proposition:

Proposition 2.2.3. *Let us consider the symmetric hyperbolic differential operator*

$$L = S\partial_t + \sum_{j=1}^{d} SA_j\partial_j$$

with S and SA_j symmetric real valued and bounded in Lipschitz norm, with $S \geqslant S_0\,\mathrm{Id}$, where $S_0 > 0$ over $[0,T]$, with $T > 0$ independent of μ. Furthermore let us consider $s \in \mathbb{R}$, $s > d/2 + 1$ and let us take

$$\lambda_s = C\left(\left|\!\left|\!\left|S\right|\!\right|\!\right|_{T,L^\infty}, \left|\!\left|\!\left|\sum_{j=1}^{d} SA_j\right|\!\right|\!\right|_{T,H^s}, \left|\!\left|\!\left|\partial_t S\right|\!\right|\!\right|_{T,L^\infty}\right).$$

Then, for any $f \in L^1([0,T];H^s(\mathbb{R}^d))$ *and* $\varphi \in H^s(\mathbb{R}^d)$ *the Cauchy problem*

$$\begin{cases} Lu = f, \ 0 < t < T \\ u(0,\cdot) = \varphi, \end{cases} \tag{2.2.13}$$

admits a unique solution $u \in \mathcal{C}([0,T];H^s(\mathbb{R}^d))$ *that verifies the energy estimate*

$$S_0 \sup_{t\in[0,T]} \left\{ e^{-\lambda_s t} \|u(t,\cdot)\|_{H^s} \right\} \lesssim \|\varphi\|_{H^s} + 2\int_0^T e^{-\lambda_s t'} \|f(t',\cdot)\|_{H^s} dt'. \tag{2.2.14}$$

For more details as well as a complete proof, we refer to [AG07].

Remark 2.2.1. *Under the same regularity assumptions, we can also infer that*

$$S_0 \sup_{t\in[0,T]} \left\{ e^{-\lambda_0 t} \|u(t,\cdot)\|_{L^2} \right\} \lesssim \|\varphi\|_{L^2} + 2\int_0^T e^{-\lambda_0 t'} \|f(t',\cdot)\|_{L^2} dt', \tag{2.2.15}$$

where

$$\lambda_0 = \frac{1}{2S_0} \left\| \frac{1}{2} \sum_{j=1}^{d} \partial_j (SA_j) - \partial_t S \right\|_{T,L^\infty}.$$

We want to apply Proposition 2.2.3. to solve the linear PDE (2.2.11a) for $\mathcal{U}^{k+1}$ in $\mathcal{C}([0,T];H^s(\mathbb{R}^d))$. First of all, we have that $\mathcal{U}^k$ and X^k are continuous in time. So, since $h_{in} \geqslant h_{min}$, by using (H_k) for a δ_0 sufficiently small, we obtain $S^k \geqslant S_0 \,\mathrm{Id}$ in $[0,T]$ for $S_0 = (1/2)\min(1, h_{min})$.

By the regularity of $\mathcal{U}^k$ and $\mathfrak{b}$, the source term $S^k B^k$ is also in H^s. More exactly, we have the following

Lemma 2.2.2. *The source term of (2.2.11a) satisfies the following linear-in-time estimate*

$$\|S^k B^k\|_{H^s} \leqslant C_F(1+T), \tag{2.2.16}$$

with the constant $C_F = C(\|\mathfrak{b}\|_{H^s}; C_f, C_v)$*, independent of* k *and of* T*.*

Proof: We have

$$\begin{aligned} \|S^k B^k\|_{H^s} &\lesssim \left(1 + \|\mathcal{U}_0^k\|_{L^\infty} + \|\mathfrak{b}\|_{L^\infty}\right) \cdot \|B^k\|_{H^s} + \left(1 + \|\mathcal{U}_0^k\|_{H^s} + \|\mathfrak{b}\|_{H^s}\right) \cdot \|B^k\|_{L^\infty} \\ &\lesssim \left(1 + \|\mathcal{U}_0^k\|_{H^s} + \|\mathfrak{b}\|_{H^s}\right) \cdot \|\mathfrak{b}\|_{H^s} \left(\|\overline{V}^k\|_{H^s} + \left|\dot{X}^k\right|\right) \end{aligned}$$

using the special structure of the matrix S^k, the Sobolev embedding $H^s(\mathbb{R}^d) \hookrightarrow L^\infty(\mathbb{R}^d)$ (which is valid since $s > d/2$) as well as the fact that the Sobolev norm is translation invariant. Then, the induction hypothesis (H_k) provides a uniform bound C_f for $\|\mathcal{U}^k\|_{H^s}$,

as well as a linear-in-time estimate for $|\dot{X}^k|$, so, since $\mathfrak{b}$ is still regular,

$$\|S^k B^k\|_{H^s} \leqslant C(\|\mathfrak{b}\|_{H^s}; C_f, C_v)(1+T).$$

□

Now we only need to verify that λ_s is bounded. For this, we have that

Lemma 2.2.3. *Assuming that (H_k) holds,*

$$\lambda_s \leqslant c(\|\mathfrak{b}\|_{H^s}; C_f, C_v)(1+T),$$

where c is a continuous nondecreasing function of its arguments.

Proof: Making use of the fact that S^k and A_j^k depend on X^k in a very simple way, throughout the function h^k, thus it is present as a translation for the function $\mathfrak{b}$, which obviously does not affect the L^∞ or H^s norms, we have that

$$|||S|||_{T,L^\infty} \leqslant 1 + |||\mathcal{U}|||_{T,L^\infty} + \|\mathfrak{b}\|_{L^\infty},$$

and that

$$\|SA_j\|_{H^s} \leqslant \|S\|_{L^\infty}\|A_j\|_{H^s} + \|S\|_{H^s}\|A_j\|_{L^\infty} \leqslant c(\|\mathfrak{b}\|_{H^s}, \|\mathcal{U}\|_{H^s}),$$

by the Sobolev embedding $H^s(\mathbb{R}^d) \hookrightarrow L^\infty(\mathbb{R}^d)$.

As for the estimate on $\|\partial_t S^k\|_{L^\infty}$, we estimate the L^∞ norm of $\partial_t h^k$, which is

$$\partial_t h^k = \partial_t \mathcal{U}_0^k + \nabla_x \mathfrak{b}(x - X^k) \cdot \dot{X}^k.$$

The second term is already controlled by (H_k). Based on the corresponding equation for $\mathcal{U}^k$ (from equation (2.2.11a)), we have that

$$\partial_t \mathcal{U}^k + \sum_{j=1}^d A_j^{k-1} \partial_j \mathcal{U}^k = -B^{k-1},$$

which implies that

$$\begin{aligned}
\|\partial_t \mathcal{U}^k\|_{L^\infty} &\leqslant \sum_{j=1}^d \|A_j^{k-1}\partial_j \mathcal{U}^k\|_{L^\infty} + \left\|\overline{V}^{k-1} \cdot \nabla_x \mathfrak{b}(. - X^{k-1}) + \nabla_x \mathfrak{b}(. - X^{k-1}) \cdot \dot{X}^{k-1}\right\|_{L^\infty} \\
&\lesssim \sum_{j=1}^d \left(1 + \|\mathcal{U}^{k-1}\|_{L^\infty} + \|\mathfrak{b}\|_{L^\infty}\right) \cdot \|\mathcal{U}^k\|_{H^s} + \|\mathfrak{b}\|_{H^s} \left(\|\mathcal{U}^{k-1}\|_{L^\infty} + \left|\dot{X}^{k-1}\right|\right) \\
&\leqslant c(\|\mathfrak{b}\|_{H^s}; C_f, C_v)(1+T),
\end{aligned}$$

by (H_k) and the regularity of $\mathfrak{b}$, as well as the Sobolev embedding $H^s(\mathbb{R}^d) \hookrightarrow W^{1,\infty}(\mathbb{R}^d)$ ($s > d/2 + 1$). Therefore, λ_s is indeed a constant independent of k, and linear in T. □

Now, we turn our attention towards the first two estimates in (H_{k+1}). For the large norm estimate, the H^s energy estimate (2.2.14) from Proposition 2.2.3. for equation (2.2.11a) of $\mathcal{U}^{k+1}$ can be stated to obtain

$$S_0 \sup_{t\in[0,T]} \left\{ e^{-\lambda_s t} \|\mathcal{U}^{k+1}(t,\cdot)\|_{H^s} \right\} \leqslant \|\mathcal{U}_{in}\|_{H^s} + 2\int_0^T e^{-\lambda_s t} \|S^k B^k\|_{H^s} dt. \tag{2.2.17}$$

The right hand side of (2.2.11a) can be estimated by Lemma 2.2.2, so we obtain

$$\left|\!\left|\!\left| \mathcal{U}^{k+1} \right|\!\right|\!\right|_{T,H^s} \leqslant \frac{1}{S_0} e^{\lambda_s T} \|\mathcal{U}_{in}\|_{H^s} + T(1+T) e^{\lambda_s T} c(\|\mathfrak{b}\|_{H^s}; C_f, C_v).$$

For C_f sufficiently large the first term in the right hand side is less than $C_f/2$. Therefore, for T small enough the second term will be less than $C_f/2$ too. This proves the first estimate of (H_{k+1}).

In order to obtain a uniform L^∞ estimate for $\mathcal{U}^{k+1} - \mathcal{U}_{in}$, we shall first of all control $\partial_t \mathcal{U}^{k+1}$ in L^∞. Just as before for $\|\partial_t \mathcal{U}^k\|_{L^\infty}$, by the large norm estimate for $\mathcal{U}^{k+1}$ we have that

$$\|\partial_t \mathcal{U}^{k+1}\|_{L^\infty} \leqslant c(\|\mathfrak{b}\|_{H^s}; C_f, C_v)(1+T).$$

Therefore we obtain

$$\left|\!\left|\!\left| \mathcal{U}^{k+1} - \mathcal{U}_{in} \right|\!\right|\!\right|_{T,L^\infty} \leqslant T \|\partial_t \mathcal{U}^{k+1}\|_{L^\infty} \leqslant c(\|\mathfrak{b}\|_{H^s}; C_f, C_v) T(1+T).$$

Hence, for a sufficiently small time T (independently of k and of μ) we get that the right hand side is less than δ_0.

Part B: existence and velocity estimate for X^{k+1}: For the existence of the solution X^{k+1} of the ODE (2.2.11b), we shall apply the Picard–Lindelöf theorem.

Lemma 2.2.4. *For $k \geq 0$, with the initial conditions $X^{k+1}(0) = 0$, and $\dot{X}^{k+1}(0) = v_{S_0}$ and the hypothesis (H_k), there exists a continuously differentiable solution X^{k+1} for the nonlinear second order non-homogeneous ODE defined in (2.2.11b) for $t \in [0, T_S]$, where $T_S = C(\mu^{1/2}, \|\mathfrak{b}\|_{H^s}; C_f)$.*

Proof: For the Picard-Lindelöf theorem, we have to show that the nonlinear functional on the right hand side of (2.2.11b) is continuous in time and uniformly Lipschitz in the spatial variable.

We recall that the functional $\mathcal{F}[\mathcal{U}^{k+1}](t, Y, Z)$ has the form of

$$\begin{aligned}\mathcal{F}[\mathcal{U}^{k+1}](t,Y,Z) = &- \frac{c_{\text{fric}}}{\sqrt{\mu}} \left(c_{solid} + \frac{1}{\tilde{M}} \int\limits_{\text{supp}(\mathfrak{b})+Y} \mathcal{U}_0^{k+1}\, dx \right) \frac{Z}{|Z| + \bar{\delta}} \\ &+ \frac{1}{\tilde{M}} \int_{\mathbb{R}^d} \mathcal{U}_0^{k+1} \nabla_x \mathfrak{b}(x - Y)\, dx.\end{aligned}$$

We already know that $\mathcal{U}_0^{k+1}$ is of class $\mathcal{C}([0,T];H^s(\mathbb{R}^d)$, so it is continuous in the time variable, regular in the spatial variable, moreover the function $\mathfrak{b}$ is regular and with a compact support, thus the integrals indeed exist and are bounded, furthermore based on the well known theorem concerning the continuity of a parametric integral, it will be continuous with respect to t.

All we need to show is that it is (locally) uniformly Lipschitz with respect to its second variable (Y,Z). Examining $\mathcal{F}[\mathcal{U}^{k+1}](t,Y,Z)$, it is clear that the second term is Lipschitz continuous due to the fact that $\mathfrak{b}$ is regular. As for the first term, since it contains a product of multiple terms with the variables Y and Z, by adding and subtracting intermediate terms they can be separated.

Let us take a closer look on these two separate terms. The integral term can be estimated due to

$$\int\limits_{\mathrm{supp}(\mathfrak{b})+Y} \mathcal{U}_0^{k+1}(t,x)\,dx = \int\limits_{\mathrm{supp}(\mathfrak{b})} \mathcal{U}_0^{k+1}(t,x-Y)\,dx,$$

and the regularity of $\mathcal{U}_0^{k+1}$. Since we chose $\overline{\delta}>0$, the function

$$Z \mapsto \frac{Z}{|Z|+\overline{\delta}}$$

is Lipschitz continuous. So, putting all the estimates together, we obtain that

$$\begin{aligned}\left|\mathcal{F}[\mathcal{U}^{k+1}](t,Y_1,Z_1)-\mathcal{F}[\mathcal{U}^{k+1}](t,Y_2,Z_2)\right| \leqslant{}& \frac{3c_{\mathrm{fric}}}{\overline{\delta}\sqrt{\mu}}\left(c_{solid}+\frac{C_f|\,\mathrm{supp}(\mathfrak{b})|}{\tilde{M}}\right)|Z_1-Z_2| \\ &+2C_fL_{\nabla_x\mathfrak{b}}\frac{|\,\mathrm{supp}(\mathfrak{b})|}{\tilde{M}}\cdot|Y_1-Y_2|;\end{aligned}$$

where L denotes the Lipschitz constant of the corresponding function in the subscript. □

One of the most important parts of the proof is the control on the solid velocity, since the solid equation contains an order $\mu^{-1/2}$ term which could potentially become huge, making the system blow up. However,

Lemma 2.2.5. *A control on the solid velocity is ensured by*

$$\left|\dot{X}^{k+1}(t)\right| \leqslant |v_{S_0}|+C_vt, \tag{2.2.18}$$

with a constant $C_v=C(\tilde{M}^{-1},\|\mathfrak{b}\|_{H^s};C_f)$ independent of k, μ and t.

Proof: By definition X^{k+1} satisfies the corresponding second order nonlinear nonhomogeneous equation in (2.2.11b) so we have that

$$\ddot{X}^{k+1}=\mathcal{F}[\mathcal{U}^{k+1}]\left(t,X^{k+1},\dot{X}^{k+1}\right),$$

thus, multiplying by $\dot{X}^{k+1}(t)$, we get that

$$\begin{aligned}\ddot{X}^{k+1}\cdot\dot{X}^{k+1} =& -\frac{c_{\text{fric}}}{\sqrt{\mu}}\left(c_{solid}+\frac{1}{\tilde{M}}\int\limits_{\text{supp}(\mathfrak{b})+X^{k+1}}\mathcal{U}_0^{k+1}\,dx\right)\frac{\left|\dot{X}^{k+1}\right|^2}{\left|\dot{X}^{k+1}\right|+\bar{\delta}}\\ &+\frac{1}{\tilde{M}}\int_{\mathbb{R}^d}\mathcal{U}_0^{k+1}\nabla_x\mathfrak{b}(x-X^{k+1})\,dx\cdot\dot{X}^{k+1}\\ \leqslant& 0+\frac{1}{\tilde{M}}\int_{\mathbb{R}^d}\mathcal{U}_0^{k+1}\nabla_x\mathfrak{b}(x-X^{k+1})\cdot\dot{X}^{k+1}\,dx,\end{aligned}$$

here the key remark is that the first, negative term disappeared from the equations. Thus, we are left with

$$\frac{1}{2}\frac{d}{dt}\left[\left|\dot{X}^{k+1}\right|^2\right]\leqslant\frac{1}{\tilde{M}}\|\mathcal{U}_0^{k+1}\|_{L^2}\|\nabla_x\mathfrak{b}\|_{L^2}\cdot|\dot{X}^{k+1}|\leqslant\frac{C_f}{\tilde{M}}\|\mathfrak{b}\|_{H^s}\left|\dot{X}^{k+1}\right|,$$

so by a Grönwall type lemma for $\dot{X}^k$, we may conclude that

$$\left|\dot{X}^k(t)\right|\leqslant|v_{S_0}|+\frac{C_f}{\tilde{M}}\|\mathfrak{b}\|_{H^s}t.$$

□

This concludes the velocity estimate for the object. Therefore, we have local-in-time existence by the Picard–Lindelöff theorem, from which the existence time is of order $\sqrt{\mu}$ due to the associated Lipschitz constant. However our velocity estimate is guaranteed for a time T_0 independent of μ, therefore the solution X^{k+1} of the ODE exists for a time T_0 independent of μ.

So we proved the existence of solutions $(\mathcal{U}^{k+1},X^{k+1})$ for the system (2.2.11), moreover we established the necessary elements for the upper bounds concerning the velocities in (H_{k+1}). □

2.2.4.4 Convergence

We want to establish the convergence of the series from (2.2.11), for that we need the L^2-norm estimates for the difference between two subsequent elements for $\mathcal{U}^k$, for X^k we shall simply estimate in $\mathbb{R}^d$-norm. We start by subtracting the equations corresponding to the k^{th} element from the equations corresponding to the $(k+1)^{\text{th}}$ element.

After the subtraction we have

$$\begin{cases} S^k\partial_t(\mathcal{U}^{k+1}-\mathcal{U}^k)+\sum_{j=1}^d S^kA_j^k\partial_j(\mathcal{U}^{k+1}-\mathcal{U}^k)= \\ =-(S^k-S^{k-1})\partial_t\mathcal{U}^k-\sum_{j=1}^d(S^kA_j^k-S^{k-1}A_j^{k-1})\partial_j\mathcal{U}^k-(S^kB^k-S^{k-1}B^{k-1}), \end{cases} \tag{2.2.19a}$$

$$\begin{cases} (\mathcal{U}^{k+1}-\mathcal{U}^k)(0,\cdot)=0; \\ \frac{d^2}{dt^2}(X^{k+1}-X^k)=\mathcal{F}[\mathcal{U}^{k+1}]\left(t,X^{k+1},\dot{X}^{k+1}\right)-\mathcal{F}[\mathcal{U}^k]\left(t,X^k,\dot{X}^k\right) \\ (X^{k+1}-X^k)(0)=0,\quad \frac{d}{dt}(X^{k+1}-X^k)(0)=0. \end{cases} \tag{2.2.19b}$$

We provide separately an appropriate estimate in this small norm for the solutions $(\mathcal{U}^{k+1}-\mathcal{U}^k)$ and $(X^{k+1}-X^k)$ of the system. The estimate for the ODE part (2.2.19b) is given by the following lemma.

Lemma 2.2.6. *For a solution $X^{k+1}-X^k$ of (2.2.19b), we have that*

$$\sup_{t\in[0,T]}|X^{k+1}(t)-X^k(t)|\lesssim C_1\frac{T}{\sqrt{\mu}}\sup_{t'\in[0,T]}\left(\left\|\mathcal{U}^{k+1}(t',\cdot)-\mathcal{U}^k(t',\cdot)\right\|_{L^2}+\left|X^{k+1}(t')-X^k(t')\right|\right), \tag{2.2.20}$$

with a constant $C_1=C(\tilde{M}^{-1},\|\mathfrak{b}\|_{H^s};C_f)$.

Notice that the right hand side of the estimate contains exactly the same differences as the ones we would like to establish an upper bound for, but due to the presence of the factor T, with T sufficiently small, it will be completely absorbed by the left hand side. However, due to the factor $\mu^{-1/2}$ these estimates are only valid for an asymptotically vanishing time of $T=\sqrt{mu}T_0$ (with T_0 independent of μ).

Proof: To treat the difference of products that arise multiple times, we introduce intermediary terms, just as we did for the verification of the Lipschitz-property. So following standard computations, we get that

$$\begin{aligned} |X^{k+1}(t)-X^k(t)| &= \left|\int_0^t\frac{d}{dt}(X^{k+1}-X^k)(s)\,ds\right| = \left|\int_0^t\int_0^s\frac{d^2}{dt^2}(X^{k+1}-X^k)(\tau)\,d\tau ds\right| \\ &\lesssim \int_0^t\int_0^s(1+T)\|\mathcal{U}^{k+1}\|_{L^2}|X^{k+1}-X^k|(\tau)\,d\tau ds \\ &\quad+\int_0^t\int_0^s\sup_{t'\in[0,T]}\left\|\mathcal{U}_0^{k+1}(t',\cdot)-\mathcal{U}_0^k(t',\cdot)\right\|_{L^2}\|\nabla_x\mathfrak{b}\|_{L^2}\,d\tau ds \\ &\quad+\int_0^t\left|\int_0^s\frac{d}{d\tau}(X^{k+1}-X^k)(\tau)\,d\tau\right|ds+\int_0^t\int_0^s|X^{k+1}-X^k|(\tau)\,d\tau ds \end{aligned}$$

Here we estimate each term by the controls of (H_k) and the Lipschitz properties, in order to obtain

$$|X^{k+1}(t)-X^k(t)| \lesssim \frac{T}{\sqrt{\mu}}\left(\sup_{t'\in[0,T]}\left\|\mathcal{U}^{k+1}(t',\cdot)-\mathcal{U}^k(t',\cdot)\right\|_{L^2}+\sup_{t'\in[0,T]}|X^{k+1}(t')-X^k(t')|\right).$$

□

For the estimate for the PDE part we have the following.

Lemma 2.2.7. *For a solution of (2.2.19a), we obtain*

$$\begin{aligned}\sup_{t\in[0,T]}\left\|\mathcal{U}^{k+1}(t,\cdot)-\mathcal{U}^k(t,\cdot)\right\|_{L^2} \lesssim & C_2T\sup_{t'\in[0,T]}\left(\left\|\mathcal{U}^k(t',\cdot)-\mathcal{U}^{k-1}(t',\cdot)\right\|_{L^2}\right)\\ &+C_2T\sup_{t'\in[0,T]}\left(\left|X^k(t')-X^{k-1}(t')\right|\right),\end{aligned}$$

with a constant $C_2=C(\tilde{M}^{-1},\|\mathfrak{b}\|_{H^s};C_f,C_v)$.

Proof: Once again we aim to use the energy estimate, since we have the linear system (2.2.19a) of the type of Proposition 2.2.3. for the variable $\mathcal{U}^{k+1}-\mathcal{U}^k$.

The same reasoning applies here as for the energy estimates section concerning the applicability of the proposition, since λ_0 is bounded, so we only need a sufficient upper bound for the right hand side of (2.2.19a), denoted by F. We shall examine it term by term.

The first two terms are handled with standard techniques to deduce

$$\|(S^k-S^{k-1})\partial_t\mathcal{U}^k\|_{L^2}\lesssim\|\mathcal{U}^k-\mathcal{U}^{k-1}\|_{L^2}+|X^k-X^{k-1}|,$$

$$\left\|(S^kA_j^k-S^{k-1}A_j^{k-1})\partial_j\mathcal{U}^k\right\|_{L^2}\lesssim\left\|\mathcal{U}^k-\mathcal{U}^{k-1}\right\|_{L^2}+|X^k-X^{k-1}|.$$

And for the third term, we deal with the product via an intermediary term, so

$$\|S^kB^k-S^{k-1}B^{k-1}\|_{L^2}\leqslant\|S^k-S^{k-1}\|_{L^2}\|B^k\|_{L^\infty}+\|S^{k-1}\|_{L^\infty}\|B^k-B^{k-1}\|_{L^2},$$

then, by using the definition of the source term, we get that

$$\begin{aligned}\|S^kB^k-S^{k-1}B^{k-1}\|_{L^2}\lesssim&(\|\mathcal{U}^k-\mathcal{U}^{k-1}\|_{L^2}+|X^k-X^{k-1}|)\|\overline{V}^k\cdot\nabla_x\mathfrak{b}(.-X^k)\|_{L^\infty}\\&+(\|\mathcal{U}^k-\mathcal{U}^{k-1}\|_{L^2}+|X^k-X^{k-1}|)\left\|\nabla_x\mathfrak{b}(.-X^k)\cdot\dot{X}^k\right\|_{L^\infty}\\&+(1+\|\mathcal{U}^{k-1}\|_{L^\infty})\left\|\overline{V}^k\cdot\nabla_x\mathfrak{b}(.-X^k)-\overline{V}^{k-1}\cdot\nabla_x\mathfrak{b}(.-X^{k-1})\right\|_{L^2}\\&+(1+\|\mathcal{U}^{k-1}\|_{L^\infty})\left\|\nabla_x\mathfrak{b}(.-X^k)\cdot\dot{X}^k-\nabla_x\mathfrak{b}(.-X^{k-1})\cdot\dot{X}^{k-1}\right\|_{L^2}.\end{aligned}$$

Again, with the apparition of intermediary terms for each product, by utilizing Lemma

2.2.5, we get that

$$\|S^k B^k - S^{k-1}B^{k-1}\|_{L^2} \lesssim (1+T) \sup_{t'\in[0,T]} \left(\|\mathcal{U}^k(t',\cdot) - \mathcal{U}^{k-1}(t',\cdot)\|_{L^2} + |X^k(t') - X^{k-1}(t')| \right).$$

Applying the energy estimate to (2.2.19a), we obtain that

$$\begin{aligned} S_0 \sup_{t\in[0,T]} \left\{ e^{-\lambda t} \|\mathcal{U}^{k+1}(t,\cdot) - \mathcal{U}^k(t,\cdot)\|_{L^2} \right\} &\leqslant 2 \int_0^T e^{-\lambda t} \|F(t,\cdot)\|_{L^2}\, dt \\ &\lesssim T(1+T) \sup_{t'\in[0,T]} \left\{ e^{-\lambda t'} \left(\left\| \mathcal{U}^k(t',\cdot) - \mathcal{U}^{k-1}(t',\cdot) \right\|_{L^2} + |X^k(t') - X^{k-1}(t')| \right) \right\}. \end{aligned}$$

□

To sum up the results from the two previous lemmas, we obtained that for $T/\sqrt{\mu}$ sufficiently small, we have that

$$\begin{aligned} &\sup_{t\in[0,T]} \left\| \mathcal{U}^{k+1}(t,\cdot) - \mathcal{U}^k(t,\cdot) \right\|_{L^2} + \sup_{t\in[0,T]} |X^{k+1}(t) - X^k(t)| \\ &\qquad \leqslant \mathfrak{c} \left(\sup_{t\in[0,T]} \left\| \mathcal{U}^k(t,\cdot) - \mathcal{U}^{k-1}(t,\cdot) \right\|_{L^2} + \sup_{t\in[0,T]} |X^k(t) - X^{k-1}(t)| \right), \end{aligned}$$

with a constant $\mathfrak{c} < 1$. This ensures the convergence in $L^\infty([0, \sqrt{\mu}T_0]; L^2(\mathbb{R}^d))$ with T_0 independent of μ.

Since we have that the H^s-norm is bounded by Proposition 2.2.3, we may extract a weakly convergent subsequence from the series, and since the limit in the sense of distributions is unique, we have convergence for the whole series in H^s too. Furthermore, again by Proposition 2.2.3 and Lemma 2.2.5, we have uniform estimates of the velocities $\dot{X}^k$ and $\mathcal{U}^k$ over a time T_0 independent of μ and of k, therefore the limit has similarly velocity estimates over a time T_0 independent of μ, which in turn guarantees its existence over such time T_0. □

This concludes the proof of the theorem, since, to deduce the regularity implied in the statement, we only have to use the convexity of the norm, following classical regularity arguments. Thus we obtained a classical solution of the coupled system (2.2.6) for a sufficiently small time T_0.

2.3 The $\mathcal{O}(\mu^2)$ asymptotic regime: The Boussinesq system

In this section, we move on to the next order regarding the asymptotic regime, that is the approximations of order μ^2. In order to simplify the computations, we consider here a weakly nonlinear regime, i.e. we assume that $\varepsilon = \mathcal{O}(\mu)$. The fluid is then governed by a

Boussinesq system. Thus, the asymptotic regime writes as follows

$$0 < \mu \leqslant \mu_{max} \ll 1, \quad \varepsilon = \mathcal{O}(\mu). \tag{BOUS}$$

At second order, the asymptotic expansion of $\overline{V}$ in terms of ζ and $\overline{V}$ (based on Proposition 3.37. of [Lan13]) is given by

$$\overline{V} = \nabla_x \psi + \frac{\mu}{3h}\nabla_x(h^3 \nabla_x \cdot \nabla_x \psi) - \frac{\mu}{2} h \nabla_x \partial_t b + \mathcal{O}(\mu^2),$$

so by making use of the definition of h, once again taking the gradient of the second equation in (2.1.22), and neglecting terms of order $\mathcal{O}(\mu^2)$, equations (2.1.22) under the Boussinesq regime (BOUS) take the form of

$$\begin{cases} \partial_t \zeta + \nabla_x \cdot (h\overline{V}) = \partial_t b, \\ \left(1 - \frac{\mu}{3}\Delta_x\right)\partial_t \overline{V} + \nabla_x \zeta + \varepsilon(\overline{V} \cdot \nabla_x)\overline{V} = -\frac{\mu}{2}\nabla_x \partial_t^2 b. \end{cases} \tag{2.3.1}$$

For the well-posedness of this Boussinesq system, see for instance [Lan13].

Remark 2.3.1. *Without the smallness assumption on $\varepsilon = \mathcal{O}(\mu)$, it is still possible to perform an asymptotic expansion at $\mathcal{O}(\mu^2)$. The resulting system is more general than the Boussinesq system (3.1.2) but also more complicated, it is known as the Serre–Green–Naghdi equations. For the justification of this general system in the fixed bottom case, please refer to [ASL08a], or to [HI15] for a moving bottom under a forced motion.*

It is well-known for the fixed bottom case that the good timescale of Boussinesq-type systems is of order ε^{-1} in order to be able to properly observe the nonlinear and dispersive effects of equations (3.1.2) (see for instance [BCL05, SX12, Bur16]). However, for a time dependent bottom (as it is in our case), one can only infer an existence time of $\mathcal{O}(1)$, due to the source term $\partial_t b$ on the right hand side of the first equation in (3.1.2). Throughout this section, we show that, with the presence of the solid in the system as well as with better estimates, a time of existence in $\varepsilon^{-1/2}$ is achievable.

2.3.1 Formal derivation of the corresponding solid motion equation

As we may observe from the Boussinesq system (3.1.2) the bottom related source terms are respectively of order $\mathcal{O}(1)$ and $\mathcal{O}(\mu)$ for the first and second equations. To ensure at least a reasonable level of consistency on the whole coupled system, we have to impose (at least) the same precision in deriving formally the equation dealing with the solid; the surface integral present in (2.1.26) will therefore be approximated at order $\mathcal{O}(\mu^2)$.

Our strategy is exactly the same as for the first order approximation case in the previous section, but it is carried out to the next order of approximation. However, it

turns out that due to the additional hypothesis on ε, the pressure formula (2.2.3) derived in Section 2 still holds in this regime, namely

Lemma 2.3.1. *Under the Boussinesq hypotheses (BOUS), the pressure takes the following form*

$$P = \frac{P_{atm}}{\varrho g H_0} + (\varepsilon\zeta - z) + \mathcal{O}(\mu^2). \tag{2.3.2}$$

Proof: The residual in (2.2.3) is of size $\mathcal{O}(\mu)$ in the SV Saint-Venant regime; however the parameter ε was set to 1 in this regime, and the same computations show that the residual is actually of size $\mathcal{O}(\varepsilon\mu)$, and therefore of $\mathcal{O}(\mu^2)$ with the Boussinesq scaling regime (BOUS). □

Remark 2.3.2. *We remark that for the Serre–Green–Naghdi system, that is without the smallness hypothesis on ε, the situation would be completely different, the expression for the pressure would take a more complex form, incorporating nonlinear effects which would lead to added mass effect for the equation of motion characterizing the solid (for more details we also refer to Section 2.3.6).*

Therefore, following the same computations as in Section 2.2.2, we obtain the same ODE for the solid displacement as (3.1.3), but with a dependence on ε as well,

$$\ddot{X}_S = -\frac{c_{\text{fric}}}{\sqrt{\mu}}\left(\frac{1}{\varepsilon}\tilde{c}_{solid} + \frac{1}{\tilde{M}}\int\limits_{\text{supp}(\mathfrak{b})+X_S}\zeta\,dx\right)\frac{\dot{X}_S}{\left|\dot{X}_S\right| + \overline{\delta}} + \frac{\varepsilon}{\tilde{M}}\int_{\mathbb{R}^d}\zeta\nabla_x\mathfrak{b}(x - X_S)\,dx. \tag{2.3.3}$$

Here, we made use of the constant of the solid $\tilde{c}_{solid}$, similar to (3.1.5), defined by

$$\tilde{c}_{solid} = \varepsilon + \frac{|\,\text{supp}(\mathfrak{b})|}{\tilde{M}}\left(\frac{P_{atm}}{\varrho g H_0} + 1\right) - \varepsilon\frac{|\,\text{Volume}_{Solid}\,|}{\tilde{M}}. \tag{2.3.4}$$

The difference between the constants c_{solid} and $\tilde{c}_{solid}$ is the ε coefficient in the latter one. Due to the additional hypothesis $\varepsilon = 1$ in (SV), it was not present in the previous section for the Saint-Venant regime, but in the Boussinesq regime (BOUS) it has to be taken into consideration.

Once again, notice the presence of the friction terms in the solid equation, which is potentially of order $(\varepsilon\sqrt{\mu})^{-1}$, so we will have to reason carefully why this doesn't pose a problem for our system. First of all, we have the following concerning the consistency of the solid equation:

Proposition 2.3.1. *Let $s_0 \geqslant 0$, and let us assume that $\zeta \in \mathcal{C}([0,T]; H^{s_0+6}(\mathbb{R}^d))$ and that $\mathfrak{b} \in H^{s_0+6}(\mathbb{R}^d)$ compactly supported. Let us suppose that $\nabla_x\psi \in \mathcal{C}([0,T]; H^{s_0+6}(\mathbb{R}^d))$. In the long wave Boussinesq regime ($\varepsilon = \mathcal{O}(\mu)$) the solid equation (2.1.26) is consistent at order $\mathcal{O}(\sqrt{\mu})$ with the model (2.3.3) on $[0,T]$ with $T > 0$.*

Proof: By the regularity assumptions and the additional hypotheses of (BOUS) (Lemmas 3.42. and 5.4. of [Lan13]), we can write that $\Phi = \psi + \mu^2 R_2$ with

$$\begin{aligned} |||R_2|||_{T,H^{s_0}} &\leqslant C(|||\zeta|||_{T,H^{s_0+4}}, \|\mathfrak{b}\|_{H^{s_0+4}})|||\nabla_x\psi|||_{T,H^{s_0+4}}, \\ |||\partial_t R_2|||_{T,H^{s_0}} &\leqslant C(|||\zeta|||_{T,H^{s_0+6}}, \|\mathfrak{b}\|_{H^{s_0+6}}, |||\nabla_x\psi|||_{T,H^{s_0+6}}), \end{aligned}$$

meaning that, we have

$$\begin{aligned} P|_{z=-1+\varepsilon b} &= \frac{P_{atm}}{\varrho g H_0} + h + \mu^2 R_{P,2}, \\ |||R_{P,2}|||_{T,H^{s_0}} &\leqslant C(|||\zeta|||_{T,H^{s_0+6}}, \|\mathfrak{b}\|_{H^{s_0+6}}, |||\nabla_x\psi|||_{T,H^{s_0+6}}). \end{aligned}$$

Hence, in the equation for the solid motion (2.1.26), we recover the approximate equation (3.1.3) with the additional error terms

$$-\sqrt{\mu}\frac{c_{\text{fric}}}{\tilde{M}}\frac{\dot{X}_S}{\left|\dot{X}_S\right| + \bar{\delta}}\int_{I(t)} R_{P,2}\,dx + \mu^2\frac{1}{\tilde{M}}\int_{I(t)} R_{P,2}\nabla_x\mathfrak{b}(x - X_S)\,dx,$$

that can be estimated as an $\mathcal{O}(\sqrt{\mu})$ total error term, that is, it is less than

$$\sqrt{\mu}C(\tilde{M}^{-1}, |||\zeta|||_{T,H^{s_0+6}}, \|\mathfrak{b}\|_{H^{s_0+6}}, |||\nabla_x\psi|||_{T,H^{s_0+6}}).$$

□

We remark that given the fact that the Boussinesq system is consistent at order μ^2 (Corollary 5.20. of [Lan13]), the consistency of the coupled fluid-solid system can only be at most of order $\sqrt{\mu}$ which is a considerable loss. In order to remedy the situation, we will address some possible extensions of the solid model in Section 2.3.6.

2.3.2 The coupled wave-structure model in the Boussinesq regime

Here we present some remarks on the right hand side of the Boussinesq system (3.1.2). Again, we have that

$$\partial_t b(t,x) = -\nabla_x\mathfrak{b}\left(x - X_S(t)\right)\cdot\dot{X}_S(t),$$

however we also have that

$$\begin{aligned} \nabla_x\partial_t^2 b(t,x) &= \nabla_x\partial_t\left(-\nabla_x\mathfrak{b}\left(x - X_S(t)\right)\cdot\dot{X}_S(t)\right) \\ &= \nabla_x\left(\nabla_x^2\mathfrak{b}\left(x - X_S(t)\right)\dot{X}_S(t)\cdot\dot{X}_S(t) - \nabla_x\mathfrak{b}\left(x - X_S(t)\right)\cdot\ddot{X}_S(t)\right). \end{aligned}$$

To sum it up, the free surface equations with a solid moving at the bottom in the case of the Boussinesq approximation take the following form

$$\begin{cases} \partial_t \zeta + \nabla_x \cdot (h\overline{V}) = \partial_t b, \\ \left(1 - \frac{\mu}{3}\Delta_x\right)\partial_t \overline{V} + \nabla_x \zeta + \varepsilon(\overline{V}\cdot\nabla_x)\overline{V} = -\frac{\mu}{2}\nabla_x \partial_t^2 b, \end{cases} \tag{2.3.5a}$$

$$\begin{aligned} \ddot{X}_S = &-\frac{c_{\text{fric}}}{\sqrt{\mu}}\left(\frac{1}{\varepsilon}\tilde{c}_{solid} + \frac{1}{\widetilde{M}}\int\limits_{\text{supp}(\mathfrak{b})+X_S} \zeta\, dx\right)\frac{\dot{X}_S}{\left|\dot{X}_S\right| + \overline{\delta}} \\ &+ \frac{\varepsilon}{\widetilde{M}}\int_{\mathbb{R}^d} \zeta \nabla_x \mathfrak{b}(x - X_S)\, dx. \end{aligned} \tag{2.3.5b}$$

2.3.3 A reformulation of the coupled fluid-solid system

Following the observations of Section 2.3.2, we may elaborate the source term of the coupled system. The free surface equations with a solid moving at the bottom in the case of the Boussinesq approximation can be written as

$$\begin{cases} \partial_t \zeta + \nabla_x \cdot (h\overline{V}) = -\nabla_x \mathfrak{b}\,(x - X_S)\cdot \dot{X}_S, \\ \left(1 - \frac{\mu}{3}\Delta_x\right)\partial_t \overline{V} + \nabla_x \zeta + \varepsilon(\overline{V}\cdot\nabla_x)\overline{V} = \\ \qquad -\frac{\mu}{2}\nabla_x\left(\nabla_x^2 \mathfrak{b}\,(x - X_S)\,\dot{X}_S\cdot\dot{X}_S - \nabla_x \mathfrak{b}\,(x - X_S)\cdot\ddot{X}_S\right), \end{cases} \tag{2.3.6a}$$

$$\begin{aligned} \ddot{X}_S = &-\frac{c_{\text{fric}}}{\sqrt{\mu}}\left(\frac{1}{\varepsilon}\tilde{c}_{solid} + \frac{1}{\widetilde{M}}\int\limits_{\text{supp}(\mathfrak{b})+X_S} \zeta\, dx\right)\frac{\dot{X}_S}{\left|\dot{X}_S\right| + \overline{\delta}} \\ &+ \frac{\varepsilon}{\widetilde{M}}\int_{\mathbb{R}^d} \zeta \nabla_x \mathfrak{b}(x - X_S)\, dx. \end{aligned} \tag{2.3.6b}$$

First of all, let us remark that a more compact formulation can be derived, just like for the nonlinear Saint-Venant equations coupled with Newton's equation (2.2.6) in Section 2.2.4.1. This formula is obtained through the same means as in the previous section, so we will apply similar notations as well. We have the following: the fluid equations (2.3.6a) for the variable $\mathcal{U} = (\zeta, \overline{V})$ can be written as

$$D_\mu \partial_t \mathcal{U} + \sum_{j=1}^{d} A_j(\mathcal{U}, X_S)\partial_j \mathcal{U} + B(\mathcal{U}, X_S) = 0, \tag{2.3.7}$$

where the matrix $A_j(\mathcal{U}, X_S)$ is the same as the one defined in the previous section, that

is

$$A_j(\mathcal{U}, X_S) = \left(\begin{array}{c|c} \varepsilon\overline{V}_j & hI_j \\ \hline I_j^\top & \varepsilon\overline{V}_j \operatorname{Id}_{d\times d} \end{array}\right) \text{ for } 1 \leqslant j \leqslant d.$$

We remark that we have the following simple decomposition

$$A_j(\mathcal{U}, X_S) = \overline{I}_j + \varepsilon\overline{A}_j(\mathcal{U}, X_S) = \left(\begin{array}{c|c} 0 & I_j \\ \hline I_j^\top & 0 \end{array}\right) + \varepsilon \left(\begin{array}{c|c} \overline{V}_j & (\zeta - b)I_j \\ \hline 0 & \overline{V}_j \operatorname{Id}_{d\times d} \end{array}\right). \tag{2.3.8}$$

Additionally, we have that

$$D_\mu = \left(\begin{array}{c|c} 1 & \\ \hline & \left(1 - \frac{\mu}{3}\Delta_x\right) \operatorname{Id}_{d\times d} \end{array}\right),$$

and the source term vector takes the following form

$$B(\mathcal{U}, X_S) = \begin{pmatrix} -\varepsilon\overline{V} \cdot \nabla_x \mathfrak{b}\left(x - X_S\right) + \nabla_x \mathfrak{b}\left(x - X_S\right) \cdot \dot{X}_S \\ \frac{\mu}{2}\nabla_x \left(\nabla_x^2 \mathfrak{b}\left(x - X_S\right) \dot{X}_S \cdot \dot{X}_S - \nabla_x \mathfrak{b}\left(x - X_S\right) \cdot \ddot{X}_S\right) \end{pmatrix}.$$

Remark 2.3.3. *Once again, we can symmetrize equation (2.3.7) with the use of the matrix*

$$S(\mathcal{U}, X_S) = \left(\begin{array}{c|c} 1 & 0 \\ \hline 0 & h \operatorname{Id}_{d\times d} \end{array}\right),$$

remarking that

$$S(\mathcal{U}, X_S) = \operatorname{Id}_{(d+1)\times(d+1)} + \varepsilon\overline{S}(\mathcal{U}, X_S) = \operatorname{Id}_{(d+1)\times(d+1)} + \varepsilon \left(\begin{array}{c|c} 0 & 0 \\ \hline 0 & (\zeta - b) \operatorname{Id}_{d\times d} \end{array}\right).$$

Let us make one further remark, concerning the second order (nonlinear) ordinary differential equation characterizing the displacement of the solid X_S in (2.3.6b). Let us

adapt the definition of the functional $\mathcal{F}[\mathcal{U}](t,Y,Z)$ introduced in Section 2.2.4.1.

$$\mathcal{F}[\mathcal{U}](t,Y,Z) = -\frac{c_{\text{fric}}}{\sqrt{\mu}}\left(\frac{1}{\varepsilon}\tilde{c}_{solid} + \frac{1}{\tilde{M}}\int\limits_{\text{supp}(b)+Y}\mathcal{U}_0\,dx\right)\frac{Z}{|Z|+\overline{\delta}} + \frac{\varepsilon}{\tilde{M}}\int_{\mathbb{R}^d}\mathcal{U}_0\nabla_x\mathfrak{b}(x-Y)\,dx.$$

The coupled system (3.1.6) has the following equivalent form

$$\begin{cases} D_\mu\partial_t\mathcal{U} + \sum\limits_{j=1}^{d} A_j(\mathcal{U},X_S)\partial_j\mathcal{U} + B(\mathcal{U},X_S) = 0, & \text{(2.3.9a)}\\ \ddot{X}_S = \mathcal{F}[\mathcal{U}]\left(t,X_S,\dot{X}_S\right). & \text{(2.3.9b)}\end{cases}$$

2.3.4 A priori estimate for the Boussinesq system coupled with Newton's equation

In this part we present the energy estimate in a Sobolev-type function space for the coupled system (3.1.6). This estimate is based on classical methods (Grönwall type inequalities), but for an energy functional adapted to the fluid-solid system. In the nonlinear Saint-Venant regime, we constructed an iterative scheme for the system which provided the necessary tools to deduce a local in time existence theorem. The heart of the proof was the energy estimate established on the linearized PDE system (Proposition 2.2.3) and a separate velocity estimate (Lemma 2.2.5.) for the solid system. Due to the additional dispersive term as well as a more complicated source term on the right hand side of system (2.3.6a), a refined analysis of the coupling terms is necessary. More precisely the right hand side with $\mu\nabla_x\partial_t^2 b$ contains a term of $\mu\ddot{X}_S$ which is asymptotically singular by equation (2.3.6b).

One additional remark concerns the time of existence of the system. We aim for a long time existence result, which involves the parameter ε. This scale was not present in the previous section since for the Saint-Venant regime (SV), we made use of the additional hypothesis of $\varepsilon = 1$. However this implies that in the Boussinesq regime (BOUS) more careful estimates are needed; we establish an existence time over a large $\mathcal{O}(\varepsilon^{-1/2})$ scale, while standard methods only provide an $\mathcal{O}(1)$ existence time when the bottom is moving, because of the $\mathcal{O}(1)$ source term $\partial_t b$ in the first equation of (3.1.2). It is however still smaller than the $\mathcal{O}\left(\varepsilon^{-1}\right)$ scale for a fixed bottom ([SX12, Bur16]).

By introducing the wave-structure energy functional

$$E_B(t) = \frac{1}{2}\int_{\mathbb{R}^d}\zeta^2\,dx + \frac{1}{2}\int_{\mathbb{R}^d}h(\overline{V}\cdot\overline{V})\,dx + \frac{1}{2}\sum_{j=1}^{d}\int_{\mathbb{R}^d}\frac{\mu}{3}h(\partial_j\overline{V}\cdot\partial_j\overline{V})\,dx + \frac{\tilde{M}}{2\varepsilon}\left|\dot{X}_S\right|^2,$$

we can establish first of all an L^2 type energy estimate for the coupled system (3.1.6),

from which we will be able to deduce a certain control on the velocity of the solid.

So, we have the following:

Proposition 2.3.2. *Let $\mu \ll 1$ sufficiently small and let us suppose that $s_0 > \max(1, d/2)$. Then any $\mathcal{U} \in \mathcal{C}^1([0,T]\times\mathbb{R}^d) \cap \mathcal{C}^1([0,T]; H^{s_0}(\mathbb{R}^d))$, $X_S \in \mathcal{C}^2([0,T])$ satisfying the coupled system (2.3.9) (or equivalently (3.1.6)), with initial data $\mathcal{U}(0,\cdot) = \mathcal{U}_{in} \in \mathcal{C}^1(\mathbb{R}^d) \cap H^{s_0}(\mathbb{R}^d)$ and $(X_S(0), \dot{X}_S(0)) = (0, v_{S_0}) \in \mathbb{R}^d \times \mathbb{R}^d$ verifies the energy estimate*

$$\sup_{t\in[0,T]} \left\{ e^{-\sqrt{\varepsilon}c_0 t} E_B(t) \right\} \leqslant 2E_B(0) + \mu c_0 T \|\mathfrak{b}\|^2_{H^3}, \tag{2.3.10}$$

where

$$c_0 = c(c_{\text{fric}}, \tilde{M}^{-1}, |||\mathcal{U}|||_{T,H^{s_0}}, |||\mathcal{U}|||_{T,W^{1,\infty}}, \|\mathfrak{b}\|_{W^{4,\infty}}).$$

Proof: We follow the standard steps of a general energy estimate, adapted for the Boussinesq system with moving bottom, paying close attention to the parameters. We start by multiplying the first equation of (2.3.6a) by ζ, and the second equation by $h\overline{V}$, after which we integrate on $\mathbb{R}^d$ with respect to the spatial variable x. This yields the following system

$$\begin{cases} \displaystyle\int_{\mathbb{R}^d} \partial_t\zeta\zeta\, dx + \int_{\mathbb{R}^d} \nabla_x\cdot(h\overline{V})\zeta\, dx = -\int_{\mathbb{R}^d} \zeta\nabla_x\mathfrak{b}\,(x-X_S)\, dx\cdot\dot{X}_S, \\ \displaystyle\int_{\mathbb{R}^d} h\left(1-\frac{\mu}{3}\Delta_x\right)\partial_t\overline{V}\cdot\overline{V}\, dx + \int_{\mathbb{R}^d} h\nabla_x\zeta\overline{V}\, dx + \varepsilon\int_{\mathbb{R}^d} h(\overline{V}\cdot\nabla_x)\overline{V}\cdot\overline{V}\, dx = \\ \qquad \displaystyle -\frac{\mu}{2}\int_{\mathbb{R}^d} h\nabla_x\left(\nabla_x^2\mathfrak{b}\,(x-X_S)\,\dot{X}_S\cdot\dot{X}_S\right)\cdot\overline{V}\, dx + \frac{\mu}{2}\int_{\mathbb{R}^d} h\nabla_x^2\mathfrak{b}\,(x-X_S)\,\ddot{X}_S\cdot\overline{V}\, dx. \end{cases}$$

Our main interest is the terms on the right hand side that represent the coupling in the source term, for the rest we shall reason briefly, since those estimates are part of the classical analysis.

The time derivative term of the second equation can be reformulated by integration by parts in the following way:

$$\begin{aligned} \int_{\mathbb{R}^d} h\left(1-\frac{\mu}{3}\Delta_x\right)\partial_t\overline{V}\cdot\overline{V}\, dx &= \frac{1}{2}\frac{d}{dt}\int_{\mathbb{R}^d} h(\overline{V}\cdot\overline{V})\, dx + \frac{1}{2}\frac{d}{dt}\sum_{j=1}^d\int_{\mathbb{R}^d}\frac{\mu}{3}h(\partial_j\overline{V}\cdot\partial_j\overline{V})\, dx \\ &\quad -\frac{1}{2}\int_{\mathbb{R}^d}\partial_t h\left(\overline{V}\cdot\overline{V} + \frac{\mu}{3}\sum_{j=1}^d(\partial_j\overline{V}\cdot\partial_j\overline{V})\right) dx + \frac{\mu}{3}\sum_{j=1}^d\int_{\mathbb{R}^d}\partial_j h(\partial_j\partial_t\overline{V}\cdot\overline{V})\, dx. \end{aligned}$$

For the first equation, by making use of an integration by parts as well as equation

(2.3.6b) on the right hand side, we get

$$\frac{1}{2}\frac{d}{dt}\int_{\mathbb{R}^d}\zeta^2\,dx+\frac{\tilde{M}}{2}\frac{1}{\varepsilon}\frac{d}{dt}\left|\dot{X}_S\right|^2+\int_{\mathbb{R}^d}\varepsilon\nabla_x\zeta\cdot\overline{V}\zeta\,dx+\int_{\mathbb{R}^d}h(\nabla_x\cdot\overline{V})\zeta\,dx=$$
$$\varepsilon\int_{\mathbb{R}^d}\nabla_x\mathfrak{b}\,(x-X_S)\cdot\overline{V}\zeta\,dx-\frac{\tilde{M}c_{\text{fric}}}{\varepsilon\sqrt{\mu}}\left(\frac{1}{\varepsilon}\tilde{c}_{solid}+\frac{1}{\tilde{M}}\int_{I(t)}\zeta\,dx\right)\frac{\left|\dot{X}_S\right|^2}{\left|\dot{X}_S\right|+\overline{\delta}},$$

$$\frac{1}{2}\frac{d}{dt}\int_{\mathbb{R}^d}h(\overline{V}\cdot\overline{V})\,dx+\frac{1}{2}\frac{d}{dt}\sum_{j=1}^{d}\int_{\mathbb{R}^d}\frac{\mu}{3}h(\partial_j\overline{V}\cdot\partial_j\overline{V})\,dx$$
$$-\frac{1}{2}\int_{\mathbb{R}^d}\partial_t h\left(\overline{V}\cdot\overline{V}+\frac{\mu}{3}\sum_{j=1}^{d}(\partial_j\overline{V}\cdot\partial_j\overline{V})\right)dx+\frac{\mu}{3}\sum_{j=1}^{d}\int_{\mathbb{R}^d}\partial_j h(\partial_j\partial_t\overline{V}\cdot\overline{V})\,dx$$
$$+\int_{\mathbb{R}^d}h\nabla_x\zeta\overline{V}\,dx+\varepsilon\int_{\mathbb{R}^d}h(\overline{V}\cdot\nabla_x)\overline{V}\cdot\overline{V}\,dx=$$
$$-\frac{\mu}{2}\int_{\mathbb{R}^d}h\nabla_x\left(\nabla_x^2\mathfrak{b}\,(x-X_S)\,\dot{X}_S\cdot\dot{X}_S\right)\cdot\overline{V}\,dx+\frac{\mu}{2}\int_{\mathbb{R}^d}h\nabla_x^2\mathfrak{b}\,(x-X_S)\,\ddot{X}_S\cdot\overline{V}\,dx.$$

Notice that by equation (2.3.6b), we have been able to substitute part of the contribution associated to the source term $\partial_t b$ as a component of the energy $E_B(t)$ on the left hand side of the first equation. This is crucial to get an extended existence time. Moreover, on the right hand side, a now nonpositive friction term appeared that can be easily controlled.

Now we add together these two equations and in what follows, by making use of term by term estimates, we arrive to a Grönwall-type inequality concerning the energy functional $E_B(t)$ (for $0\leqslant t\leqslant T$) which then allows us to properly conclude the demonstration. Hence we are left with

$$\frac{d}{dt}E_B(t)=A_B+B_B+C_B+D_B+F_B+G_B,\tag{2.3.11}$$

where

$$A_B:=\frac{1}{2}\int_{\mathbb{R}^d}\partial_t h\left(\overline{V}\cdot\overline{V}+\frac{\mu}{3}\sum_{j=1}^{d}(\partial_j\overline{V}\cdot\partial_j\overline{V})\right)dx,\tag{2.3.12}$$

$$B_B:=-\frac{\mu}{3}\sum_{j=1}^{d}\int_{\mathbb{R}^d}\partial_j h(\partial_j\partial_t\overline{V}\cdot\overline{V})\,dx,\tag{2.3.13}$$

$$C_B:=-\int_{\mathbb{R}^d}\varepsilon\nabla_x\zeta\cdot\overline{V}\zeta\,dx-\int_{\mathbb{R}^d}h(\nabla_x\cdot\overline{V})\zeta\,dx-\int_{\mathbb{R}^d}h\nabla_x\zeta\overline{V}\,dx\tag{2.3.14}$$
$$-\varepsilon\int_{\mathbb{R}^d}h(\overline{V}\cdot\nabla_x)\overline{V}\cdot\overline{V}\,dx,\tag{2.3.15}$$

$$D_B := \varepsilon \int_{\mathbb{R}^d} \nabla_x \mathfrak{b}\,(x - X_S) \cdot \overline{V} \zeta \, dx - \frac{\tilde{M} c_{\text{fric}}}{\varepsilon \sqrt{\mu}} \left(\frac{1}{\varepsilon} \tilde{c}_{solid} + \frac{1}{\tilde{M}} \int_{I(t)} \zeta \, dx \right) \frac{\left| \dot{X}_S \right|^2}{\left| \dot{X}_S \right| + \bar{\delta}}, \tag{2.3.16}$$

$$F_B := -\frac{\mu}{2} \int_{\mathbb{R}^d} h \nabla_x \left(\nabla_x^2 \mathfrak{b}\,(x - X_S)\, \dot{X}_S \cdot \dot{X}_S \right) \cdot \overline{V} \, dx, \tag{2.3.17}$$

$$G_B := \frac{\mu}{2} \int_{\mathbb{R}^d} h \nabla_x^2 \mathfrak{b}\,(x - X_S)\, \ddot{X}_S \cdot \overline{V} \, dx. \tag{2.3.18}$$

Now we proceed to estimate each term on the right hand side. By making use of the first equation of the Boussinesq system (3.1.6), namely that

$$\partial_t h = -\varepsilon \nabla_x \cdot (h \overline{V}),$$

we can establish that

$$A_B \leqslant \varepsilon c(\|\mathcal{U}\|_{W^{1,\infty}}, \|\mathfrak{b}\|_{W^{1,\infty}}) \left(\|\overline{V}\|_{L^2}^2 + \frac{\mu}{3} \|\overline{V}\|_{H^1}^2 \right).$$

As for the term B_B, we aim to estimate the L^2 norm of the mixed derivative term $\partial_j \partial_t \overline{V}$. By making use of the second equation of the system (3.1.6), we have

$$\begin{aligned} \frac{\mu}{3} \partial_j \partial_t \overline{V} = &\left(1 - \frac{\mu}{3} \Delta_x\right)^{-1} \left(-\frac{\mu}{3} \partial_j \nabla_x \right) \zeta + \left(1 - \frac{\mu}{3} \Delta_x\right)^{-1} \varepsilon \left(-\frac{\mu}{3} \partial_j ((\overline{V} \cdot \nabla_x) \overline{V}) \right) \\ &+ \frac{\mu}{2} \left(1 - \frac{\mu}{3} \Delta_x\right)^{-1} \left(-\frac{\mu}{3} \partial_j \nabla_x \right) \partial_t^2 b. \end{aligned} \tag{2.3.19}$$

Let us estimate each term separately. Given the fact that $\left(1 - \frac{\mu}{3} \Delta_x\right)^{-1} \left(-\frac{\mu}{3} \partial_j \nabla_x \right)$ is a zeroth order differential operator whose symbol is uniformly bounded with respect to μ, we can easily deduce that

$$\left\| \left(1 - \frac{\mu}{3} \Delta_x\right)^{-1} \left(-\frac{\mu}{3} \partial_j \nabla_x \right) \zeta \right\|_{L^2} \lesssim \|\zeta\|_{L^2}.$$

For the second term, first of all, we have that the operator $\left(1 - \frac{\mu}{3} \Delta_x\right)^{-1} \mu \partial_j$ has a symbol of order -1, uniformly bounded with respect to μ, therefore

$$\left\| \left(1 - \frac{\mu}{3} \Delta_x\right)^{-1} \varepsilon \left(-\frac{\mu}{3} \partial_j ((\overline{V} \cdot \nabla_x) \overline{V}) \right) \right\|_{L^2} \lesssim \varepsilon \|(\overline{V} \cdot \nabla_x) \overline{V})\|_{H^{-1}},$$

from which, by a classical product estimate, we have that for $s_0 \geqslant d/2$, $-1 > -s_0$

$$\|(\overline{V} \cdot \nabla_x) \overline{V})\|_{H^{-1}} \lesssim \|\overline{V}\|_{H^{s_0}} \|\nabla_x \cdot \overline{V}\|_{H^{-1}} \lesssim \|\overline{V}\|_{H^{s_0}} \|\overline{V}\|_{L^2}.$$

As for the third term from (2.3.19), we use the chain rule for $\partial_t^2 b$, as well as the fact that

$\left(1-\frac{\mu}{3}\Delta_x\right)^{-1}$ is uniformly bounded in μ as an differential operator of order 0. This yields

$$\mu^2\left\|\left(1-\frac{\mu}{3}\Delta_x\right)^{-1}(-\partial_j\nabla_x)\,\partial_t^2 b\right\|_{L^2}\lesssim\mu^2(\|\mathfrak{b}\|_{W^{4,\infty}}|\dot{X}_S|^2+\|\mathfrak{b}\|_{H^3}|\ddot{X}_S|),$$

where we made use of the fact that $\mathfrak{b}$ is compactly supported. Here we can estimate $\mu^2|\ddot{X}_S|$ directly from equation (2.3.6b) due to the additional smallness parameter. More exactly we have that

$$\mu^2\frac{c_{\text{fric}}}{\sqrt{\mu}\varepsilon}\tilde{c}_{solid}\leqslant\sqrt{\mu}C(c_{\text{fric}},\|\mathfrak{b}\|_{L^\infty})\quad\text{ and }\quad\frac{|\dot{X}_S|}{|\dot{X}_S|+\overline{\delta}}\leqslant 1,$$

which allows us to infer that

$$\mu^2|\ddot{X}_S|\leqslant\sqrt{\mu}C(c_{\text{fric}},\|\mathfrak{b}\|_{W^{1,\infty}},\|\zeta\|_{L^\infty})$$

To sum it up, we have obtained the following estimate:

$$\left\|\frac{\mu}{3}\partial_j\partial_t\overline{V}\right\|_{L^2}\lesssim\|\zeta\|_{L^2}+\varepsilon c(\|\mathcal{U}\|_{H^{s_0}})\|\overline{V}\|_{L^2}+\mu^2|\dot{X}_S|^2+\sqrt{\mu}\|\mathfrak{b}\|_{H^3}.\tag{2.3.20}$$

Thus we get

$$B_B\leqslant\varepsilon c(\|\mathcal{U}\|_{W^{1,\infty}},\|\mathfrak{b}\|_{W^{4,\infty}})\left[\|\zeta\|_{L^2}\|\overline{V}\|_{L^2}+\varepsilon c(\|\mathcal{U}\|_{H^{s_0}})\|\overline{V}\|_{L^2}^2+\left|\dot{X}_S\right|^2+\sqrt{\mu}\|\mathfrak{b}\|_{H^3}\|\overline{V}\|_{L^2}\right],$$

here the last term can be estimated as $\|\nabla_x\mathfrak{b}\|_{L^2}^2+\|\overline{V}\|_{L^2}^2$ as well.

The integrals incorporating the nonlinear spatial derivative terms correspond to

$$C_B=\sum_{j=1}^d\int_{\mathbb{R}^d}SA_j(\mathcal{U})\partial_j\mathcal{U}\cdot\mathcal{U}\,dx=-\frac{1}{2}\sum_{j=1}^d\int_{\mathbb{R}^d}\partial_j(SA_j)(\mathcal{U})\mathcal{U}\cdot\mathcal{U}\,dx,$$

to which we can easily find an upper bound, giving

$$C_B\leqslant\varepsilon c(\|\mathcal{U}\|_{W^{1,\infty}},\|\mathfrak{b}\|_{W^{1,\infty}})\|\mathcal{U}\|_{L^2}^2.$$

For the first two source terms for the system, basic L^∞-norm estimates and Cauchy-Schwartz inequalities provide the necessary means to conclude

$$\begin{aligned}D_B&\leqslant\varepsilon c(\|\mathfrak{b}\|_{W^{1,\infty}})\|\zeta\|_{L^2}\|\overline{V}\|_{L^2}+0,\\F_B&\leqslant\mu c(\|\mathcal{U}\|_{W^{1,\infty}},\|\mathfrak{b}\|_{W^{3,\infty}})\left|\dot{X}_S\right|^2.\end{aligned}$$

We remark that the friction term can be straightforwardly bounded above by 0 in the estimate for D_B.

We leave the last source term, G_B, as it is due to the presence of $\ddot{X}_S(t)$; according to equation (2.3.6b), it requires some attention to avoid problems arising from the friction part (the asymptotically singular terms).

So, to sum up the previous estimates, we get that

$$\begin{aligned}\frac{d}{dt}E_B(t) \leqslant &+ \varepsilon c(\|\mathcal{U}\|_{W^{1,\infty}}, \|\mathfrak{b}\|_{W^{1,\infty}}) \left(\|\overline{V}\|_{L^2}^2 + \frac{\mu}{3}\|\nabla_x \cdot \overline{V}\|_{L^2}^2\right) \\ &+ \varepsilon c(\|\mathcal{U}\|_{W^{1,\infty}}, \|\mathfrak{b}\|_{W^{1,\infty}}) \left[\|\zeta\|_{L^2}\|\overline{V}\|_{L^2} + \varepsilon c(\|\mathcal{U}\|_{H^{s_0}})\|\overline{V}\|_{L^2}^2 + \sqrt{\mu}\|\overline{V}\|_{L^2}^2 + \|\mathcal{U}\|_{L^2}^2\right] \\ &+ \varepsilon c(\|\mathcal{U}\|_{W^{1,\infty}}, \|\mathfrak{b}\|_{W^{4,\infty}})\|\mathcal{U}\|_{L^2}^2(\mu^2|\dot{X}_S|^2 + \sqrt{\mu}\|\mathfrak{b}\|_{H^3}^2) \\ &+ \varepsilon c(\|\mathfrak{b}\|_{W^{1,\infty}})\|\zeta\|_{L^2}\|\overline{V}\|_{L^2} + 0 + \mu c(\|\mathcal{U}\|_{W^{1,\infty}}, \|\mathfrak{b}\|_{W^{3,\infty}}) \left|\dot{X}_S\right|^2 \\ &+ G_B.\end{aligned}$$

So we may deduce that

$$\frac{d}{dt}E_B(t) \leqslant \varepsilon c(\|\mathcal{U}\|_{H^{s_0}}, \|\mathcal{U}\|_{W^{1,\infty}}, \|\mathfrak{b}\|_{W^{4,\infty}}) \left(E_B(t) + \sqrt{\mu}\|\mathfrak{b}\|_{H^3}^2\right) + G_B \tag{2.3.21}$$

from which by integrating with respect to the time variable t (keeping in mind that $0 \leqslant t \leqslant T$), we obtain

$$E_B(t) - E_B(0) \leqslant \varepsilon c_0 \int_0^t E_B(\tau)\, d\tau + \sqrt{\mu}\varepsilon c_0 t\|\mathfrak{b}\|_{H^3}^2 + \int_0^t G_B\, d\tau, \tag{2.3.22}$$

where we made use of the constant

$$c_0 = c(|||\mathcal{U}|||_{T,H^{s_0}}, |||\mathcal{U}|||_{T,W^{1,\infty}}, \|\mathfrak{b}\|_{W^{4,\infty}}).$$

Lemma 2.3.2. *The remaining source term G_B satisfies the following estimate for all $0 \leqslant t \leqslant T$,*

$$\begin{aligned}\frac{\mu}{2}\int_0^t \int_{\mathbb{R}^d} h\nabla_x^2\mathfrak{b}\,(x - X_S)\,\ddot{X}_S \cdot \overline{V}\, dx\, d\tau \leqslant &\ \mu c(\|\mathfrak{b}\|_{W^{2,\infty}}, |||\mathcal{U}|||_{T,L^\infty})(E_B(t) + E_B(0)) \\ &+ \sqrt{\varepsilon}c(c_{\text{fric}}, \tilde{M}^{-1}, \|\mathfrak{b}\|_{W^{4,\infty}}, |||\mathcal{U}|||_{T,H^{s_0}}, |||\mathcal{U}|||_{T,W^{1,\infty}}) \int_0^t E_B(\tau)\, d\tau \\ &+ \mu c(\|\mathfrak{b}\|_{W^{4,\infty}}, |||\mathcal{U}|||_{T,W^{1,\infty}}) \int_0^t \|\mathfrak{b}\|_{H^3}^2\, d\tau.\end{aligned}$$

Proof: To handle the source term, first of all we apply an integration by parts in the time

variable. This yields

$$\begin{aligned}\mu\int_{\mathbb{R}^d}\int_0^t h\nabla_x^2\mathfrak{b}\left(x-X_S\right)\ddot{X}_S\cdot\overline{V}\,d\tau\,dx &= \mu\int_{\mathbb{R}^d} h\nabla_x^2\mathfrak{b}\left(x-X_S\right)\dot{X}_S\cdot\overline{V}(t,x)\,dx\\ &-\mu\int_{\mathbb{R}^d} h\nabla_x^2\mathfrak{b}\left(x-0\right)v_{S_0}\cdot\overline{V}_{in}(x)\,dx-\mu\int_{\mathbb{R}^d}\partial_t h\nabla_x^2\mathfrak{b}\left(x-X_S\right)\dot{X}_S\cdot\overline{V}(t,x)\,dx\\ &+\mu\int_0^t\int_{\mathbb{R}^d} h\nabla_x(\nabla_x^2\mathfrak{b}\left(x-X_S(\tau)\right)\dot{X}_S(\tau)\cdot\dot{X}_S(\tau))\cdot\overline{V}\,dx\,d\tau\\ &-\mu\int_0^t\int_{\mathbb{R}^d} h\nabla_x^2\mathfrak{b}\left(x-X_S(\tau)\right)\dot{X}_S(\tau)\cdot\partial_t\overline{V}\,dx\,d\tau.\end{aligned}$$

The first two boundary terms can be estimated similarly, for the first term we have that

$$\mu\int_{\mathbb{R}^d} h\nabla_x^2\mathfrak{b}\left(x-X_S\right)\dot{X}_S\cdot\overline{V}(t,x)\,dx\leqslant\mu c(\|\mathfrak{b}\|_{W^{2,\infty}},\|\mathcal{U}\|_{L^\infty})(|\dot{X}_S|^2+\|\overline{V}\|_{L^2}^2),$$

and we can deduce an identical estimate for the initial data. Here we used the fact that $\mathfrak{b}$ is compactly supported, and as such the integrals can be calculated on $\mathrm{supp}(\mathfrak{b})$. Since we assume that μ is sufficiently small, this estimate with the energy term will be absorbed by the energy term on the left hand side of (2.3.22).

Once again making use of the first equation of (3.1.6) we obtain

$$\mu\int_{\mathbb{R}^d}\partial_t h\nabla_x^2\mathfrak{b}\left(x-X_S\right)\dot{X}_S\cdot\overline{V}(t,x)\,dx\leqslant\mu\varepsilon c(\|\mathfrak{b}\|_{W^{2,\infty}},\|\mathcal{U}\|_{W^{1,\infty}})(|\dot{X}_S|^2+\|\overline{V}\|_{L^2}^2).$$

The integral on the support of $\mathfrak{b}$ gives

$$\begin{aligned}&\mu\int_{\mathbb{R}^d} h\nabla_x(\nabla_x^2\mathfrak{b}\left(x-X_S(\tau)\right)\dot{X}_S\cdot\dot{X}_S)\cdot\overline{V}\,dx\,d\tau\leqslant\\ &\leqslant\mu c(\|\mathfrak{b}\|_{L^\infty},\|\mathcal{U}\|_{L^\infty})|X_S|^2\|\nabla_x^3\mathfrak{b}\|_{L^2(\mathrm{supp}(\mathfrak{b}))}\|\overline{V}\|_{L^2(\mathrm{supp}(\mathfrak{b}))}\\ &\leqslant\mu c(\|\mathfrak{b}\|_{W^{3,\infty}},\|\mathcal{U}\|_{L^\infty})|X_S|^2.\end{aligned}$$

Finally, by an integration by parts with respect to the spatial variable, we get that

$$\begin{aligned}\int_0^t\int_{\mathbb{R}^d}\nabla_x^2\mathfrak{b}\left(x-X_S(\tau)\right)\dot{X}_S(\tau)\cdot\partial_t\overline{V}\,dx\,d\tau &=\\ =\int_0^t\int_{\mathbb{R}^d}\nabla_x\mathfrak{b}\left(x-X_S(\tau)\right)\cdot\dot{X}_S(\tau)(\nabla_x\cdot\partial_t\overline{V})\,dx\,d\tau,&\end{aligned}$$

from which we deduce that

$$\begin{aligned}
&\mu\int_0^t\int_{\mathbb{R}^d} h\nabla_x^2\mathfrak{b}\left(x-X_S(\tau)\right)\dot{X}_S\cdot\partial_t\overline{V}\,dx\,d\tau\leqslant\\
&\leqslant c(\|\mathfrak{b}\|_{W^{2,\infty}},|||\mathcal{U}|||_{T,L^\infty})\int_0^t|\dot{X}_S|\left\|\frac{\mu}{3}\nabla_x\cdot\partial_t\overline{V}\right\|_{L^2}dx\,d\tau\\
&\leqslant\sqrt{\varepsilon}c(\|\mathfrak{b}\|_{W^{2,\infty}},|||\mathcal{U}|||_{T,L^\infty})\int_0^t\frac{|\dot{X}_S(\tau)|}{\sqrt{\varepsilon}}\left(\|\zeta\|_{L^2}+\varepsilon c(\|\mathcal{U}\|_{H^{s_0}})\|\overline{V}\|_{L^2}\right)d\tau\\
&\quad+\sqrt{\varepsilon}c(\|\mathfrak{b}\|_{W^{2,\infty}},|||\mathcal{U}|||_{T,L^\infty})\int_0^t\frac{|\dot{X}_S(\tau)|}{\sqrt{\varepsilon}}\left(\sqrt{\mu}\|\overline{V}\|_{L^2}+\mu^2|\dot{X}_S|\right)d\tau,\\
&\quad+\mu c(\|\mathfrak{b}\|_{W^{1,\infty}},|||\mathcal{U}|||_{T,W^{1,\infty}})\int_0^t\|\mathfrak{b}\|_{H^3}^2\,d\tau
\end{aligned}$$

where we made use of our previous observation adapted to $\mu\nabla_x\cdot\partial_t\overline{V}$ (inequality (2.3.20)). Remarking that $\varepsilon^{-1/2}|\dot{X}_S|\leqslant E_B^{1/2}$ by definition, we obtain

$$\begin{aligned}
\mu\int_0^t\int_{\mathbb{R}^d}h\nabla_x^2\mathfrak{b}\left(x-X_S(\tau)\right)\dot{X}_S(\tau)\cdot\partial_t\overline{V}\,dx\,d\tau\leqslant\\
\leqslant\sqrt{\varepsilon}c(c_{\text{fric}},\tilde{M}^{-1},\|\mathfrak{b}\|_{W^{2,\infty}},|||\mathcal{U}|||_{T,H^{s_0}})\int_0^t E_B(\tau)\,d\tau\\
+\mu c(\|\mathfrak{b}\|_{W^{1,\infty}},|||\mathcal{U}|||_{T,W^{1,\infty}})\int_0^t\|\mathfrak{b}\|_{H^3}^2\,d\tau,
\end{aligned}$$

which in turn allows us to conclude this lemma. □

So by Lemma 2.3.2. and inequality (2.3.22), we obtain that for μ sufficiently small

$$E_B(t)\leqslant 2E_B(0)+\sqrt{\varepsilon}\tilde{c}_0\int_0^t E_B(\tau)\,d\tau+\mu\tilde{c}_0t\|\mathfrak{b}\|_{H^3}^2,\tag{2.3.23}$$

with the constant

$$\tilde{c}_0=c(c_{\text{fric}},\tilde{M}^{-1},|||\mathcal{U}|||_{T,H^{s_0}},|||\mathcal{U}|||_{T,W^{1,\infty}},\|\mathfrak{b}\|_{W^{4,\infty}}).$$

Thus, by Grönwall's inequality, we can conclude the energy estimate. □

This concludes the L^2-estimates (case $s=0$). Let us mention some consequences concerning the velocity of the solid.

Corollary 2.3.1. *This energy estimate provides us with a natural control on the solid velocity, namely*

$$\sup_{t\in[0,T]}\left\{e^{-\sqrt{\varepsilon}c_0t}\left|\dot{X}_S(t)\right|^2\right\}\leqslant\varepsilon\|\mathcal{U}_{in}\|_{\mathcal{X}^0}^2+|v_{S_0}|^2+\varepsilon\mu c_0T\|\mathfrak{b}\|_{H^3}^2,\tag{2.3.24}$$

where

$$c_0=c(c_{\text{fric}},\tilde{M}^{-1},|||\mathcal{U}|||_{T,W^{1,\infty}},|||\mathcal{U}|||_{T,H^{s_0}},\|\mathfrak{b}\|_{W^{4,\infty}}).$$

This implies that the solid velocity stays bounded on a $\mathcal{O}(\varepsilon^{-1/2})$ timescale as long as c_0 stays bounded.

Remark 2.3.4. *Following the steps of Lemma 2.2.5. we would have obtained the velocity estimate*

$$\left|\dot{X}_S(t)\right| \leqslant |v_{S_0}| + \varepsilon \frac{\|\mathcal{U}\|_{L^\infty}\|b\|_{W^{1,\infty}}}{\tilde{M}} t, \tag{2.3.25}$$

which is a worse estimate than the one presented in the previous corollary and it cannot be used to obtain an extended existence time.

Remark 2.3.5. *By the identity*

$$\dot{X}_S(t) = \sqrt{\varepsilon}\frac{\dot{X}_S(t)}{\sqrt{\varepsilon}},$$

from (3.1.12) of Corollary 3.1.1, it is easy to see that if the initial velocity is of order $\sqrt{\varepsilon}$, that is $\varepsilon^{-1/2}v_{S_0}$ is uniformly bounded in μ and ε, then the scaled solid velocity $\varepsilon^{-1/2}\dot{X}_S(t)$ stays uniformly bounded. Moreover, this uniform bound is valid up until a time of order $\mathcal{O}(\varepsilon^{-1/2})$ as long as c_0 remains bounded.

For higher order energy estimates we are going to make use of this estimate and the differential operator $\Lambda^s = (1-\Delta_x)^{s/2}$. The energy functional associated to these estimates writes as

$$\begin{aligned} E_B^s(t) =& \frac{1}{2}\int_{\mathbb{R}^d}(\Lambda^s\zeta)^2\,dx + \frac{1}{2}\int_{\mathbb{R}^d} h(\Lambda^s\overline{V}\cdot\Lambda^s\overline{V})\,dx \\ &+ \frac{1}{2}\sum_{j=1}^{d}\int_{\mathbb{R}^d}\frac{\mu}{3}h(\partial_j\Lambda^s\overline{V}\cdot\partial_j\Lambda^s\overline{V})\,dx + \frac{\tilde{M}}{2\varepsilon}\left|\dot{X}_S\right|^2. \end{aligned}$$

Due to the special structure of our system, let us define the following adapted Sobolev space to provide a uniformly formulated energy estimate.

Definition 2.3.1. *The Sobolev-type space $\mathcal{X}^s$ is given by*

$$\mathcal{X}^s(\mathbb{R}^d) = \left\{\mathcal{U} = (\zeta, \overline{V}) \in L^2(\mathbb{R}^d) \text{ such that } \|\mathcal{U}\|_{\mathcal{X}^s} < \infty\right\},$$

where

$$\|\mathcal{U}\|_{\mathcal{X}^s} = \|\zeta\|_{H^s} + \|\overline{V}\|_{H^s} + \sqrt{\mu}\|\overline{V}\|_{H^{s+1}}.$$

The last term in the $\mathcal{X}^s$ norm appeared due to the necessity to control the dispersive smoothing through $\sqrt{\mu}$ times the partial derivatives.

We have to modify certain parts of the proof, due to the fact that some of the cancellations used above cease to work anymore. More precisely, we have that

Proposition 2.3.3. *Let $\mu \ll 1$ sufficiently small and let us take $s \in \mathbb{R}$ with $s > d/2+1$. Let us take $\mathcal{U} \in \mathcal{C}([0,T];\mathcal{X}^s(\mathbb{R}^d)) \cap C^1([0,T];\mathcal{X}^{s-1}(\mathbb{R}^d))$, $X_S \in \mathcal{C}^1([0,T])$ satisfying the*

coupled system (2.3.9) (or equivalently (3.1.6)), with initial data $\mathcal{U}(0,\cdot) \in \mathcal{X}^s(\mathbb{R}^d)$ *and* $(X_S(0), \dot{X}_S(0)) = (0, \sqrt{\varepsilon}V_{S_0}) \in \mathbb{R}^d \times \mathbb{R}^d$. *Then* $\mathcal{U}$, X_S *verifies the energy estimate*

$$\sup_{t\in[0,T]} \left\{ e^{-\sqrt{\varepsilon}c_s t} \left(\frac{1}{2}\|\mathcal{U}\|^2_{\mathcal{X}^s} + \frac{1}{2\varepsilon}\left|\dot{X}_S\right|^2 \right) \right\} \leqslant 2\|\mathcal{U}(0,\cdot)\|^2_{\mathcal{X}^s} + 2\left|V_{S_0}\right|^2 + \sqrt{\varepsilon}Tc_s\|\mathfrak{b}\|^2_{H^{s+3}},$$

where

$$c_s = c(c_{\text{fric}}, \tilde{M}^{-1}, |||\mathcal{U}|||_{T,H^s}, \|\mathfrak{b}\|_{H^{s+3}}).$$

Remark 2.3.6. *Notice that taking into account the coupling effect for the a priori estimate ensured that the constant in the exponential stays of order* $\sqrt{\varepsilon}$, *which guarantees a proper control on the fluid velocity over a time* $\mathcal{O}(\varepsilon^{-1/2})$, *which is better than what the general theory would imply for a time dependent bottom variation.*

Proof: We start by applying the operator Λ^s on the symmetrized equation ((2.3.9) multiplied by $S(\mathcal{U}, X_S)$), and we would like to use the techniques presented for the case of $s = 0$, treating $\Lambda^s\mathcal{U}$ as our new unknown. Thus we are left with

$$\begin{aligned} S(\mathcal{U}, X_S)D_\mu\partial_t\Lambda^s\mathcal{U} + \sum_{j=1}^{d} SA_j(\mathcal{U}, X_S)\partial_j\Lambda^s\mathcal{U} + \Lambda^s SB(\mathcal{U}, X_S) \\ + [\Lambda^s, S(\mathcal{U}, X_S)]D_\mu\partial_t\mathcal{U} + \sum_{j=1}^{d}[\Lambda^s, SA_j(\mathcal{U}, X_S)]\partial_j\mathcal{U} = 0. \end{aligned} \tag{2.3.26}$$

Notice the presence of the additional commutator terms in the equation.

Our main idea is the same as before, after multiplying the equation by $\Lambda^s\mathcal{U}$ and integrating over $\mathbb{R}^d$, we make use of similar estimates as in the first part for the L^2 estimate to obtain a Grönwall type inequality for the corresponding modified energy functional $E^s_B(t)$.

For the first two terms of our new equation, which correspond to the time derivative and nonlinear terms of the original equation (2.3.30a), they may be treated similarly as before, obtaining the same estimates with the same constants, only for H^s-norm instead of L^2-norm.

The main difference is the presence of the commutators in equation (2.3.26) due to Λ^s, and the treatment of the source term since the cancellation obtained by using the ODE (2.3.6b) does not work anymore. We will make use of the well-known Kato-Ponce inequality (for this we have $s > 0$) as well as Sobolev-embedding results (for these, the condition $s > d/2 + 1$ is necessary) to establish commutator estimates. Namely, we have that for $f \in H^s$, $g \in H^{s-1}$

$$\|[\Lambda_s, f]g\|_{L^2} \lesssim \|f\|_{H^s}\|g\|_{L^\infty} + \|f\|_{W^{1,\infty}}\|g\|_{H^{s-1}} \lesssim \|f\|_{H^s}\|g\|_{H^{s-1}},$$

the latter inequality coming from the embedding $H^s(\mathbb{R}^d) \hookrightarrow W^{1,\infty}(\mathbb{R}^d)$. We also have that

for $f \in H^s$, $g \in H^s$, and $s > d/2$

$$\|\Lambda_s(fg)\|_{L^2} \lesssim \|f\|_{H^s}\|g\|_{H^s}.$$

So, by the decomposition of the symmetrizer matrix, we may write that

$$\begin{aligned}\left|\int_{\mathbb{R}^d}[\Lambda^s, S(\mathcal{U}, X_S)]D_\mu\partial_t\mathcal{U}\cdot\Lambda^s\mathcal{U}\,dx\right| &= \left|\int_{\mathbb{R}^d}[\Lambda^s, \varepsilon\overline{S}(\mathcal{U}, X_S)]D_\mu\partial_t\mathcal{U}\cdot\Lambda^s\mathcal{U}\,dx\right| \\ &\lesssim \varepsilon(\|\mathcal{U}\|_{H^s}+\|\mathfrak{b}\|_{H^s})\left\|\sum_{j=1}^d SA_j(\mathcal{U}, X_S)\partial_j\mathcal{U}+SB(\mathcal{U}, X_S)\right\|_{H^{s-1}}\cdot\|\mathcal{U}\|_{H^s} \\ &\lesssim \varepsilon c(\|\mathcal{U}\|_{H^s}, \|\mathfrak{b}\|_{H^s})\|\mathcal{U}\|_{H^s}^2 + \varepsilon c(\|\mathcal{U}\|_{H^s}, \|\mathfrak{b}\|_{H^s})\|SB(\mathcal{U}, X_S)\|_{H^s}\|\mathcal{U}\|_{H^s}.\end{aligned}$$

Here we made use of equation (2.3.9) to handle the time derivative. The additional term will be absorbed by the source term in equation (2.3.26).

Additionally we have that

$$\begin{aligned}\left|\int_{\mathbb{R}^d}\sum_{j=1}^d[\Lambda^s, SA_j(\mathcal{U}, X_S)]\partial_j\mathcal{U}\cdot\Lambda^s\mathcal{U}\,dx\right| &= \left|\int_{\mathbb{R}^d}\sum_{j=1}^d[\Lambda^s, \varepsilon S\overline{A}_j(\mathcal{U}, X_S)]\partial_j\mathcal{U}\cdot\Lambda^s\mathcal{U}\,dx\right| \\ \lesssim \varepsilon\sum_{j=1}^d\left\|S\overline{A}_j(\mathcal{U}, X_S)\right\|_{H^s}\|\partial_j\mathcal{U}\|_{H^{s-1}}\|\mathcal{U}\|_{H^s} &\lesssim \varepsilon c(\|\mathcal{U}\|_{H^s}, \|\mathfrak{b}\|_{H^s})\|\mathcal{U}\|_{H^s}^2.\end{aligned}$$

In both these commutator estimates, we made use of the fact that the constant diagonal matrix component trivially cancels out in the commutator.

Finally, attention has to be paid to the source term too, since for instance now we can't apply the ODE (2.3.6b) to treat the original right hand side of the first equation due to the presence of the operator Λ^s. Thus we are left with

$$\begin{aligned}\int_{\mathbb{R}^d}\Lambda^s\zeta\Lambda^s\nabla_x\mathfrak{b}\,(x-X_S)\,dx\cdot\dot{X}_S &\leqslant \sqrt{\varepsilon}\frac{|\dot{X}_S|}{\sqrt{\varepsilon}}\|\zeta\|_{H^s}\|\nabla_x\mathfrak{b}\|_{H^s} \\ &\leqslant \sqrt{\varepsilon}c(\|\mathcal{U}\|_{H^s})\left(\frac{1}{\varepsilon}|\dot{X}_S|^2+\|\nabla_x\mathfrak{b}\|_{H^s}^2\right).\end{aligned} \tag{2.3.27}$$

Here we remark that $|\dot{X}_S|^2 \leqslant 2\varepsilon E_B^s$. Notice that it is at this point that we can no longer use the cancellation, thus loosing a smallness factor.

Moreover, we are required to estimate terms which involve the operator Λ^s applied to a product, this is handled by the commutator estimates, giving us

$$\varepsilon\int_{\mathbb{R}^d}\Lambda^s(\nabla_x\mathfrak{b}\,(x-X_S)\cdot\overline{V})\Lambda^s\zeta\,dx \leqslant \varepsilon c(\|\mathfrak{b}\|_{H^{s+1}})\|\mathcal{U}\|_{H^s}^2,$$

and with a simple upper bound, we have

$$\frac{\mu}{2}\int_{\mathbb{R}^d} h\Lambda^s\nabla_x\left(\nabla_x^2\mathfrak{b}\,(x-X_S)\,\dot{X}_S\cdot\dot{X}_S\right)\cdot\Lambda^s\overline{V}\,dx\leqslant\mu c(\|\mathcal{U}\|_{H^s},\|\mathfrak{b}\|_{H^{s+3}})\left|\dot{X}_S\right|^2.$$

At last, just as with Lemma 2.3.2. we can deduce the following estimate

$$\begin{aligned}\mu\int_{\mathbb{R}^d}\int_0^t h\Lambda^s\nabla_x^2\mathfrak{b}\,(x-X_S(\tau))\,\ddot{X}_S(\tau)\cdot\Lambda^s\overline{V}\,d\tau\,dx&\leqslant\mu c(|||\mathcal{U}|||_{T,H^s},\|\mathfrak{b}\|_{H^{s+2}})(E_B^s(t)+E_B^s(0))\\&+\sqrt{\varepsilon}c(c_{\text{fric}},\tilde{M}^{-1},|||\mathcal{U}|||_{T,H^s},\|\mathfrak{b}\|_{H^{s+3}})\int_0^t E_B^s(\tau)\,d\tau\\&+\mu c(|||\mathcal{U}|||_{T,H^s},\|\mathfrak{b}\|_{W^{1,\infty}})t\|\nabla_x\mathfrak{b}\|_{H^{s+2}}^2.\end{aligned}$$

To sum it up, after an integration with respect to the time variable, with the definition of the energy functional $E_B^s(t)$ and the velocity estimate obtained from the L^2 estimate (Corollary 3.1.1.), we may write that

$$E_B^s(t)\leqslant 2E_B^s(0)+\sqrt{\varepsilon}\tilde{c}_s t\|\mathfrak{b}\|_{H^{s+3}}^2+\sqrt{\varepsilon}\tilde{c}_s\int_0^t E_B^s(\tau)\,d\tau,\tag{2.3.28}$$

with the constant

$$\tilde{c}_s=c(c_{\text{fric}},\tilde{M}^{-1},|||\mathcal{U}|||_{T,H^s},\|\mathfrak{b}\|_{H^{s+3}}).$$

So we have the right terms in order to complete the estimate, again with Grönwall's lemma. □

2.3.5 Local in time existence theorem

The energy estimate allows us to establish the main existence theorem for the coupled Boussinesq system, which states as follows

Theorem 2.3.1. *Let us consider the coupled system defined by equations (3.1.6). Let us suppose that for the initial value ζ_{in} and $\mathfrak{b}$ the lower bound condition (2.1.1)*

$$\exists h_{min}>0,\ \forall X\in\mathbb{R}^d,\ 1+\varepsilon\zeta(X)-\varepsilon\mathfrak{b}(X)\geqslant h_{min}\tag{2.3.29}$$

is satisfied. If the initial values ζ_{in} and $\overline{V}_{in}$ are in $\mathcal{X}^s(\mathbb{R}^d)$ with $s\in\mathbb{R}$, $s>d/2+1$, and $V_{S_0}\in\mathbb{R}^d$ then there exists a maximal $T_0>0$ independent of ε such that there is a unique solution

$$\begin{aligned}&(\zeta,\overline{V})\in C\left(\left[0,\frac{T_0}{\sqrt{\varepsilon}}\right];\mathcal{X}^s(\mathbb{R}^d)\right)\cap C^1\left(\left[0,\frac{T_0}{\sqrt{\varepsilon}}\right];\mathcal{X}^{s-1}(\mathbb{R}^d)\right),\\&X_S\in C^2\left(\left[0,\frac{T_0}{\sqrt{\varepsilon}}\right]\right)\end{aligned}$$

with uniformly bounded norms for the system (3.1.6) with initial conditions $(\zeta_{in},\overline{V}_{in})$ and

$(0, \sqrt{\varepsilon}V_{S_0})$.

Proof: For this demonstration we shall follow the footsteps of a classical Friedrichs type reasoning for (in general) symmetric hyperbolic systems, found for example in Chapter 16 of [Tay97]. The reason for this has already been evoked in the previous section, an iterative scheme is not adapted to the nonlinear coupled Boussinesq system because it does not allow for the cancellation of the coupling terms in the energy estimates. With a carefully chosen Friedrichs smoothing of the equations, these cancellations can be preserved.

1. A regularized system: We shall first of all regularize the system with the help of the Friedrichs mollifier J_δ.

Definition 2.3.2. *For every $u \in L^2(\mathbb{R}^d)$ we have that for $\xi \in \mathbb{R}^d$*

$$\widehat{J_\delta u}(\xi) = \varphi(\delta\xi)\hat{u}(\xi),$$

with φ a regular real valued even function defined on $\mathbb{R}^d$ with compact support, such that $\varphi(0) = 1$.

A slightly modified classical property of the mollifier entails the followings

Lemma 2.3.3. (1) *For every $s, t \in \mathbb{R}$, the operator J_δ acts from $\mathcal{X}^s$ onto $\mathcal{X}^t$, moreover there exists a constant $C(s, t, \delta)$ such that*

$$\|J_\delta u\|_{\mathcal{X}^t} \leqslant C(s, t, \delta)\|u\|_{\mathcal{X}^s}$$

for every $u \in \mathcal{X}^s$. (2) *J_δ as a linear operator is continuous every $L^p(\mathbb{R}^d)$, $1 \leqslant p \leqslant \infty$, furthermore for all $u \in L^p(\mathbb{R}^d)$*

$$\|J_\delta u\|_{L^p} \leqslant C\|u\|_{L^p}$$

with a constant C independent of δ.

Using the mollifier, we propose the following symmetric regularized system

$$\begin{cases} S(J_\delta\mathcal{U}^\delta, X_S^\delta)D_\mu\partial_t\mathcal{U}^\delta + \sum_{j=1}^{d} J_\delta S(J_\delta\mathcal{U}^\delta, X_S^\delta)A_j(J_\delta\mathcal{U}^\delta, X_S^\delta)J_\delta\partial_j\mathcal{U}^\delta = \\ \qquad\qquad = S(J_\delta\mathcal{U}^\delta, X_S^\delta)J_\delta B(J_\delta\mathcal{U}^\delta, X_S^\delta), & \text{(2.3.30a)} \\ \ddot{X}_S^\delta(t) = \mathcal{F}[J_\delta\mathcal{U}_0^\delta]\left(t, X_S^\delta, \dot{X}_S^\delta\right), & \text{(2.3.30b)} \\ \mathcal{U}^\delta(0,\cdot) = \mathcal{U}_{in}, \left(X_S^\delta, \dot{X}_S^\delta\right)(0) = (0, v_{S_0}). \end{cases}$$

Based on Lemma 2.3.3, we may deduce that the regularized system (2.3.30) is in fact an ODE (in the Fourier space) on any $\mathcal{X}^s$ Banach-space, the regularization guarantees that the nonlinear operator on the right hand side in its canonical form is regular thus

uniformly Lipschitz and continuous in time. So by the Picard–Lindelöf theorem we may deduce that there exists a solution $\mathcal{U}^\delta \in C([0,T_\delta];\mathcal{X}^s)$ and $X_S^\delta \in C^2([0,T_\delta])$.

2. A priori estimate for the regularization: Following the steps of the a priori estimates proved in the previous section, the estimate in Proposition 2.3.3 holds for our regularized system as well, since by the careful choice of regularization in system (2.3.30) the cancellations are preserved. So we have that

$$\|\mathcal{U}^\delta\|_{\mathcal{X}^s}^2 + \frac{1}{\varepsilon}\left|\dot{X}_S^\delta(t)\right|^2 \leqslant e^{\lambda t}\left(\|\mathcal{U}_{in}\|_{\mathcal{X}^s}^2 + |v_{S_0}|^2 + \sqrt{\varepsilon}c_s t\|\mathfrak{b}\|_{H^{s+3}}^2\right), \tag{2.3.31}$$

with $\lambda = \sqrt{\varepsilon}c_s$, $t \in [0,T_\delta]$.

3. Uniformization of the time interval: Here the hypothesis $s > d/2+1$ is important since we want to make use of the Sobolev embedding $H^s \hookrightarrow W^{1,\infty}$.

Lemma 2.3.4. *The regularized problem (2.3.30) has a solution on $[0,\varepsilon^{-1/2}T_0]$ with T_0 independent of δ and ε.*

We have an estimate of the form

$$\frac{d}{dt}E_B^s(\mathcal{U}^\delta, X_S^\delta)(t) \leqslant \sqrt{\varepsilon}c(c_{\text{fric}}, \tilde{M}^{-1}, \left|\!\left|\!\left|\mathcal{U}^\delta\right|\!\right|\!\right|_{T,H^s}, \|\mathfrak{b}\|_{H^{s+3}})\left(E_B^s(\mathcal{U}^\delta, X_S^\delta)(t) + \|\mathfrak{b}\|_{H^{s+3}}^2\right),$$

just before using Grönwall's lemma in the higher order energy estimates. By a change of variable of the time parameter of the form $t = \varepsilon^{-1/2}t'$, it is clear to see that we have an uniform upper bound for a long time regime (with the variable t'). This implies that solutions to the regularized system (2.3.30) exist for a time $\varepsilon^{-1/2}T_{0,\delta}$ with $T_{0,\delta}$ independent of ε.

Furthermore, we have that for every $\tilde{T} > 0$, $t \in \left[0, \min\{\tilde{T}, \varepsilon^{-1/2}T_{0,\delta}\}\right]$

$$\frac{d}{dt}\left(\|\mathcal{U}^\delta(t,\cdot)\|_{\mathcal{X}^s}^2 + \frac{1}{\varepsilon}\left|\dot{X}_S^\delta(t)\right|^2\right) \leqslant F\left(\|\mathcal{U}^\delta(t,\cdot)\|_{\mathcal{X}^s}^2 + \frac{1}{\varepsilon}\left|\dot{X}_S^\delta(t)\right|^2\right) \tag{2.3.32}$$

with F being a regular function independent of δ. By the Picard–Lindelöf theorem, there exists $T_0 > 0$ ($\varepsilon^{-1/2}T_0 \leqslant \tilde{T}$) such that the ordinary differential equation

$$\begin{cases} y'(t) = F(y(t)) \\ y(0) = \|\mathcal{U}_{in}\|_{\mathcal{X}^s}^2 + |V_{S_0}|^2 \end{cases}$$

has a unique solution on $[0,\varepsilon^{-1/2}T_0]$. By Grönwall's lemma and a standard comparison theorem for ODEs we deduce that

$$\|\mathcal{U}^\delta(t,\cdot)\|_{\mathcal{X}^s}^2 + \frac{1}{\varepsilon}\left|\dot{X}_S^\delta(t)\right|^2 \leqslant y(t).$$

□

4. Convergence: Let us define the following supplementary function space

$$E^s_{T_0} = L^\infty\left(\left[0, \frac{T_0}{\sqrt{\varepsilon}}\right]; \mathcal{X}^s\right) \cap W^{1,\infty}\left(\left[0, \frac{T_0}{\sqrt{\varepsilon}}\right]; \mathcal{X}^{s-1}\right).$$

Solutions $\mathcal{U}^\delta$ of the regularized problem clearly belong to $E^s_{T_0}$ with $X^\delta_S \in W^{1,\infty}$. Thus, the family $\{\mathcal{U}^\delta\}_\delta$ is bounded in $E^s_{T_0}$ so it has a weakly convergent subsequence in $E^s_{T_0}$ towards a function $\mathcal{U} \in E^s_{T_0}$.

Since the inclusion $H^s_{loc}(\mathbb{R}^d) \hookrightarrow H^{s-1}_{loc}(\mathbb{R}^d)$ is compact, by the Arzela–Ascoli theorem we may extract a strongly convergent subsequence from it in $C([0, \varepsilon^{-1/2}T_0]; \mathcal{X}^{s-1}_{loc})$ locally.

By interpolation inequalities we have that $\mathcal{U} \in C^\sigma([0, \varepsilon^{-1/2}T_0]; \mathcal{X}^{s-\sigma}_{loc})$ for each $\sigma \in (0, 1)$. Moreover, since the inclusion $H^{s-\sigma}(\mathbb{R}^d) \hookrightarrow C^1(\mathbb{R}^d)$ is also compact for sufficiently small $\sigma > 0$, we may deduce that the subsequence is converging in $C([0, \varepsilon^{-1/2}T_0]; C^1_{loc}(\mathbb{R}^d))$, with X^δ_S converging in $C^1[0, \varepsilon^{-1/2}T_0]$. With this subsequence we shall no problem in passing to the limit in δ for the regularized system (2.3.30) in the sense of distributions, leading to a solution of the problem in $E^s_{T_0}$.

5. Additional regularity: In fact, by being more careful with the estimates, we may deduce that the solution $\mathcal{U}$ is in

$$C\left(\left[0, \frac{T_0}{\sqrt{\varepsilon}}\right]; \mathcal{X}^s\right) \cap C^1\left(\left[0, \frac{T_0}{\sqrt{\varepsilon}}\right]; \mathcal{X}^{s-1}\right).$$

Essentially, the main idea is to prove that the norm $\|\mathcal{U}(t,\cdot)\|_{\mathcal{X}^s}$ is in fact a (Lipschitz-)continuous function of t, since it is the limit of $\|J_\delta \mathcal{U}(t,\cdot)\|_{\mathcal{X}^s}$. For more details, we refer to Chapter 16 of [Tay97].

6. Uniqueness: By taking the difference of two solutions for the system (3.1.6), they consequently satisfy a similar system, thus by the previous a priori estimate, with 0 right hand side, we may conclude that this difference has to be 0 as well. □

This concludes the proof of the well-posedness theorem concerning the coupled fluid-solid system in the Boussinesq regime (3.1.6). As one can clearly see from the demonstration, Remark 2.3.6. on the nature of the time of existence stays valid, so solutions are guaranteed over a time of order $\mathcal{O}(\varepsilon^{-1/2})$.

2.3.6 Towards a more refined solid model

As we remarked in the beginning of the analysis of the Boussinesq regime, the solid equation was consistent with the full Newton equation only at $\mathcal{O}(\sqrt{\mu})$ (Proposition 2.3.1.). In order to be more consistent with the equation, we have to continue the asymptotic development of Φ with respect to μ, since the loss of consistency is due to the integral

term

$$-\frac{c_{\text{fric}}}{\tilde{M}\mu^{3/2}}\frac{\dot{X}_S}{|\dot{X}_S|+\overline{\delta}}\int_{I(t)} P_{z=-1+\mu b}\,dx.$$

For this, let us briefly elaborate an additional term in the asymptotic development. By Proposition 3.37. of [Lan13] we have that

$$\Phi(x,z)=\psi(x)-\mu\left(\frac{z^2}{2}+z\right)\Delta_x\psi+\mu z\partial_t b+\mathcal{O}(\mu^2), \tag{2.3.33}$$

which gives us

$$\varepsilon\partial_t\Phi=\varepsilon\partial_t\psi(x)-\varepsilon\mu\left(\frac{z^2}{2}+z\right)\Delta_x\partial_t\psi+\varepsilon\mu z\partial_{tt}b+\mathcal{O}(\varepsilon\mu^2),$$

as well as

$$\frac{\varepsilon^2}{2}|\nabla_x\Phi|^2=\frac{\varepsilon^2}{2}|\nabla_x\psi|^2+\mathcal{O}(\varepsilon^2\mu),\quad \frac{\varepsilon^2}{2\mu}|\partial_z\Phi|^2=\mathcal{O}(\varepsilon^2\mu).$$

This means that the pressure formula (2.2.3) takes the form

$$P(x,z)=\frac{P_{atm}}{\varrho g H_0}-z+\varepsilon\zeta-\varepsilon\mu\left(\frac{z^2}{2}+z\right)\Delta_x\zeta-\varepsilon\mu z\partial_{tt}b+\mathcal{O}(\varepsilon\mu^2),$$

so an evaluation at the bottom gives

$$P_{bott}=\frac{P_{atm}}{\varrho g H_0}+h+\frac{1}{2}\varepsilon\mu\Delta_x\zeta+\varepsilon\mu\partial_{tt}b+\mathcal{O}(\varepsilon\mu^2), \tag{2.3.34}$$

and as such its integral over the support of the bottom ($I(t)$) is

$$\int_{I(t)} P_{z=-1+\mu b}\,dx=\tilde{M}(\tilde{c}_{solid}-\varepsilon)+\varepsilon\int_{I(t)}\zeta\,dx+\frac{\varepsilon\mu}{2}\int_{I(t)}\Delta_x\zeta\,dx+\mathcal{O}(\varepsilon\mu^2).$$

By keeping the approximation of the pressure for the pressure term in the Newton's equation (2.1.26), we can recover a solid equation consistent at order $\mathcal{O}(\mu^{3/2})$ of the form

$$\begin{aligned}\ddot{X}_S=&-\frac{c_{\text{fric}}}{\sqrt{\mu}}\left(\frac{1}{\varepsilon}\tilde{c}_{solid}+\frac{1}{\tilde{M}}\int\limits_{\text{supp}(\mathfrak{b})+X_S}\zeta\,dx+\frac{\mu}{2\tilde{M}}\int\limits_{\text{supp}(\mathfrak{b})+X_S}\Delta_x\zeta\,dx\right)\frac{\dot{X}_S}{\left|\dot{X}_S\right|+\overline{\delta}}\\&+\frac{\varepsilon}{\tilde{M}}\int_{\mathbb{R}^d}\zeta\nabla_x\mathfrak{b}(x-X_S)\,dx.\end{aligned} \tag{2.3.35}$$

One may obtain the same results for this model as the ones presented in Theorem 2.3.1.

We would like to point out one particularity of the aforementioned computations. The

integral of $\varepsilon\mu\partial_t^2 b$ disappeared due to the fact that b is smooth and of support compact. If one were to use the refined pressure formula (2.3.34) to compute the integral in the pressure term of Newton's equation as well, one would find an additional nonzero term, namely

$$\varepsilon\mu \int_{\mathbb{R}^d} (\nabla_x b \cdot \ddot{X}_S)\nabla_x b \, dx =: \mathcal{M}_{\nabla_x b}\ddot{X}_S, \tag{2.3.36}$$

where the linear map $\mathcal{M}_{\nabla_x b}$ can be represented as a matrix, that is, in addition, positive semi-definite. In fact $\mathcal{M}_{\nabla_x b}$ stands for the so called added mass effect, or virtual mass effect, corresponding to an added inertia due to the solid accelerating/decelerating in the fluid medium, thus deflecting/moving some volume of the surrounding fluid as well. As one can see, in the weakly nonlinear Boussinesq regime (BOUS) this term was not present since it was of order $\mathcal{O}(\mu^2)$, however if one were to study the general second order asymptotic regime (meaning the Serre–Green–Naghdi equations), that is without the additional assumption of $\varepsilon = \mathcal{O}(\mu)$, this term (and many other nonlinearities) would be present.

Conclusion

In the present paper, we established a coupled physical model of the water waves problem with a freely moving object on the bottom of the fluid domain. We deduced the exact coupled system and analyzed two different shallow water asymptotic regimes (with respect to the shallowness parameter μ): the nonlinear Saint-Venant system and the Boussinesq system. We established local in time existence results as well as a uniqueness theorem for both cases and we improved the existence time for the weakly nonlinear Boussinesq regime.

Another possible approach would be to consider the full Green–Naghdi system for the $\mathcal{O}(\mu^2)$ asymptotic regime and establish the coupled system and possibly well-posedness results for it. This would yield a non-hydrostatic pressure formula, and consequently a more complex equation for the solid motion, incorporating the added mass effect, briefly elaborated in the last section.

An even more general scenario can be envisioned, that is to handle the full problem formulated in the first section, treating the coupled problem (2.1.22) with (2.1.26).

To complement the theoretical results, a numerical study is to follow this article in order to verify the applicability of the system as well as to compare it with other existing methods to treat wave-structure interaction problems ([DNZ15], [ACDNn17]).

Chapter 3

The incidence of a freely moving bottom on wave propagation

Contents

Version française abregée

La compréhension et la prédiction de la génération et de l'évolution des vagues occupe les ingénieurs marins et les océanographes depuis des années. En 1871 Joseph Boussinesq ([Bou71]) a introduit le premier modèle du problème des vagues intégrant des variables horizontalement moyennées. Ce modèle a été modifié et adapté pour de nombreux régimes physiques et mathématiques différents ([Per67], [Nwo93], [BCS02], [Lan13]).

La mise en oeuvre d'un fond qui évolue en temps dans ces modèles pose des défis à la fois théoriques et numériques. Il existe des adaptations basées principalement sur des expériences physiques ([Wu87], [TW92], [Che03]), mais leur justification rigoureuse n'est faite que pour certains modèles ([Igu11]). L'objectif de cette étude est la mise en oeuvre d'un schéma numérique pour un modèle intégrant un objet qui se déplace au fond sous l'action du mouvement des vagues ([Ben17]).

Bien que l'étude numérique d'un solide immergé ne soit pas nouvelle, notre approche est motivée par une analyse théorique approfondie du système couplé, contrairement aux considérations expérimentales ou aux motivations numériques qui sont présentes en général dans la littérature.

Le système couplé : Nous nous intéressons à un modèle de deux dimensions physiques, une horizontale (coordonnée x) et une verticale (coordonnée z) (voir Figure 3.1). Les variables (adimensionnées) du système sont l'élévation de la surface libre ζ, la vitesse horizontale verticalement moyennée $\overline{V}$, et le déplacement du solide X. L'évolution du fond du domaine du fluide est décrite par $b(t,x) = \mathfrak{b}\,(x - X(t))$, où $\mathfrak{b}$ correspond à l'état initial du solide.

Il y a également trois paramètres dans le système qui caractérisent le régime physique dans lequel on se place : μ est le paramètre de faible profondeur, ε le paramètre de l'amplitude des vagues et β le paramètre de la topographie du fond.

Donc, les équations à surface libre en présence d'un solide au fond dans le régime de Boussinesq faiblement non-linéaire sont données par

$$\begin{cases} \partial_t \zeta = E(\zeta, \overline{V}, X, \dot{X}), & \text{(3.0.1a)} \\ \partial_t \overline{U} = F(\zeta, \overline{V}, X, \dot{X}, \ddot{X}), & \\ \ddot{X} = G(\zeta, X, \dot{X}), & \text{(3.0.1b)} \end{cases}$$

où

$$\overline{U} = \overline{U}(\overline{V}) = \overline{V} - \frac{\mu}{3}\partial_{xx}\overline{V}.$$

Les termes à droite s'écrivent

$$E(\zeta, \overline{V}, X, \dot{X}) = -\partial_x(h\overline{V}) - \frac{\beta}{\varepsilon}\partial_x \mathfrak{b}(x - X)\dot{X},$$
$$F(\zeta, \overline{V}, X, \dot{X}, \ddot{X}) = -\partial_x\zeta - \frac{\varepsilon}{2}\partial_x(\overline{V}^2) - \frac{\mu\beta}{2\varepsilon}\partial_{xxx}\mathfrak{b}(x - X)(\dot{X})^2 + \frac{\mu\beta}{2\varepsilon}\partial_{xx}\mathfrak{b}(x - X)\ddot{X},$$
$$G(\zeta, X, \dot{X}) = -\frac{c_{fric}}{\beta\sqrt{\mu}}F_{normal}(\zeta, X)\frac{\dot{X}}{|\dot{X}| + \delta} + \frac{\varepsilon}{\tilde{M}}\int_{\mathbb{R}} \zeta\partial_x\mathfrak{b}(x - X)\, dx.$$

Pour le dernier terme, c_{fric} représente le coefficient de friction, le quatrième paramètre du modèle, δ est un petit constant mathématique, de plus

$$F_{normal}(X, \zeta) = \beta + c_{solid} + \frac{\varepsilon}{\tilde{M}}\int_{\mathrm{supp}(\mathfrak{b})+X} \zeta\, dx, \tag{3.0.2}$$

avec les notations suivantes :

$$c_{solid} = \frac{|\,\mathrm{supp}(\mathfrak{b})|}{\tilde{M}}\left(\frac{P_{atm}}{\varrho g H_0} + 1\right) - \frac{\beta}{\tilde{M}}\int_{\mathrm{supp}(\mathfrak{b})} b\, dx, \qquad \tilde{M} = \frac{M}{\varrho L a_{bott}}.$$

Le schéma numérique : Nous mettons en oeuvre un schéma numérique de différences finies qui repose sur une approche de maillage décalé ([LM07]). Nous avons amélioré leur modèle en raffinant la précision de certaines sous-étapes afin d'obtenir un schéma qui converge en ordre 4 en temps ainsi qu'en espace également pour les quantités du fluide.

Le maillage est décalé au sens où l'élévation de la surface libre (ζ) et la fonction décrivant la topographie du fond (b) sont définies sur les points du maillage, en revanche, la vitesse moyennée ($\overline{V}$) existe sur les points de milieu du maillage. Les équations d'évolution seront définies sur les espaces correspondant aux espaces de définition de ces quantités du fluide. Le passage entre un vecteur défini sur les point de la maille et un vecteur défini sur les points du milieu est assuré par une interpolation centrée sur 4 points.

Pour la discrétisation en espace, nous appliquons des schémas de différences finies centrales d'ordre 4. Pour la discrétisation en temps nous avons choisi l'algorithme de prédiction-correction d'Adams qui consiste en deux sous-étapes :

1. L'étape de la prédiction par un schéma multi-étape explicite d'Adams–Bashforth pour l'équation (3.0.1a)

$$\zeta_i^{n+1^*} = \zeta_i^n + \frac{\Delta t}{12}\left(23E_i^n - 16E_i^{n-1} + 5E_i^{n-2}\right),$$

et de même pour $\overline{V}_{i+1/2}^{n+1^*}$. En outre, c'est à ce point qu'on applique une discrétisation adaptée pour l'équation qui caractérise le mouvement du solide :

$$X^{n+1} = \overline{G}(\zeta^n, X^n, X^{n-1}, X^{n-2}), \tag{3.0.3}$$

avec $\overline{G}$ définie par (3.2.6). Notons que cette partie du schéma n'est que d'ordre 2 (contrairement au reste du schéma, qui est d'ordre 4 en temps)

2. La correction utilise un schéma multi-étapes implicite d'Adams–Moulton de la forme

$$\zeta_i^{n+1} = \zeta_i^n + \frac{\Delta t}{24}\left(9E(\zeta_i^{n+1^*}, \overline{V}_{i+1/2}^{n+1^*}, X^{n+1}) + 19E_i^n - 5E_i^{n-1} + E_i^{n-2}\right).$$

Quelques résultats des simulations numériques : Tout d'abord, nous remarquons qu'il est possible d'effectuer une analyse de stabilité de von Neumann pour le système linéarisé ([LM07]). Cela nous fournit une condition de Courant–Friedrichs–Lewy de la forme suivante :

$$\sqrt{gH_0}\frac{\Delta t}{\Delta x} \leqslant \frac{1}{2},$$

à respecter dans les simulations.

Nous avons effectué une suite d'expériences numériques pour vérifier l'ordre de convergence. Dans le cas d'un fond plat, où le système admet une solution d'onde solitaire qui permet de mesurer l'erreur de la solution exacte, nous avons trouvé un ordre de convergence proche de 4, qui est la valeur théorique (Figures 3.2). Nous avons obtenu des résultats similaires dans le cadre d'un fond fixe non-plat, cette fois en mesurant l'erreur relative avec une solution approchée (Figure 3.3). Dans le cas d'un solide pouvant se déplacer au fond, nous détectons une baisse d'ordre, l'ordre est de 3 en espace et de 2 en temps (Figure 3.4), ce qui reste cohérent avec nos attentes.

En suivant l'amplitude d'une vague qui passe au-dessus du solide (en regardant plusieurs régimes physiques), nous apercevons une diminution légère dans le cas où le solide peut bouger (Figures 3.9, 3.10). Cette diminution devient plus importante pour de petites valeurs du coefficient de friction ($\sim 10^{-3}$).

Nous avons également mesuré les effets des vagues sur le mouvement du solide. Notamment, nous avons mis en évidence des effets d'amortissement hydrodynamique pour de petites valeurs c_{fric}. La Figure 3.13 montre que le ralentissement dû à la force de pression joue un rôle important dans la dynamique et l'évolution du mouvement de l'objet.

Nous avons réalisé des expériences en temps long aussi, c'est-à-dire des simulations avec des trains de vagues qui s'approchent du solide, situé au fond. Les résultats (Figures 3.15 et 3.16) montrent une évolution quasi-périodique de la position avec un déplacement total positif vers la direction du mouvement des vagues, dont l'évolution temporelle n'est pas linéaire.

Introduction

Understanding and predicting surface wave propagation and transformation has been one of the central elements of coastal engineering and oceanography for the past few

decades. In 1871 Boussinesq introduced the first depth averaged model ([Bou71]). It originally described a physical situation with horizontal bottom and was later generalized for variable depths by Peregrine ([Per67]). This kind of models has played a crucial role in water wave modeling, especially in shallow water regions (such as the shoaling zone for coastal waves). From a mathematical point of view, these equations arise as shallow water asymptotic limits of the full water waves problem (for a thorough discussion on the subject, please refer to [Lan13]) and incorporate (weakly) dispersive and (weakly) nonlinear effects. Nowadays many reformulations and generalizations of the original Boussinesq system exist: for example Nwogu's extended equation ([Nwo93]) or the abcd-system introduced in [BCS02], to cite a few of the most important ones.

There has been some articles considering the case of moving bottoms. After observing solitary waves by disturbances of the bottom topography advancing at critical speed ([Wu87]) Wu et al. formally derived a set of generalized channel type Boussinesq systems ([TW92]). Their work was extended later on in a formal study on more general long wave regimes ([Che03]). Tsunami research has also proved to be a main motivation factor for the consideration of time dependent topographies (see for instance [Igu11], where the asymptotic models are fully justified), as well as the study of waves generated by submarine landslides [DK13, Mel15]. All these references share the assumption that the motion of bottom is prescribed, and therefore not influenced by the propagation of the waves.

In this work, we address the more complex situation of a bottom moving under the pressure forces exerted by the waves as they propagate at the surface. Contrary to the previous configuration, this is a two-way coupling: the motion of the solid influences the motion of the wave as above, but the motion of the solid is itself governed by the propagation of the waves. In [Ben17], a model was derived to model this wave-structure interaction. It consists in a weakly nonlinear Boussinesq model with topography terms coupled to a second order ODE describing the motion of the solid under pressure and friction forces.

A first physical motivation for such a model stems, for example, from marine energy engineering, and most notably submerged wave energy converters (submerged pressure differential devices, see [AELS14] and references therein) and oscillating wave surge converters (WaveRollers and Submerged plate devices, [GIL+14]). Note that there have also been recent theoretical and numerical works on a related wave-structure interaction problem based on depth averaged models and where the object is not lying at the bottom but floating at the surface [Lan17], [Boc18], [IL18] [BEKRE17]. One of the goals of this work is to bring some qualitative and quantitative answers on wave induced motion at the bottom. A second motivation is coastal protection. In order to diminish the impact of storm waves on coastal structures, submarine structure are sometimes built to change the topography and hereby the location of wave breaking. The possibility of having moving and/or elastic structures to decrease the energy of the waves has also been considered recently. This is another goal of this work to assess the influence of a freely moving bottom on wave breaking.

Although the numerical study of immersed structures is not entirely new, our approach is heavily based on a theoretical analysis of the general system, rather than experimental or numerical considerations usually present in the corresponding bibliography. An approach with numerous physical and biological applications was developed by Cottet et al. ([CM06], [CMM08]) based on a level set formulation, adapting an immersed boundary method and general elasticity theory (see also [FGG07]). Modeling underwater landslides provides for an excellent example of such systems, we refer to [DK13] and references therein for recent developpments. Numerical models adapted to tsunami generation due to seabed deformations were presented for example in [GN07] or [Mit09]. From a control theory point of view, Zuazua et al. ([DNZ15]) performed an analytical and numerical analysis on underwater wave generator models. Perhaps one of the most relevant existing studies concerns a submerged spring-block model and the associated experimental and numerical observations ([AMMM15], [ACDNn17]).

The structure of the article is as follows. After a brief introduction, we present the weakly nonlinear Boussinesq system in a fluid domain with a flat bottom topography and with a solid object lying on the bottom, capable of moving horizontally under the pressure forces created by the waves. Following our previous work, this coupled system admits a unique solution for a long time scale ([Ben17]).

In the third section we detail the finite difference numerical scheme adapted to this system. We elaborate a fourth order accurate staggered grid system for the variables concerning the movement of the fluid, following the footsteps of Lin and Man ([LM07]). As for the time discretization, an adapted fourth order accurate Adams–Bashforth predictor-corrector method is implemented, incorporating the discretized ordinary differential equation characterizing the solid displacement via a modified central finite difference scheme. We end this section with some remarks on the boundary conditions implemented and on certain useful properties of our adaptation.

Section 4 details the numerical experiments concerning the model. The convergence of the finite difference scheme is measured to be almost of order 4 in time and in space for a flat bottom as well as for large coefficients of friction, greatly improving the reference staggered grid model (of order 2 only) in [LM07] over a flat bottom. An order 3 mesh convergence and an order 2 convergence in time is observed for small coefficients of friction. The transformation of a passing wave over the solid is detailed in various different physical regimes. Wave shoaling effects are examined and compared to a system with the same parameters admitting a fixed solid object on the bottom instead of a freely moving one. The effects of the friction on the motion of the solid are also measured, revealing that the solid comes to a halt after the wave has passed over it. Measuring the solid motion also indicates hydrodynamical damping effects reminiscent to the ones attributed to dead-water phenomena, closely tied to internal wave generation (for more details, we refer to [Ekm04], [MVD11], [Duc11], [Duc12]). Long term effects by a wave train test are also presented at the end of the section.

3.1 The governing equations

3.1.1 The physical regime

We work in two spatial dimensions, and denote the horizontal coordinate by x and the vertical coordinate by z. The time parameter shall be $t \in \mathbb{R}^+$. The physical domain occupied by the fluid is

$$\Omega_t = \{(x,z) \in \mathbb{R} \times \mathbb{R} \,:\, -H_0 + b(t,x) < z < \zeta(t,x)\}\,,$$

where H_0 is the typical water depth at rest and the functions $\zeta(t,x)$ and $b(t,x)$ stand for the free surface elevation and the bottom topography variation respectively (see Figure 2.1).

The solid on the bottom is supposed to be moving only in the horizontal direction, its displacement vector is denoted by $X(t)$, consequently its velocity is given by $v(t) = \dot{X}(t)$. Therefore we have that

$$b(t,x) = \mathfrak{b}\,(x - X(t))\,, \tag{3.1.1}$$

with $\mathfrak{b}$ corresponding to the initial state of the solid, at $t = 0$ (without loss of generality, we assume that $X(0) = 0$). This function $\mathfrak{b}$ is of class $\mathcal{C}^\infty(\mathbb{R})$ and compactly supported.

The solid is supposed to be rigid and homogeneous with a given mass M, in frictional contact with the flat bottom of the domain. Its motion is governed by Newton's second law, and the main difficulty consists in computing the hydrodynamical force exerted by the fluid.

The fluid itself is assumed to be homogeneous, inviscid, incompressible, and irrotational. In full generality Its dynamics are described by the full water waves problem, that is, by the free surface Euler equations (see for instance [Lan13]). As said in the introduction we choose here to describe the fluid dynamics by a simpler asymptotic model, namely, a Boussinesq system.

The weakly nonlinear Boussinesq system considered here is a shallow water asymptotic model, and we therefore have to introduce characteristic scales of the problem to perform shallow water asymptotics. First of all H_0 denotes the typical base water depth at rest, and L, the characteristic horizontal scale of the wave motion; the solid horizontal size is assumed to be of the same order. Moreover we denote by a_{surf}, the order of the free surface amplitude, and a_{bott}, the height of the solid.

Using these quantities, we can introduce several dimensionless quantities:

- shallowness parameter $\mu = \dfrac{H_0^2}{L^2}$,
- nonlinearity (or amplitude) parameter $\varepsilon = \dfrac{a_{surf}}{H_0}$,

- bottom topography parameter $\beta = \dfrac{a_{bott}}{H_0}$.

These parameters play an important role in the formulation of the governing equations.

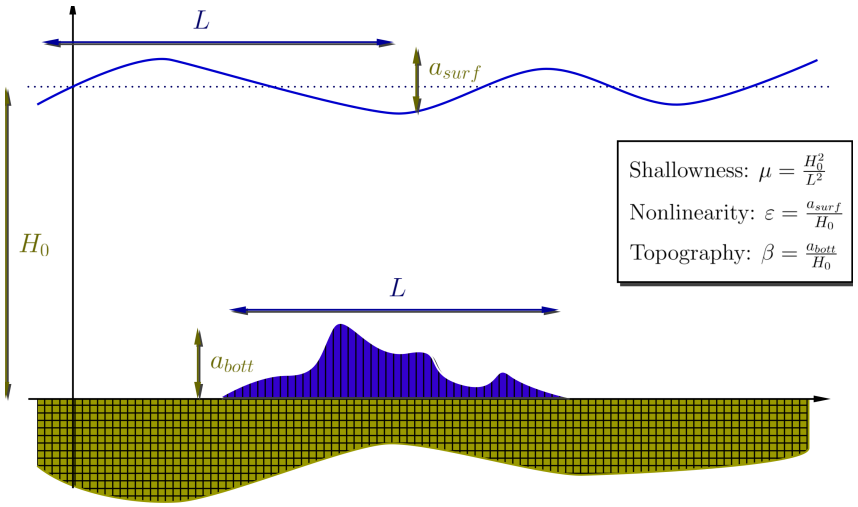

Figure 3.1 – The characteristic scales of the coupled water waves problem

3.1.2 The coupled Boussinesq system

We consider here a shallow water and weakly nonlinear regime, i.e. we assume that μ is small and that $\varepsilon = \mathcal{O}(\mu)$, and we also suppose that the height of the solid is relatively small (meaning $\beta = \mathcal{O}(\mu)$). The fluid is then governed by a Boussinesq system. Thus, the asymptotic regime writes as

$$0 \leqslant \mu \leqslant \mu_{max} \ll 1, \quad \varepsilon = \mathcal{O}(\mu),\ \beta = \mathcal{O}(\mu). \tag{BOUS}$$

In this regime, Boussinesq systems are known to approximate the full water waves equations with a $O(\mu^2)$ precision (see for instance [Lan13]). In the case of a moving bottom, such a Boussinesq system is given by the equations

$$\begin{cases} \partial_t \zeta + \partial_x (h\overline{V}) = \dfrac{\beta}{\varepsilon} \partial_t b, \\ \left(1 - \dfrac{\mu}{3}\partial_{xx}\right) \partial_t \overline{V} + \partial_x \zeta + \varepsilon (\overline{V} \cdot \partial_x)\overline{V} = -\dfrac{\mu\beta}{2\varepsilon} \partial_x \partial_t^2 b, \end{cases} \tag{3.1.2}$$

with $h = 1 + \varepsilon\zeta - \beta b$ denoting the nondimensionalized fluid height while $\overline{V}$ stands for the (dimensionless) vertically averaged horizontal velocity

$$\overline{V}(t,x) = \frac{1}{h} \int_{-1+\beta b}^{\varepsilon\zeta} V(t,x,z)\, dz,$$

with V being the dimensionless horizontal component of the velocity field of the fluid. In the equation, the variables are classically the nondimensionalized forms of the corresponding physical quantities described in the previous section (see [Lan13] and more specifically [Ben17] for details on the non-dimensionalization process). To recover the quantities with the proper dimensions, it is enough to multiply the function or variable by its corresponding characteristic scale (e.g. $\zeta \rightsquigarrow a_{surf}\zeta$, $x \rightsquigarrow Lx$, etc.).

Remark 3.1.1. *Without the smallness assumption on ε, and on β, it is still possible to perform an asymptotic expansion at $\mathcal{O}(\mu^2)$. The resulting system is more general than the Boussinesq system (3.1.2) but also more complicated, it is known as the Serre–Green–Naghdi equations (see for example [HI15]).*

Following the derivation presented in [Ben17], Newton's second law for the solid displacement can be written in dimensionless form as

$$\ddot{X} = -\frac{c_{fric}}{\beta\sqrt{\mu}} F_{normal}(X,\zeta)\frac{\dot{X}}{\left|\dot{X}\right| + \delta} + \frac{\varepsilon}{\tilde{M}}\int_{\mathbb{R}} \zeta \partial_x b \, dx. \tag{3.1.3}$$

In this expression, the first term of the right-hand-side correspond to friction forces, and the second one to the pressure forces exerted by the fluid on the solid.
In the formula for the friction forces, $\frac{1}{\beta}F_{normal}$ denotes the norm of the normal force exerted by the flat bottom on the solid,

$$\frac{1}{\beta}F_{normal}(X,\zeta) = 1 + \frac{c_{solid}}{\beta} + \frac{\varepsilon}{\beta\tilde{M}}\int_{\mathrm{supp}(\mathfrak{b})+X} \zeta \, dx, \tag{3.1.4}$$

where c_{solid} and $\tilde{M}$ are quantities that depend only on the physical parameters of the solid,

$$c_{solid} = \frac{|\,\mathrm{supp}(\mathfrak{b})|}{\tilde{M}}\left(\frac{P_{atm}}{\varrho g H_0} + 1\right) - \frac{\beta}{\tilde{M}}\int_{\mathrm{supp}(\mathfrak{b})} b \, dx, \tag{3.1.5}$$

and

$$\tilde{M} = \frac{M}{\varrho L a_{bott}}$$

(P_{atm} stands for the atmospheric pressure, g the gravitational acceleration constant, ρ for the volumic mass of the fluid, and M for the mass of the object). The friction coefficient c_{fric} in the expression for the friction force plays an important role in the mathematical, physical and numerical analysis of the problem. The actual measurement of this coefficient is rather difficult, especially in a complex physical system such as the current one, mainly because its value depends on many other physical parameters (like the material structure of the surfaces, the temperature, the pressure, the velocity of the sliding, etc.). Generally speaking a coefficient of $10^{-2} \sim 10^{-3}$ corresponds to a relatively frictionless sliding, and values in the range of 1 signify an important friction between the contact media. Finally, δ is an artificial parameter introduced in [Ben17] to avoid the singularity in the friction force when the solid stops (a more accurate description, left for further works, is to distinguish

between static and dynamic friction forces); the value of this parameter is taken to be sufficiently small ($\sim 10^{-10}$) in order to be much smaller than all the other parameters considered here.

Remark 3.1.2. *The first term in c_{solid} corresponds to the the contribution of the atmospheric pressure to the pressure at the bottom. The second term corresponds to the hydrostatic pressure contribution due to the water column. It is of interest to consider configurations where these two contributions are of comparable importance,*

$$\frac{P_{atm}}{\varrho g H_0} \sim 1 \qquad \Longleftrightarrow \qquad H_0 \sim 10m,$$

for $P_{atm} \sim 1000hPa$ and $\rho \sim 1000kg.m^{-3}$. In our numerical simulations, we shall therefore take $H_0 = 10m$; with smaller values, the effects of the atmospheric pressure would be predominant and for larger values, this would be the pressure of the water column.

To sum it up, the Boussinesq equations coupled with a freely moving object at the bottom take the following form

$$\begin{cases} \partial_t \zeta + \partial_x (h\overline{V}) = \dfrac{\beta}{\varepsilon} \partial_t b, \\ \left(1 - \dfrac{\mu}{3}\partial_{xx}\right) \partial_t \overline{V} + \partial_x \zeta + \varepsilon (\overline{V} \cdot \partial_x)\overline{V} = -\dfrac{\mu\beta}{2\varepsilon} \partial_x \partial_{tt} b, \end{cases} \tag{3.1.6a}$$

$$\ddot{X} = -\frac{c_{fric}}{\beta\sqrt{\mu}} F_{normal}(\zeta, X) \frac{\dot{X}}{\left|\dot{X}\right| + \delta} + \frac{\varepsilon}{\tilde{M}} \int_{\mathbb{R}} \zeta \partial_x b \, dx, \tag{3.1.6b}$$

where we recall that $b(t,x) = \mathfrak{b}(x - X(t))$.
With the numerical scheme in mind, we can rewrite this system in a more compact form as follows

$$\begin{cases} \partial_t \zeta = E(\zeta, \overline{V}, X, \dot{X}), \\ \partial_t \overline{U} = F(\zeta, \overline{V}, X, \dot{X}, \ddot{X}), \end{cases} \tag{3.1.7a}$$

$$\ddot{X} = G(\zeta, X, \dot{X}), \tag{3.1.7b}$$

where

$$\overline{U} = \overline{U}(\overline{V}) = \overline{V} - \frac{\mu}{3}\partial_{xx}\overline{V}. \tag{3.1.8}$$

The remaining terms are given by

$$E(\zeta, \overline{V}, X, \dot{X}) = -\partial_x(h\overline{V}) - \frac{\beta}{\varepsilon}\partial_x \mathfrak{b}(x - X)\dot{X}, \tag{3.1.9a}$$

$$F(\zeta, \overline{V}, X, \dot{X}, \ddot{X}) = -\partial_x\zeta - \frac{\varepsilon}{2}\partial_x(\overline{V}^2) - \frac{\mu\beta}{2\varepsilon}\partial_{xxx}\mathfrak{b}(x - X)(\dot{X})^2 + \frac{\mu\beta}{2\varepsilon}\partial_{xx}\mathfrak{b}(x - X)\ddot{X} \tag{3.1.9b}$$

$$G(\zeta, X, \dot{X}) = -\frac{c_{fric}}{\beta\sqrt{\mu}}F_{normal}(\zeta, X)\frac{\dot{X}}{|\dot{X}| + \delta} + \frac{\varepsilon}{\tilde{M}}\int_{\mathbb{R}} \zeta\partial_x\mathfrak{b}(x - X)\, dx, \tag{3.1.9c}$$

where we recall that F_{normal} is given by (3.1.4).

3.1.3 Relevant properties of the system

The mathematical analysis of the coupled system (3.1.6)-(3.1.6b) is performed in [Ben17]. One of the difficulties to get a uniform existence time is the singular term $1/\beta\sqrt{\mu}$ in the expression (3.1.7b) for G. One has to take advantage of the structure of this term to show that it is a dissipative term that does not contribute to the growth of the energy. The numerical scheme we shall use to describe the wave-structure interaction must be carefully chosen in order to reproduce this mechanism at the discrete level (otherwise singular $O(1/\beta\sqrt{\mu})$ error terms would appear). Due to the importance of this issue, we recall here the uniform L^2-type a priori estimate for (3.1.6)-(3.1.6b) obtained in [Ben17]. Let us first introduce the wave-structure energy functional

$$E_B(t) = \frac{1}{2}\int_{\mathbb{R}} \zeta^2\, dx + \frac{1}{2}\int_{\mathbb{R}} h(\overline{V})^2\, dx + \frac{1}{2}\int_{\mathbb{R}} \frac{\mu}{3}h(\partial_x\overline{V})^2\, dx + \frac{\beta}{2\varepsilon^2}\tilde{M}\left|\dot{X}\right|^2; \tag{3.1.10}$$

the first term accounts for the potential energy of the waves, the second and third for their kinetic energy, and the last one for the kinetic energy of the solid. We have the following ([Ben17]):

Proposition 3.1.1. *Let $\mu \leq \mu_{max}$ and $s_0 > 3/2$. Then any $\mathcal{U} \in \mathcal{C}^1([0,T]; H^{s_0})$ and $X \in \mathcal{C}^2([0,T])$ satisfying the coupled system (3.1.6), with initial data $\mathcal{U}(0,\cdot) = \mathcal{U}_{in} \in H^{s_0}$ and $(X(0), \dot{X}(0)) = (0, v_{S_0}) \in \mathbb{R}\times\mathbb{R}$ verify the energy estimate*

$$\sup_{t\in[0,T]}\left\{e^{-\sqrt{\beta}c_0 t}E_B(t)\right\} \leqslant 2E_B(0) + 2\mu c_0 T\|\mathfrak{b}\|^2_{H^3}, \tag{3.1.11}$$

where

$$c_0 = c(\sup_{t\in[0,T]}\|\mathcal{U}(t,\cdot)\|_{H^{s_0}}, \|b\|_{W^{3,\infty}}).$$

Sketch of proof. It follows a standard energy estimate argument; we multiply the first equation of (3.1.6) by ζ and the second equation by $h\overline{V}$, and we integrate over $\mathbb{R}$ with

respect to x. We also multiply the equation on X by $\frac{\tilde{M}\beta}{\varepsilon^2}\dot{X}$ and add the three resulting equations to obtain

$$\frac{d}{dt}E_B = \frac{\beta}{\varepsilon}\Big[\int \partial_t b\zeta + \dot{X}\int \zeta\partial_x b\Big] - c_{fric}\tilde{M}\frac{1}{\varepsilon^2\sqrt{\mu}}F_{normal}\frac{|\dot{X}|^2}{|\dot{X}|+\delta} + \text{l.o.t.},$$

where l.o.t. stand for terms that can be controlled by a Gronwall type argument. Recalling that $b(t,x) = \mathfrak{b}(x - X(t))$, the first term between brackets vanishes. The second term of the right-hand-side being obviously negative, a control of E_B follows from a Gronwall type argument (see [Ben17] for details). The fact that the contribution of the (singular) friction term is negative is crucial to obtain the uniform estimate stated in the proposition. This property should be preserved by the numerical scheme. □

Using this proposition, it is easy to obtain the following corollary that provides a uniform control on the velocity. A numerical scheme that would not respect the sign property used in the proof of the proposition would lead to considerable errors in the solid velocity.

Corollary 3.1.1. *This energy estimate provides us with a natural control on the solid velocity, namely*

$$\sup_{t\in[0,T]}\left\{e^{-\sqrt{\beta}c_0 t}\tilde{M}\left|\dot{X}(t)\right|^2\right\} \leqslant 4\frac{\varepsilon^2}{\beta}E_B(0) + 4\frac{\varepsilon^2\mu}{\beta}c_0 T\|\mathfrak{b}\|^2_{H^3}, \tag{3.1.12}$$

where c_0 is as before.

3.2 The discretized model

In this section we present the numerical scheme we use to compute numerical solutions to (3.1.9a)-(3.1.9b). We follow the ideas of Lin and Man ([LM07]) who used a staggered grid approach for the numerical simulation of a Boussinesq system in the case of a flat bottom. We improve their model by reaching a fourth order overall accuracy in space and time, and extend the scheme in order to take into account non flat topographies. We then propose a second order numerical scheme for the wave-structure interaction that reproduces at the discrete level dissipative structure of the singular term used to derive Corollary 3.1.1.

3.2.1 The finite difference scheme on a staggered grid

Since the solid motion is time dependent only ($X(t)$ does not depend on the horizontal coordinate x), spatial discretization only concerns the fluid variables, for which we aim for a fourth order precision.

In their article, Lin and Man obtained a stable and accurate model for a Boussinesq type system (the Nwogu equations). They observed good conservative properties for the fluid system, attributed mainly to the staggered grid method they implemented, which is an important factor for long-term measurements; furthermore this scheme is well-adapted to accurate energy measurements of the system.

We implement their staggered grid method in which the "scalar" quantities, such as the surface elevation ζ, the bottom topography b and the fluid height h, are defined on the grid points, and the "vectorial" variable, the averaged velocity $\overline{V}$ (that is still a scalar since we are only working in one horizontal dimension) is defined on the mid-points of the mesh. The mesh size will be chosen as Δx, numbered by $i = 1, 2, \dots N_{space}$. The discrete equation for ζ (based on (3.1.9a)) will be defined for mesh points and the equation for $\overline{V}$ (from equation (3.1.9b)) for the mid-points.

In order to be able to do this, we will have to define the "scalar" quantities for the mid-points as well, we shall do so by a four point centered fourth order interpolation, that is,

$$\zeta_{i+1/2} = \frac{-\zeta_{i-1} + 9\zeta_i + 9\zeta_{i+1} - \zeta_{i+2}}{16}.$$

In the reference article [LM07], only a linear interpolation was used. Even though it was not mentioned at all, we believe it to be one of the main reasons for the loss of mesh convergence in their scheme (they observe only a second order convergence).

For the spatial discretization in general, we chose fourth order accurate central finite difference schemes for the different orders of derivatives. In their work, Lin and Man chose only second order schemes for the higher order derivatives which is another reason for the resulted loss in mesh convergence in their case. In our implementation even higher order derivatives are discretized by fourth order schemes.

Observing the right hand sides of equations (3.1.7a) we may separate four different types of terms. Once again, we emphasize on the fact that the first equation will act on mesh points while the second one will be defined on mid-points of the grid.

- First order derivative on grid points for a "scalar" quantity, this concerns the term $\partial_x \mathfrak{b}$, and equivalently first order derivative on mid-points for "vectorial" variables, this concerns the term $\partial_x(\overline{V}^2)$. For this case, the classical four point central difference scheme of order 4 writes as

$$(\partial_x \mathfrak{b})_i = \frac{\mathfrak{b}_{i-2} - 8\mathfrak{b}_{i-1} + 8\mathfrak{b}_{i+1} - \mathfrak{b}_{i+2}}{12\Delta x}, \tag{3.2.1}$$

  and similarly for the derivative of $\overline{V}^2$ with mid-points.

- First order derivative on mid-points for a quantity having values in grid points, this concerns the term $\partial_x(h\overline{V})$, and equivalently first order derivative on grid points for quantities having values in mid-points, this concerns the term $\partial_x \zeta$. For this case,

the adapted four point central difference scheme of order 4 writes as

$$(\partial_x \zeta)_{i+1/2} = \frac{\zeta_{i-1} - 27\zeta_i + 27\zeta_{i+1} - \zeta_{i+2}}{24\Delta x}, \tag{3.2.2}$$

and similarly for the derivative of $h\overline{V}$ with mid-points.

- Second order derivative on mid-points for quantities having values at grid points, this concerns both $\partial_{xx}\mathfrak{b}$ and $\partial_{xx}\overline{V}$. A classical fourth order accurate central finite difference scheme is implemented, meaning

$$(\partial_{xx}\mathfrak{b})_{i+1/2} = \frac{-\mathfrak{b}_{i-3/2} + 16\mathfrak{b}_{i-1/2} - 30\mathfrak{b}_{i+1/2} + 16\mathfrak{b}_{i+3/2} - \mathfrak{b}_{i+5/2}}{12(\Delta x)^2}, \tag{3.2.3}$$

and similarly for $\overline{V}$.

- Third order derivative on mid-points for a term having values on grid points, this concerns $\partial_{xxx}\mathfrak{b}$. Once again, a fourth order accurate central scheme is applied,

$$(\partial_{xxx}\mathfrak{b})_{i+1/2} = \frac{\mathfrak{b}_{i-5/2} - 8\mathfrak{b}_{i-3/2} + 13\mathfrak{b}_{i-1/2} - 13\mathfrak{b}_{i+3/2} + 8\mathfrak{b}_{i+5/2} - \mathfrak{b}_{i+7/2}}{8(\Delta x)^3}. \tag{3.2.4}$$

The high accuracy guarantees that we can capture more precisely the nonlinear interaction between the fluid and the solid without posing problems for the numerical scheme due to the necessity of information on many grid points, since the solid is localized to its support (the middle section of the wave tank, as explained in Section 3.2.4).

3.2.2 Time stepping with Adams–Bashforth

As elaborated in [LM07], we adapt a fourth order accurate Adams predictor-corrector method. Starting from the initial condition at time $t = 0$, the first two values of the quantities may be generated by a fourth order classic Runge–Kutta (RK4) time stepping algorithm. Let us suppose that currently we are at time step $n \geqslant 2$ and as such, all information on the main variables (ζ, $\overline{V}$, and X) is known. The method consists of two steps:

1. First, the predictor step is implemented on the fluid equations (equations (3.1.7a)) by the explicit third order Adams–Bashforth scheme

$$\begin{aligned}
\zeta_i^{n+1^*} &= \zeta_i^n + \frac{\Delta t}{12}\left(23E_i^n - 16E_i^{n-1} + 5E_i^{n-2}\right), \\
\overline{U}_{i+1/2}^{n+1^*} &= \overline{U}_{i+1/2}^n + \frac{\Delta t}{12}\left(23F_{i+1/2}^n - 16F_{i+1/2}^{n-1} + 5F_{i+1/2}^{n-2}\right),
\end{aligned}$$

in addition we apply the algorithm for calculating the solid position (presented in

the following section),

$$X^{n+1} = \overline{G}(\zeta^n, X^n, X^{n-1}, X^{n-2}). \tag{3.2.5}$$

2. With the knowledge of the predicted values, the next step is the correction by a fourth order Adams–Moulton method

$$\zeta_i^{n+1} = \zeta_i^n + \frac{\Delta t}{24}\left(9E(\zeta_i^{n+1^*}, \overline{V}_{i+1/2}^{n+1^*}, X^{n+1}) + 19E_i^n - 5E_i^{n-1} + E_i^{n-2}\right),$$
$$\overline{U}_{i+1/2}^{n+1} = \overline{U}_{i+1/2}^n + \frac{\Delta t}{24}\left(9F(\zeta_i^{n+1^*}, \overline{V}_{i+1/2}^{n+1^*}, X^{n+1}) + 19F_{i+1/2}^n - 5F_{i+1/2}^{n-1} + F_{i+1/2}^{n-2}\right).$$

Remark 3.2.1. *Additionally, the predictor-corrector method can be iterated to guarantee even more accuracy for the algorithm.*

We remark that in [LM07], the same algorithm was used in the case of a flat bottom but with an observed convergence of order 2 instead of the theoretical order 4 in the time variable.

3.2.3 Time discretization for the solid motion

Equation (3.1.7b) is an ODE which involves no further spatial discretization. We shall discretize it in time, considering a time step Δt indexed by $n = 1, 2, \dots N_{time}$. We have to be careful though, since this equation is coupled to the first two equations of the system, having the source terms depending on X, $\dot{X}$, and $\ddot{X}$ as well, and as such it is incorporated in the Adams scheme presented in the previous section.

Notice the presence of integrals of the fluid variables in the expression $G(\zeta, X, \dot{X})$,

$$G(\zeta, X, \dot{X}) = -\frac{c_{fric}}{\beta\sqrt{\mu}} F_{normal}(\zeta, X)\frac{\dot{X}}{|\dot{X}| + \delta} + \frac{\varepsilon}{\tilde{M}}\int_{\mathbb{R}} \zeta \partial_x \mathfrak{b}(x - X)\, dx, \tag{3.2.6}$$

which implies some restrictions for calculating the numerical integral since these variables are only known for grid and mid-points. For further details, please refer to Section 3.2.5.

Another remark concerns the order of magnitude of G. We are working with a regime where the shallowness parameter μ is supposed to be small, meaning that the first term in the expression for G is at least of order $\mathcal{O}(\beta^{-1}\mu^{-1/2})$ while the second term is small, of order $\mathcal{O}(\varepsilon)$. The fact that G is large can lead to numerical instabilities in the computation of the solid motion; as explained in Proposition 3.1.1, we have however a control on the solid velocity inherited from dissipative properties of the coupled system. We want to achieve a similar property for the discretized system, that is a similar dissipation of the discrete energy which in turn ensures that oscillations or other instabilities do not appear in the simulation.

First of all, we can write that

$$G(\zeta, X, \dot{X}) = -C(\zeta, X)\frac{\dot{X}}{|\dot{X}| + \delta} + \overline{C}(\zeta, X), \tag{3.2.7}$$

where we introduced the following two quantities

$$C(\zeta, X) = \frac{c_{fric}}{\sqrt{\mu}}\left(1 + \frac{c_{solid}}{\beta} + \frac{\varepsilon}{\tilde{M}\beta}\int_{\mathrm{supp}(\mathfrak{b})+X} \zeta\, dx\right), \tag{3.2.8a}$$

$$\overline{C}(\zeta, X) = \frac{\varepsilon}{\tilde{M}}\int_{\mathbb{R}} \zeta \partial_x \mathfrak{b}(x - X)\, dx. \tag{3.2.8b}$$

We wish to construct an appropriate numerical scheme. Let us suppose that we are at time step n, so that quantities ζ^n, $\overline{V}^n$, and X^n are known up until the index n. This implies that the constants $C^n = C(\zeta^n, X^n)$ and $\overline{C}^n = \overline{C}(\zeta^n, X^n)$ are also known (since they do not involve any time differentiation).

We base our discretization on the reformulation (3.2.7) of the equation at hand. Let us apply a second order accurate central finite difference scheme on the acceleration $\ddot{X}$ and on the velocity $\dot{X}$, furthermore let us apply a second order accurate backwards finite difference scheme for its absolute value $|\dot{X}|$. This yields

$$\frac{X^{n+1} - 2X^n + X^{n-1}}{(\Delta t)^2} = -C^n \frac{\frac{X^{n+1} - X^{n-1}}{2\Delta t}}{\left|\frac{3X^n - 4X^{n-1} + X^{n-2}}{2\Delta t}\right| + \delta} + \overline{C}^n, \tag{3.2.9}$$

so by rearranging the terms we get that

$$\left(1 + (\Delta t)^2 \frac{C^n}{|3X^n - 4X^{n-1} + X^{n-2}| + 2\Delta t\delta}\right) X^{n+1} \\ = 2X^n - \left(1 - (\Delta t)^2 \frac{C^n}{|3X^n - 4X^{n-1} + X^{n-2}| + 2\Delta t\delta}\right) X^{n-1} + (\Delta t)^2 \overline{C}^n.$$

Notice that by the definition of C, the factor of X^{n+1} is strictly positive, thus we may multiply by its inverse to obtain an explicit formula for X^{n+1}, namely

$$X^{n+1} = \overline{G}(\zeta^n, X^n, X^{n-1}, X^{n-2}), \tag{3.2.10}$$

where

$$\overline{G}(\zeta^n, X^n, X^{n-1}, X^{n-2}) = \frac{2X^n - \left(1 - (\Delta t)^2 \frac{C^n}{|3X^n - 4X^{n-1} + X^{n-2}| + 2\Delta t\delta}\right) X^{n-1} + (\Delta t)^2 \overline{C}^n}{1 + (\Delta t)^2 \frac{C^n}{|3X^n - 4X^{n-1} + X^{n-2}| + 2\Delta t\delta}}.$$

Remark 3.2.2. *Notice that we choose the same order for the central finite difference*

schemes for the first and second order derivatives. The accuracy of the backwards finite difference scheme for the absolute value of the velocity estimate was chosen accordingly, and may be adapted.

The important property of this discretization is that the friction term plays also a dissipative role at the discrete level, reproducing the property used to derive Corollary 3.1.1 in the continuous case. Note that the second term in (3.2.12) corresponds to the time discretization of $\frac{\varepsilon}{\tilde{M}} \int_0^t \int \zeta \partial_x b$; if we were to perform a discrete energy estimate for the full wave-structure system, this term would cancel as in the proof of Proposition 3.1.1 with the contribution of the source term in the equation on ζ.

Lemma 3.2.1. *Owing to equation (3.2.9), the velocity associated to the displacement*

$$\dot{X}^n := \frac{X^{n+1} - X^{n-1}}{2\Delta t} \tag{3.2.11}$$

verifies the following

$$\frac{1}{2}\left|\frac{X^{n+1} - X^n}{(\Delta t)}\right|^2 \leqslant \frac{1}{2}\left|\frac{X^1 - X^0}{(\Delta t)}\right|^2 + (\Delta t)\sum_{k=1}^{n} \overline{C}^k \dot{X}^k. \tag{3.2.12}$$

Proof: Let us multiply equation (3.2.9) by $\dot{X}^n$. Then, we obtain

$$\frac{(X^{n+1} - X^n)^2 - (X^n - X^{n-1})^2}{2(\Delta t)^3} = -C^n \frac{(\dot{X}^n)^2}{\left|\frac{3X^n - 4X^{n-1} + X^{n-2}}{2\Delta t}\right| + \delta} + \overline{C}^n \dot{X}^n.$$

Notice first of all that the first term on the right hand side is non-positive. Summing over n, we therefore get

$$\frac{(X^{n+1} - X^n)^2}{2(\Delta t)^2} \leq \frac{(X^1 - X^0)^2}{2(\Delta t)^2} + (\Delta t)\sum_{k=1}^{n} \overline{C}^k \dot{X}^k,$$

which yields the result. □

3.2.4 The wave tank and its boundaries

Notice that the weakly nonlinear Boussinesq system (3.1.2) is cast on $\mathbb{R}$ which is clearly not the case for numerical models. Hence we consider the discretized model in a wave tank of sufficiently large size (it shall be detailed for each experiment in the next section). The idea is to place the solid in the middle of the tank and numerically generate the waves (soliton or wave train) near the solid, therefore allowing us to focus on the middle section of the tank, the effects of boundary conditions imposed on the horizontal limits would be negligible. In all the cases, the width of the wave tank is taken to be at least $100L$ with

L being the wavelength of a wave, and the analysis is focused on the central $20L \sim 30L$ wide region of the domain. As for the boundary conditions, for the sake of clarity, solid walls are implemented, implying reflective boundaries for the fluid variables. This means Neumann-type boundary condition for the "scalar" parameters ζ and h (the derivative equals to 0) and Dirichlet-type boundary condition on the fluid velocity $\overline{V}$ (equals to 0).

Variables for the solid are not concerned by these limiting conditions since they are independent of the spatial variable. The only technical effect is that the simulation is to be stopped when the object touches the boundary. As evoked before, due to the size of the wave tank, this scenario does not happen in the numerical experiments considered here.

3.2.5 Further remarks

The first remark concerns a reference solution for the Boussinesq system with completely flat bottom topography. It is known that a solitary wave solution (soliton) exists for this equation (see for example [BC16]). Naturally, by introducing a solid object on the bottom of the fluid domain, this referential solution will not stay a solitary wave propagating at a constant speed, it will be transformed, deformed according to the governing equations and the change in bottom topography. Nevertheless it serves as a basic tool to analyze the effects of the object on a single wave, as it will be done during the first half of the next section.

Some words should be mentioned about the effect of the solid displacement X on the fluid equations in (3.1.6a). Due to the horizontal motion of the object, it is present in the variable b as a translation. Since there are multiple instances when derivatives of the bottom topography function are taken, the order of the operations has to be established with respect to the discretization.

In our algorithm, at each time step, the actual bottom surface shall be calculated via the translation by X^n of the initial state $\mathfrak{b}$ and then it is discretized on the grid points and the mid-points as well. If we were to discretize the initial bottom topography and then translate it, it is clear that the fitting of the translated discrete bottom to the actual grid would create additional error terms which could potentially decrease the overall accuracy.

However we shall mention that our approach works mainly because the initial bottom surface $\mathfrak{b}$ as a function defined on $\mathbb{R}$ is known, so that we can discretize any translated instance of it. It would not be possible without accurate interpolations, if the solid height was initially given only on grid points.

An important remark concerns the integral terms present in the solid equation (3.1.3). Except for the volume of the solid, these integrals involve integration over the support of the object (at its current state) of fluid variables that are initially only defined on mesh points (or mid-points). As such the applicable accurate methods are somewhat limited. In our situation we chose a third order Simpson method (resulting in a global error of

order 4) and it writes as follows

$$\int_{j\Delta x}^{k\Delta x} \zeta(x)\,dx \approx \Delta x \frac{1}{6}\left(\zeta_j + \zeta_k + 2\sum_{l=j+1}^{k-1}\zeta_l + 4\sum_{l=j}^{k-1}\zeta_{l+1/2}\right). \tag{3.2.13}$$

3.3 Numerical results

In this part we present several numerical experiments for different one dimensional wave propagation and transformation scenarios. The effects of a solid allowed to move will be compared to a fixed solid case to highlight the main features of this new approach.

As explained in Remark 3.1.2, the appropriate base water depth for our case is (at least) 10 meters (due to the difference in the order of magnitude of the coefficients). As such, comparable physical experiments are not exactly available.

For our study in general, the wave tank is taken with the following physical parameters: its width is exactly 1000 (meters), its height is $H_0 = 20$. The attributed shallowness parameter is then determined by the choice of the wavelength L, with the two main cases being $L = 40$ for $\mu = 0.25$, and $L = 20\sqrt{10}$ for $\mu = 0.1$. This implies that the wave-tank is 25 wavelengths long in the former case and approximately 16 wavelengths long in the latter case. The principal observational area is in the vertical section $[400, 600]$ of the wave tank.

The solid will be considered to be given by a truncated Gaussian function, the discrete truncation determined by an error term $\epsilon = 10^{-4}$, that is

$$\mathfrak{b}(x) = b_0(x)\mathbf{1}(b_0 > \epsilon), \qquad \text{where } b_0(x) = a_{bott}\exp\left(-10\left(\frac{x}{L}\right)^2\right).$$

As for its physical parameters, the default choice for the mass parameter is chosen to be $\tilde{M} = \frac{2}{3}$, corresponding to an approximate solid density of $\varrho_S = 2\frac{g}{cm^3}$. The vertical size as well as the coefficient of the friction will be varied during most of the simulations.

3.3.1 Order of the numerical scheme

The first set of tests concerns the verification of the convergence of the scheme. In [LM07] the overall algorithm for the fluid equations was second order accurate both in time and in space. Since we made some adaptations on the original scheme, it is reasonable to verify how this has affected the order of the convergence. In the case of a flat bottom, we improve substantially the accuracy compared to [LM07] since we observe a convergence of order 3.5 in space and 3.8 in time. Moreover, these orders are conserved for a non-flat topography. When the solid is allowed to move, the order of convergence becomes 3 in space and 2 in time (which is not surprising since a proposed a second order discretization

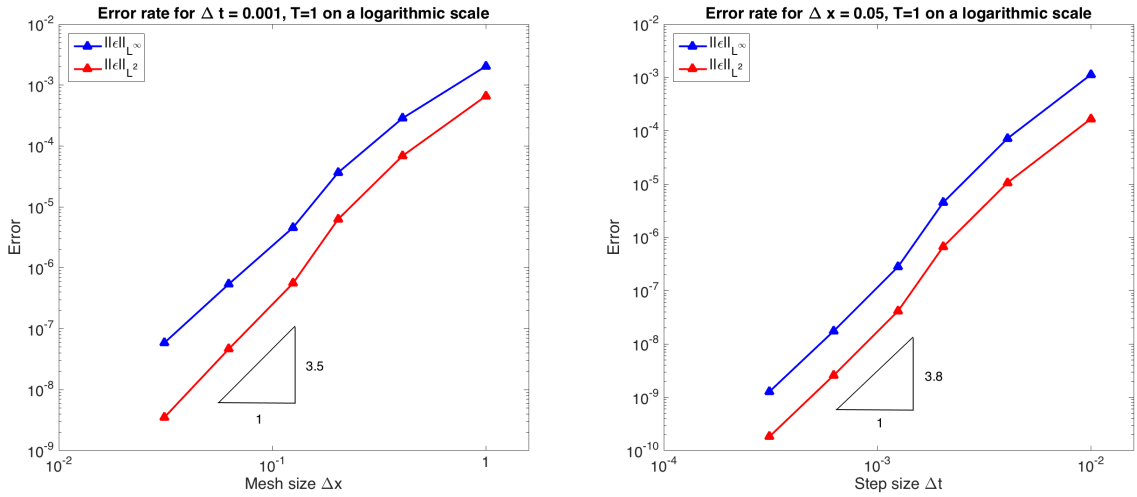

(a) $\mu = \varepsilon = 0.1$ solitary wave evolution, spatial error

(b) $\mu = \varepsilon = 0.1$ solitary wave evolution, temporal error

Figure 3.2 – Discretization error for solitary wave evolution over flat bottom

of the ODE for the solid motion).

3.3.1.1 Convergence of the scheme over a flat bottom topography

First of all, we consider the wave tank without the presence of the solid and its effects. This means that we are considering the simplified algorithm for a flat bottom case. The convergence is then checked numerically by the exact traveling wave solution for (3.1.2) with $b \equiv 0$. The existence of a solitary wave solution is a well known fact, for explicit computations, please refer to [Che98], for a more general approach, one may see [BC16] for example. By searching the solution for (3.1.2) as a solitary traveling wave with constant speed $c > 1$ ($\zeta = \zeta_c = \zeta_c(x - ct)$, $\overline{V} = \overline{V}_c = \overline{V}_c(x - ct)$) it is easy to check that the velocity profile has to satisfy

$$-(\overline{V}_c)'' = -\frac{3}{\mu c}\overline{V}_c\left(c - \frac{1}{c - \varepsilon\overline{V}_c} - \frac{\varepsilon}{2}\overline{V}_c\right), \tag{3.3.1}$$

with $\overline{V}_c < c/\varepsilon$. From the velocity profile, the surface elevation then can be recovered simply by

$$\zeta_c = \frac{\overline{V}_c}{c - \varepsilon\overline{V}_c}. \tag{3.3.2}$$

With this at our disposal, the solitary wave solution serving as a reference can be reconstructed by a fourth order Runge-Kutta method (in order to avoid any influence on the accuracy of the overall scheme).

As elaborated in Section 3.4 of [LM07], a von Neumann stability analysis can be carried out for the linearized system. Since no changes have been made in the time discretization of the fluid equations (system (3.1.2)), their analysis can be adapted in a straightforward way to our case too, leading to a CFL condition of the form:

$$\sqrt{gH_0}\frac{\Delta t}{\Delta x} \leqslant 0.5. \tag{3.3.3}$$

In order to respect this stability condition, in what follows we set $\Delta x = 0.05$ and $\Delta t = 0.001$.

Two basic verification tests have been designed, each one testing for the wave-tank and wave parameters $\mu = \varepsilon = 0.1$. The simulation is run for a time $T = 1$.

The first test measures the error of the spatial discretization, compared to the solitary wave solution, by fixing the time step Δt sufficiently small ($\Delta t = 0.001$) and varying the spatial discretization's step size, giving us $\Delta x = 2^{-k}$ for $k \in \{0, 1, 2, 3, 4, 5\}$. We measure the L^2 and L^∞ norms of the error for the surface elevation ζ. Figure 3.2a shows the results, on a logarithmic scale. The scheme is behaving as an algorithm of order 3.5 in the spatial discretization.

The second test measures the total error, compared to the solitary wave solution, by fixing the CFL-ratio at 0.05, varying the time discretization's step size, giving us $\Delta t = 0.01 \cdot 2^{-k}$ for $k \in \{0, 1, 2, 3, 4, 5\}$, and Δx respectively. Once again we measure the L^2 and L^∞ norms of the error for the surface elevation ζ. Figure 3.2b shows the results, on a logarithmic scale. The scheme is behaving as an algorithm of order 3.8 for the time discretization, an almost order 4 convergence which would be the ideal scenario for the applied Adams predictor-corrector method.

Therefore we have established a major improvement over [LM07], by an accurate interpolation, and more coherent accuracy in the finite difference schemes, one can indeed obtain an almost fourth order convergence.

3.3.1.2 Convergence of the scheme for a non-flat bottom topography

Lacking an explicit solution for the non-flat bottom case, we performed a relative error analysis to test the global convergence of the full coupled system as well, meaning that as a reference solution we calculated the surface elevation for $\Delta x = 0.01$, $\Delta t = 10^{-4}$ and we compared it to the calculated surface elevations for less refined mesh sizes and time steps. Two physically different testing parameters were chosen, the first one corresponding to an immobile solid at the bottom, the second one representing the case of the fully coupled problem where solid motion is observed. For the first case, the physical parameters of the system were chosen to be $\mu = \varepsilon = 0.1$, $\beta = 0.3$, with a frictional coefficient of $c_{fric} = 0.01$. The simulation is run for a time $T = 5$.

Figure 3.3 shows the relative error of the surface elevation compared to our choice

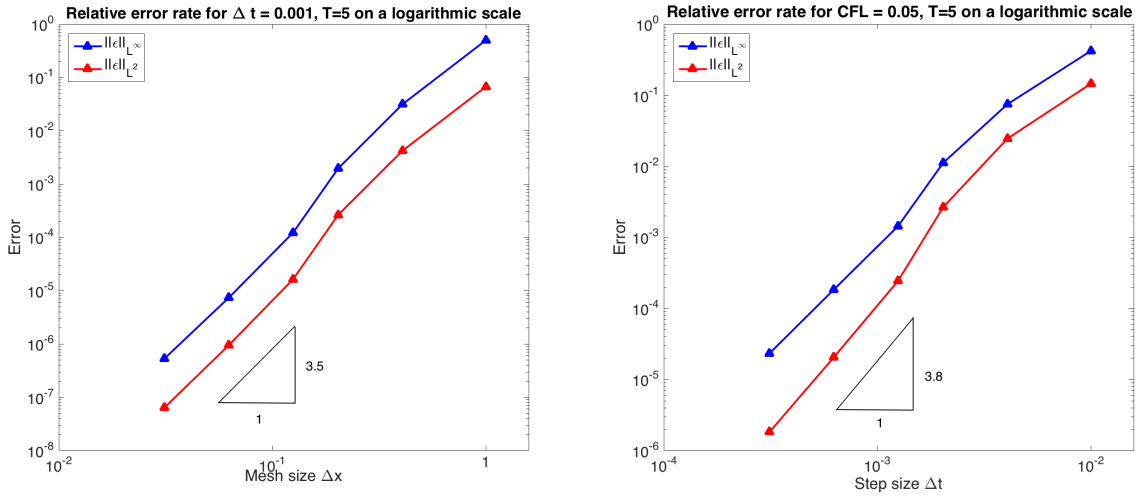

(a) $\mu = \varepsilon = 0.1$ solitary wave evolution, spatial error

(b) $\mu = \varepsilon = 0.1$ solitary wave evolution, temporal error, fixed CFL-ratio

Figure 3.3 – Discretization error for solitary wave evolution over non-flat bottom ($\beta = 0.3$, $c_{fric} = 0.01$)

of reference solution (in L^2 and L^∞ norms), carried out for either a fixed time step ($\Delta t = 0.001$), or a fixed CFL-ratio (0.05) dividing by 2 the other step parameter for each consecutive measurement. One can observe that the overall spatial discretization stays of order 3.5, and the temporal error stays in the previously observed order of 3.8 too.

For the second case, the physical parameters of the system were chosen to be $\mu = \varepsilon = 0.2$, $\beta = 0.4$, with a frictional coefficient of $c_{fric} = 0.001$. The simulation is run until a time $T = 5$ allowing for sufficiently long interaction between the solid and the incoming wave.

Figure 3.4 shows the relative errors (in L^2 and L^∞ norms) for the surface elevation, carried out once again for either a fixed time step ($\Delta t = 0.001$), or for a fixed CFL-ratio (0.05). One can observe that the overall spatial discretization has stayed at an order 3.5, attributed to the loss in accuracy represented by the observable solid motion. Notice also that we have a temporal convergence rate of 2, attributed to the fact that the time discretization scheme for the solid was chosen to be only of order 2.

3.3.2 Transformation of a wave passing over a fixed and a moving obstacle

In this part we present the two main characteristic situations that have been observed during the ensemble of the simulations, each with a passing wave and a breaking wave case. Two representative examples were chosen, showing step by step the “transformation”

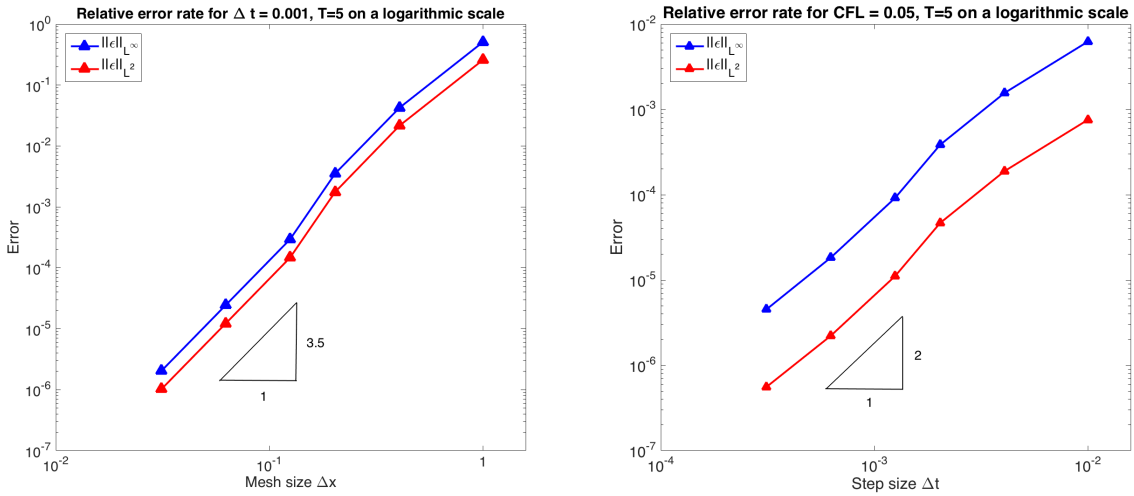

(a) Relative spatial error for $\Delta t = 0.001$ (b) Relative error for fixed CFL-ratio

Figure 3.4 – L^2 and L^∞ error for a wave evolution over time $T = 5$ ($\mu = \varepsilon = 0.2$, $\beta = 0.4$, $c_{fric} = 0.001$)

of a single passing wave over the solid, first for a highly frictional case, then for the almost perfect sliding case. As initial conditions, the approaching wave is taken to be the solitary wave solution for the flat bottom case.

3.3.2.1 The regime of a large coefficient of friction

The first example presents a wave passing over the solid (here essentially fixed because of the large friction coefficient), getting slightly perturbed by the bottom topography irregularity (the presence of the solid) and continuing its trajectory with a modified amplitude and an altered form. With a shallowness parameter of $\mu = 0.1$, the initial wave amplitude is taken as 4 (meaning $\varepsilon = 0.2$). The solid has a maximal vertical size of 6 and is subjected to a frictional sliding on the bottom, with a coefficient of $c_{fric} = 0.5$.

In Figure 3.5 this passing wave is plotted (red) at different time steps. As a reference, the flat bottom solitary wave is also visualized (green), propagating at a constant speed, and allowing for a better qualitative comparison for the changes the approaching wave undergoes. The solid is centered around the horizontal coordinate $x = 500$ with a numerical support spanning through the interval $[480, 520]$, for a better visibility, it has been omitted from the figure.

In the first figures the wave approaches the solid, and thus wave shoaling is observed (its amplitude increases) until its peak at around time step 4200, after which the wave crest passes over the peak of the solid and drops (step 5400), due to the drop in the bottom topography. After this drop the initial wave, now slightly asymmetric, continues onward, with an amplitude (slightly) less than its initial value.

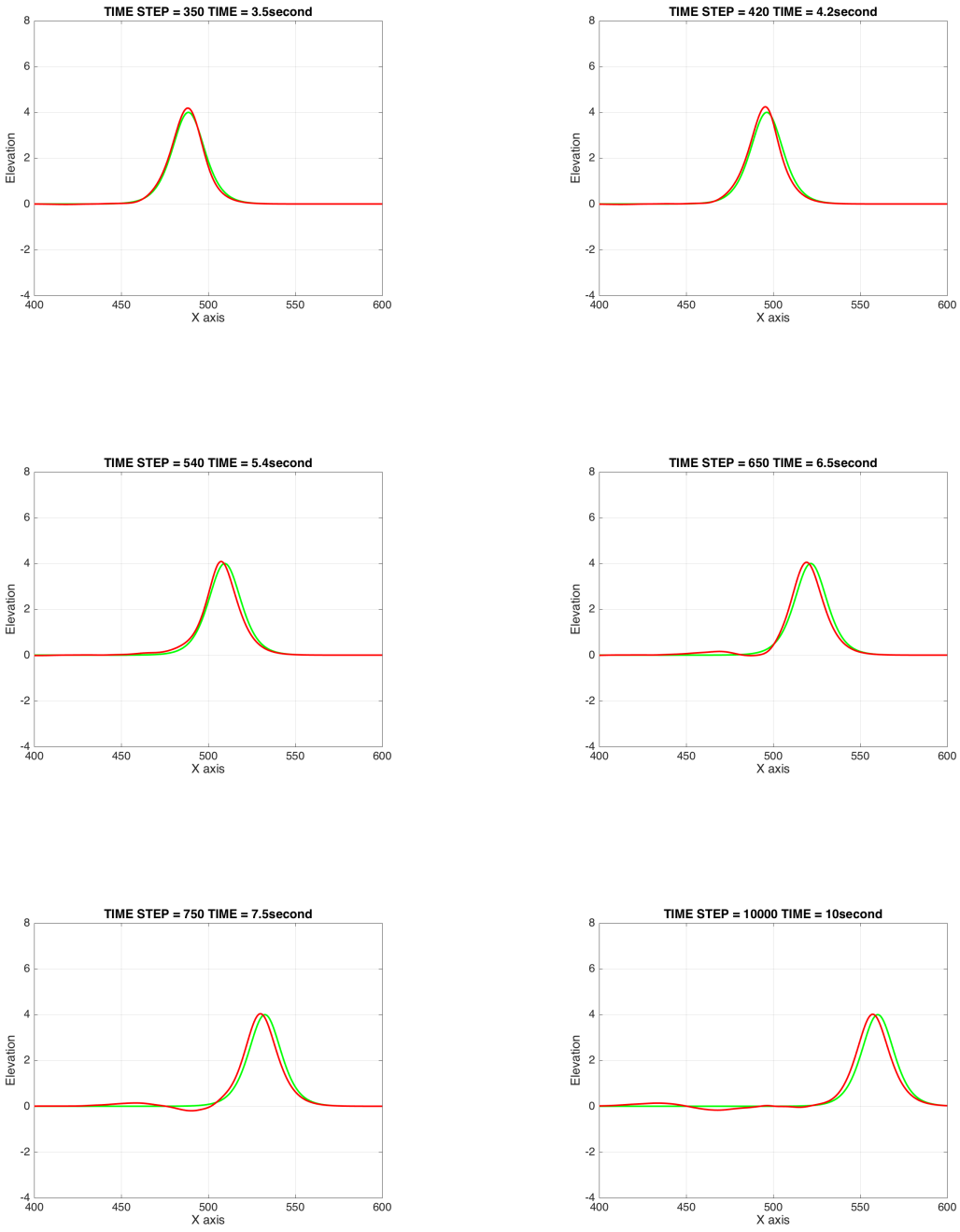

Figure 3.5 – Evolution of a passing wave ($\mu = 0.1$, $\varepsilon = 0.2$) over a small obstacle ($\beta = 0.3$, $c_{fric} = 0.5$); red curve is the passing wave, green curve is the reference soliton for flat bottom

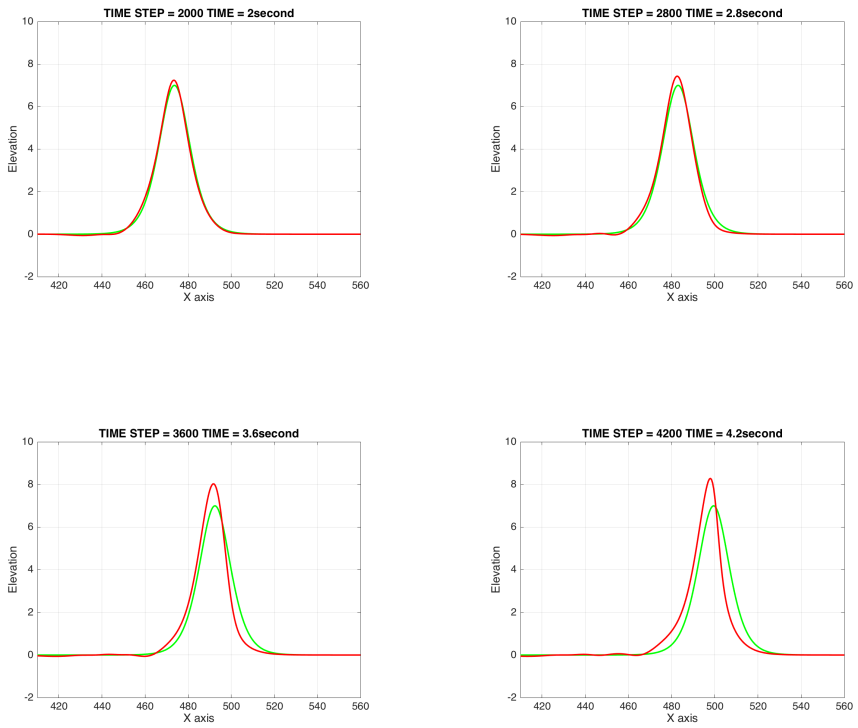

Figure 3.6 – Evolution of an approaching large wave ($\mu = 0.25$, $\varepsilon = 0.35$ and breaking when reaching the obstacle ($\beta = 0.5$, $c_{fric} = 0.5$); red curve is the approaching wave, green curve is the reference soliton for flat bottom

Moreover the wave became out of phase due to the "bump" in its motion. One can also observe a backwards going small amplitude long wavelength wave created by the drop after passing over the solid (starting from the back trough at around step 6500). It is important to remark that due to the high frictional term, essentially no solid displacement was observed.

The set of images in Figure 3.6 depict the wave breaking encountered during the simulations for regimes with a large coefficient of friction. In this case a numerical condition was detected in the experiments that signals a possible wave-breaking due to a steepening wave slope (for more details, see Section 3.3.4).

A plunging (or spilling) type wave-breaking is most commonly indicated by a critical increase in steepness in the middle section of the front wave slope, and was observed for relatively large wave amplitudes with a large object at the bottom. For a representative test case, a wave of wavelength 40 is chosen over a base water depth of 20, with initial amplitude 7. The solid has a maximal height of 10 and is sliding on the bottom with a dynamical friction coefficient of $c_{fric} = 0.5$. As represented in Figure 3.6, the wave ap-

proaching the solid increases in amplitude, just like before, however this increase becomes critical as the wave crest approaches the solid peak. The flat bottom solitary wave is represented only as a reference.

3.3.2.2 The regime of a small coefficient of friction

We show here a second set of examples, with a much smaller friction coefficient so that a solid displacement is observed. Such a displacement occurs regardless of the vertical dimension of the solid and appears to be more relevant in intermediate to high wave amplitude regimes. As a test case, we chose $c_{fric} = 0.001$ for a solid height of 8. The wave amplitude is chosen to be 4 with a shallowness parameter of the system $\mu = 0.1$.

As it can be seen from Figure 3.7 the incoming wave gains amplitude as it starts to pass over the solid. At this moment, the friction term characterizing the solid motion becomes less important than the pressure force created by the wave and, as a result, the solid slides for a long distance.

In the meantime the solid starts propagating with increased velocity, thus further amplifying its amplitude (time step 5400). When the wave peak finally passes over the top of the solid, it drops due to the downwards slope in the bottom topography (time step 6000, generating secondary waves traveling backwards (time step 6400). Notice that the passing wave has a significant loss in amplitude (almost 10%) and an attenuated shape (time step 9000).

An interesting feature is the incidence of the fact that the solid can move on the type of wave breaking we observe. We consider here an almost frictionless ($c_{fric} \ll 0.01$) sliding case for large solid objects and intermediate to large wave amplitudes (see Figure 3.8). The approaching wave gains in amplitude due to the slope presented by the object, further amplified by the fact that the solid starts propagating as well. In these critical cases however, the solid velocity becomes comparable to the velocity of the wave, thus maintaining the critical position of the wave (time step $4000 - 4500$, the wave peak propagates with the solid peak). A solid displacement of 5 to 20 meters can be detected. The critical increase in steepness is detected closer to the front trough, implying a characteristically different wave breaking (surging waves).

3.3.3 Amplitude of the transmitted wave for a fixed and moving obstacle

The following simulations measure the effect of a bottom topography deformation (a solid object) on a single passing wave, most notably the variation of the amplitude. We will compare the amplitude of a single wave approaching the solid with the amplitude of the transmitted leading wave. The main interest is to observe the difference between the cases when the solid is allowed to move and the case where the solid is fixed to the

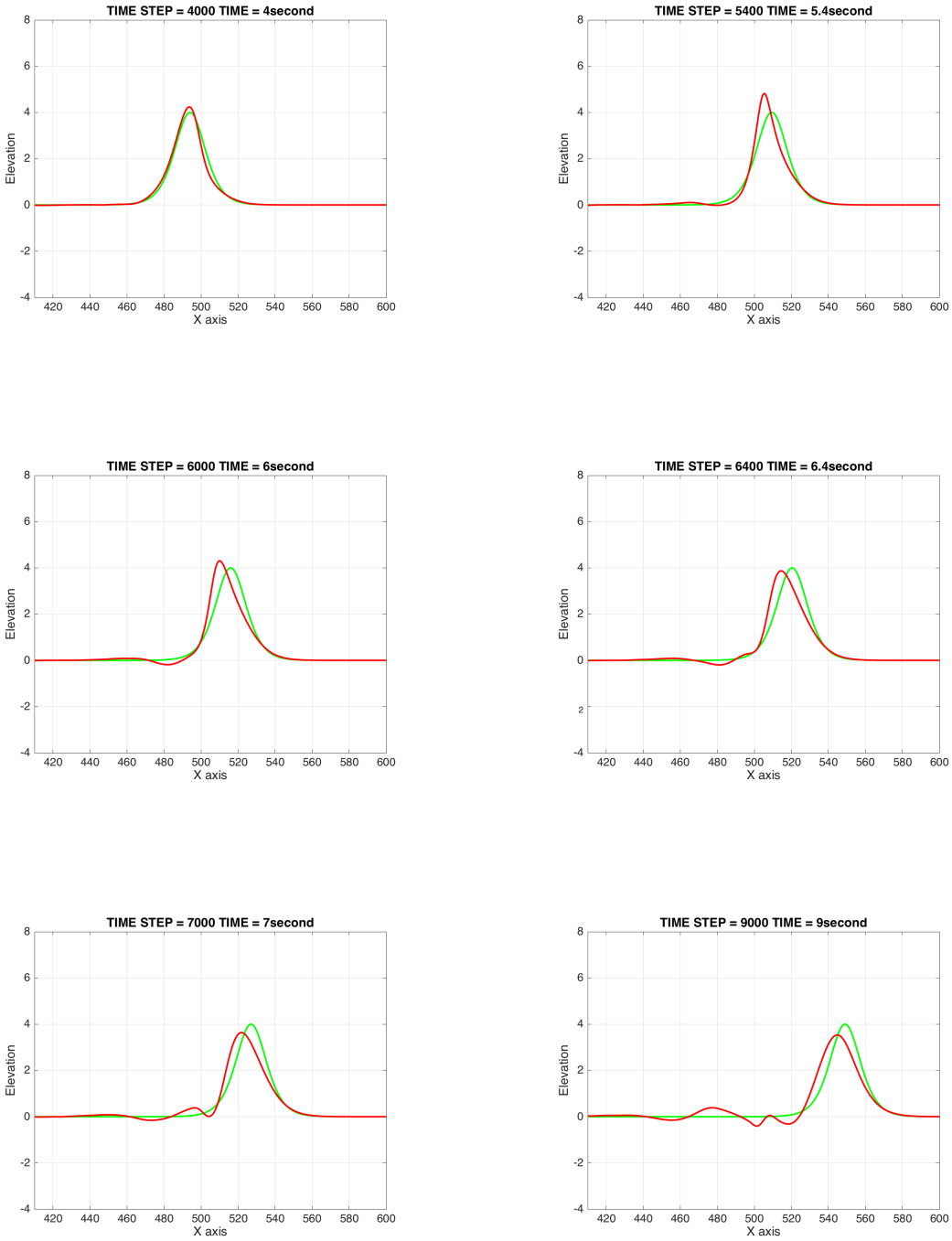

Figure 3.7 – Evolution of a passing wave ($\mu = 0.1$, $\varepsilon = 0.2$) over a larger sliding obstacle ($\beta = 0.4$, $c_{fric} = 0.001$); red curve is the passing wave, green curve is the reference soliton for flat bottom

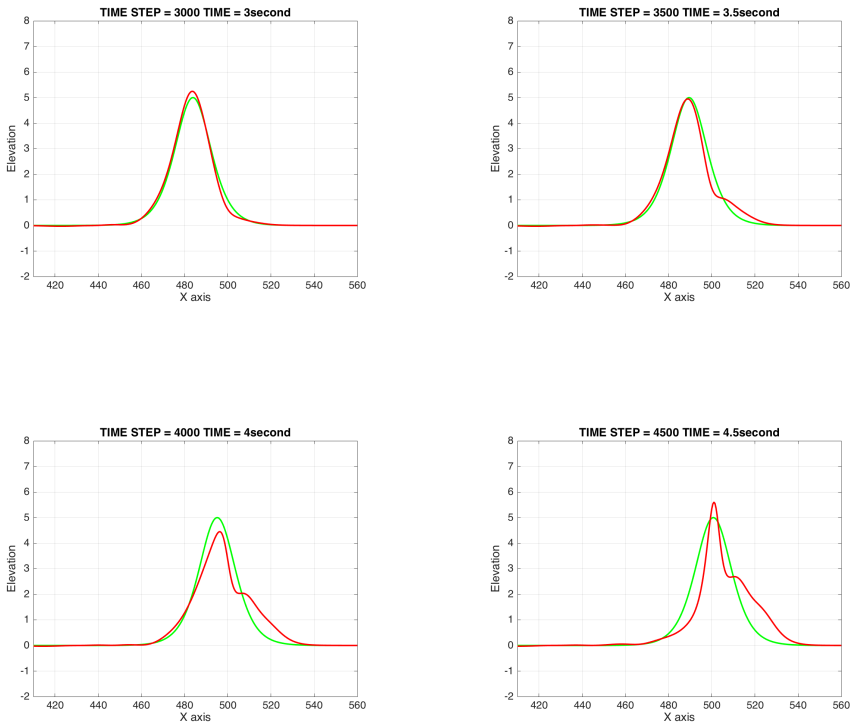

Figure 3.8 – Evolution of an approaching wave ($\mu = 0.25$, $\varepsilon = 0.25$) over an almost perfectly sliding large solid ($\beta = 0.5$, $c_{fric} = 0.001$); red curve is the approaching wave, green curve is the reference soliton for flat bottom

bottom.

A solitary wave for the flat bottom case is taken as an initial condition, situated two wavelengths from the solid object, traveling towards it. Throughout the simulations a characteristic base wavelength of $L = 40$ is taken for a uniform shallowness parameter of $\mu = 0.25$.

We consider 3 different (vertical) sizes for the solid, a small object corresponding to $\beta = 0.1$, a medium sized object with $\beta = 0.3$ and a relatively large object for $\beta = 0.5$. For each of these three cases we examine the qualitative effects of the solid. We are testing three different frictional domains as well, an almost frictionless, perfect sliding, with $c_{fric} = 0.001$, a relatively smooth sliding for $c_{fric} = 0.01$, and a hard frictional sliding for $c_{fric} = 0.5$. The results will be compared to the two reference cases: one being the simulation running for the same time for a flat bottom, giving a 1 to 1 ratio between the entering and the leaving wave amplitude, the other one being the case when the same initial object is fixed to the ground, not being allowed to move throughout the simulation, meaning that $b(t, x) = \mathfrak{b}(x)$ is independent of the time.

For a small object ($\beta = 0.1$, see Figure 3.9a) we observe that the 1 to 1 ratio for amplitude variation for a flat bottom is essentially preserved for both the fixed bottom and the cases of a solid with frictional motion with relatively large frictional coefficient. Only an almost negligible (10^{-3}) drop in amplitude is detected in all these situations.

The decrease in amplitude is measurable however in the $c_{fric} = 0.001$ regime for wave amplitudes above 4. This relative drop in amplitude increases with the height of the incoming wave.

For the $\beta = 0.3$ intermediate vertical solid scale, the simulation results are summarized in Figure 3.9b. One can notice similar effects as the ones concluded in the previous case for a small sized solid. Except for the almost perfect sliding, the other cases respect the 1: 1 ratio of wave amplitudes.

The impact of the solid is more visible in the almost perfect sliding case, since the considerable drop in amplitude is observed for smaller waves as well. The drop in amplitude amounts for up to 12% amplitude loss for the higher waves. Here we note that for intermediate sized waves, the initial wave is completely absorbed by the new wave produced by the solid motion, which is a longer and much flatter wave (thus the remarkable drop in amplitude). For small wave amplitudes, this is not observed, since the generated pressure force on the bottom is not large enough to create significant solid motion.

Finally, the results for the $\beta = 0.5$ case (Figure 3.10) indicate an even more complicated behavior. Amplitude decrease is observed for all the non flat bottom cases, with the drop of the amplitude being more and more important the freer the object can move (the less friction is imposed). The heavily frictional case ($c_{fric} = 0.5$) still matches quite well the fixed bottom scenario but the other two test cases show a more important decrease in wave amplitude.

Another feature, made clearer in the zoomed image (Figure 3.10b) is a slight layering

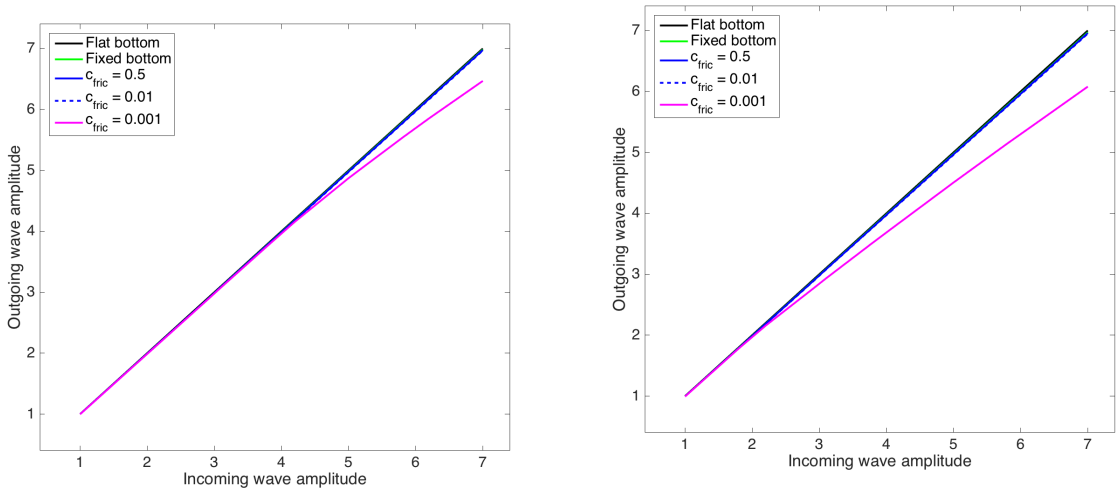

(a) Change in wave amplitude over a small solid

(b) Change in wave amplitude over a medium sized solid

Figure 3.9 – Wave amplitude variation for small ($\beta = 0.1$) to medium ($\beta = 0.3$) sized solid ($\mu = 0.25$)

between the cases in the presence of a solid, with the fixed bottom case being the closest to preserving the amplitude, closely followed by the hard frictional case, signifying that these two regimes are physically close to each other. Notice that the less important the friction is in the system, the more the amplitude is dropping, especially for middle to high wave amplitudes.

The main difference however is the newfound presence of wave breaking, meaning the simulation was stopped because the numerical condition for the initial wave breaking phase was observed (for more details, please refer to the next section). Not only can we observe wave breaking for all non flat bottom cases, but also there is a slight difference between the fixed and the moving bottom cases too (further examined in the next section).

For the nearly negligible friction ($c_{fric} = 0.001$) surging waves are observed, highlighting the fact that for a larger solid in almost perfect sliding, solid motion can also lead to critical wave transformation. The phenomenon was already described in the last part of the previous section.

To sum it up, we observed that allowing bottom motion, especially for an almost frictionless sliding, accounts for a measurable decrease in wave amplitude. This is due to the fact that part of the energy of the wave is transferred to the solid as a kinetic energy, propelling its motion on the bottom.

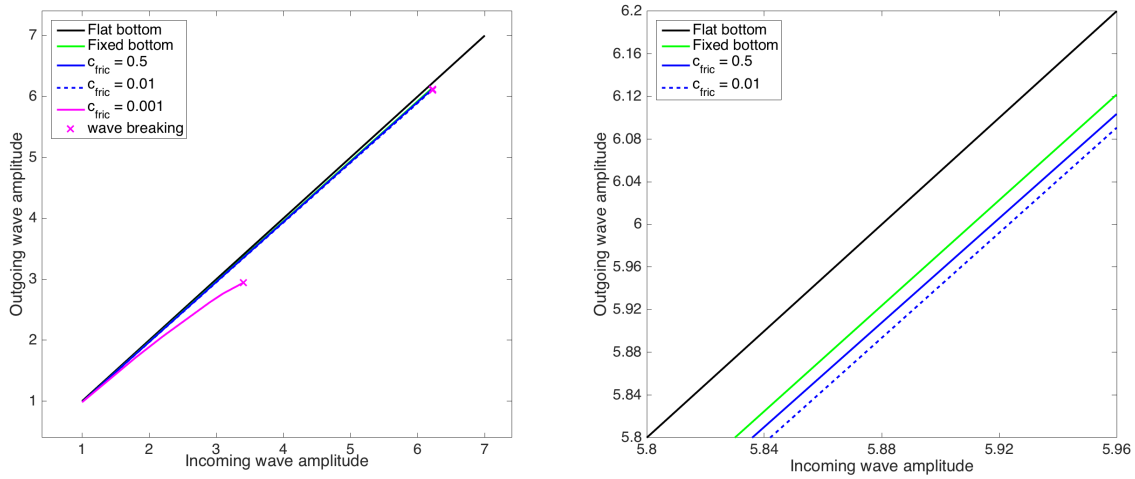

(a) Change in wave amplitude for a passing solitary wave

(b) Zoom to the subcritical section of the amplitudes

Figure 3.10 – Wave amplitude variation for a large ($\beta = 0.5$) solid ($\mu = 0.25$)

3.3.4 An effect of bottom displacement on the wave breaking

In this section we summarize the numerical test cases related to the simulations in which a numerical pre-condition for wave-breaking was observed. It manifested in the fact that the wave became too steep, indicating that physically the wave entered in a wave surging phase, closely followed by the breaking or plunging of the wave.

A sufficient, but rather lenient numerical condition for wave breaking in our case (based on [Sou88]) is the following

$$\max_i \frac{\zeta_{i+1} - \zeta_i}{\Delta x} > 1. \tag{3.3.4}$$

For a more detailed analysis on wave breaking conditions for Boussinesq type models, we refer to [BCL+12] and [KR17].

With a series of experiments we now examine the position of the wave breaking point according to this criteria for different parameter choices. We chose a maximal solid height of $H_0/2$ giving us a topography parameter of $\beta = 0.5$. For this case wave breaking could be observed for large wave amplitudes. We implement two different frictional situations ($c_{fric} = 0.001$, and $c_{fric} = 0.5$), as well as the reference case for a fixed bottom.

A single traveling wave of wavelength $L = 40$ is sent $2L$ distance away from the solid and with a wave amplitude as the principal parameter for the simulations. As a reference, the position of the wave at the moment of the numerical wave breaking point is given by the position of the wave crest. The simulations have also been carried out for the case of a fixed bottom, having the topography of the initial solid state.

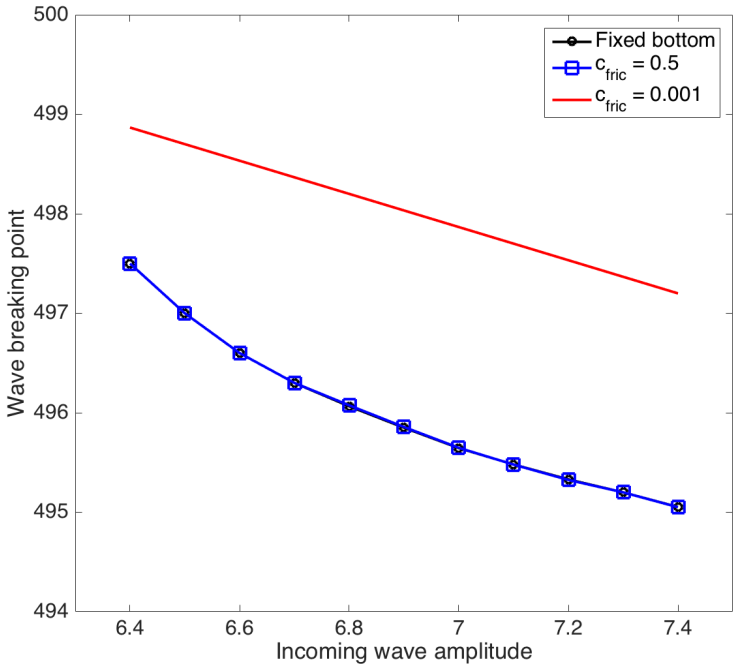

Figure 3.11 – Wave breaking point for large amplitude incoming waves ($\mu = 0.25$, $\beta = 0.5$)

The main interest of this numerical experiment is to see the effect of a solid that is allowed to move on the wave breaking point. As it can be seen from the results (Figure 3.11) the $c_{fric} = 0.5$ frictional case and the fixed bottom barely differ. Actually the same was observed for other c_{fric} values as well (in the range of 0.01 to 1).

In the case when the object is sliding almost frictionlessly ($c_{fric} = 0.001$) however, the position of the wave crest is much further away from the initial position. The qualitative difference is due to the change of the nature of the wave breaking (as it was remarked in Section 3.3.2). Nevertheless a measurable delay is observed for the wave breaking point, owing to the fact that the initial wave loses some of its energy while the new, frontal wave is created by the solid.

3.3.5 Observations on the hydrodynamical damping

The previous simulations gave us some insight on the effects of a moving solid on the wave motion. Now we reverse our point of view, so to speak, in order to examine the inverse, that is how the waves affect the solid motion.

Our numerical simulations show that if c_{fric} is of order $10^{-4} \sim 10^{-5}$, the solid takes and extended amount of time before finally coming to a halt (Figure 3.12), creating small amplitude, large wavelength waves in front of and behind it. By creating such waves, its

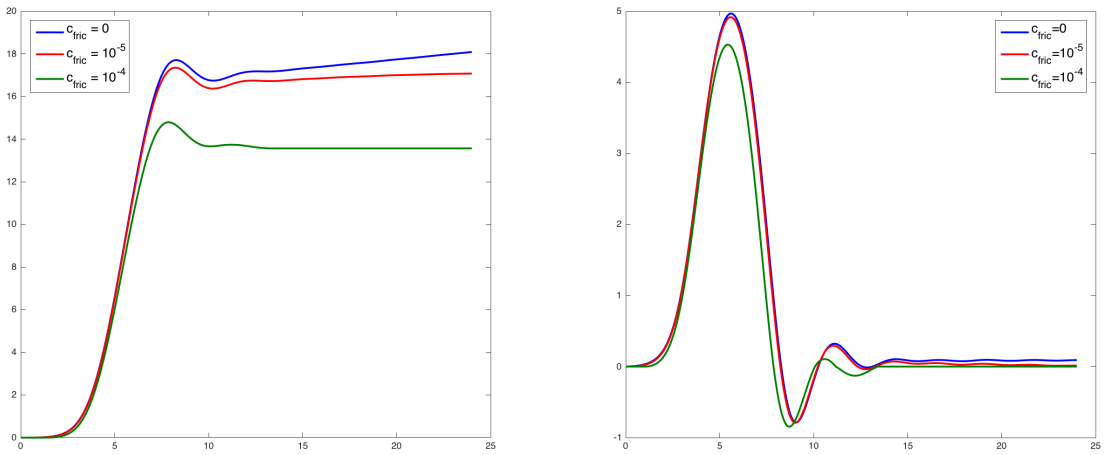

(a) Solid position

(b) Solid velocity

Figure 3.12 – Solid motion for low coefficients of friction ($\mu = \varepsilon = 0.2$, $\beta = 0.4$)

motion is damped by a phenomenon similar to the dead-water phenomenon, described in detail for Boussinesq type models for example in [Duc12].

In the limiting situation of $c_{fric} = 0$ it continues its motion without stopping. Notice the rapidly stabilized oscillatory behavior in the velocity profile of the solid (Figure 3.12b), further highlighting the small amplitude wave-generation around the peak of the solid.

The hydrodynamic effects are shown not only by the change in direction for the solid motion as well as the increased changes in velocity. In Figure 3.13 we compared two situations: as a reference the standard model was left running for the whole time ($T = 24$), for the second simulation the pressure term was removed at the moment when the velocity hit its maximal value, taking into consideration only the frictional damping of the system.

As it can be clearly seen, without the hydrodynamic effects the solid velocity decreases essentially linearly, as it is dictated by the corresponding equation of motion, the solid slowly comes to a halt. The hydrodynamic damping not only increases the deceleration process but it also keeps the solid relatively close to its initial position.

3.3.6 Measurements of the solid displacement

Three additional sets of simulations were conducted in order to measure the effects of friction on the system, as well as to highlight long term effects by means of simulating an approaching wave train.

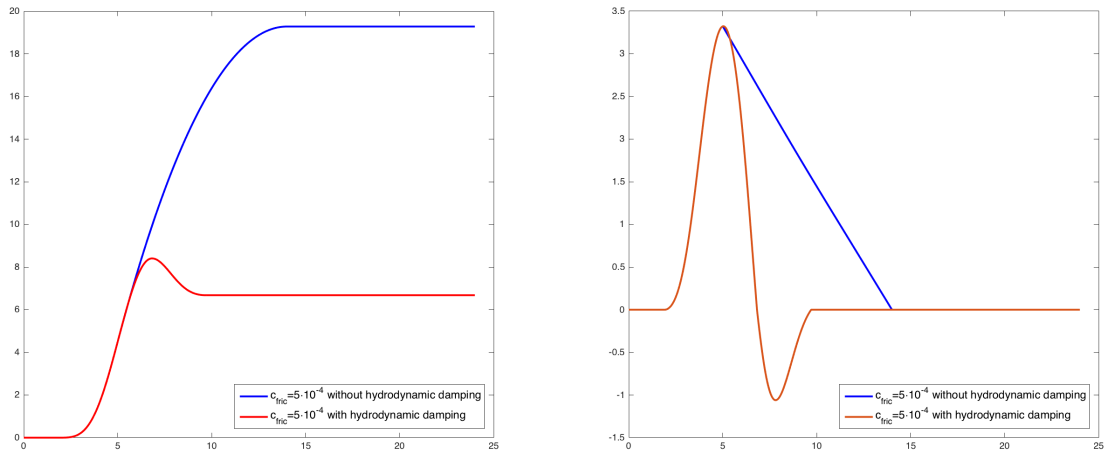

(a) Solid position

(b) Solid velocity

Figure 3.13 – Solid motion with and without hydrodynamic damping ($\mu = \varepsilon = 0.2$, $\beta = 0.4$, $c_{fric} = 0.0005$)

3.3.6.1 Solid displacement for varying coefficients of friction

For the physical parameters $\beta = 0.3$ and $\varepsilon = 0.25$, while the friction coefficient is varied from 0.001 to 0.003. Figure 3.14 shows the change in the solid motion for this case.

We remark a significant drop in the maximal solid displacement, attributed to the qualitative change of the system from a frictional to a frictionless sliding. The critical values for c_{fric} for this transformation depend on the shape of the object as well as its physical parameters.

Furthermore we remark that the solid does in fact stop in its motion, a property due to not only the damping effect of the frictional forces but to the hydrodynamic damping as well. The latter one is clearly visible by the fact that the solid motion changes direction after the wave peak passes over it and rapidly looses velocity by the time the wave leaves the interaction zone.

3.3.6.2 Solid displacement for varying wave amplitudes

The second one consists of measuring the effect of a single traveling wave on the solid motion, for a relatively frictionless sliding ($c_{fric} = 0.001$). The maximal vertical size of the solid is 6, with waves having an amplitude in the range $[3, 5]$. It also serves as a reference case for the wave train simulations presented later on.

On Figure 3.15 we can see the almost perfect "oscillation circle" for the solid position, meaning that after the approaching wave pushes the solid forward, it passes over the

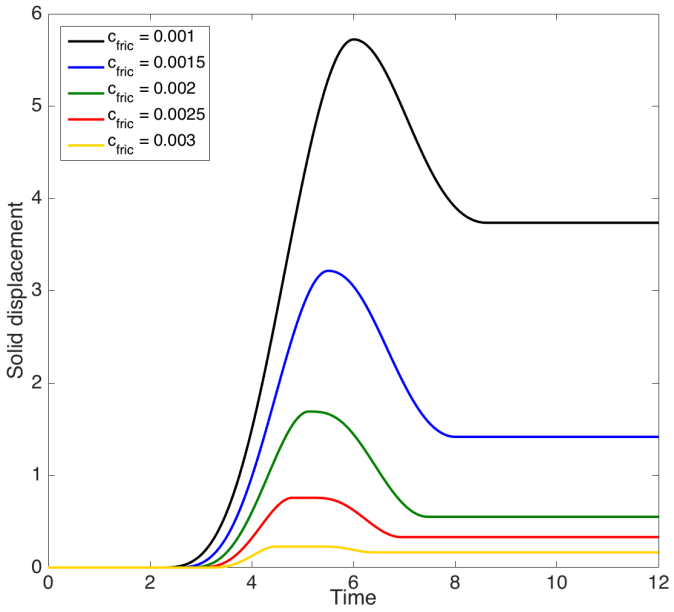

Figure 3.14 – Solid displacement for a varying coefficients of friction ($\mu = \varepsilon = 0.25$, $\beta = 0.3$)

object, and then it pushes the solid backwards, making it return nearly to its initial state. Notice the slight asymmetry of the curves as well as the rather extended calming phase, attributed mainly to the slowing effects of frictional forces.

The final set of numerical experiments concerns the long term effects of wave motion on a solid that is allowed to move freely, subjected to a frictional sliding on the bottom of the wave tank. This was carried out by simulations on a long time scale, it involves sending a wave train consisting of 10 consecutive solitary waves in the direction of the solid and measuring the evolution of the solid displacement.

The wave tank is now taken to be twice as large as before, with a length of 2000 to properly accommodate the wave train. A medium sized solid is chosen ($\beta = 0.3$) for intermediate wave amplitudes (ε ranging from 0.15 to 0.25) with a wavelength of $L = 40$. The simulation is run for a time of $T = 54$, allowing for 7 waves to pass over the solid.

The evolution of the position of the center of the mass is plotted in Figure 3.16, corresponding to an almost perfect sliding ($c_{fric} = 0.001$). We observe solid displacement of order 1 for each passing wave, as well as some qualitative differences in the wave cycles.

There is a positive net solid displacement per incoming wave, resulting in the solid getting further and further away from the initial position after each passing wave in the train. We remark that the displacement per passing wave is not constant, attributing to an overall nonlinear increase in distance. This is due to the fact that a passing wave is perturbed by the solid, resulting in backwards traveling small amplitude long waves (as

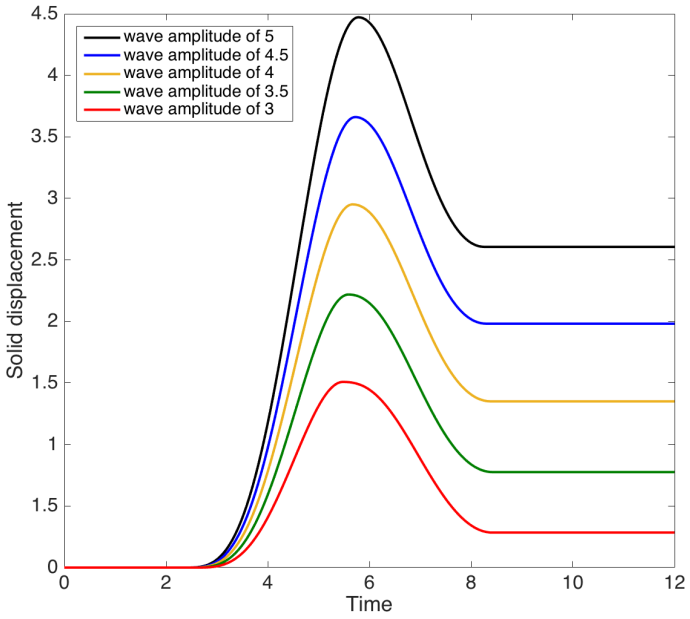

Figure 3.15 – Evolution of the solid position due to a single solitary wave, with frictional sliding ($\mu = 0.25$, $\beta = 0.3$, $c_{fric} = 0.001$)

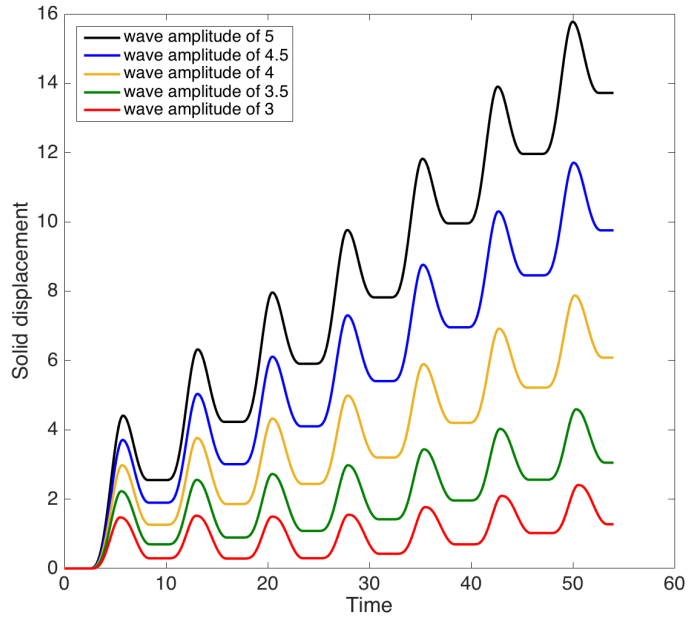

Figure 3.16 – Evolution of the solid position due to a wave train, with almost perfect sliding ($\mu = 0.25$, $\beta = 0.3$, $c_{fric} = 0.001$)

pointed out in Section 3.3.2), meaning that later members of the wave train get perturbed even before reaching the interaction zone. This results in a non-constant incoming wave amplitude even though initially it was constant.

Also, comparing the effects of a single wave (Figure 3.15) with a wave train (Figure 3.16), we can notice that, even though the elements of the wave train were launched sufficiently apart to avoid undesired interactions with each other, due to the extended period of time it takes for the frictional and hydrodynamic damping to slow down the solid motion, nonlinear effects are observable in the solid displacement.

3.4 Conclusion

In the present paper, we propose a modeling of the interactions of waves with an object lying on the bottom and allowed to move. To this end, we use the models developed in ([Ben17]), propose a new numerical code to simulate these wave-structure interactions (and which significantly extend and improve existing codes for fixed, flat, topographies). We then use this code to exhibit new interesting features of this kind of wave structure interaction, and in particular we show that the displacement of the solid object has an incidence on the size of the transmitted wave and on wave breaking (more precisely on its location and on its type). This is of particularly interest for applications to the protection of coastal areas from wave damages. We also exhibit interesting features of the solid motion, such as nonlinear effects and hydrodynamical damping; these aspects are interesting for applications to wave energies. This is to our knowledge the first time that these phenomena are exhibited as they require to take into action the wave-structure coupling in both ways (influence of the waves on the solid motion and vice versa); we believe that they suggest several interesting developments, both from the PDE and numerical viewpoints.

Conclusion

This thesis was dedicated to a series of studies of two particular problems emerging from the domain of fluid-structure interaction. The main emphasis was on an asymptotic analysis concerning these problems, in order to ascertain qualitative and quantitative properties of the associated coupled systems, as well as to further existing works in which, in a certain sense, less degree of freedom was supposed.

1 Contributions of the thesis

The basic configuration of the two main problems involved the presence of an incompressible, irrotational, perfect fluid in a certain domain with the addition of a rigid, solid body in the system. The asymptotic analysis intervened through physical parameters, supposed to be small, that describe not only the size or the inertia of the object but, in certain cases, they incorporate information on the fluid domain as well.

The first, and often the most difficult, task was the establishment of the well-posedness of the arising system of equations, a delicate problem due to the fact that it involves the treatment of a coupled ODE-PDE system for which methods and hypotheses are not necessarily compatible. The second task was to establish the effects of the coupling on the system, more specifically to gain more understanding on the influence of the solid motion on the fluid dynamics. In the case when the main difficulty was the complexity of the underlying partial differential equations, numerical simulations were implemented. On the other hand, in the case when the asymptotic analysis itself proved to be mathematically challenging, ideas coming from other physical problems and associated formal computations were applied.

1.1 Multiple scale analysis of a toy model

Chapter 1 detailed an asymptotic analysis based on a multiple-scale approach, of a system of second order non-linear ordinary differential equations. This system arises as a simplified model for the motion of a rigid body immersed in a two-dimensional perfect fluid. The fluid is assumed to be irrotational and is confined in a bounded domain. The

unknowns of the model represent the position of the object, that is the position of its center of mass and the angle of rotation; the equations arise from Newton's second law with the consideration of a Kutta-Joukowski type lift force.

A detailed analysis is carried out on this system when the solid inertia (mass and/or diameter) tends to 0. The study revolves around three main topics, each of them presenting a specific issue that often arises as part of a singular perturbation problem. First and foremost, the evolution of the position vector of the center of mass is dictated by an equation reminiscent of the equation describing the trajectory of a charged particle in classical electromagnetic field theory ([Kru58]). We established an asymptotic development up to arbitrary order with respect to the (infinitesimal) mass parameter for the position by an adaptation of the so called guiding center approximation. In particular, we have that the motion is dictated by the classical point-vortex system at zeroth order.

The angular variable evolves according to a slowly-in-time modulated non-linear pendulum equation, and experiences qualitatively different behavior depending on the initial data. This is brought to light by Sections 1.4 and 1.5 of Chapter 1 in which the characteristic behavior of a solution is established for small angular momentum (small diameter). For small initial data, the dominant effect is the periodicity of the equation, a two-timescale asymptotic development can be derived based on the results of [BH88]. The slow time modulation can lead to instabilities due to the cumulated effects over a long timespan, therefore we introduced an adapted shift and a corresponding scaling for the fast time variable to ensure the boundedness of the terms in the development.

For larger initial data, the "trajectories" of the system (in a dynamical sense) are dominated by the instabilities near the generalized homoclinic trajectories. Hence the corresponding solution is propagated by the flow towards a neighborhood of the normally invariant manifold in which the map behaves like a Smale horseshoe map, implying chaotic behavior in the weakest sense.

1.2 Wave-structure interaction for shallow waters

Chapters 2 and 3 address the mathematical description of a setting in which the solid object is lying at the bottom of a layer of fluid and moves under the forces created by waves traveling on the surface of this layer. More precisely, the water waves problem is considered in a fluid domain with a flat bottom topography and with an object lying on the bottom, allowed to move horizontally under the pressure forces created by the waves, and in frictional contact with the bottom itself.

Section 2.1 of Chapter 2 establishes the mathematical setting of the physical problem, such as the dynamics of the fluid and the mechanics of the solid motion, and prepare the terrain to the analysis of the models in shallow water asymptotic regimes. More specifically, the case of the (nonlinear) Saint-Venant system, and the (weakly nonlinear) Boussinesq system are examined as far as the fluid dynamics is concerned. An existence and uniqueness theorem is proved for the coupled fluid-solid system in both cases. More-

over, by making use of certain annulations in the corresponding energy estimates, as well as the particular structure of the coupling terms, one is able to go beyond the standard scale for the existence time of solutions to the Boussinesq system with a moving bottom, resulting in long time existence results, improving on what the general theory would dictate ([Mel15]), but still not as good as the ones obtained for the *abcd*-system (in the case of a fixed bottom) ([Bur16]).

Motivated principally by the latter results, a finite difference scheme is implemented for the Boussinesq system coupled with the solid object. The fluid quantities are discretized on a staggered grid, improving the results of [LM07] in terms of precision and convergence for the flat bottom case, as well as generalizing the algorithm for possible applications over a generic moving bottom setting. The solid motion is discretized in time based on central finite difference scheme of lower order than the scheme applied for the PDE part of the coupled system, however it retains the overall dissipative characteristics of the equation (originating from the friction).

A series of numerical experiments were carried out in Section 3.3 of Chapter 3. The moving bottom case is compared with a system where the same object is fixed to the bottom in order to observe the qualitative and quantitative differences in wave transformation. In general a loss of wave amplitude is observed. The influence of the friction on the whole system is also measured, indicating differences for small and large coefficients of friction. Overall, hydrodynamic damping effects reminiscent to the dead-water phenomenon can be established. The simulations involving a wave train approaching the solid show in particular the complex nature of the interaction between the object and the waves.

2 Research perspectives

Naturally, one can envision many directions in which the works presented here can be continued. These are, but not limited to, straightforward generalizations or natural continuations of the preceding studies of which we would like to elaborate a couple.

2.1 Asymptotic analysis of the coupled toy model

The system (1.1.1), albeit a decoupled system of EDOs, involves two variables with their respective smallness parameters that influence their corresponding evolution. Chapter 1 highlighted the complex dynamical background of these variables when one treats them separately. Therefore, a natural extension of this work would be to consider an asymptotic expansion of the two variables at the same time. This would require a multiple-scale approach incorporating the features of both the high frequency, low amplitude gyration around the guiding center (essentially a point-vortex), as well as the shifted modulation of the angular variable.

This perspective becomes even more interesting if one considers the more general equations derived in Section 1.2. System (1.2.18) presents the full equations at order $\mathcal{O}(\varepsilon)$, that are fully coupled. The asymptotic analysis for this system would require a thorough multiple-scale development in order to properly handle the coupling between the two variables.

2.2 Convergence issues

Chapter 1 presents results for the convergence of the two variables of the model towards their zeroth order approximation in their respective asymptotic regime. It was proven in Corollary 1.3.2 that we have convergence in $\mathcal{C}^\infty$ between the two point-vortex systems. Theorem 1.4.1 prepares the ground for a first order asymptotic development. From this point on, one hopes to obtain eventually a convergence result in $W^{1,\infty}$ just as for the massive point-vortex system, however establishing properly controled error estimate for this nonlinear system is highly non-trivial. Furthermore, by continuing the development, one expects to find a better approximation, therefore improving the associated convergence results too.

2.3 Modeling underwater landslides

One of the main limitations of the physical model presented in Section 2.1 of Chapter 2 is that it is only applicable to a flat bottom surface. The limitation does not arise from the fluid dynamics model, since it is capable of handling an arbitrary (but sufficiently regular in the sense of Sobolev) bottom topography variation ([Mel15]). The restriction comes from our physical considerations on the solid, most notably its rigidity. This implies that the solid is non-deformable, meaning that in particular, if initially the part of the solid in direct contact with the bottom is flat, it will stay flat during the entirety of its motion. One can see that this excludes any type of angles, curves, or peaks concerning the immovable part of the bottom.

The flat bottom hypothesis does not pose significant difficulties when one considers applications originating from coastal engineering, where this assumption is quite common and not really restrictive. However, when one wishes to handle submarine landslides ([CKS11], [DK13]), slopes in the reference topography are unavoidable. This is especially true when modeling underwater landslide generated tsunamis, which is an environmentally important and physically complex issue ([TBC01], [GW05]). Therefore an extension of the presented model is planned to incorporate nontrivial bottom topographies by alleviating the rigidity assumption on the solid.

2.4 Static and dynamic friction laws

Another issue with the solid model presented in Section 2.1 of Chapter 2 concerns the friction law applied in the determination of the friction force in Newton's second law. More precisely, a kinetic (dynamic)-only friction law is applied to describe this force term. This involves the implicit assumption that the friction force is zero if there is no solid motion (the velocity of the solid is zero). However, it is well known ([Ber06]) that this does not reflect the physical reality properly. By the third law of Coulomb, one has that the friction force at any instance verifies the inequality

$$|\mathbf{F}_{fric}| \leqslant c_{fric}|\mathbf{F}_{normal}|.$$

In particular, when the solid is not moving, a strict inequality is in effect, signifying that the net force acting on the solid is not enough to surpass the static friction effects blocking the solid motion. Mathematically speaking it is represented by a jump condition in the motion, leading to discontinuities and non-uniqueness in the solution of the corresponding ODE.

Another complication arises from the fact that the coefficient associated with the static friction (the strict inequality) is in fact not equal to the coefficient of the dynamic friction (when the solid is in motion), with the former being larger, according to experiments.

2.5 Coupling for more general shallow water models

A direct continuation of the works presented in Chapter 2 is to consider more precise shallow water models. A natural step towards this goal would be to incorporate the Serre–Green–Naghdi equations instead of the Boussinesq equations. The advantage is that in this asymptotic regime no additional hypothesis is made on ε or on β, we obtain the general second order approximation of the form

$$\begin{aligned} \partial_t\zeta + \nabla_x \cdot (h\overline{V}) &= \frac{\beta}{\varepsilon}\partial_t b, \\ (1+\mu\mathcal{T})\partial_t\overline{V} + \nabla_x\zeta + \varepsilon(\overline{V}\cdot\nabla_x)\overline{V} + \mu\varepsilon(\mathcal{Q}(\overline{V}) + \mathcal{Q}_b(\overline{V})) &= \mu\mathbf{mb}, \end{aligned} \tag{2.1}$$

where we have the following operators

$$\begin{aligned} \mathcal{T}V = &-\frac{1}{3h}\nabla_x(h^3\nabla_x\cdot V) \\ &+\beta\frac{1}{2h}\left(\nabla_x(h^2\nabla_x b\cdot V) - h^2\nabla_x b\nabla_x\cdot V\right) + \beta^2\nabla_x b\nabla_x b\cdot V; \end{aligned}$$

$$\mathcal{Q}(\overline{V}) = -\frac{1}{3h}\nabla_x\left(h^3\left((\overline{V}\cdot\nabla_x)(\nabla_x\cdot\overline{V}) - (\nabla_x\cdot\overline{V})^2\right)\right),$$
$$\mathcal{Q}_b(\overline{V}) = \frac{\beta}{2h}\Big(\nabla_x(h^2(\overline{V}\cdot\nabla_x)^2 b) - h^2((\overline{V}\cdot\nabla_x)(\nabla_x\cdot\overline{V}) - (\nabla_x\cdot\overline{V})^2)\nabla_x b\Big) + \beta^2((\overline{V}\cdot\nabla_x)^2 b)\nabla_x b;$$

and finally

$$\mathbf{mb} = -\frac{\beta}{2\varepsilon}\Big(\nabla_x(h\partial_t^2 b) + (\varepsilon\nabla_x\zeta + \beta\nabla_x b)\partial_t^2 b\Big) - \frac{\beta^2}{2\varepsilon}\nabla_x(\partial_t b)^2 - \frac{\beta}{2}\Big(-\nabla_x(\partial_t b\nabla_x\cdot(h\overline{V})) + \nabla_x\cdot(h\overline{V})\nabla_x\partial_t b + \nabla_x\nabla_x\cdot(\partial_t b h\overline{V}\Big).$$

The aim would be to establish the coupled system with the solid moving on the bottom just as in the case of the weakly nonlinear Boussinesq regime. Owing to structural similarities, one hopes to obtain a good control on the associated energy which would imply eventually a local existence and uniqueness result for the system, however proper treatment of the nonlinear terms is highly challenging.

In this regime, the wave-solid interaction is expected to be more complex, and some phenomena such as the added mass effect would be relevant, while they could be neglected in the weakly nonlinear regime considered in this thesis.

Appendix A

On Grönwall type inequalities

Throughout the different parts of this thesis we made use of inequalities and estimates for differential equations (ordinary as well as partial) under the common designation of "Grönwall's inequality". Here we would like to clarify this, since the applied inequalities were not necessarily the classical Grönwall's lemma nor a straightforward adaptation.

First of all, we have the following non-linear generalization of the original inequality ([Bih56]).

Proposition A.0.1. *Let $f : [a, b] \to \mathbb{R}^+$ be a continuous function that satisfies the integral inequality*

$$f(t) \leqslant A + \int_a^t \Psi(s)\phi(f(s))\, ds, \quad t \in [a, b], \tag{A.0.1}$$

where $A \geqslant 0$, $\Psi : [a, b] \to \mathbb{R}^+$ is continuous, and $\phi : \mathbb{R}^+ \to \mathbb{R}^+\backslash\{0\}$ is continuous and monotone increasing. Then the estimation

$$f(t) \leqslant \Phi^{-1}\left(\Phi(A) + \int_a^t \Psi(s)\, ds\right), \quad t \in [a, b] \tag{A.0.2}$$

holds, where $\Phi : \mathbb{R}^+ \to \mathbb{R}$ is given by

$$\Phi(x) := \int_{x_0}^x \frac{1}{\phi(s)}\, ds.$$

Proof: Let us denote by $g(t)$ the following function:

$$g(t) := \int_a^t \Psi(s)\phi(f(s))\, ds, \quad t \in [a, b].$$

We have that $g(a) = 0$, therefore by the definition g and inequality (A.0.1) we obtain

$$\frac{d}{dt}g(t) = \Psi(t)\phi(f(t)) \leqslant \Psi(t)\phi(A + g(t))$$

for any $t \in [a,b]$. So, integrating over $[a,t]$ yields

$$\int_0^{f(t)} \frac{1}{\phi(A+s')}\, ds' \leqslant \int_a^t \Psi(s)\, ds.$$

Hence, by the definition of Φ we get that

$$\Phi(A+f(t)) - \Phi(A) \leqslant \int_a^t \Psi(s)\, ds$$

for any $t \in [a,b]$. Since the function Φ is also monotone increasing, the result follows from this estimate and (A.0.1). □

This estimate was used for instance in the estimates in Lemma 2.3.2. of Section 2.3.4.

Another, more classical generalization of Grönwall's lemma is the following, often used for norm estimates for differential equations in Hilbert spaces.

Proposition A.0.2. *Let $f : [a,b] \to \mathbb{R}$ be a continuous function that satisfies the integral inequality*

$$\frac{1}{2} f^2(t) \leqslant \frac{1}{2} f_0^2 + \int_a^t \Psi(s) f(s)\, ds, \quad t \in [a,b], \tag{A.0.3}$$

where $f_0 \geqslant 0$, $\Psi : [a,b] \to \mathbb{R}^+$ is continuous. Then the estimation

$$|f(t)| \leqslant |f_0| + \int_a^t \Psi(s)\, ds, \quad t \in [a,b] \tag{A.0.4}$$

holds.

Proof: For $\varepsilon > 0$ let g_ε be defined by

$$g_\varepsilon(t) := \frac{1}{2}(f_0^2 + \varepsilon^2) + \int_a^t \Psi(s) f(s)\, ds, \quad t \in [a,b],$$

a quantity that is always positive, since, by (A.0.3) we have

$$\frac{1}{2} f^2(t) \leqslant g_\varepsilon(t).$$

The chain rule yields

$$g_\varepsilon'(t) = \Psi(t) f(t), \quad t \in [a,b],$$

from which one infers that

$$g_\varepsilon'(t) \leqslant \Psi(t) \sqrt{2 g_\varepsilon(t)}.$$

By integrating over $[a,t]$ we obtain that

$$\sqrt{2g_\varepsilon(t)} - \sqrt{2g_\varepsilon(a)} = \int_a^t \frac{g_\varepsilon'(s)}{\sqrt{2g_\varepsilon(s)}}\, ds \leqslant \int_a^t \Psi(s)\, ds.$$

Therefore we deduce that

$$\begin{aligned} |f(t)| &\leqslant \sqrt{2g_\varepsilon(a)} + \int_a^t \Psi(s)\,ds \\ &\leqslant |f_0| + \varepsilon + \int_a^t \Psi(s)\,ds, \end{aligned}$$

which is valid for every $\varepsilon > 0$. This implies the desired estimate. □

This Grönwall type inequality was used in the demonstration of Lemma 2.2.5. in Section 2.2.4.3 part B, throughout section 2.3.4 for the proof of the energy estimates in Propositions 3.1.1 and 2.3.3, and in Lemma 3.2.1. of Section 3.2.3.

Bibliography

[ABZ11] Thomas Alazard, Nicolas Burq, and Claude Zuily. On the water-wave equations with surface tension. *Duke Mathematical Journal*, 158(3):413–499, 2011.

[ABZ14] Thomas Alazard, Nicolas Burq, and Claude Zuily. On the Cauchy problem for gravity water waves. *Inventiones Mathematicae*, 198(1):71–163, 2014.

[ACDNn17] Stéphane Abadie, Marcela Cruchaga, Benoit Ducassou, and Jonathan Nuñez. A fictitious domain approach based on a viscosity penalty method to simulate wave/structure interaction. *Journal of Hydraulic Research*, 55(6):847–862, 2017.

[AELS14] Reza Alam, Ryan Elandt, Marcus Lehmann, and Mostafa Shakeri. The Wave Carpet: Development of a Submerged Pressure Differential Wave Energy Converter, 2014. 30th Symposium on Naval Hydrodynamics, Hobart, Australia.

[AG07] Serge Alinhac and Patrick Gérard. *Pseudo-differential operators and the Nash–Moser theorem*, volume 82 of *Graduate Studies in Mathematics*. American Mathematical Society, 2007.

[AMMM15] Stéphane Abadie, Manuel Martin Medina, Cyril Mokrani, and Denis Morichon. Déplacement d'une structure soumise à l'impact d'un front d'onde, 2015. Rencontres Universitaires de Génie Civil, Bayonne, France.

[ASL08a] Borys Alvarez-Samaniego and David Lannes. Large time existence for 3D water-waves and asymptotics. *Inventiones Mathematicae*, 171(3):485–541, 2008.

[ASL08b] Borys Alvarez-Samaniego and David Lannes. A Nash–Moser theorem for singular evolution equations. Applications to the Serre and Green–Naghdi equations. *Indiana University Mathematics Journal*, 57(1):97–131, 2008.

[Bar04] Eric Barthélemy. Nonlinear shallow water theories for coastal waves. *Surveys in Geophysics*, 25(3-4):315–337, 2004.

[BC98] Jerry Lloyd Bona and Min Chen. A Boussinesq system for two-way propagation of nonlinear dispersive waves. *Physica D: Nonlinear Phenomena*, 116(1–2):191–224, 1998.

[BC16] Stevan Bellec and Mathieu Colin. On the existence of solitary waves for Boussinesq type equations and cauchy problem for a new conservative model. *Advances in Differential Equations*, 21(9-10):945–976, 2016.

[BCL05] Jerry Lloyd Bona, Thierry Colin, and David Lannes. Long wave approximations for water waves. *Archive for Rational Mechanics and Analysis*, 178(3):373–410, 2005.

[BCL+12] Philippe Bonneton, Florent Chazel, David Lannes, Fabien Marche, and Marion Tissier. A new approach to handle wave breaking in fully non-linear Boussinesq models. *Coastal Engineering*, 67:54–66, 2012.

[BCS02] Jerry Lloyd Bona, Min Chen, and Jean-Claud Saut. Boussinesq equations and other systems for small-amplitude long waves in nonlinear dispersive media. I: Derivation and linear theory. *Journal of Nonlinear Science*, 12(4):283–318, 2002.

[BEKRE17] Umberto Bosi, Allan Peter Engsig-Karup, Mario Ricchiuto, and Claes Eskilsson. Toward unified spectral boussinesq modeling for wave energy converters, 2017. Conference Paper, 19th International Conference on Finite Elements in FLow Problems, Rome.

[Ben17] Krisztián Benyó. Wave-structure interaction for long wave models in the presence of a freely moving object on the bottom, 2017. preprint, submitted, hal-01665775.

[Ben18a] Krisztián Benyó. Multiple-scale analysis of the dynamics of a point particle in a two dimensional perfect incompressible and irrotational flow, 2018. preprint.

[Ben18b] Krisztián Benyó. Numerical analysis of the weakly nonlinear Boussinesq system with a freely moving body on the bottom, 2018. preprint, submitted, hal-01791764.

[Ber06] Jean-Marie Berthelot. *Mécanique des solides rigides*. Tec and Doc Lavoisier, 2006.

[BG59] Jerome Berkowitz and Clifford S. Gardner. On the asymptotic series expansion of the motion of a charged particle in slowly varying fields. *Communications on Pure and Applied Mathematics*, 12:501–512, 1959.

[BH88] F. Jay Bourland and Richard Haberman. The modulated phase shift for strongly nonlinear, slowly varying, and weakly dampened oscillators. *SIAM Journal of Applied Mathematics*, 48(4):737–748, 1988.

[Bih56] Imre Bihari. A generalization of a lemma of Bellman and its application to uniqueness problems for differential equations. *Acta Mathematica Hungarica*, 7(1):81–94, 1956.

[Boc18] Edoardo Bocchi. Floating structures in shallow waters: local well-posedness in the axisymmetric case, 2018. preprint; hal-01714437.

[Bou71] Joseph V. Boussinesq. Théorie générale des mouvements qui sont propagés dans un canal rectangulaire horizontal. *Comptes Rendus des Séances de l'Académie des Sciences, Paris*, 73:256–260, 1871.

[BPVM+06] Augusto Beléndez, Carolina Pascual Villalobos, David Méndez, Tarsicio Beléndez, and Cristian Neipp. Exact solution for the nonlinear pendulum. *Revista Brasileira de Ensino de Física*, 29(4):645–648, 2006.

[Bra18] Marco Bravin. On the weak uniqueness of "viscous incompressible fluid + rigid body" system with Navier slip-with-friction conditions in a 2D bounded domain, 2018. preprint, hal-01740859.

[BS06] Hans-Joachim Bungartz and Michael Schäfer. *Fluid-structure interaction: Modelling, Simulation, Optimisation*, volume 53 of *Lecture Notes in Computational Science and Engineering*. Springer Verlag, 2006.

[Bur16] Cosmin Burtea. New long time existence results for a class of Boussinesq-type systems. *Journal de Mathématiques Pures et Appliquées*, 109(2):203–236, 2016.

[CGNS05] Walter Craig, Philippe Guyenne, David P. Nicholls, and Catherine Sulem. Hamiltonian long-wave expansions for water waves over a rough bottom. *Proceedings of the Royal Society of London, Section A*, 461:839–873, 2005.

[Cha07] Florent Chazel. Influence of bottom topography on long water waves. *ESAIM: Mathematical Modeling and Numerical Analysis*, 41(4):771–799, 2007.

[Che98] Min Chen. Exact traveling-wave solutions to bidirectional wave equations. *International Journal of Theoretical Physics*, 37(5):1547–1567, 1998.

[Che03] Min Chen. Equations for bi-directional waves over an uneven bottom. *Mathematics and Computers in Simulation*, 62(1-2):3–9, 2003.

[CK96] Julian D. Cole and Jirair K. Kevorkian. *Multiple scale and singular perturbation methods*, volume 114 of *Applied Mathematical Sciences*. Springer Verlag, 1996.

[CKS11] Leonid B. Chubarov, Gayaz S. Khakimzyanov, and Nina Shokina. Numerical modelling of surface water waves arising due to movement of underwater landslide on irregular bottom slope. *Notes on Numerical Fluid Mechanics and Multidisciplinary Design*, 115:75–91, 2011. Computational Science and High Performance Computing IV.

[CL15] Angel Castro and David Lannes. Well-posedness and shallow-water stability for a new Hamiltonian formulation of the water waves equations with vorticity. *Indiana University Mathematics Journal*, 64(4):1169–1270, 2015.

[CLS12] Walter Craig, David Lannes, and Catherine Sulem. Water waves over a rough bottom in the shallow water regime. *Annales de l'Institut Henri Poincaré (C) Non Linear Analysis*, 29(2):233–259, 2012.

[CM06] Georges-Henri Cottet and Emmanuel Maitre. A level set method for fluid-structure interactions with immersed surfaces. *Mathematical Models and Methods in Applied Sciences*, 16(3):415–438, 2006.

[CMM08] Georges-Henri Cottet, Emmanuel Maitre, and Thomas Milcent. Eulerian formulation and level set models for incompressible fluid-structure interaction. *ESAIM: Mathematical Modelling and Numerical Analysis*, 42(3):471–492, 2008.

[Cra85] Walter Craig. An existence theory for water waves and the Boussinesq and Korteweg–de Vries scaling limits. *Communications in Partial Differential Equations*, 10(8):787–1003, 1985.

[CS93] Walter Craig and Catherine Sulem. Numerical simulation of gravity waves. *Journal of Computational Physics*, 108(1):73–83, 1993.

[CSMT00] Carlos Conca, Jorge H. San Martin, and Marius Tucsnak. Existence of solutions for the equations modelling the motion of a rigid body in a viscous fluid. *Communications in Partical Differential Equations*, 25(5-6):1019–1042, 2000.

[CSS92] Walter Craig, Catherine Sulem, and Pierre-Louis Sulem. Nonlinear modulation of gravity waves: a rigorous approach. *Nonlinearity*, 5(2):497–522, 1992.

[CW05] Jacky Cresson and Stephen Wiggins. A Smale-Birkhoff theorem for normally hyperbolic manifolds, 2005. preprint.

[CW15] Jacky Cresson and Stephen Wiggins. A lambda-lemma for normally hyperbolic invariant manifolds. *Regular and Chaotic Dynamics*, 20(1):94–108, 2015.

[DK13] Denis Dutykh and Henrik Kalisch. Boussinesq modeling of surface waves due to underwater landslides. *Nonlinear Processes in Geophysics*, 20:267–285, 2013.

[DNZ15] Denys Dutykh, Hayk Nersisyan, and Enrique Zuazua. Generation of 2D water waves by moving bottom disturbances. *IMA Journal of Applied Mathematics*, 80(4):1235–1253, 2015.

[Dor17] Adrien Doradoux. Simulation numérique d'écoulements diphasiques autour d'un solide mobile, 2017. Thesis dissertation.

[dP16] Thibault de Poyferré. A priori estimates for water waves with emerging bottom, 2016. preprint, arXiv:1612.04103.

[Duc11] Vincent Duchêne. Asymptotic models for the generation of internal waves by a moving ship, and the dead-water phenomenon. *Nonlinearity*, 24(8):2281–2323, 2011.

[Duc12] Vincent Duchêne. Boussinesq/Boussinesq systems for internal waves with a free surface, and the KdV approximation. *ESAIM: Mathematical Modelling and Numerical Analysis*, 46(1):145–185, 2012.

[Ekm04] Vagn Walfrid Ekman. On dead water. *Scientific Results of the Norwegian North Polar Expedition 1893-1896*, 5(15):1–150, 1904.

[Fen71] Neil Fenichel. Persistence and smoothness of invariant manifolds for flows. *Indiana University Mathematical Journal*, 21(3):193–226, 1971.

[FGG07] Miguel A. Fernández, Jean-Fréderic Gerbeau, and Céline Grandmont. A projection semi-implicit scheme for the coupling of an elastic structure with an incompressible fluid. *International Journal for Numerical Methods in Engineering*, 69(4):794–821, 2007.

[GH83] John Guckenheimer and Philip Holmes. *Nonlinear Oscillations, Dynamical Systems, and Bifurcations of Vector Fields*, volume 42 of *Applied Mathematical Sciences*. Springer Verlag, 1983.

[GIL+14] Mateus das Neves Gomes, Liércio André Isoldi, Max Letzow, Luiz Alberto Oliveira Rocha, Elizaldo Domingues dos Santos, Flávio Medeiros Seibt, and Jeferson Avila Souza. Computational modeling applied to the study of wave energy converters (WEC). *Marine Systems and Ocean Technology*, 9(2):77–84, 2014.

[GKSW95] Stephan T. Grilli, James T. Kirby, Ravishankar Subramanya, and Ge Wei. A fully nonlinear Boussinesq model for surface waves. Part 1. Highly nonlinear unsteady waves. *Journal of Fluid Mechanics*, 294:71–92, 1995.

[GLS14] Olivier Glass, Christophe Lacave, and Franck Sueur. On the motion of a small body immersed in a two dimensional incompressible perfect fluid. *Bulletin de la Société Mathématique de France*, 142(3):489–536, 2014.

[GLS16] Olivier Glass, Christophe Lacave, and Franck Sueur. On the motion of a small light body immersed in a two dimensional incompressible perfect fluid with vorticity. *Communications of Mathematical Physics*, 341(3):1015–1065, 2016.

[GM00] Céline Grandmont and Yvon Maday. Existence for an unsteady fluid-structure interaction problem. *ESAIM: Mathematical Modeling and Numerical Analysis*, 34(3):609–636, 2000.

[GMS18] Olivier Glass, Alexandre Munnier, and Franck Sueur. Point vortex dynamics as zero-radius limits of the motion of a rigid body in an irrotational fluid. *Inventiones Mathematicae*, 2018.

[GN07] Philippe Guyenne and David P. Nicholls. A high-order spectral method for nonlinear water waves over moving bottom topography. *SIAM Journal of Scientific Computing*, 30(1):81–101, 2007.

[Gre04] Walter Greiner. *Classical mechanics: point particles and relativity*. Classical Theoretical Physics. Springer Verlag, 2004.

[GS15] Olivier Glass and Franck Sueur. Uniqueness results for weak solutions of two-dimensional fluid-solid systems. *Archive for Rational Mechanics and Analysis*, 218(2):907–944, 2015.

[GVH14] David Gérard-Varet and Matthieu Hillairet. Existence of weak solutions up to collision for viscous fluid-solid systems with slip. *Communications on Pure and Applied Mathematics*, 67(12):2022–2076, 2014.

[GW05] Stéphan T. Grilli and Philip Watts. Tsunami generation by submarine mass failure. I: Modeling, experimentail validation, and sensitivity analysis. *Journal of Waterway, Port, Coastal, and Ocean Engineering*, 131(6):283–297, 2005.

[HI15] Fujiwara Hiroyasu and Tatsuo Iguchi. A shallow water approximation for water waves over a moving bottom. *Advanced studies in pure mathematics*, 64:77–88, 2015.

[HM93] Stuart P. Hastings and J. Bryce McLeod. Chaotic motion of a pendulum with oscillatory forcing. *The American Mathematical Monthly*, 100(6):563–572, 1993.

[HPS77] Morris W. Hirsch, Charles C. Pugh, and Michael Shub. *Invariant manifolds*, volume 583 of *Springer Lecture Notes in Mathematics*. Springer Verlag, 1977.

[Igu09] Tatsuo Iguchi. A shallow water approximation for water waves. *Journal of Mathematics of Kyoto University*, 49(1):13–55, 2009.

[Igu11] Tatsuo Iguchi. A mathematical analysis of tsunami generation in shallow water due to seabed deformation. *Proceedings of the Royal Society of Edinburgh Section A: Mathematics*, 141(3):551–608, 2011.

[IL18] Tatsuo Iguchi and David Lannes. Hyperbolic free boundary problems and applications to wave-structure interactions, 2018. preprint; arXiv:1806.07704.

[KB43] Nikolay M. Krylov and Nikolay N. Bogoliubov. *Introduction to non-linear mechanics*, volume 11 of *Applied Mathematics*. Princeton University Press, 1943. Originally published in 1937 in Russian by Izd-vo Akad. Nat. USSR, Kiev.

[KL84] Tosio Kato and Chi Yuen Lai. Nonlinear evolution equations and the Euler flow. *Journal of Functional Analysis*, 56(1):15–28, 1984.

[KN86] Tadayoshi Kano and Takaaki Nishida. A mathematical justification for Korteweg–de Vries equation and Boussinesq equation of water surface waves. *Osaka Journal of Mathematics*, 23(2):389–413, 1986.

[KO85] Rangachary Kannan and Rafael Ortega. Periodic solutions of pendulum-type equations. *Journal of Differential Equations*, 59:123–144, 1985.

[KR17] Maria Kazolea and Mario Ricchiuto. On wave breaking for Boussinesq-type models, 2017. Research Report: hal-01581954.

[Kru58] Martin Kruskal. The Gyration of a Charged Particle. *AEC Research and Development Report*, 1958. Project Matterhorn, Princeton University.

[Kru64] Martin Kruskal. Asymptotology. *Lectures presented at the seminar on plasma physics*, pages 373–397, 1964.

[Kuz59] Gregory Evgeny Kuzmak. Asymptotic solutions of nonlinear second order differential equations with variable coefficients. *Journal of Applied Mathematics and Mechanics*, 23(3):730–744, 1959.

[Lan05] David Lannes. Well-posedness of the water-waves equations. *Journal of the American Mathematical Society*, 18(3):605–654, 2005.

[Lan13] David Lannes. *The water waves problem: mathematical analysis and asymptotics*, volume 188 of *Mathematical Surveys and Monographs*. American Mathematical Society, 2013.

[Lan17] David Lannes. On the dynamics of floating structures. *Annals of Partial Differential Equations*, 3(1), 2017.

[LB10] Emmanuel Lefrançois and Jean-Paul Boufflet. An introduction to fluid-structure interaction: Application to the piston problem. *SIAM Review*, 52(4):747–767, 2010.

[Li06] Yi A. Li. A shallow-water approximation to the full water wave problem. *Communications on Pure and Applied Mathematics*, 59(9):1225–1285, 2006.

[Lin83] Anders Lindstedt. Sur la forme des expressions des distances mutuelles dans le problème des trois corps. *Compte-Rendus de l'Académie des Sciences*, 97:1276–1353, 1883.

[Lin05] Hans Lindblad. Well-posedness for the motion of an incompressible liquid with free surface boundary. *Annals of Mathematics*, 162(1):109–194, 2005.

[LM07] Penghzi Lin and Chuanjian Man. A staggered-grid numerical algorithm for the extended Boussinesq equations. *Applied Mathematical Modelling*, 31(2):349–368, 2007.

[LM17] David Lannes and Guy Métivier. The shoreline problem for the one-dimensional shallow water and Green–Naghdi equations, 2017. preprint, hal-01614321.

[Luk66] John Christian Luke. A perturbation method for nonlinear dispersive wave problems. *Proceedings of the Royal Society of London, Series A*, 292(1430):403–412, 1966.

[Luk67] Jon Christian Luke. A variational principle for a fluid with a free surface. *Journal of Fluid Mechanics*, 27(2):395–397, 1967.

[MA11] Akbar Mohebbi and Zohreh Asgari. Efficient numerical algorithms for the solution of "good" Boussinesq equation in water wave propagation. *Computer Physics Communications*, 182(12):2464–2470, 2011.

[MB03] Andrew J. Majda and Andrea L. Bertozzi. *Vorticity and incompressible flow*. Cambridge Texts in Applied Mathematics. Cambridge University Press, 2003.

[Mel63] Vladimir K. Melnikov. On the stability of the center for time-periodic perturbations. *Transactions of the Moscow Mathematical Society*, 12:1–57, 1963.

[Mel15] Benjamin Melinand. A mathematical study of meteo and landlside tsunamis: the Proudman resonance. *Nonlinearity*, 28:4037–4080, 2015.

[Mil77] John W. Miles. On Hamilton's principle for surface waves. *Journal of Fluid Mechanics*, 83(1):153–158, 1977.

[Mit09] Dimitrios E. Mitsotakis. Boussinesq systems in two space dimensions over a variable bottom for the generation and propagation of tsunami waves. *Mathematics and Computers in Simulation*, 80(4):860–873, 2009.

[MS86] Kenneth R. Meyer and George R. Sell. Homoclinic orbits and Bernoulli bundles in almost periodic systems. *Institute of Mathematics and Its Applications, Preprint Series*, 285:1–23, 1986. University of Minnesota.

[MVD11] Matthieu Mercier, Romain Vasseur, and Thierry Dauxois. Resurrecting dead-water phenomenon. *Nonlinear Processes in Geophysics*, 18:193–208, 2011.

[Mé17] Benjamin Mélinand. Coriolis effect on water waves. *ESAIM: Mathematical Modelling and Numerical Analysis*, 51(5):1957–1985, 2017.

[Neu15] John Charles Neu. *Singular Perturbation in the Physical Sciences*, volume 167 of *Graduate Studies in Mathematics*. American Mathematical Society, 2015.

[Nwo93] Okey Nwogu. Alternative form of Boussinesq equations for nearshore wave propagation. *ASCE Journal of Waterway, Port, Coastal, and Ocean Engineering*, 119(6):618–638, 1993.

[ORT07] Jaime Ortega, Lionel Rosier, and Takéo Takahashi. On the motion of a rigid body immersed in a bidimensional incompressible perfect fluid. *Annales de l'Institut Henri Poincaré (C) Non Linear Analysis*, 24(1):139–165, 2007.

[Ovs74] Lev V. Ovsjannikov. To the shallow water theory foundation. *Archives of Mechanics*, 26:407–422, 1974.

[Pal86] Kenneth J. Palmer. Transversal heteroclinic points and Cherry's example of a nonintegrable Hamiltonian system. *Journal of Differential Equations*, 65(3):321–360, 1986.

[Per67] D. Howell Peregrine. Long waves on a beach. *Journal of Fluid Mechanics*, 27(4):815–827, 1967.

[Pes05] Bernard Peseux. Introduction au couplage fluide-structure, 2005. Cours en Ligne (CEL), DEA Nantes.

[Poi90] Henri Poincaré. Sur le problème des trois corps et les équations de la dynamique. *Acta Mathematica*, 13:1–270, 1890.

[Poi92] Henri Poincaré. *Les méthodes nouvelles de la mécanique célèste*. Gauthier-Villars, 1892.

[PR83] George C. Papanicolaou and Rodolfo R. Rosales. Gravity waves in a channel with a rough bottom. *Studies in Applied Mathematics*, 68(2):89–102, 1983.

[Rob83] Clark Robinson. Sustained resonance for a nonlinear system with slowly varying coefficients. *SIAM Journal of Mathematical Analysis*, 14(5):847–860, 1983.

[Sma65] Stephen Smale. Diffeomorphisms with many periodic points. *Differential and Combinatorial Topology*, pages 63–80, 1965. A Symposium in Honor of Marston Morse.

[Sou88] Howard Neil Southgate. Wave Breaking - a review of techniques for calculating energy losses in breaking waves, 1988. Technical Report, Hydraulics Research Wallington.

[Sue17] Franck Sueur. Motion of a particle immersed in a two dimensional incompressible perfect fluid and point vortex dynamics. *Particles in flows, Advances in Mathematical Fluid Mechanics*, 3:139–216, 2017.

[Sul05] Pierre-Louis Sulem. Introduction to the Guiding Center Theory. *Fields Institute Communications*, 46:109–147, 2005. Topics in Kinetic Theory.

[SW00] Guido Schneider and C. Eugene Wayne. The long-wave limit for the water wave problem I. The case of zero surface tension. *Communications on Pure and Applied Mathematics*, 53(12):1475–1535, 2000.

[SX12] Jean-Claude Saut and Li Xu. The Cauchy problem on large time for surface waves Boussinesq systems. *Journal de Mathématiques Pures et Appliquées*, 97(6):635–662, 2012.

[Tay97] Michael E. Taylor. *Partial Differential Equations: Nonlinear Equations*, volume 117 of *Applied Mathematical Sciences*. Springer, 1997.

[TBC01] Stefano Tinti, Elisabetta Bortolucci, and Cinzia Chiavettieri. Tsunami excitation by submarine slides in shallow-water approximation. *Pure and Applied Geophysics*, 158(4):759–797, 2001.

[TC08] Takéo Takahashi and Patricio Cumsille. Well-posedness for the system modelling the motion of a rigid body of arbitrary form in an incompressible viscous fluid. *Czechoslovak Mathematical Journal*, 58(4):961–992, 2008.

[Tur87] Bruce Turkington. On the evolution of a concentrated vortex in an ideal fluid. *Archive for Rational Mechanics and Analysis*, 97(1):75–87, 1987.

[TW92] Michelle H. Teng and Theodore Y. Wu. Nonlinear water waves in channels of arbitrary shape. *Journal of Fluid Mechanics*, 242:211–233, 1992.

[Wig88a] Stephen Wiggins. *Global bifurcations and chaos*, volume 73 of *Applied Mathematical Sciences*. Springer Verlag, 1988.

[Wig88b] Stephen Wiggins. On the detection and dynamical consequences of orbits homoclinic to hyperbolic periodic orbits and normally hyperbolic invariant tori in a class of ordinary differential equations. *SIAM Journal of Applied Mathematics*, 48(2):262–285, 1988.

[Wu87] Theodore Yao-Tsu Wu. Generation of upstream advancing solitons by moving disturbances. *Journal of Fluid Mechanics*, 184:75–99, 1987.

[Wu97] Sijue Wu. Well-posedness in Sobolev spaces of the full water wave problem in 2-D. *Inventiones Mathematicae*, 130(1):39–72, 1997.

[Wu99] Sijue Wu. Well-posedness in Sobolev spaces of the full water wave problem in 3-D. *Journal of the American Mathematical Society*, 12(2):445–495, 1999.

[Yos82] Hideaki Yosihara. Gravity waves on the free surface of an incompressible perfect fluid of finite depth. *Publications of the Research Institute for Mathematical Sciences*, 18(1):49–96, 1982.

[Zak68] Vladimir E. Zakharov. Stability of periodic water waves of finite amplitude on the surface of a deep fluid. *Journal of Applied Mechanics and Technical Physics*, 9(2):190–194, 1968.